QUANTIFICATION OF COMPLEX DNA DAMAGE BY IONISING RADIATION: AN EXPERIMENTAL AND THEORETICAL APPROACH

A thesis submitted for the degree of Doctor of Philosophy

by

Jonathan Fulford

Department of Biological Sciences, Brunel University

May 2000

Abstract

Ionising radiation potentially produces a broad spectrum of damage in DNA including single and double strand breaks (ssb and dsb) and base damages. It has been hypothesised that sites of complex damage within cellular DNA have particular biological significance due to an associated decreased efficiency in repair. The aim of this study is to gain further understanding of the formation of complex DNA damage.

Irradiations of plasmid DNA illustrate that an increase in ionising density of the radiation results in a decrease in ssb yields/Gy but an increase in dsb per ssb, indicative of an increase in the number of complex damage sites per simple isolated damage site. As the mechanism for damage formation shifts from purely indirect at low scavenging capacities to a significant proportion of direct at higher scavenging capacities the proportion of complex damage increases. Comparisons with the yields of ssb and dsb simulated by Monte-Carlo calculations for Al_K USX and α-particles also indicate this correspondence.

The ionisation density of low energy, secondary electrons produced by photons was assessed experimentally from the dependence of the yield of OH radicals escaping intra-track recombination on photon energy. As energy decreases the OH radical yield initially decreases reflecting an increased ionisation density. However, with further decrease in photon energy the yield of OH radicals increases in line with theoretical calculations.

Base damage yields were determined for low and high ionising density radiation over a range of scavenging capacities. As scavenging capacity increases the base damage:ssb ratios increases implying a contribution from electrons to base damage. It is proposed that base damage contributes to DNA damage complexity. Complex damage analysis reveals that at cell mimetic scavenging capacities, 23 % and 72 % of ssb have an additional spatially close damage site following γ-ray and α-particle irradiation respectively.

Table of Contents

Chapter 1
Introduction

Chapter 2
Materials and Methods

Chapter 3
Comparison of the Yield of ssb and dsb Induced in Plasmid DNA by ^{60}Co γ-ray, Al_K USX and α-particle Irradiation: Dependence on the Concentration of OH Radical Scavengers

Chapter 4
The Simulation of 1.5 keV electron and α-particle Tracks and Subsequent Comparison of the Yields of DNA ssb and dsb with those Determined Experimentally

Chapter 5
Determination the Yields of Radiation-Induced Base Damage Revealed by Enzymes: Dependence of these Yields Upon Scavenging Capacity and Radiation Quality

Chapter 6
Experimental Procedures for Obtaining DNA Samples at Variable Humidities

List of Tables

List of Figures

Acknowledgements

I am grateful to the Radiation and Genome Stability Unit, Harwell for providing me with a studentship funded by the Commission of the European Community (Contract No. F14-CT95-0011c).

I would like to thank my supervisors; Pete O'Neill and Dudley Goodhead at the MRC and Janet Arrand at Brunel. In particular I would like to thank Pete for always being helpful and encouraging, even if he did make me do lots of Work in Progress's and both him and Dudley for giving me the chance to do a Ph.D in the first place even though, having found out I was a QPR supporter, it may well have only been because they felt sorry for me

Thank you to Hooshang Nikjoo for supplying the track codes and for all of his assistance and advice in the simulations which were undertaken and Siobhan Cunniffe, Jo Buckingham, Stuart Townsend, Mark Hill, Charlotte Bolton, Dave Stevens and Paul Bonner for their help with experiments and irradiations.

Thanks to all of my friends at the MRC, especially Emma, Melanie and Helen my companion in Ph.D land, who always made it a pleasant place to work and of course play football. Special mention to Debbie who provided a very special friendship and one which I now miss very much.

Chapter 1

Introduction

1.1. Historical Introduction

X-rays were discovered in 1895 by Wilhelm K. Roentgen, a German physicist, and were so named because at first he didn't understand what they were. Within a year the French physicist Antoine Henri Becquerel discovered that crystals of a uranium compound would darken photographic plates even if the plates were not exposed to light. He proposed that uranium gave off energy in the form of radiation. Subsequent experiments by the British physicist Ernest Rutherford showed that this radiation consisted of particles he named alphas and betas.

The detrimental effects of ionising radiation on biological tissue were discovered soon after these initial discoveries by Roentgen and Becquerel. In 1896 Grubbé (1933) described how long exposures to X-rays of the back of his hand led to erythema and oedema. Within a year, X-rays were being used as a potential therapeutic agent. Long term effects of radiation subsequently became apparent when cancers were reported in radiation workers and radiologists.

Subsequent biological studies have revealed a whole spectrum of cellular and genetic consequences of exposure to ionising radiation. When long term effects and specifically cancer induction are considered there is overwhelming evidence to support DNA as the critical target with which radiation interacts (Datta *et al.* 1976, Frankenberg *et al.* 1981, Frankenberg-Schwager 1990, Folkard *et al.* 1995).

1.2. The Hazards of Radiation

Why is radiation capable of causing damage, which may induce death at the cellular level or cancer at the organism level? The answer probably lies in the type of damage that is produced. The actual energy deposited within a body or cell is extremely small. A dose of about 4 Gy (Vriesendorp and van Bekkum 1984) is considered sufficient to kill half of the people who receive it. In an average person this corresponds to the deposition of only 280 J or sufficient energy to raise the temperature of a cup of water by about ¼ of a degree. However energy is not deposited equally throughout the body. Indeed, energy deposition is not uniform even in a volume as small as a cell. Radiation

deposits energy in the form of so-called tracks (Mozumder and Magee 1966, Goodhead 1992). Tracks consist of a series of discrete energy depositions, which occur along the path that the radiation traverses. Such depositions consist of single ionisation or excitation events of atoms or molecules. Thus energy deposition is not even uniform at an atomic level. One atom may receive energy sufficient to cause ionisation whereas an adjacent atom may receive none. However, different types of radiation do not give equivalent levels of critical damage within biological systems. If, for example cells exposed to 10 Gy of ^{60}Co γ-ray irradiation are compared with those exposed to 10 Gy from an α-particle source, survival levels are not comparable, with a greater number of cells killed by the α-particles (see reviews, Elkind 1984, Hall 1994). Potentially, this may be explained by the characteristics of the radiation tracks associated with the two radiation types. Energy deposition events associated with γ-rays are sparsely distributed with a relatively large average distance between separate events. However for α-particle tracks, energy depositions are much closer together with large volumes of a typical cell being unaffected by the passage of the particle but small regions receiving a large number of energy depositions (Goodhead and Nikjoo 1989). It is this lack of uniformity in distribution that is one of the unique features of radiation as a damaging agent. Mechanisms within a cell exist for the repair of damaged sites on a macroscopic scale (Friedberg *et al.* 1995). However it is conceptually easy to imagine that if a number of damage sites occur in close vicinity then repair may not be as straightforward as a single isolated damage site (Chaudhry and Weinfeld 1995, Harrison *et al.* 1998).

It is the difference in the spatial distribution of energy deposition events between radiations such as γ-rays and α-particles and the effect that this has on the ability of cells to subsequently process the damage, that is thought to give rise to differences in damage distribution and hence cell survival or cancer induction. Subsequently, it is necessary to think not only about the total amount of damage associated with a particular radiation but also the proximity of one damaged site to another. Thus the concept of 'clustered damage' or 'multiply damaged sites', defined as a number of damage sites occurring spatially close to one another, is of prime biological importance (Goodhead *et al.*1985, Ward 1988, 1994, Goodhead 1989, 1994, Goodhead and Nikjoo 1989).

Radiations such as α-particles and γ-rays have different physical characteristics. α-particles typically have a very short range being completely absorbed by a few cm of air. Thus, for a cell to receive a significant dose from an α-particle it is necessary for it to be close to the α-particle emitter. By contrast hard γ-rays have a very low (exponential) attenuation through matter, having a significant probability of passing through a considerable thickness of lead. Hence it is still possible to receive a significant dose from a γ-ray source located some distance away. An α-particle emitter however that is actually present within the body, for example, through ingestion or inhalation, may be considered to pose a potentially large risk. A natural gaseous source of α-particle emitters is radon and its short lived daughters. Radon-222 (^{222}Rn) is a decay product of radium-226 (^{226}Ra) which is the fifth daughter of uranium-238 (^{238}U). ^{238}U and ^{226}Ra are both naturally occurring in rocks and soil to varying degrees and so ^{222}Rn, which exists as a gas above -61.8^0 C becomes ubiquitous, with its concentration increasing in areas where there is a rich source or poor ventilation. Radon decays with a half-life of 3.82 days to ^{218}Po, which in turn decays to ^{214}Pb in both cases by the emission of a α particle. Subsequent β decay by ^{214}Pb leads to the formation of ^{214}Po, another α emitter. The α-particles from radon and its daughters have energies of 5.49-7.69 MeV and these are mostly stopped by clothes or by the thicker superficial layers of the skin. Consequently the risk associated with radon via external irradiation will be minimal to all body tissue with the possible exception of skin. Only if it is present internally will any significant dose arise in internal tissues. Radon is found in varying levels in the environment and is present at particularly high concentrations in areas where fissured granite rock is abundant.

Because of its prevalence and the possible risk associated with an α-particle emitter, attention has turned to addressing the possible risk associated with radon (NCRP 1984, National Research Council, BEIR IV 1988, BEIR VI 1998). According to the BEIR IV report the "evaluation of the lung-cancer risk associated with radon daughters was the most challenging faced by the committee." However, epidemiological studies of the risks associated with radon have serious limitations. Firstly, lung cancer has a relatively high incidence in the population as a whole and so any additional cases attributable to radon must be detectable against this background. Secondly in the case of additional cases detected, the large number of other causes of lung cancer must be considered. Because of these two factors, large studies are required to remove the possibility of

natural statistical fluctuations in case numbers and the influence of other cancer causing factors. Thirdly, since cancer is a disease that takes a long time to develop, any study will need to be undertaken over very long time-scales. Fourthly, because the most robust epidemiological data are from high exposures to miner cohorts long extrapolations are required for application of the risk to common public exposures. Because of these limitations, attention has turned to the possibility of developing mechanistic models based on computer simulations to guide the radiation risk estimation. However, the reliability of such simulations must be tested against experimentally determined benchmarks. Such results also give an indication, in the case of disparity between simulation and experiment of those areas within the simulation that are unsatisfactory. Thus, it is necessary to generate reliable experimental benchmarks that will test any simulation, but are practical to undertake. If there is good agreement between simulation and experiment, any subsequent predictions by the extrapolation of simulations to low dose, low dose rate scenarios that are generally not experimentally feasible, may be treated with a reasonable level of confidence.

1.3. Interaction of Radiation with Matter

Ionising radiation may be sub-divided into two distinct types; electromagnetic and particulate. The interactions with matter undergone by these two forms of radiation are distinct and need to be considered separately.

1.3.1. Electromagnetic

There are three distinct types of photon interaction; photoelectric, Compton scattering and pair production. The total probability per unit length μ for removal of a photon incident upon a material is known as the total linear attenuation coefficient. It is equal to the sum of the respective probability coefficients for photoelectric absorption (τ), Compton scattering (σ) and pair production (κ):

$$\mu=\tau+\sigma+\kappa$$

The relative importance of these three processes with photon energy and the atomic mass Z of the absorber is illustrated in figure 1.1. The fractional loss in intensity (I) in crossing any thickness dx of material is

$$dI/I= -\mu dx \quad \text{and thus} \quad I=I_0e^{-\mu t} \text{ in passing through a thickness t}$$

The mass attenuation coefficient is a more commonly used term and is equal to μ/ρ where ρ represents the density of the medium. A typical mass attenuation coefficient for a target such as aluminium is illustrated in figure 1.2.

1.3.1.1. Photoelectric Effect

In this case a photon is completely absorbed by an atom and one of the atomic electrons, subsequently known as a photoelectron, is released. The kinetic energy of the electron (KE_e) is given by;

$$KE_e=E_\gamma-B_e$$

Where E_γ represents the energy of the incoming photon and B_e the binding energy of the electron. The photoelectric effect is most significant for photons below 100 keV increasing rapidly with atomic number Z of the absorbing material (approximately Z^4) and decreasing rapidly with photon energy (approximately E_γ^{-3}). Additionally there are discontinuous absorption probabilities corresponding to binding energies of particular electronic shells. For example, if the binding energy of a K-shell electron in a particular atom is 50 keV then photons with energy less than this value cannot release K-shell photoelectrons. When photon energy is increased above 50 keV the availability of the K-shell electrons to participate in the photoelectric absorption process leads to a sudden increase in the probability of absorption (referred to as the cross section), known as the K edge. Figure 1.3 shows a typical photoabsorption cross section for DNA (Hieda 1994).

In addition to the photoelectron, the photoelectric interaction also creates an ionised atom with a vacancy present in one of its bound shells, which if the γ-ray is of sufficient energy will probably arise in the K-shell. This vacancy will be filled via the capture of a free electron and/or rearrangement of the other electrons present in the outer shells of the atom. As a result, one or more characteristic X-rays may also be generated. In a proportion of the cases, an Auger electron is emitted instead of X-rays as a mechanism to remove the excitation energy.

1.3.1.2. Compton Scattering

Compton scattering is predominantly an outer shell process whereby a photon scatters from a nearly free atomic electron transferring a variable amount of energy. The photon is scattered through angles with varying cross section probability and transfers an

amount of energy dependent upon the scattering angle. The energy of the scattered photon is given by

$h\nu' = h\nu/\{1+h\nu(1-\cos\theta)/m_0c^2\}$

where θ represents the scattering angle, m_0 the rest mass of an electron and $h\nu$ and $h\nu'$ the energy of the photon before and after scattering respectively.

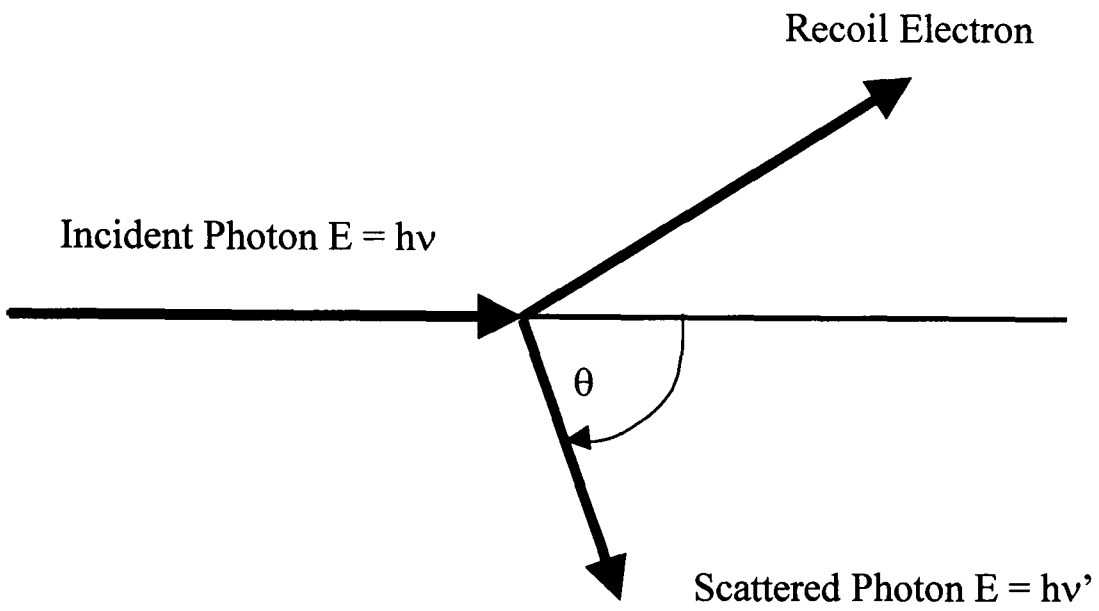

1.3.1.3. Pair Production

Pair production is the process where a photon creates an electron-positron pair.

$$E_\gamma = T^+ + 2m_ec^2 + T^-$$

where T^+ and T^- represent the kinetic energies of the electron and positron respectively. As a result of the $2m_ec^2$ term for the rest masses of the two particles created, there is a threshold for pair production of 1.022 MeV below which the process cannot take place. As a result the process is important only for photons of high energy.

1.3.2. Charged Particles

1.3.2.1. Linear Stopping Power/Specific Energy Loss

In a given absorber, the loss of energy (E) per unit path length (x) is given by

$S = -dE/dx$ where S is defined as the linear stopping power.

For particles with a constant charge, the value of S increases as the particle velocity decreases as given by the Bethe formula.

$$-dE/dx = \frac{4\pi e^4 z^2 NB}{m_0 v^2}$$

where $B = Z\{\ln(2m_0v^2/I) - \ln(1-v^2/c^2) - v^2/c^2\}$ which for non-relativistic particles reduces to $Z\{\ln(2m_0v^2/I)\}$

where v and z are the velocity and charge of the primary particle, N and Z are the number density and atomic number of the absorber atoms and m_0 and e are the rest mass and charge of the electron respectively.

As the expression B varies slowly with particle energy, dE/dx effectively varies inversely with particle energy. For charged particles, dE/dx is proportional to z^2. Thus, for example, an α-particle loses energy at four times the rate of a proton of the same velocity.

The Bethe formula however breaks down at low particle energies when a positively charged particle, such as an α-particle picks up electrons from the absorber, reducing its effective charge. At the end of the track the particle becomes a neutral atom.

1.3.2.2. α-particles

Under normal radioactive decay processes α particles travel at a speed where relativistic corrections may be neglected. They interact with matter primarily via the Coulomb force interacting with the electrons of the matter they traverse. It is also possible for interactions with nuclei through Rutherford scattering, although this is rare. If only the Coulombic interaction is considered, the proximity of the encounter may be sufficient to cause either electronic excitation within the absorber or ionisation. In either case, energy is transferred to an electron in the absorber resulting in a loss of energy from the α particle. The maximum energy transferred in any one interaction is approximately $1/2000^{th}$ of the alpha particle energy, so that an α particle requires many interactions to bring it to rest. At any given time the particle interacts with a large number of electrons simultaneously resulting in a continuous decrease in its velocity until it stops. Due to the large momentum and as interactions occur in all directions simultaneously, there is little deviation in the direction of the particle track. It is only at the track end when the particle velocity is very slow that single interactions may cause path deviation. In the event of a particularly close encounter, an electron may have sufficient energy transferred to it for it to go on and create further ionisations and excitations. Such electrons are known as delta rays (δ-rays) and represent an indirect way by which the energy of a charged particle may be transferred to an absorbing medium. δ-rays represent a mechanism by which energy may be deposited some distance from the main radiation track.

1.3.2.3. Electrons

In comparison to heavily charged particles such as α particles, fast electrons lose less energy per unit track length. As their mass is equal to that of the orbital electrons with which they interact, a much larger fraction of their energy may be lost in a single encounter leading to greater deviation from the original path direction. Additionally, electron-nuclear interactions may result in abrupt changes in direction. Due to these sharp rapid deviations, energy is also lost via radiative processes known as Bremsstrahlung. Thus the linear stopping power for electrons is the sum of the collisional and radiative losses. Generally radiative losses are significant only in absorber materials of high atomic number and for high electron energies.

1.4. Interaction of Radiation with Water

The interactions of radiation with water and the time-scale of events can be summarised as below (Kupperman 1967, Buxton 1987, Farhataziz and Rogers 1987, Bensasson *et al.* 1993).

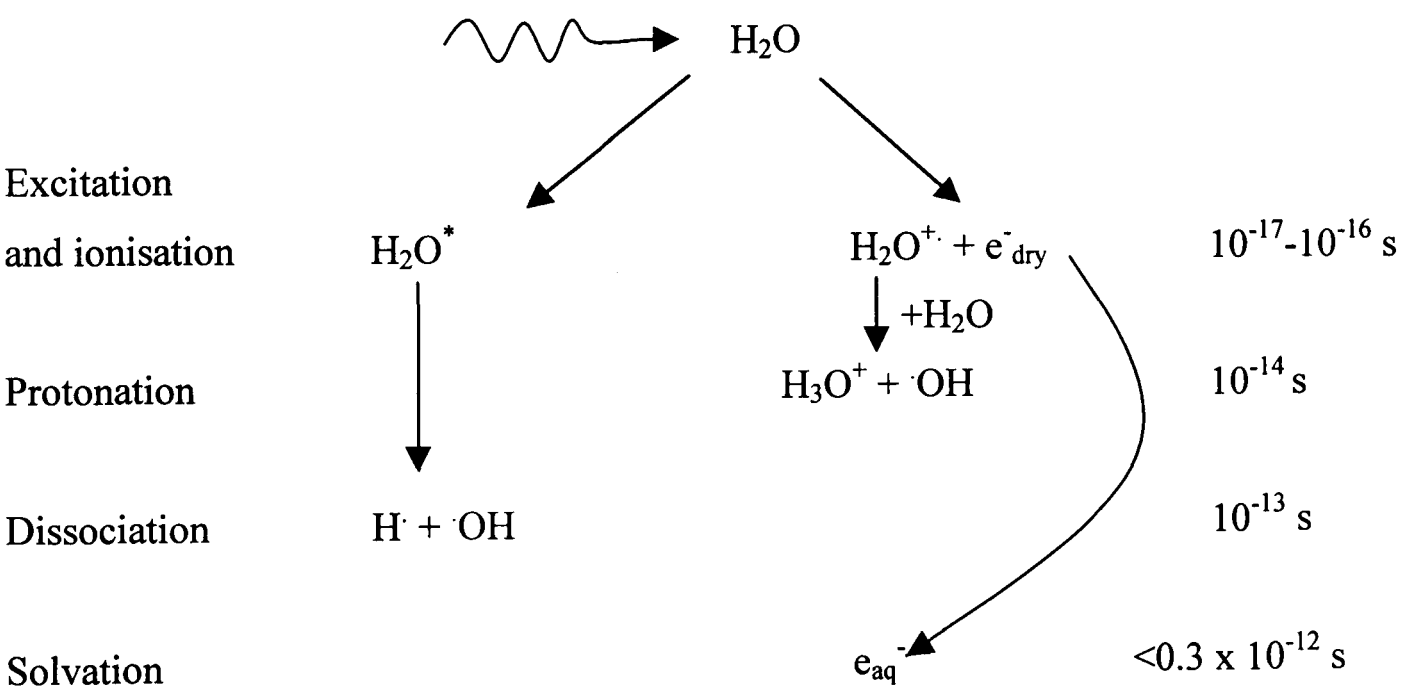

All of these processes are practically diffusion controlled and radicals that escape intra-track recombination events may subsequently interact with any radical scavengers present within the solution. The scavenging capacity of a solution is defined as the concentration of the scavenger within the solution multiplied by the reaction rate constant of the scavenger with the radical of interest (Buxton *et al.* 1988). The rate constants of OH radicals, which are considered specifically important in inducing DNA damage, with two common scavengers, Tris and ethanol are 1.5×10^9 and 1.9×10^9 mol^{-1} dm^3 s^{-1} respectively (Buxton *et al.* 1988).

1.5. Track Structure and LET

Linear Energy Transfer (LET) is the average energy transferred per unit length of charged particles of a given type and energy i.e. for the charged particle, the LET in a medium is given by dE/dl, where dE is the average energy locally imparted to the medium by the particle in traversing a distance dl. However, a particle traversing a medium continually loses energy, and hence its LET continually varies. In addition, at the microscopic level the distribution of energy deposition is far from uniform (see figure 1.4) and the value of LET gives no measure of this variation. Subsequently the concept of LET is only of use as a broad indication of some of the qualities associated with a particular radiation. It is common to describe neutral radiations as having a LET equivalent to the mean LET of the secondary particles from their interactions in the medium. For γ–rays and X-rays these secondary particles are mostly electrons and for neutrons they are mostly recoil protons and nuclear fragments. The assignment of mean values obscures the fact that the secondary particles cover a wide spectrum of LETs Typical values for ^{60}Co γ-rays and orthovoltage X-rays are between 0.3 and 2 keV μm^{-1}, for natural α-particles ~ 100 keV μm^{-1} and for heavier charged particles up to about 2000 keV μm^{-1} or even 16,000 keV μm^{-1} for slow uranium ions.

The yield of species produced following the passage of a radiation track depends both on the ionisation density of the radiation and the time at which the species present are sampled. Figure 1.5 illustrates an example of the spatial and temporal distribution of radiation-induced species produced in water by a 10 keV electron track (Terrissol and Beaudré 1990). Initially the distribution of species generated by the passage of a radiation track is very non-homogeneous. However with increasing time the species may interact with one another or diffuse to eventually give an approximately

homogeneous distribution. From pulse radiolysis determination of the yields of e^-_{aq} and hydroxyl radicals, the majority of intra-track events involving water radicals are complete within 10^{-6} s (Jonah *et al.* 1973, 1976) (figure 1.6). Simulations also predict that the majority of intra-track radical-radical interactions in water occur at times $<10^{-6}$s (Turner *et al.* 1988), after which the remaining radicals may be regarded as homogeneously distributed (figure 1.7) (Pimblott and LaVerne 1997, 1998). The likelihood of intra-track radical-radical interactions depends upon the distance between sites of radical formation i.e. the ionising density of the radiation track which is dependent on the type and energy of the radiation (Magee and Chatterjee 1978, Yamaguchi 1989, Hill and Smith 1994, Hieda *et al.* 1994, Watanabe *et al.* 1995) (see track schematic figure 1.8). For instance, decreases in photon or electron energy result in corresponding increases in ionisation density. It is anticipated that densely ionising radiations result in a large number of intra-track radical-radical events since the average distance between sites of radical formation is small. In contrast, a ^{60}Co γ-ray radiation track gives relatively smaller numbers of intra-track radical-radical events due to its sparsely ionising nature and the proportionally larger average distance between sites of radical formation. These differences are schematically shown in figure 1.8, parts 1 and 2. As ionising density increases a greater number of intra-track radical-radical events occur. In table 1.1 the radiation chemical yields, expressed as G values, are presented for species present at $> 10^{-6}$ s for the radiolysis of water using different LET radiation. As the LET of the radiation increases from ^{60}Co γ-rays to 32 MeV α-particles to 12 MeV α-particles, a corresponding decrease occurs in the yields of escaping species. This dependence on radiation quality is consistent with increased ionisation density, leading to an increased probability of intra-track recombination and therefore decreased yields of homogeneously distributed species. For the dependence of the radical yield on the photon energy of the radiation, it has been postulated from simulations (Magee and Chatterjee 1978, 1980, Yamaguchi 1989, Hieda *et al.* 1994, Hill and Smith 1994, Watanabe *et al.* 1995) that the yield of hydroxyl radicals, generated from radiation tracks in water and which escape intra-track recombination events to become homogeneously distributed, is dependent upon the energy of the photon. Simulations have postulated that the yield of homogeneously distributed hydroxyl radicals decreases as the energy of the incident photon is reduced but that with very low energy photons, < 1 keV, the yield increases (Magee and Chatterjee 1978, Yamaguchi 1989,

Terrissol and Beaudré 1990, Hill and Smith 1994). In addition to the average distance between the sites of radical formation, another factor which influences the number of intra-track radical-radical events is the absolute number of radicals generated. This is illustrated in figure 1.8, part 3. For instance with extremely low energy photons small numbers of radicals are generated. Thus, although the average distance between adjacent radicals may be very small, any one radical has few other radicals in the vicinity. Hence, a small solid angle exists around a radical within which diffusion in that direction may result in interaction with another radical compared with the higher energy track scenario presented for α-particle radiation. To date few studies have investigated experimentally the dependence of yield of water radicals on photon energy and those which have, have examined the yield of ferric ions (Fricke dosimetry) which decreases with decreasing photon energy in the range 1MeV to 2 keV (Freyer *et al.* 1989, Watanabe *et al.* 1995, Yamaguchi 1997).

At times > 10^{-7} s the OH radicals are considered to be homogeneously distributed. The effect of radical scavengers is to limit the mean diffusion distance of species from their site of formation; in effect limiting their potential to become homogeneously distributed. Hence, by varying the concentration of the scavengers it is possible to sample effectively the distribution of the species produced by the radiation at different times. This is illustrated in figure 1.7 which effectively reflects figure 1.6 where higher scavenging capacities result in earlier sampling times and thus greater yields of OH radicals for high energy electron irradiation since the scavengers compete with intra-track radical-radical reactions. At low scavenging capacities radicals potentially diffuse large distances and hence become homogeneously distributed with radical yields reaching a plateau. Therefore, only homogeneously distributed radicals interact with the scavenger in competition with radical-radical interactions.

1.6. DNA Structure and Damage Formation

1.6.1. Structure of DNA

DNA consists of a ladder wrapped helically around a central axis, with the two rails of the ladder made up of alternating deoxyribose sugar rings and phosphate groups. The rungs of the ladder consist of purine-pyrimidine base pairs forming a double helix as

illustrated in figure 1.9. These bases are either purines (adenine or guanine) or pyrimidines (cytosine or thymine) with the complementary bases adenine and thymine always bonding via two hydrogen bonds and guanine and cytosine always bonding via three hydrogen bonds. The order of these bases on the DNA strand is the basis of genetic information.

The points of attachment of base pairs do not lie directly opposite each other, which dictates the geometry of the DNA double helix. The edge of the base pairs, along which the angle between attachments is less than 180^0, is called the minor groove edge, whereas the one forming an angle greater than 180^0 is known as the major groove edge. When base pairs are stacked into a helix, the sugar phosphate backbones build the walls of the minor and major grooves which wind around the helix with the base edges forming the floors of the grooves.

There are two fundamental types of DNA conformation known as A DNA and B DNA. The two forms differ mainly in the positioning of the base pairs around the helix axis and in the angle of inclination of the bases with respect to the axis. In B DNA, the base pairs are stacked almost perpendicular to the helix axis with an average of 10 base pairs per turn of the helix and a spacing of 3.4 Å between bases. In A DNA the angle of inclination of the base pairs from the perpendicular is between 13^0 and 19^0 with about 11 base pairs per turn and an average distance between base pairs of 2.9 Å.

The form that DNA adopts is dependent upon humidity and therefore the water content of the DNA (for review see Saenger 1988). The B configuration is stable at a relative humidities of approximately 80 % and above, whereas the A configuration is adopted at humidities < 80 %. DNA does not exist as an isolated molecule. Instead, a large number of water molecules are bound to it. The bound water is not homogeneously distributed around the DNA (see figure 1.10). At less than 65 % relative humidity, corresponding to Γ = 5-6, where Γ is defined as the number of moles of water per mole of nucleotide, hydration occurs at the oxygens of the phosphate group. Hydration of functional amino, imino and keto groups of the bases occurs above 65 % relative humidity with the addition of 8-9 more water molecules. At relative humidities greater than 80 %, the primary hydration shell is complete when Γ = 20. Further increases in hydration are accompanied by swelling of the sample. Of these 20 water molecules, 11 or 12 are in direct contact with the DNA forming the inner, primary hydration shell which is impermeable to cations (Tunis and Hearst 1968). Upon cooling to significantly

below 0^0 C, the water of hydration of the B-form does not freeze into an ice like state (Falk *et al.* 1970). The remaining 8 or 9 water molecules comprise the outer, primary hydration shell. A second hydration shell exists, which although indistinguishable from bulk water in terms of permeability to cations and ability to form ice, has slightly different properties to those of bulk water (Wolf and Hanlon 1975).

1.6.2. DNA Damage

1.6.2.1. Radical Generated DNA Damage

Ionising radiation induces damage in DNA via the direct and the indirect effects. In the direct effect, the radiation track overlays the DNA and its associated bound water and interacts directly, to deposit energy, producing ionisations and excitations (see section 1.3). Alternatively, in the indirect effect, damage arises as a result of energy being deposited to molecules in the neighbourhood of DNA, giving rise to radicals which subsequently diffuse to and interact with DNA as shown in figure 1.11 using the OH radical as an example. Of all the radicals generated in water (see section 1.4) it is widely accepted that the OH radical is the principal species which causes DNA strand breaks and other biologically relevant DNA damage (Chapman *et al.* 1973, Roots and Okada 1975, von Sonntag 1987, O'Neill and Fielden 1993). The OH radical interacts mainly by addition to the nucleobases or by H-atom abstraction from the sugar moiety examples of which are illustrated in figure 1.12.

For irradiation of DNA in aqueous solution the contribution of diffusible radicals relative to directly produced DNA radicals is determined by the radical scavenging conditions of the solution (Krisch *et al.* 1991, Milligan *et al.* 1993, 1994, 1996 a and b, Jones *et al.* 1994). The scavenging capacity of a solution is defined as the concentration of the scavenger within the solution multiplied by the reaction constant of the scavenger with the radical of interest (Buxton *et al.* 1988). Scavengers which react with OH radicals, effectively remove them as potential DNA damaging agents to an extent dependent upon the scavenger concentration. Therefore, for a given radiation dose the yield of OH radicals which interact with the DNA decreases with increasing scavenger concentration leading to a reduction in the amount of DNA damage (Krisch *et al.* 1991, Milligan *et al.* 1993, 1994, 1996a and b). Effectively, the concentration of scavengers dictates the radius around a DNA target within which a radical, if formed, may diffuse and cause DNA damage (see figure 1.11). As the concentration of the scavenging

solution increases, mean radical diffusion distances decrease, resulting in fewer radicals at a given radiation dose interacting with the DNA. Consequently, the proportion of damage attributable to the direct deposition of energy will increase relative to the proportion of water radical mediated indirect damage. At scavenger concentrations representative of those found within a cell, the mean diffusion distances of OH radicals is approximately 4-6 nm (Roots and Okada 1975, Chapman and Gillespie 1981). At these scavenging capacities the relative contribution of indirect DNA damage determined for cells varies from about 60 % to 30 % for irradiation with low and high LET respectively (Chapman *et al.* 1979, Roots *et al.* 1985, deLara *et al.* 1995).

1.6.2.2. Types of DNA Damage

Damage to DNA falls into a number of categories, dependent upon the site of damage formation. The types and forms of DNA interaction have been summarised in a number of reviews (Ward 1981, 1988, Hutchinson 1985, von Sonntag 1987, O'Neill and Fielden 1993, Breen and Murphy 1995, Pogozelski and Tullius 1998) and the rate constants of reactions of e^-_{aq}, OH radicals and H radicals with DNA and its constituents are well documented (Anbar *et al.* 1973, 1975, Ross 1975, Farhataziz and Ross 1977, Deeble and von Sonntag 1985, Buxton *et al.* 1988). A number of damage types such as modified sugars and crosslinks may be formed but single and double strand breaks (ssb and dsb) have been the main focus for investigation although some studies have examined the induction of base damage (bd).

Strand Breaks

A single strand break, which involves cleavage of the phosphate diester bond between the phosphate and the deoxyribose, leads to loss of base and strand separation. A double strand break results from the breakage of both DNA strands within a given separation of base pairs. The exact value for base pair separation depends upon the ionic strength of the environment around the DNA. Experimentally this value has been shown to vary from 34 bp to 3 bp as the ionic strength varies from 10^{-3} mol dm^{-3} to 0.1 mol dm^{-3} (Freifelder and Trumbo 1969, van der Schans 1978, van Touw *et al.* 1985, von Sonntag 1987). Simulations of radiation induced DNA dsb have used a value of 10 base pairs (Nikjoo *et al.* 1994a).

The majority of strand break experiments on DNA in solution have focused on the use of low LET radiation. However, some studies have utilised α-particles, neutrons, heavy

ions and low energy photons to assess the role of radiation characteristics on damage yields. To assess the importance of radiation induced strand breaks, plasmid DNA, minichromosomes and cells have all been examined and the relative abundance of ssb, dsb and more complex damage determined.

For low LET radiation in the presence of oxygen, the yield of DNA strand breaks in aqueous solution irradiated by low LET radiation depends upon the competition between DNA and any scavenger present for the OH radical (see section 1.6.2.1) (Krisch *et al.* 1991, Udovičić *et al.* 1991, Milligan *et al.* 1993). There is strong evidence that the reaction between e^-_{aq} and DNA does don't contribute to ssb formation (Jones and O'Neill 1991). The yields of both ssb and dsb induced by γ-ray radiation decrease with increasing scavenging capacity and as such, the kinetics of the reaction between DNA and the OH radical have been examined (Grossweiner 1978, Udovičić *et al.* 1991, Milligan *et al.* 1996c). It has been found that due to the non-homogeneous energy deposition associated with radiation and the subsequent non-homogeneous production of OH radicals (see figure 1.5) homogeneous competition kinetics may not be applicable when the scavenger concentration is high. Milligan *et al.* (1993, 1996c), irradiated plasmid and SV40 DNA with γ-rays and showed that simple competition kinetics apply for DNA concentrations varying between 10 and 1000 μg/ml, at low scavenging capacities where the diffusion distance of OH radicals > the length of the DNA, so that the log of the ssb yield is proportional to the log of DNA concentration. However, at higher concentrations of DNA, the ssb yield approaches a plateau value and is not adequately described by simple competition kinetics.

Mechanisms for the generation of strand breaks and the subsequent influence of radiation quality and scavenging capacity on their yields has been the focus of a number of studies with strand break yields decreasing with increasing scavenging capacity. The lifetime of the OH radical is proportional to the reciprocal of the scavenging capacity and therefore as the scavenging capacity increases there is a corresponding decrease in the OH radical lifetime (Roots and Okada 1975). Single strand break induction by γ-ray irradiation of SV40 viral DNA (Krisch *et al.* 1991, Ayene *et al.* 1995) is linear with dose i.e. it represents a one-hit response over a scavenging capacity range from 10^5 to 10^{10} s^{-1}. However, dsb induction shifts from a mainly quadratic (two-hit) dose response at very low scavenger capacities to an almost pure linear dose response at scavenging capacities > 10^7 s^{-1}. At low scavenging

capacities, it was hypothesised that the majority of dsbs are due to two independent OH radicals from different tracks causing ssbs, one on each strand, sufficiently close together that they give rise to a dsb. At higher scavenging capacities (> 10^7 s^{-1}) dsbs from single track events are hypothesised to constitute the main pathway involving the formation of multiple DNA damages in close proximity. The linear dose response for dsb induction at high scavenging capacities may be interpreted in terms of the hypothesis of Goodhead *et al.* (1980) and Ward (1981) where one-hit dsbs arise as a result of local clusters of OH radicals and directly produced radicals in DNA from single track energy deposition events near to the DNA (Krisch *et al.* 1991, Jones *et al.* 1993). An alternative mechanism to explain a linear dose dependence for dsb induction was proposed by Siddiqi and Bothe (1987) whereby a single OH may give rise to a dsb. This mechanism involves an OH radical initially attacking a DNA strand to induce a ssb and subsequently the radical site becomes located on an adjacent sugar moiety. The secondary radical is then transferred to the complementary DNA strand, where it induces a second ssb, resulting in a dsb. As the scavenger capacity is increased it is suggested that this radical transfer mechanism for dsb formation is greater than that resulting from the direct effect up to scavenging capacities of approximately 10^9 s^{-1} (Siddiqi and Bothe 1987).

In addition to experimental assessment, the mechanisms for dsb formation have also been examined by theoretical analysis (Xapos and Pogozelski 1996, Pogozelski *et al.* 1999). It was considered that dsbs formed in proportion to dose, referred to as αdsbs, may be induced via three processes (Spotheim-Maurizot *et al.* 1990); 1) The action of a single OH radical which results in a ssb and the transfer of the radical site to the complementary strand causing the formation of a second strand break as described above (Siddiqi and Bothe 1987) 2) Two or more OH radicals formed by a single track event, and 3) Energy deposits from a single track occuring within the DNA or its associated bound water (Goodhead 1994, Ward 1994). Mechanisms 1) and 2) will be dependent upon scavenging conditions whereas for 3) the direct energy depositions will be independent of scavenger concentration but hybrid dsb, whereby one strand is broken due to a direct energy deposit and the complementary strand by a diffusible radical formed within the cluster, will have a dependence on scavenging capacity. Fitting of experimental data for the yields of DNA strand breaks (Spotheim-Maurizot *et al.* 1990, Krisch *et al.* 1991, Taucher-Scholz *et al.* 1992, Jones *et al.* 1993, Klimczak *et*

al. 1993) obtained under variable scavenging conditions and utilising different radiations, to a mechanistic model (as distinct from Monte Carlo modelling) (Xapos and Pogozelski 1996) leads to predictions of the relative importance of the different mechanisms for dsb formation. For γ-ray irradiations at low scavenger concentrations, clustered damage sites are predicted to contribute little to the total number of αdsbs and therefore all αdsbs must result from the radical transfer mechanism. At scavenger capacities greater than 10^8 s^{-1} dsbs arising from clustered damage sites become significant, increasing in importance with increasing scavenging capacity up to values of 10^{10} s^{-1} where all αdsbs will result from clustered damage sites. For high LET radiation, even at low scavenger levels the majority of αdsbs are as a result of clustered damage sites. At a scavenging capacity of $4x10^7$ s^{-1} for α-particle irradiation, over 80% of αdsbs are of this form. However at these low scavenger values, the majority of the clustered damage sites partly result from OH radicals interacting with DNA forming hybrid dsb and hence are potentially scavengeable. As the scavenger concentration increases so too does the proportion of non-scavengable αdsbs contributing to clustered damage sites. At a scavenging capacity < 10^8 s^{-1} Klimczak *et al.* (1993) proposed that the majority of αdsb are produced from a single OH radical since the yield of ssb and αdsb are linearly dependent upon scavenging capacity. At higher scavenger capacities the yield of αdsb is no longer linearly dependent upon scavenging capacity, indicative of a non-scavengable component contributing to yields of αdsb i.e. as a result of directly produced complex damage. In contrast, a number of studies (Prise *et al.* 1993, 1999a, Milligan *et al.* 1995) examining the chemical repair of DNA strand breaks, using thiols as opposed to biochemical repair using enzymes, have concluded that two independently produced radicals are the precursors to the majority of dsbs. Such a finding argues against a major contribution by a single radical mechanism involving inter-strand radical transfer but is consistent with dsbs being formed at the sites of clustered energy depositions.

Irrespective of the radiation, the yields of ssb and dsb decrease with increasing scavenging capacity (Krisch *et al.* 1991, Milligan *et al.* 1993, 1996a and b, Milligan and Ward 1994). In addition, at a constant scavenging capacity, the yields of both ssb and dsb are found to decrease with increasing ionisation density of the radiation (Spotheim-Maurizot *et al.* 1990, Jones *et al.* 1993, Peak *et al.* 1995, Stankus *et al.* 1995, Hodgkins *et al.* 1996b, Milligan *et al.* 1996a). The role of ionisation density in

determining the amount of DNA damage has been assessed by a number of groups by comparing the relative yields of ssb and dsb over a range of scavenging capacities following γ-ray and α-particle irradiation. From irradiations of SV40, it was concluded that the yields of ssb following irradiation with ^{4}He ions (α-particles) are about a factor of 10 less than that following ^{137}Cs γ-ray irradiation (Jones *et al.* 1993). The yield of ssb induced by α-particle irradiation decreases with increasing scavenging capacity, however, with a less steep dependence than that exhibited following γ-ray irradiation. The ratio of ssb:dsb is considered to be an indicator of the relative contribution of isolated damage characterised by a ssb to more complex damage as represented by a dsb induced within the DNA. Following ^{4}He ion irradiation the ratio of ssb:dsb remains essentially constant over the scavenging capacity employed ($6.6x10^{6}$ s^{-1} to $1.3x10^{10}$ s^{-1}) with a value of approximately 10:1 whereas following γ-ray irradiation the ratio of ssb:dsb varies between approximately 60 and 30 over the same scavenging range (Jones *et al.* 1993). Using SV40 molecules and plasmid DNA, the ratio of ssb:dsb for γ-ray irradiation has been determined to vary from approximately 150 to 40 as the scavenging capacity varies from $3x10^{6}$ s^{-1} to $1.5x10^{8}$ s^{-1} (Krisch *et al.* 1991), from 150:1 to 60:1 over a scavenging capacity range of $2x10^{8}$ s^{-1} to $6x10^{9}$ s^{-1} (Klimczak *et al.* 1993) and from 70:1 to 40:1 over a scavenging capacity range of $1.5x10^{7}$ to $3x10^{8}$ s^{-1} (Hodgkins *et al.* 1996a). One study indicated that the ratio of ssb:dsb is equal to approximately 100:1 over a scavenging capacity range of $6.6x10^{6}$ s^{-1} to $6.6x10^{9}$ s^{-1} (Milligan *et al.* 1996a). For α-particle irradiation, the ratios of ssb:dsb are approximately constant with a value of 13:1 over a scavenging capacity range of $1.5x10^{7}$ to $3x10^{8}$ s^{-1} (Hodgkins *et al.* 1996b) and 25:1 to 15:1 over a scavenging range of $6.6x10^{6}$ s^{-1} to $6.6x10^{9}$ s^{-1} (Milligan *et al.* 1996a). In summary the ratios of ssb:dsb decrease from approximately 150:1 at low scavenging capacities ($1x10^{6}$ s^{-1}) to 20-30:1 at high scavenging capacities equivalent to cell mimetic values ($3x10^{8}$ s^{-1}) following γ-ray irradiation. However following α-particle irradiation, similar decreases in the ratios of ssb:dsb with increasing scavenging capacities are not seen where the ratio of ssb:dsb is not strongly dependent upon the scavenging capacity.

DNA damage yields induced in plasmid DNA in aqueous solution following neutron irradiation, a high LET radiation source, relative to those induced by ^{60}Co γ-rays have been undertaken for various neutron energies. Following exposure to 0.85 MeV neutrons, relative yields of ssb and dsb are 0.20 and 0.68 of those following γ-ray

irradiation at low scavenger concentrations (Peak *et al.* 1995). At high scavenging capacities, yields of ssb induced by γ-rays are reduced by about a factor of 7 relative to those at low scavenging capacities whereas the yields of ssb and dsb induced by neutrons are reduced by a factor of approximately 2.5. Fast neutrons with a flat energy spectrum from 34 MeV to low energies are half as efficient as ^{60}Co γ-rays at inducing ssb in plasmid DNA at low scavenger concentrations (50 mmol dm^{-3} potassium phosphate) but 1.5 times more efficient at inducing dsbs (Spotheim-Maurizot *et al.* 1990) leading to a ratio of ssb:dsb of 56:1 and 20:1 for photons and neutrons respectively. At low scavenging capacities ($1.5x10^7$ s^{-1}), irradiation with fission neutrons with an LET approximately 30 times that of ^{60}Co γ-rays (Stankus *et al.* 1995) leads to plasmid yields of ssb approximately one third of those induced by γ-ray irradiation. It was postulated that the majority of damage induced under these conditions results from the indirect effect of radiation leading to an estimate of the G-value for OH radicals of 0.088 μmol J^{-1}. Therefore generally, the yields of ssb and dsb induced by neutrons are less than those induced by γ-ray radiation.

The effectiveness of high LET heavy ions in inducing strand breaks in DNA has been undertaken to evaluate the influence of track ionisation density in cells and DNA in solution (Roots *et al.* 1985, Heilmann *et al.* 1993, 1995, Löbrich *et al.* 1996, Nygren and Ahnström 1996) and SV40 DNA (Stanton *et al.* 1993, Taucher-Scholz and Kraft 1999). Irradiations of SV40 DNA at a scavenging capacity of $1.5x10^7$ s^{-1} have been carried out for a wide range of ion species from helium to uranium with LET values varying from 5 to 16,000 keV/μm (Taucher-Scholz and Kraft 1999). Up to 40 keV/μm, the total energy deposition determines the cross section for ssbs and up to 400 keV μm^{-1} the cross section for dsb. At higher LET values the cross sections are essentially independent of LET but with individual responses observed for the different particles. For each ion species, this LET independence occurs at a lower LET for ssb than that for dsb resulting in a decrease in the ratio of ssb:dsb from 70:1 for X–rays to 6:1 for particles with a LET value of 500 keV/μm. This change in the ratio of ssb:dsb is indicative of the influence of track recombination events (see section 1.5) due to a high local deposition of energy events which favour the formation of dsbs. For dsb induced by high LET radiation, the increased ionisation density leads to very high local energy depositions giving rise to clustered dsb damage i.e. more than one dsb induced per track. It has been shown in cellular systems (Rydberg 1996, Newman *et al.* 1997) and

via calculations (Chatterjee and Holley 1993, Hutchinson 1996) that small DNA fragments are produced resulting from a multiple number of dsb sites in close vicinity from a single track. These close related dsb are only detected as single dsb by gel electrophoresis.

Rather than just determining the relative proportion of dsb, that may be classified as a simple form of complex damage, from the ratio of ssb:dsb, the presence of complex damage may be assessed by examining the potential repairability of the damage. Reduced extent of repairability of damage sites has been interpreted as resulting from an increased complexity of damage (see section 1.8). The assumption is supported by the decreased efficiency of repair enzymes to excise damage with specifically synthesised complex damage sites (Chaudrey and Weinfeld 1995, Harrison *et al.* 1998, David-Cardonnier *et al.* 2000). The ability of cell extracts to rejoin radiation-induced ssb in plasmid DNA has been used as an indicator of the presence of complex ssb damage (Hodgkins *et al.* 1996a and b, Cunniffe and O'Neill 1999). Following γ-ray and α-particle irradiation, plasmid DNA was incubated for 3 h with cell free extracts and the yields of ssb determined. It was assumed that simple ssb are readily rejoined by the extract whereas those ssb that are not rejoined reflect the presence of associated damage within a few base pairs. At low scavenging capacities, the majority of ssb induced by γ-ray irradiation are rejoined, whereas at high scavenging capacities a greatly reduced proportion of ssb are rejoined. For α-particle irradiation under equivalent scavenging capacities the majority of ssb remain un-rejoined. It was also found that some ssb are converted into additional dsbs following the addition of cell extracts. At cellular mimetic scavenging conditions 50% of α-particle induced ssb are converted into dsb, in contrast to only 12% conversion of ssb induced by γ-ray irradiation. Comparisons between the rejoining of ssb induced by γ-ray and Al_K ultrasoft X-ray (USX) irradiation by cell extracts also illustrate a reduced degree of repair for ssb induced by more densely ionising Al_K USX irradiation (Cunniffe and O'Neill 1999). It was proposed that the extent of rejoining of ssb decreases with increased complexity of the DNA ssb, predicted from the ionising density of the radiation and the changes in scavenging capacity.

Irradiations of plasmid DNA in the presence of N-(2-thioethyl)-1, 3-diaminopropane (WR-1065), which reacts rapidly with radicals located on DNA resulting in chemical repair leads to a reduction in the induction of strand breaks. The extent of ssb induction

for both γ-ray and α-particle irradiation is linearly dependent upon the concentration of WR-1065 (Milligan *et al.* 1996a). Since the gradient of the reduction factor on concentration is greater for low LET γ-ray irradiation it was suggested that strand breaks arising with higher LET radiation are less repairable by thiols, due to the breaks arising from a greater number of radicals within a cluster for high LET. The conclusion therefore, is that radical clustering on the DNA is repaired less efficiently by thiols than are damage sites induced by single radical species (Prise *et al.* 1994, Milligan *et al.* 1997).

The difference in DNA damage complexity associated with radiation quality is also obtained from cellular studies. Comparisons of the extent of rejoining of cellular DNA dsb induced by ^{60}Co γ-rays or ^{238}Pu α-particles followed by 3 h repair shows that over 90% of dsb are rejoined in the γ-ray exposed samples compared with only 30-50% for those exposed to α-particles (Blöcher 1988, Jenner *et al.* 1992, 1993, Prise *et al.* 1998). For cells incubated for 3 hours following irradiation in 0.5 mol dm^{-3} DMSO, 90% of the dsbs induced by γ-ray irradiation are rejoined. In contrast under the same conditions, dsbs induced by α-particles are reduced by <13% following incubation for 3 h at 37^{0} C (deLara *et al.* 1995). Therefore the majority of non-scavengable dsbs induced by α-particles are not readily rejoined in contrast to those induced by γ-ray irradiation. The ability to rejoin dsbs has been postulated as being the primary reason for the RBE (Relative Biological Efficiency) of α-particles (Blöcher 1988). However, it is not only the rejoining of dsbs that is biologically significant, the fidelity of the rejoining will also be crucial. Löbrich (1998) has shown that approximately 25 % of dsbs induced by X-ray irradiation are incorrectly rejoined. After high LET irradiation, less efficient rejoining takes place, together with an impaired ability for correct rejoining of dsb.

Therefore, the majority of the studies to date infer that the extent of rejoining of dsb decreases as the LET of the radiation increases and of those that are rejoined an increasing yield are rejoined incorrectly with increasing LET. These studies have highlighted the possible influence of damage complexity on the ability of cells to process such damage.

Base Damage

Irradiation of DNA in aqueous solution also results in bases being chemically modified or released, since both pyrimidines and purines readily react with radiation induced water radicals. Solvated electrons and the hydroxyl radical react with DNA at almost diffusion controlled rates, whereas the hydrogen atom interacts at almost two orders of magnitude slower. Although in principle the H-atom may abstract hydrogen from the sugar within the DNA it reacts almost exclusively by addition to the base (Deeble and von Sonntag 1985). In the case of DNA irradiated in aerated, aqueous solutions, pyrimidine radicals react with oxygen and are converted into the corresponding peroxyl radicals in a reaction which is almost diffusion controlled (Adams and Wilson 1969a and b, Willson 1970, O'Neill and Fielden 1993). However the low oxygen uptake in purine systems indicates that the majority of purine radicals, do not react with oxygen (Isildar *et al.* 1982). For a full description of the free radical chemistry of DNA, readers are referred to a number of detailed descriptions (von Sonntag 1987, Steenken 1989, O'Neill and Fielden 1993, Breen and Murphy 1995, Burrows and Muller 1998, Pogozelski and Tullius 1998).

Sites of base damage or modification are of interest on two counts. Firstly, they arise within cells naturally at a very high rate in organisms that rely on oxygen for their metabolic energy source due to the production of oxidising species such as the superoxide radical, the hydroxyl radical and hydrogen peroxide (Cadenas 1989, Sies 1991, Ames *et al.* 1993). A high level of background oxidative DNA damage together with mutagenic potential suggests that this type of damage may be an important contributor to cancer induction. Secondly, studies examining DNA damage have concentrated on the yields of dsb as a measure of the formation of complex damage induced by ionising irradiation. However, the presence of base damage sites in close proximity to strand break sites contributes to the spectrum of complex damages, and hence detection and quantification of base damage provides additional insights into the complexity of DNA damage formation by ionising radiation.

In response to the spontaneous induction of base damage sites, a large number of repair enzymes are present within the cell. DNA glycosylases constitute a class of enzymes whose role in the repair process is base excision through hydrolysis of the base-sugar (N-C glycosylic) bond of modified or incorrect bases giving rise to abasic (AP) sites (Sancar and Sancar 1988, Friedberg *et al.* 1995). Several glycosylases also display AP lyase activity that converts an AP site into a strand break. Two glycosylases used

experimentally as damage probes are Endonuclease III (Nth) and Formamidopyrimidine Glycosylase (Fpg) derived from *E.coli* and whose site specificities are summarised in table 2.4. Fpg has been found to remove oxidised purines and in particular 2,6-diamino-4-hydroxy-5-N-methyl formamidopyrimidine (FAPy) (Breimer 1984) or intact (but oxidised) imidazole rings 7,8-dihydro-8-oxo-2'deoxyguanine (8oxoG) (Tchou *et al.* 1991) and displays strand cleaving activity that acts at AP sites in DNA (O'Connor and Laval 1989, Boiteux *et al.* 1992). Nth excises oxidised pyrimidines (Demple and Linn 1980, Katcher and Wallace 1983, Breimer and Lindahl 1984, Wallace 1988, 1994, Dizdaroglu *et al.* 1993) and cleaves AP sites. The range of substrates recognised includes thymine glycol, dihydrothymine (Demple and Linn 1980) and a range of 5,6-saturated and fragmented pyrimidine derivatives.

Studies on ssb formation in γ-ray irradiated DNA in solution following incubation with Fpg and/or Nth indicate that the enzymes act additively in the conversion of radiation induced base damage sites into ssb (Milligan *et al.* 1999). The increase in the yields of ssb following enzyme treatment was interpreted to result from the conversion of base damage sites into ssb (see section 2.4.2.2). Fpg and Nth have been used to quantify the number of base damage sites following γ-ray or X–ray irradiation, predominantly at low scavenging capacities where the majority of damage sites are produced by single OH radical interactions (Milligan *et al.* 1996b, 1999). At low scavenging capacities ($1.5x10^6$ s^{-1} and $1.5x10^7$ s^{-1}) the presence of Fpg leads to approximately two enzyme sensitive sites per prompt ssb (Milligan *et al.* 1996b, 1999) whereas, Epe *et al.* (1993) reported approximately equivalent yields of Fpg sensitive base damage site and ssb in γ-ray irradiated DNA in solution. Other studies with Fpg confirmed that approximately equivalent numbers of Fpg sensitive sites and prompt ssb are induced by low-LET radiation at low scavenging capacities (Häring *et al.* 1994, Epe *et al.* 1996, Kuipers and Lafleur 1998). Nth treatment of DNA irradiated in solution at low scavenging capacities ($1.5x10^6$ s^{-1} and $1.5x10^7$ s^{-1}) gives an increased yield of ssb of approximately 2.5 i.e. 1.5 Nth sensitive sites per prompt ssb (Milligan *et al.*1996b, 1999) whereas Epe *et al.* (1993) reported an increase in yields of ssb by a factor of approximately 1.6 i.e. 0.6 Nth sensitive sites per ssb. Other studies with Nth confirmed that less than 1 Nth sensitive site is formed per ssb following low-LET irradiation at low scavenging capacities e.g. 0.4-0.6 Nth sensitive sites per ssb (Häring *et al.* 1994, Epe *et al.* 1996, Kuipers and Lafleur 1998). In contrast to the majority of other studies for γ-ray

irradiation of DNA carried out under scavenging capacities of $1.5x10^7$ s^{-1} and $3.0x10^8$ s^{-1}, Prise *et al.* (1999b) measured high yields of enzyme sensitive sites i.e. 2.7 and 3.5 Nth sensitive sites per ssb respectively. This study also presented the first data on the yield of enzyme sensitive base damage sites induced by α-particle irradiation of DNA. Under the same scavenging conditions as for γ-ray irradiation, yields of ssb increase by factors of 1.8 and 2.5 respectively i.e. 0.8 and 1.5 Nth sensitive sites per ssb. Therefore the majority of studies indicate that the yield of enzyme sensitive sites per prompt ssb induced by irradiation of DNA is ~0.5-1.5 after Nth treatment and ~1-2 after Fpg treatment.

A recent study has shown that certain secondary radicals produced from the scavenger may also cause base modifications (Milligan *et al.* 1999). After irradiation of DNA by γ-rays at a high scavenging capacity ($6.6x10^9$ s^{-1}) using DMSO, the yield of ssb increases following Fpg or Nth treatment by factors of approximately 30 and 20 respectively. It was argued that these very large increases in base damage yields at high concentrations of DMSO result from the formation of base damage through the interaction of DNA with the resulting methylperoxyl radical. This latter radical is formed from the interaction of DMSO with OH radicals and the resulting methyl radical interacting with oxygen. Strand break damage is not directly produced but base damage sites are formed which are recognised by Fpg and Nth. The formation of DNA damage by hydrated electrons is minimised since the irradiations are carried out in the presence of oxygen. No decrease in either the yield of base damage or prompt ssb was seen when the oxygen concentration was increased and thus electron induced damage is thought to be insignificant.

The use of base excision repair enzymes has proved useful in gaining information on radiation-induced DNA base modifications and has the potential to be used to reveal clustered damage sites which involve base modifications. Analytical chemical techniques have been used to characterise base damage, however there is significant controversy concerning the appropriate methods to use (Douki *et al.* 1996, 1999, Cadet *et al.* 1997). Therefore, base excision repair enzymes have been used as probes of base damage as well as of complex damage involving base damage sites in the studies described later.

In mammalian cells, the repair of DNA damage such as individual ssbs or base damage sites is very rapid and efficient and occurs via the process of excision repair (Wallace

1994, Friedberg *et al.* 1995). In simple terms the initial process of base excision repair or nucleotide excision repair involves a length of the nucleotide strand containing the damaged region being excised by endonucleases (figure 1.13). DNA polymerases then act to construct a new sequence of nucleotides using the undamaged strand as a template. Finally, when the repair replication has been carried out the new section of DNA is linked to the intact region by ligase enzymes. However if damage occurs to both strands in the same location to within a few base pairs then repair may not be so straightforward. No template exists and thus it is possible for genetic information to be lost or misrepair to take place. If a number of DNA damage sites are present in close proximity this clustered damage may effect the ability of an enzyme to recognise and/or bind to the relevant area and interfere with the repair capability of a cell. Hence the spatial characteristics of the energy depositions associated with a given radiation type may have critical implications in the recognition and/or repair of the DNA damage that ensues.

The interaction of radiation with DNA may give rise to spatially close ssb and base damage sites or multiple base damage sites. The base excision repair enzymes convert these base damage sites into strand breaks. It is hypothesised that for complex damage, enzyme activity may be inhibited or may induce dsbs via the conversion of base damage sites into ssb in close vicinity to a pre-existing ssb. Some initial studies have reported the effect of clustered DNA damage on the efficiency of base excision repair enzymes to excise base damage. Nth has been used to examine its ability to process complex damage sites in DNA (Chaudhry and Weinfeld 1995) and to assess whether in attempting repair of such spatially close lesions, dsbs are inadvertently formed. Model systems have been examined with damaged bases, either dihydrothymine (DHT), or abasic sites, 1, 3, 5, or 7 base pairs apart on opposite strands. In the case of substrates containing DHT sites five and seven base pairs apart some dsbs were formed although in small numbers relative to the formation of ssbs. In the case of DHT sites one or three base pairs apart no dsbs were generated. It was suggested that the action of the enzyme is inhibited by the proximity of a second DHT damage site. Specifically the glycosylase activity of Nth is inhibited by the close vicinity of DHT whereas abasic sites in close proximity are rapidly converted by Nth into dsbs. That dsbs are produced irrespective of the distance abasic sites are apart, indicates that the enzyme cleaves both abasic sites. Therefore inhibition of AP lyase activity was not detected. Oligonucleotide substrates have also been constructed containing a site of pyrimidine damage or an abasic site 1,3

or 6 base pairs away from a ssb on the opposite strand (Harrison *et al.* 1998). In agreement with the previous finding Nth was able to cleave an AP site irrespective of the distance away from the strand break site, whereas cleavage of a base damage (thymine glycol or DHT) one base pair away from the gap was reduced relative to cleavage three or six base pairs away. The efficiency of cleavage of the lesion increased as the distance between base damage lesion and strand break was increased. Studies of the efficiency of Nth, Fpg or nuclear extracts from a Ku deficient CHO cell line to induce a ssb on an oligonucleotide containing an AP site, DHT, 8-oxoG or 8-oxoA 1,3 or 5 bp away from either an AP site or DHT has revealed DHT excision is much more affected than cleavage of an AP site by the presence of another damage (David-Cordonnier *et al.* 2000). This inhibition of DHT excision is most significant in the presence of an AP site on the opposite strand and may have implications on minimising the probability of the formation of dsb when a clustered damage is present.

To assess the contribution of base damage to DNA complex damage (section 1.8), the number of additional dsb, revealed by treatment with Nth, after irradiation of plasmid DNA has been determined with ^{60}Co γ-ray and α-particle irradiation (Prise *et al.* 1999b). It was inferred that an increase in dsb following Nth treatment is an indication of the number of complex sites, representing a base damage in close proximity to a ssb on the opposite strand or two spatially close base damage sites, but on different strands. Irradiations of plasmid DNA carried out at scavenging capacities of 1.5×10^7 s^{-1} and 3.0×10^8 s^{-1} lead to increases in the number of dsb following treatment with Nth by factors of 4.2 and 5.2 for γ-ray irradiation and 1.6 and 1.3 for α-particle irradiation respectively. Thus either α-particle irradiation leads to less base damage sites per ssb relative to γ-ray irradiation or detection by the Nth is less efficient following α-particle irradiation, potentially as a result of complex damage inhibiting enzyme activity as discussed above (Chaudhry and Weinfeld 1995, Harrison *et al.* 1998, David-Cordonnier *et al.* 2000).

1.6.2.3. Effects of Heat

The temperature at which a DNA sample is maintained following irradiation is known to contribute to the amount of damage subsequently detected. Many alterations at the sugar moiety have been detected in irradiated DNA (Ward and Kuo 1976, von Sonntag *et al.* 1981, von Sonntag 1987, Breen and Murphy 1995), and three distinct reaction

product classes identified; 1) free deoxyribose radiation products with both phosphate linkages broken and the unaltered base released 2) altered sugars moieties bound by one phosphate linkage to a broken DNA strand and the unaltered base released 3) altered sugars (fragmented and/or oxidised) with both phosphate linkages intact and either the unaltered base released or remaining attached. Types 1) and 2) correspond to direct strand breaks whereas 3) is categorised as a radiation-induced labile site: i.e. may give rise to strand breaks following subsequent post-irradiation heat treatment (Henle *et al.* 1995). From a cellular point of view, these labile sites are significant as they represent damage, which although potentially lethal may be repaired (Ward *et al.* 1984, Ward 1985). Studies undertaken to quantify the additional strand breaks resulting from either increased post-irradiation temperature or due to alkali hydrolysis of labile sites (Lücke-Huhle 1975, Flick *et al.* 1989, Roots *et al.* 1990) have postulated that the same damage is responsible for both effects. However to date the structure of radiation-induced labile sites remains unknown.

Several studies have shown that the yield of γ-ray induced strand breaks in SV40 DNA increases with temperature (2^0 C-37^0 C) (Jones *et al.* 1994a, Tomita *et al.* 1995). Irradiation of DNA at 23^0 C resulted in an approximate 50 % increase of ssb relative to that for irradiation at 2^0 C and an approximate 20 % decrease relative to 37^0 C (Jones *et al.* 1994a). For dsb, the yield at room temperature is twice that determined at 2^0 C and approximately half the value determined at 37^0 C. In addition, the time course of the yield of strand breaks for samples irradiated at 2^0 C, but incubated at 37^0 C, show that the yield of single strand break reaches an initial maximum after 5 h with a half-maximum value at 1.5 h. After 5 h, a much slower increase in the yield of ssb occurs up to at least 18 h post irradiation. In comparison the dependence of the yield of dsb on time shows two distinct time domains. Initially there is a rapid increase in dsb yield which is complete within 2 h, with a midpoint of 15 min and results in an approximate twofold increase. It was argued that the additional dsb arise from hydrolysis of labile sites that are proximal to other pre-existing ssbs or other labile sites. Further enhancement of dsbs on a longer timescale are thought to be due to either a) recruitment of independent, spatially separate ssbs into dsbs by duplex melting or b) single sites of initial damage acting to give dsbs. The reason why heat treatment results in such large increases in the yields of dsb may represent an increase in the maximum distance between two independent ssb which gives rise to a dsb. Plasmid DNA has

been used to examine the maximum distance between two independently induced ssbs on opposite strands that could give rise to a dsb (Van Touw *et al.* 1985). For irradiated DNA either maintained at room temperature or heated to 55^0 C for 3.5 h, the interstrand separation of ssb to give a dsb was determined to be 29±6 and 102±13 bp respectively. In plasmid DNA at 4 ^{0}C, ssbs greater than 6 bp apart do not give rise to dsbs whereas at 25^0 C this value rises to 9 bp (Hanai *et al.* 1998).

Therefore the extent of radiation induced damage depends upon the temperature at which the samples are irradiated and at which they are subsequently processed.

1.7. Computer Simulations of Radiation Induced DNA Damage

Computer simulations are a relatively new field of scientific investigation having been used for only approximately 20 years within the radiation field. The sophistication of such simulations has been partially dependent upon the expertise of the programmers developing them but primarily dependent upon the computing power available. In recent years, with the rapid increases in computer technology there has been a corresponding increase in the level of complexity within simulations. Simulations of track structure have developed significantly over the last decade with Monte Carlo codes having been developed which describe the molecular chemical interactions along the tracks of ionising radiation (Paretzke 1987, Nikjoo *et al.* 1998) and describe with increasing sophistication the models of the DNA used within the simulation (Chatterjee and Holley 1993, Umrania *et al.* 1995, Nikjoo *et al.* 1997). Simulations have been employed in a wide range of fields and a wide range of areas within the radiation field itself e.g. understanding the differences between low and high LET radiations (Goodhead 1994), examination of clustered damage (Goodhead 1994, Ward 1994) and low dose exposure to radon (National Research Council 1998). Simulations are based on determining the products of the interaction of a radiation field within a target substance and then following these products in time and space and examining how they interact with each other and with other products within the target (for review see Paretzke 1987). All of the calculations however are statistical in nature to reflect the basic stochastic processes. All events have a probability associated with them rather than there being defined outcomes. Thus for example, if an electron track is analysed, the incoming electron will have a probability of interacting with a given target atom which is dependent upon several factors such as; the electron velocity, the physical

characteristics of the target atom i.e. atomic number and mass, the closeness of approach etc (Tomita *et al.* 1997). In addition, a range of interactions may occur, giving rise to various products with variable energies associated with them. Such parameters are summarised in a concept known as the cross-section which is an experimentally determined value expressing the probability of interaction between a specific incoming particle of specific velocity interacting with a specific target and giving rise to a specific product (for summary see Paretzke 1987, Varma and Chatterjee 1994). A large number of cross-sections are subsequently required to describe the probability of, for example; a total elastic interaction, total inelastic, total excitation, charge transfer and doubly differential which gives the probability of a specific energy loss and the angle of travel of the outgoing particle. Because of the very large number of interactions that are possible within a wide range of targets, experimentally determined cross-section values are not available for all combinations. Specifically the majority of experimental data have been measured in water vapour. Data for other materials such as liquid water or DNA are limited due to experiments being difficult to undertake or completely impractical (for review of cross-sections used by various codes see Nikjoo *et al.* 1994b and c). It has subsequently been necessary to evaluate cross-sections theoretically extrapolating from the determined experimental values. For example, in the determination of cross-sections from liquid water it is necessary to use the experimentally determined values from water vapour and correct for the increased molecular density and increased number and complexity of molecular interactions (Paretzke 1987). The determination of the site of all ionisation and excitations associated with the passage of an incoming particle constitutes the physical track of the radiation. The radicals and molecular products that subsequently arise at these points gives rise to the chemical track. To examine the effects of the indirect effect, radicals that have been generated are allowed to diffuse randomly for a period of time during which they will interact and react with various molecules that are present. The likelihood of interaction will depend upon the species present and the closeness of approach. Again, experimentally determined values for the maximum interaction radius between species are used (Nikjoo *et al.* 1997). If species pass within a distance less than this value then the radical species are assumed to interact and a product formed which is again followed as it diffuses. Such a procedure is continued until all of the chemically reactive species have been reacted and effectively removed. Again, because of the random nature of the diffusion process a variable product yield may arise from

an identical chemical track. If a DNA target is introduced into a simulation those ionisations that occur within the volume occupied within the volume defined for the DNA are considered to give rise to direct damage. If radicals produced by the chemical track diffuse and interact with the DNA target then this is considered to constitute indirect damage (see section 2.7 for full details)

Because of the statistical nature of all of the interactions associated with a track it is necessary for any one study to repeat the process a large number of times so that reliable average values are obtained.

In the simulation studies that were initially undertaken to determine the absolute yield of strand break within DNA, only direct energy depositions were considered (Charlton *et al.* 1989, Holley *et al.* 1990). However, more recently the diffusion of radicals for DNA irradiated within water, has been included within such simulations (Terrissol and Beaudré 1990, Michalik 1992, Nikjoo *et al.* 1994b, 1997, 1999, Tomita *et al.* 1997, 1998, Moiseenko *et al.* 1998a and b). Even for those simulations that have included the diffusion of radicals, diffusion has been restricted to distances which are characteristic of those found within the cellular environment. No work has been undertaken to determine the yields of strand breaks yields at scavenging capacities significantly different to that within cells.

Work has also been restricted to certain radiations. As a result of the increased computing time necessary to examine DNA damage with high energy radiations the majority of work has examined low energy electrons and photons (Goodhead and Brenner 1983, Charlton *et al.* 1989, Goodhead and Nikjoo 1989, Nikjoo and Goodhead 1991, Nikjoo *et al.* 1994a, Friedland *et al.* 1998) with some additional work undertaken examining irradiation with high LET radiations; α-particles and heavy ions (Charlton *et al.* 1989, Nikjoo *et al.* 1994a, 1999, Holley and Chatterjee 1996). When complex damage has been considered, DNA damage analysis has principally focused on the relative yields of ssb and dsb, however there has recently been some analysis investigating the contribution of base damage sites to complex damage formation (Nikjoo *et al.* 1999). At scavenging capacities which lead to a mean OH radical diffusion distance equivalent to that found within the cellular environment, it was calculated (Nikjoo *et al.* 1999) that electrons with energy $\leq$ 4.5 keV have ratios of ssb:dsb of 13-15 whereas 2 MeV α-particles have a ratio of ssb:dsb of 4. For both electron and α-particle simulations the ratio of base damage:ssb is approximately 2.

Approximately 30 % of dsb following low LET irradiation are complex (i.e. have additional breaks in close vicinity) but with the inclusion of base damage this rise to approximately 60 %, whereas for high LET irradiation these values rise from approximately 70 % to 90 % following inclusion of base damage.

1.8. Clustered Damage

The non-uniform deposition of energy characteristic of ionising radiation statistically results in sites where radiation damages are spatially close, within a few tens of base pairs of each other. These regions are known as clustered DNA damage or multiply damaged sites (MDS). A clustered damage site generally occurs when a radiation track passes through or near to the DNA and deposits energy either in the DNA, in the water molecules in the close vicinity of the DNA, or does both. The direct energy deposition events give rise to DNA damage which are possibly supplemented by diffusible water radicals. The contribution of water radicals to damage will be dependent upon both the LET of the radiation and the OH radical scavenging capacity of the solution surrounding the DNA as discussed in section 1.5 and 1.6.2.1. These clustered lesions are thought to be biologically significant (Goodhead *et al.* 1980, 1985, Ward 1985, Goodhead 1989, 1992). In essence the concept of clustered damage or multiply damaged sites implies a site containing several elemental damages close to one another, be it a ssb near another ssb, a ssb near a base modification etc. Figure 1.14 schematically represents an example of a clustered DNA damage. It is hypothesised that the complexity of clustered DNA damage increases with the LET of the radiation and that the biological significance of such damage sites may lie in them being less repairable (Goodhead *et al.* 1980, 1985, Ward 1985, Goodhead 1989, 1992). The majority of information that has been obtained in reference to complex damage has arisen from simulations of DNA damage although experimental evidence is now becoming available.

From table 1.2, which shows the number of lesions produced by 1 Gy of low LET radiation, it can be seen that even a dose of only 1 Gy gives less than 1 lethal event and approximately one chromosome aberration in contrast to the large number of ssb induced. It was assumed therefore that ssb have no biological significance. A similar argument may be made for individual base damage sites which again, although numerous do not seem to lead to lethal events. As a result of this, it has been hypothesised that complex lesions including dsb may be more significant due to their

reduced abundance. However the argument as applied to base damage sites and ssb may be directed to dsb, as there is no 1:1 relationship between the induced yield of dsb and cellular effects although some dsb induced in cells have been inferred to be less repairable (Goodhead *et al.* 1993). The question therefore arises as to whether lethal lesions constitute a particular type of damage e.g. a damage that is difficult to repair or whether it is their precise location, either relative to a target or to each other which is of significance. Track structure simulations of DNA damage allow an examination of the energy deposition of different LET radiations at the nanometer level with DNA or its immediate environment (Goodhead 1987, Paretzke 1987). These simulations indicate that any small DNA segment has a very low probability of experiencing either direct or indirect damage associated with a specific radiation track. For example a 6 base pair segment in a γ-ray irradiated cell has probabilities of about 10^{-6} and 10^{-4} per Gy of undergoing a direct ionisation or being within 4-6 nm of a primary radical respectively (Goodhead and Hikjoo 1989, Nikjoo *et al.* 1991), which is the average diffusion distance of an OH radical within the cellular environment (Roots and Okada 1975, Ward 1991).Therefore, a dsb is likely to be associated with ionisations from a single primary track rather than from two distinct tracks at low doses based upon these probabilities. From a large number of cellular studies it has been confirmed that increasing the LET of the radiation results in increased cellular effects e.g. cell inactivation, mutations, aberrations etc (Cox *et al.* 1977, Thacker *et al.* 1982, Thacker 1992). However, for a constant dose the number of cells that are actually hit with higher LET radiation is lower than that for low LET due to the decreased number of tracks per Gy with high LET radiation. The fact that fewer cells are actually hit has also been confirmed from track structure simulations (Goodhead and Nikjoo 1989). In addition, the number of dsbs induced has been shown to show little dependence on LET (Prise *et al.* 1987, Jenner *et al.* 1992, 1993). For example even slow α-particles give a relative biological effectiveness (RBE) for dsb induction of around 1 relative to ^{60}Co γ-rays. The lack of strong LET dependence on dsb induction suggests that dsb do not result predominantly from single ionisations, in which case their abundance would increase with decreasing LET, nor from large clusters of closely located ionisations in which case abundance would greatly increase with increasing LET. Instead it is implied that the majority of measured dsb result from relatively small local clusters from single tracks (Charlton *et al.* 1989, Goodhead and Nikjoo 1989, Brenner and Ward 1992,

Michalik 1992). More recently, it was proposed that the yield of dsb induced by α-particles is under-estimated due to the formation of dsbs within distances of a few tens of base pairs, with such associated damaged sites being measured experimentally as single dsb (Hutchinson 1996, Rydberg 1996, Newman *et al.* 1997). However the disparity between the relationship of cellular manifestations of damage and LET and between dsb induction and LET persists. It tends to indicate the possibility that damage of a greater complexity than a simple dsb may be involved for significant biological effects to arise.

It is important to stress that neither the larger-scale nor the small-scale characteristics of a radiation track are uniform. All radiation effects are mediated by the passage of charged particles. In the event of an incoming photon interacting with a target, electrons are generated which, subsequently pass through a medium giving rise to further ionisations and excitations. The exact location of these events will be different with each track. If Monte Carlo simulations are undertaken, the location of every event within a radiation track may be determined. Subsequently the analysis of these spatial patterns should give a reasonable representation of the distribution of DNA damage within cells at the nanometer level. One major feature of all radiations is the abundance of very low energy secondary electrons from which all depositions take place within a few tens of nanometers because of the very short range of these electrons. From simulations, the types and frequencies of DNA damage produced by different radiations may be examined by randomly overlaying a DNA target on a 3-D simulation of a radiation track and repeating the process a very large number of times, using many simulated tracks, to allow for track stochastics, to obtain statistically meaningful data. From these approaches it was found that the most likely event is a single ionisation for any radiation but particularly for low-LET. However more complex events such as dsb with other damage sites in close vicinity arise even for low-LET radiation (Goodhead and Nikjoo 1989, Nikjoo *et al.* 1991). Although technically dsbs they are quite different from a simple dsb break and may compromise the cellular recognition and repair mechanism. Although such complex events may arise for low LET radiation they are found to increase in frequency and complexity as the LET is increased (Goodhead 1992). In addition uniquely severe clusters may arise with high LET radiation. The question is whether the frequency of occurrence of complex events correlates with significant biological end points and if so, what is specific about them that makes them

significant from a biological standpoint. From considering simple volume targets of DNA it is possible to evaluate the absolute frequency distributions of energy deposition by individual tracks. The actual size of the biological target has a large effect on the frequency of clusters. There is an increased frequency of severe clusters if for example bound water or protein is included within the DNA target (Goodhead and Nikjoo 1989, Brenner and Ward 1992, Michalik 1992). However, all radiations, irrespective of LET produces sparse ionisations or small clusters with the highest frequency i.e. a slow α-particle track will still produce all of the types of break that are characteristic of a high energy photon but with an altered frequency distribution (Goodhead *et al.* 1985, Goodhead and Nikjoo 1989, Brenner and Ward 1992, Michalik 1992). It was suggested that cells will be more efficient at repairing with high fidelity more minor damage associated with sparse ionisations and the efficiency of repairing complex damage decreases with high LET (Goodhead *et al.* 1980, 1985, Ward 1985, Goodhead 1989, 1992). It was suggested by Goodhead *et al.* (1993) that decreased ability of repair with increased complexity of damage might result in residual cellular consequences being dominated by the less frequent but more complex components of the damage spectrum following radiation exposure, that is they have greater biological 'severity'. Such damage sites may be of such complexity that they cannot ever be repaired with full fidelity irrespective of the time available. This is supported by work determining the number of dsb necessary for a lethal event in a cell following exposure to different agents. Fox and Prise (1992) determined that for slow α-particles a dose resulting in 20 dsb was required for cell lethality whereas for fast electrons and hard X-rays a dose resulting in nearly 100 dsb was required. If a chemical agent such as hydrogen peroxide is used a concentration sufficient to give several hundred dsb is required for cell lethality. Such data suggests a wide spectra of dsb of differing complexity are formed and thus have differing repair potentials.

1.8.1. Ultra-soft Irradiations

Ultrasoft X-rays (USX) with energies <5 keV, are not a source of radiation that is of immediate biological concern within the environment. This is because of their high attenuation, and thus very limited penetration into target materials, in which they are absorbed almost exclusively by the photoelectric process. USX radiation sources are used as a tool since they effectively allow the biological effects of low energy

secondary electrons associated with the track ends of higher energy radiation sources to be studied (figure 1.15). All ionising radiations produce large numbers of low energy secondary electrons as they pass through material. For example, low linear energy transfer (LET) radiation i.e. γ-rays, X-rays and high-energy electrons produce low energy secondary electrons that contribute approximately 30% of the absorbed dose (Nikjoo and Goodhead 1991). Such low energy electrons have limited range and hence deposit all of their energy within a small volume potentially forming clusters of energy deposition (figure 1.16). From work examining the role of clustered damage within biological systems, the role of high local depositions of energy relative to more sparse depositions in causing significant damage has been raised. Because USX sources are effectively representative of the high ionisation density track ends of low LET radiations a comparison of the biological effects between the two radiations gives an indication of the relative importance of the densely ionising and sparsely ionising parts of the track (Goodhead and Thacker 1977, Goodhead *et al.* 1979, 1980, 1981, Frankenberg *et al.* 1990, Goodhead and Nikjoo 1990, Botchway *et al.* 1997). An increase in ionisation density is generally considered to give rise to an increased proportion of complex damage which is less susceptible to cellular repair mechanisms than damage produced by more sparsely distributed ionisations. A large number of studies have employed characteristic ultra-soft X-rays and have highlighted these low energy secondary electrons to be potentially the predominant contributor to biologically-effective, DNA damage (Goodhead and Thacker 1977, Frankenberg *et al.* 1981, Hieda *et al.* 1986, 1994, 1996, Prise *et al.* 1987, Kobayashi *et al.* 1987, Goodhead and Nikjoo 1989, Botchway *et al.* 1997). The role of the energy cluster size distribution may be investigated by varying the energy of the USX.

As discussed in section 1.7 the amount and type of complex damage associated with high LET radiations has been investigated with computer simulations. However it is desirable to have some experimentally determinable measure of complexity. As previously discussed, although not directly correlated with cellular end points, the formation of double strand breaks (dsbs) have been taken to be an indication of the potential of a radiation track to form complex damage. Thus the ratio of ssb:dsb can be regarded as a potential measure of the ratio of simple:complex damage associated with a particular radiation.

1.9. Quantification of Damage Induced in Plasmid DNA

If the results determined from a computer simulation are to be compared with those obtained from an experimental system, it is advantageous to develop a simple and well-defined experimental set-up. In this way, the number of variables that have to be modelled is reduced and hence computing time is kept to a minimum. In addition, the relationship between closeness of fit between experiment and simulation can be examined in more detail and the exact effects of altering variables within the simulation assessed. Rather than utilising a cellular system it is beneficial to examine a simpler biological system in which repair does not take place and only yields of induced damage are effectively determined. A plasmid system represents a system of choice.

Plasmids are circular molecules of DNA that lead independent existences in bacterial cells. Plasmids carry genes which are often beneficial to the host bacteria affording them protection to various factors. For example the ability to survive certain antibiotics is often due to the presence in the bacterium of a plasmid carrying antibiotic resistant genes. All plasmids possess at least one DNA sequence that acts as an origin of replication to allow plasmids to multiply independently of the host bacterial chromosomes. Some smaller plasmids utilise the host cells own DNA replicative enzymes whereas some of the larger ones carry genes that are specific for plasmid replication. The copy number of a plasmid refers to how many plasmid molecules are normally found within a host cell. Although a plasmid will have a twisted form due to the repulsion of the phosphate backbone, in its undamaged state it will form a closed loop, which can effectively be represented as the closed circular form, illustrated in figure 1.17. However if it receives a single strand break the plasmid will revert to a relaxed state to give the open circular form. In the event of receiving a double strand break the plasmid will completely unwind and enter the linear form. If an electric field is applied the plasmid moves towards the positive charge. However if the plasmid is within a restrictive medium such as a gel when the field is applied, the three possible forms of the plasmid, the closed, open and linear will have different mobilities. Subsequently, after a period of time three different bands arise corresponding to the three different forms. These forms are subsequently quantified and the relative proportion of the three forms compared. Such a determination may be used as a representation of the amount of radiation damage induced to plasmid DNA. The question of variations in sensitivity of open circular and closed circular plasmid DNA has been assessed by Ozols *et al.* (1999). γ-ray irradiations carried out on undamaged

and pre-irradiated plasmid reveal equivalent numbers of new ssbs induced in the two plasmid forms. It was subsequently concluded that there is no effect on radiosensitivity of the conformation of the plasmid.

1.10. Aims

The objective of the current study is to extend the knowledge of complex damage, determined both experimentally and predicted via computer simulations. The majority of experimental data assessing the role of ionisation density of the radiation on DNA damage have focused on the yields of ssb and dsb obtained following low LET irradiation such as high energy X-rays, γ-rays and electrons. One aim of the current study is to focus on the yield of strand breaks in plasmid DNA following irradiation with high LET radiation such as α-particles and on Al_K USX, as this latter radiation has an ionisation track representative of the high ionisation density track ends of low LET radiation. The use of such a radiation allows direct comparisons to be made of the relative importance of low and high LET radiation in contributing to complex damage within plasmid DNA.

The relative importance of indirect and direct mechanisms in contributing to DNA damage, specifically complex, is assessed by varying the scavenging capacity of the solution containing the plasmid DNA and irradiating with α-particle, Al_K USX and γ-ray radiations. In this way the source of radiation damage may be shifted from predominantly isolated OH radical mediation to damage predominantly resulting from direct energy deposition. Additional analysis of the direct effect may be made by attempting to irradiate dried DNA at varying humidity thereby altering bound water levels.

An additional experimental parameter which will significantly alter the degree of complexity associated with plasmid DNA damage is the inclusion of base damage. To date little information is available on the yields of base damage sites present within DNA. An aim of the study is to use enzymes which convert sites of base damage into strand breaks. Both the number of isolated base damage sites and the number of prompt ssb previously considered as being representative of isolated damage sites but which are in close vicinity to a base damage site may be assessed. In the latter case this represents an additional class of complex damage which may be quantified.

The majority of computer simulations have been undertaken at scavenging capacities representative of those found within the cellular environment. Although this may be a biologically significant scavenging capacity at which to undertake simulations, it may mean that simulations are in fact mechanistically in error but fitted so that they correspond with the available experimental data. If there were indeed mechanistic errors these should become manifest when the scavenging capacity is varied. A principle aim therefore of the current study is to provide benchmarks for subsequent simulations and also to undertake some direct comparisons between experimental and simulated data. By undertaking simulations at a range of scavenging capacities the robustness of the simulation to correspond accurately to experimentally determined yields of strand breaks may be assessed. Simulations may also give further insight into the spectrum of damage that arises and the dependence of the relative yields of damage types on scavenging capacity and radiation energy. For example, the aim is to determine the relative contributions of the direct and indirect effect and the amounts and types of complex damage that arise for simulations of Al_K USX and α-particle irradiation for comparison with experimentally obtained data.

Table 1.1.

G values expressed as μmol J^{-1} of primary species in the radiolysis of water using radiation of different LET at 10^{-6} s (Appleby and Schwarz 1969, Burns 1981).

	$\cdot OH$	e^-_{aq}	$H\cdot$	H_2O_2	H_2	$HO_2\cdot$
^{60}Co γ-rays	0.29	0.28	0.06	0.06	0.04	0.003
32 MeV α-particles	0.10	0.07	0.04	0.10	0.10	0.005
12 MeV α-particles	0.06	0.04	0.03	0.11	0.11	0.007

Table. 1.2.

Damage associated with 1Gy of low-LET radiation in a mammalian cell (Goodhead 1994).

Initial Physical damage	
Ionisations in cell nucleus	~100 000
Ionisations directly in DNA	~2000
Excitations directly in DNA	~2000

Selected biochemical damage (Ward 1988)	
DNA single-strand breaks	1000
8-Hydroxyadenine	700
T* (thymine damage)	250
DNA double-strand breaks	40
DNA-protein cross links	150

Selected cellular effects	
Lethal events	~0.2-0.8
Chromosome aberrations	~1
Hprt mutations	$\sim 10^{-5}$

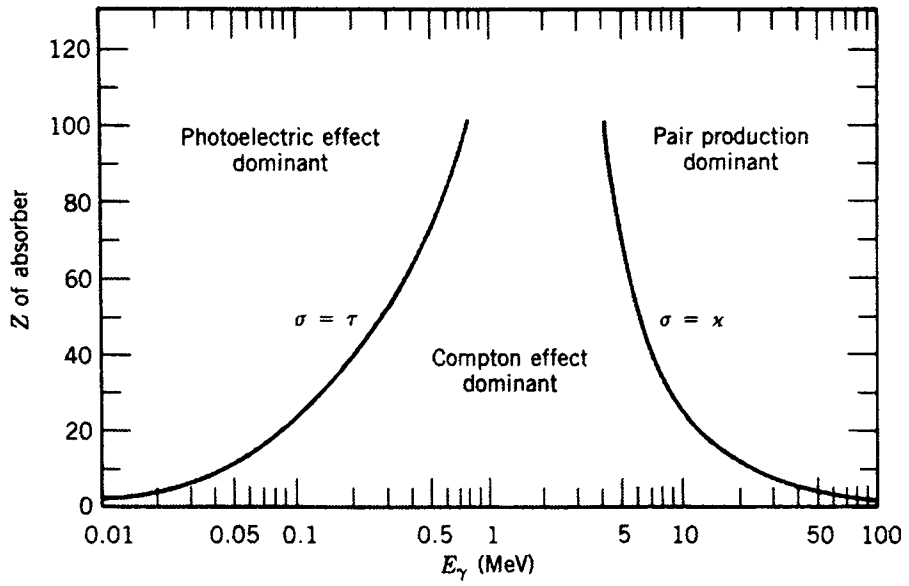

Figure 1.1.

Relative importance of γ-ray interactions with varying photon energy and varying target Z (Krane 1988).

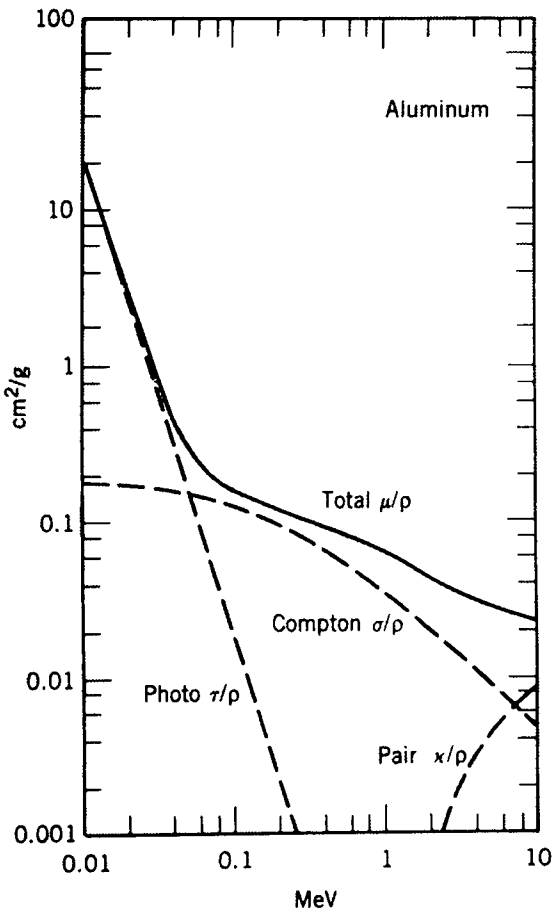

Figure 1.2.

Variation of photon mass attenuation coefficient for an aluminium target with photon energy (Krane 1988).

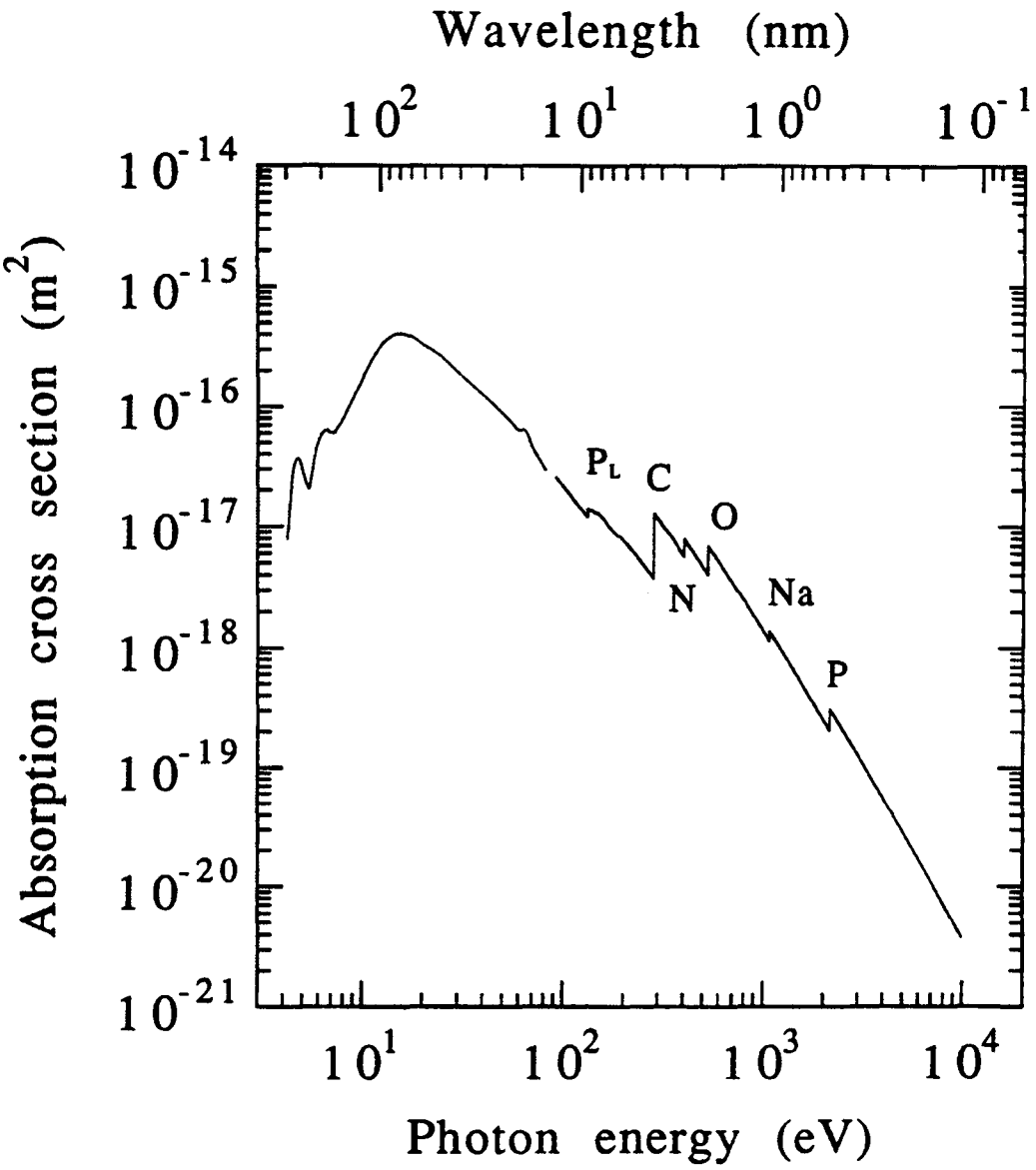

Figure 1.3.

Variation in photoabsorption cross section for a DNA target with varying photon energy (Hieda 1994).

Figure 1.4.

Schematic of radiation tracks in chromatin fibre illustrating the difference in ionisation density associated with tracks of different LET.

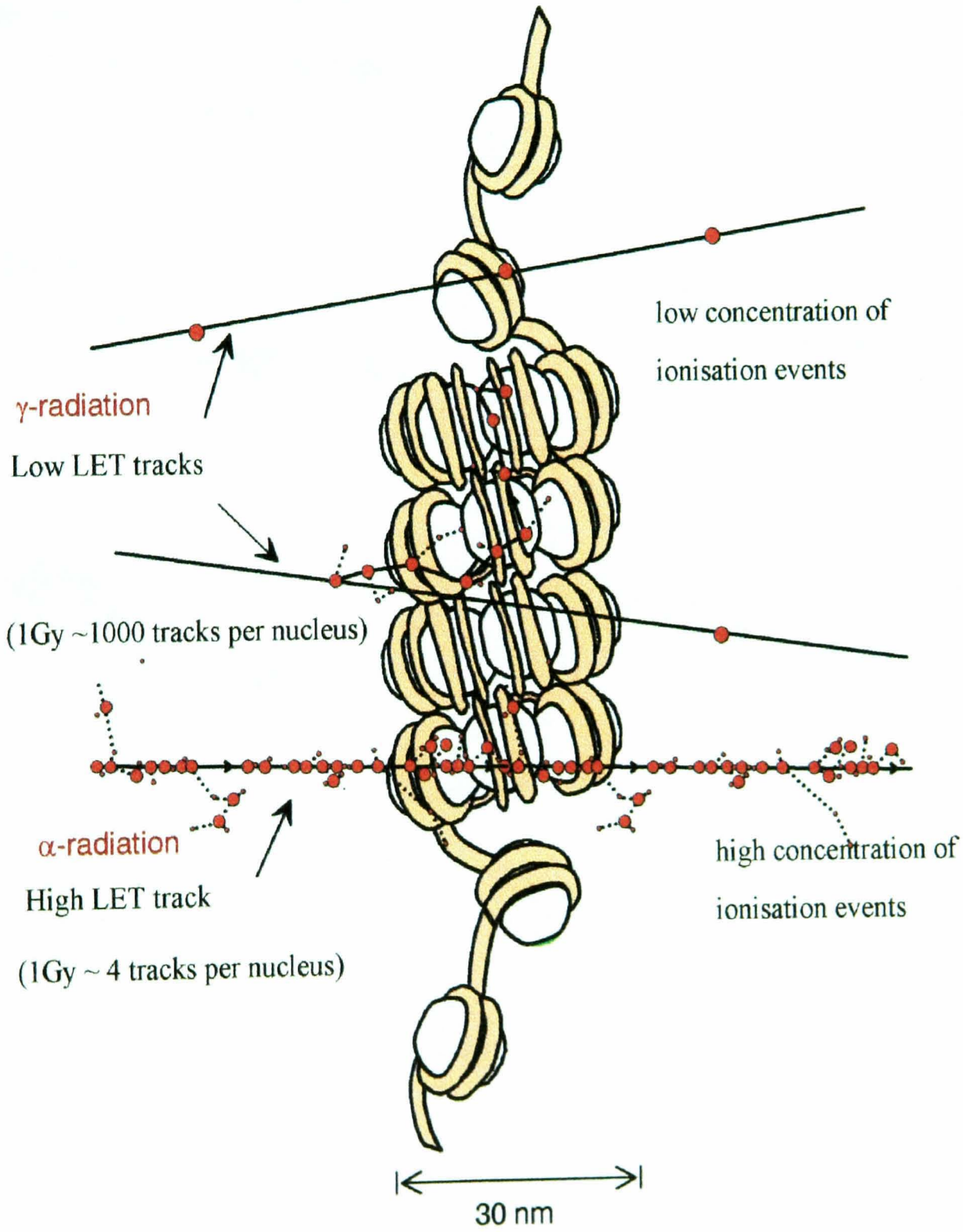

Figure 1.5.

Development of one 10 keV electron track in liquid water in space and time (Terrissol and Beaudré 1990). Each dot represents one radical species and N represents the number of species present at the time considered.

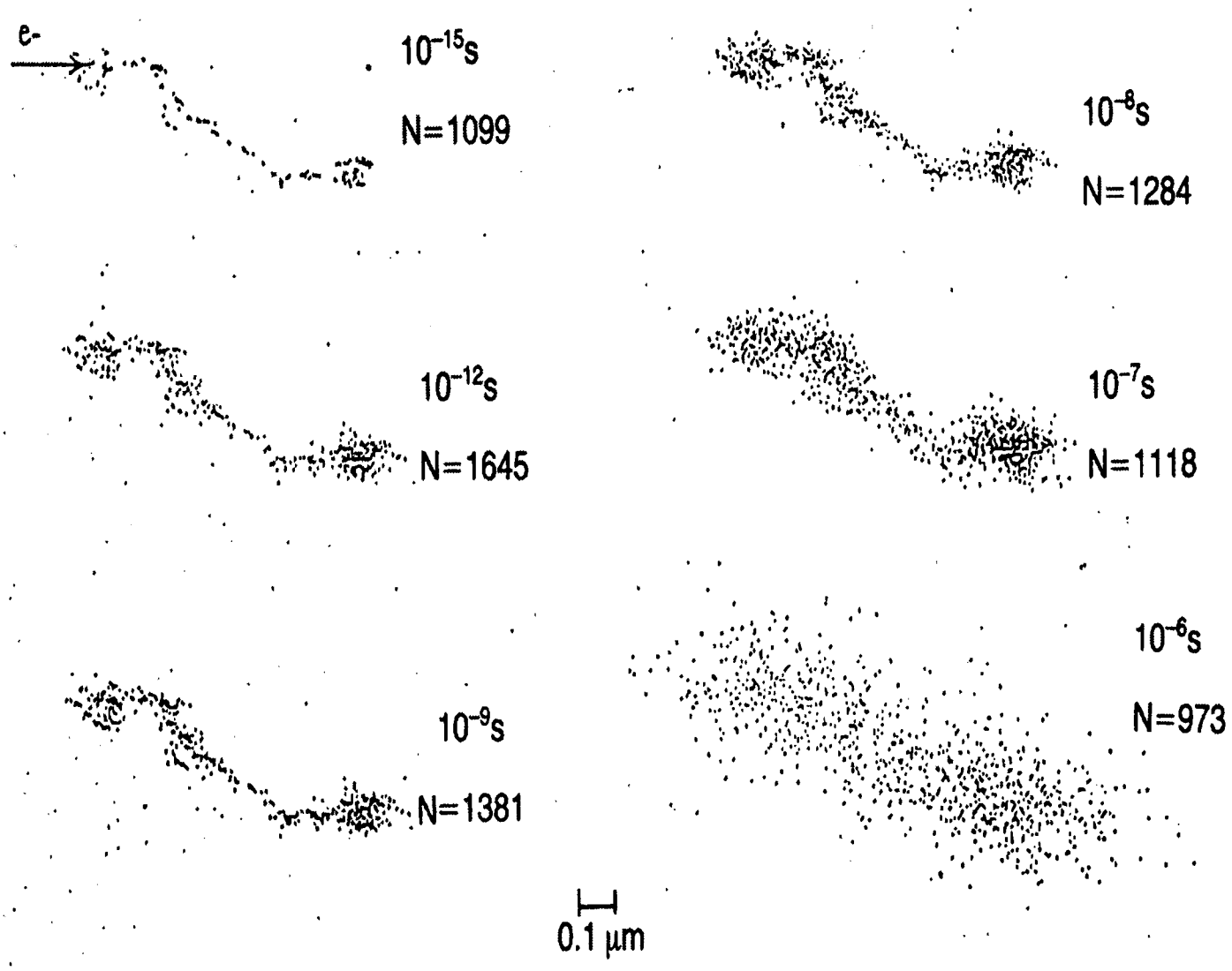

Figure 1.6.

Illustration of calculated (Turner *et al.* 1988) and measured (Jonah *et al.* 1976, Jonah and Miller 1977) time-dependent yields of the OH radical. G-value is expressed in molecules/100 eV. Taken from Turner *et al.* (1988).

● Jonah *et al.* (1976), ○ Jonah and Miller (1977)

—— Turner *et al.* (1988)

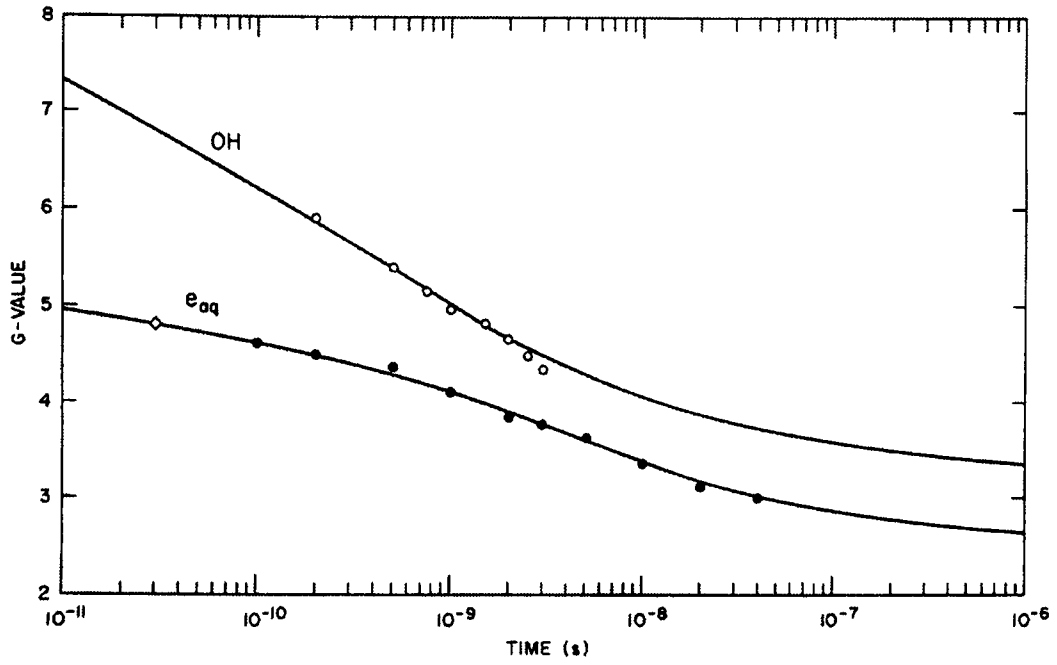

Figure 1.7.

Hydroxyl radical yield dependence on scavenging capacity (of hydroxyl scavenger s_{OH}) in aerated water. G-value is expressed in molecules/100 eV. Taken from LaVerne and Pimblott (1993b).

❑ Diffusion kinetics calculation- LaVerne and Pimblott (1993b)

▲ Schuler and Behar (1983) ■ ● Draganić *et al.* (1969)

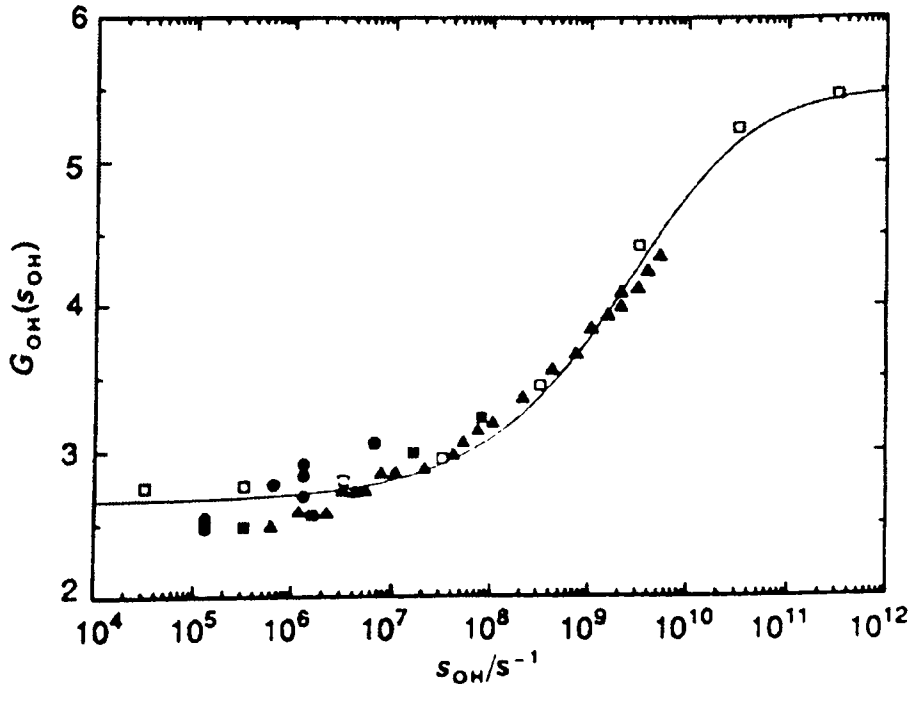

Figure 1.8.

A schematic illustrating radiation track events.

1. Densely ionising tracks.

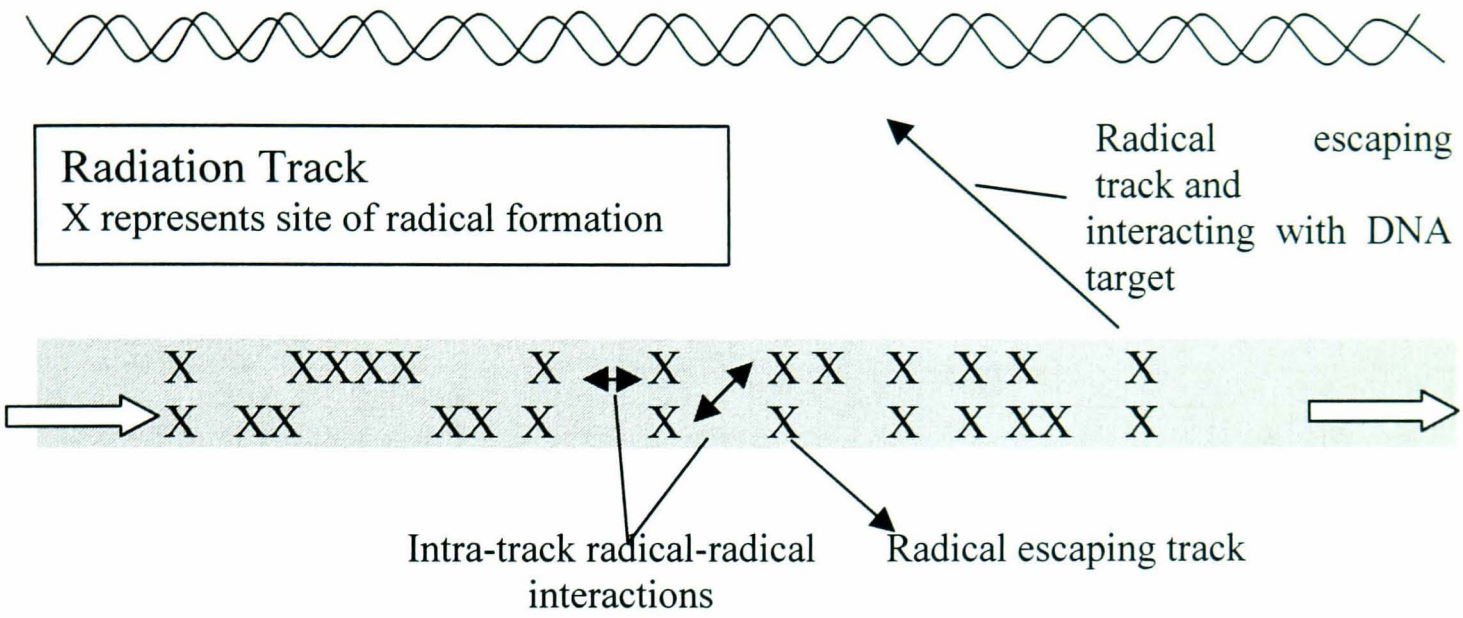

2. Less densely ionising tracks.

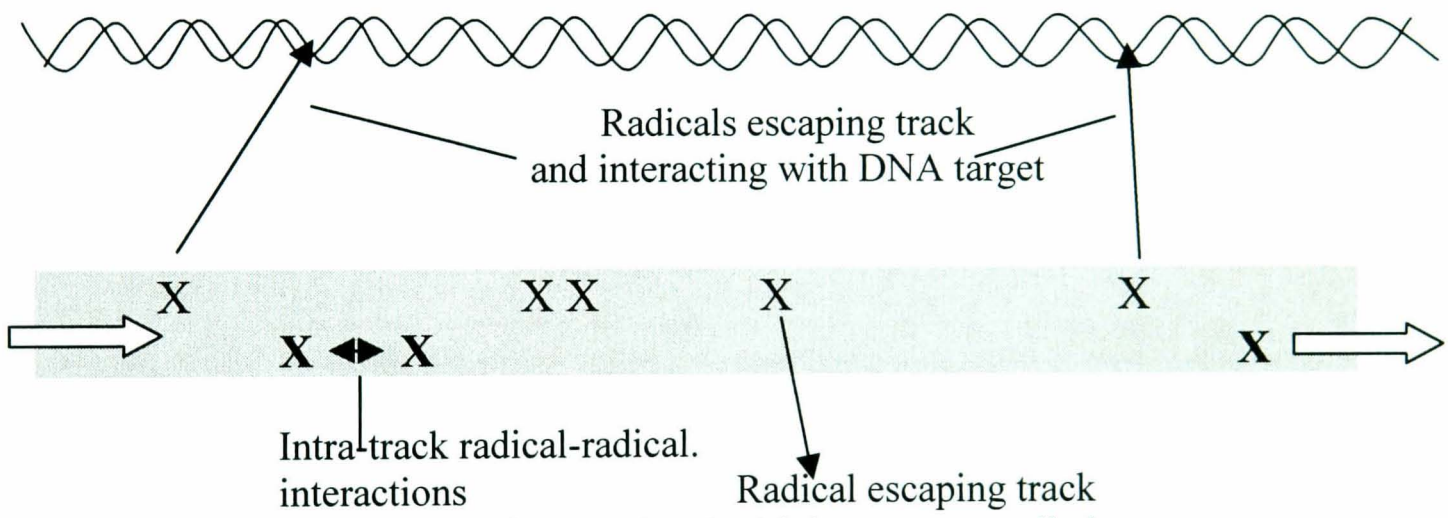

3. Short densely ionising tracks associated with low energy radiation.

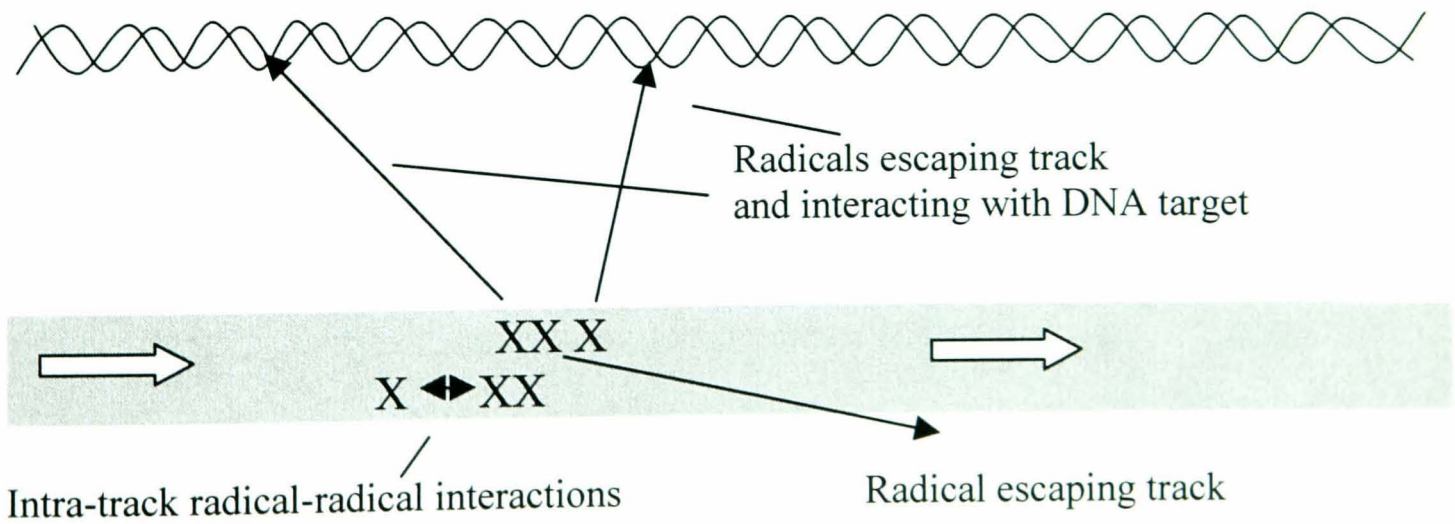

Figure 1.9.

DNA and its bases.

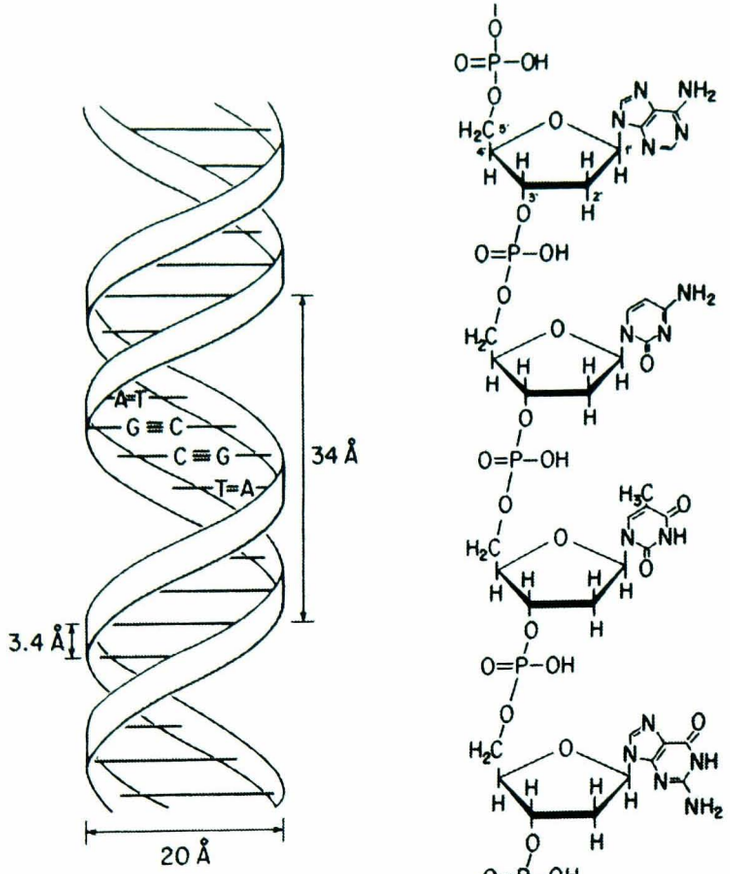

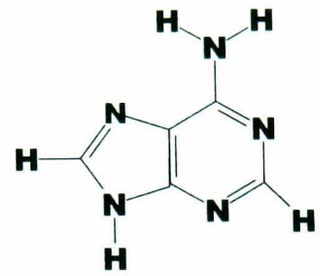

Adenine

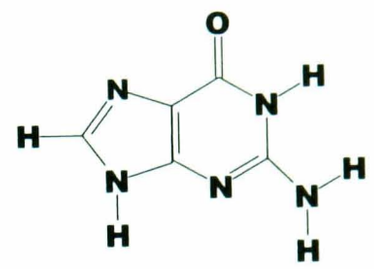

Guanine

Purine Bases

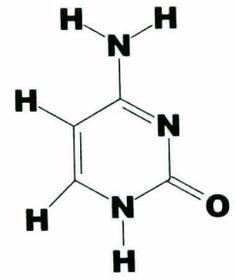

Cytosine

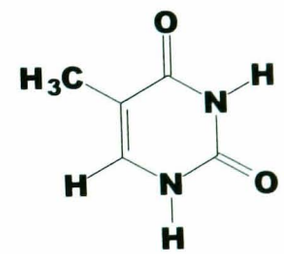

Thymine

Pyrimidine Bases

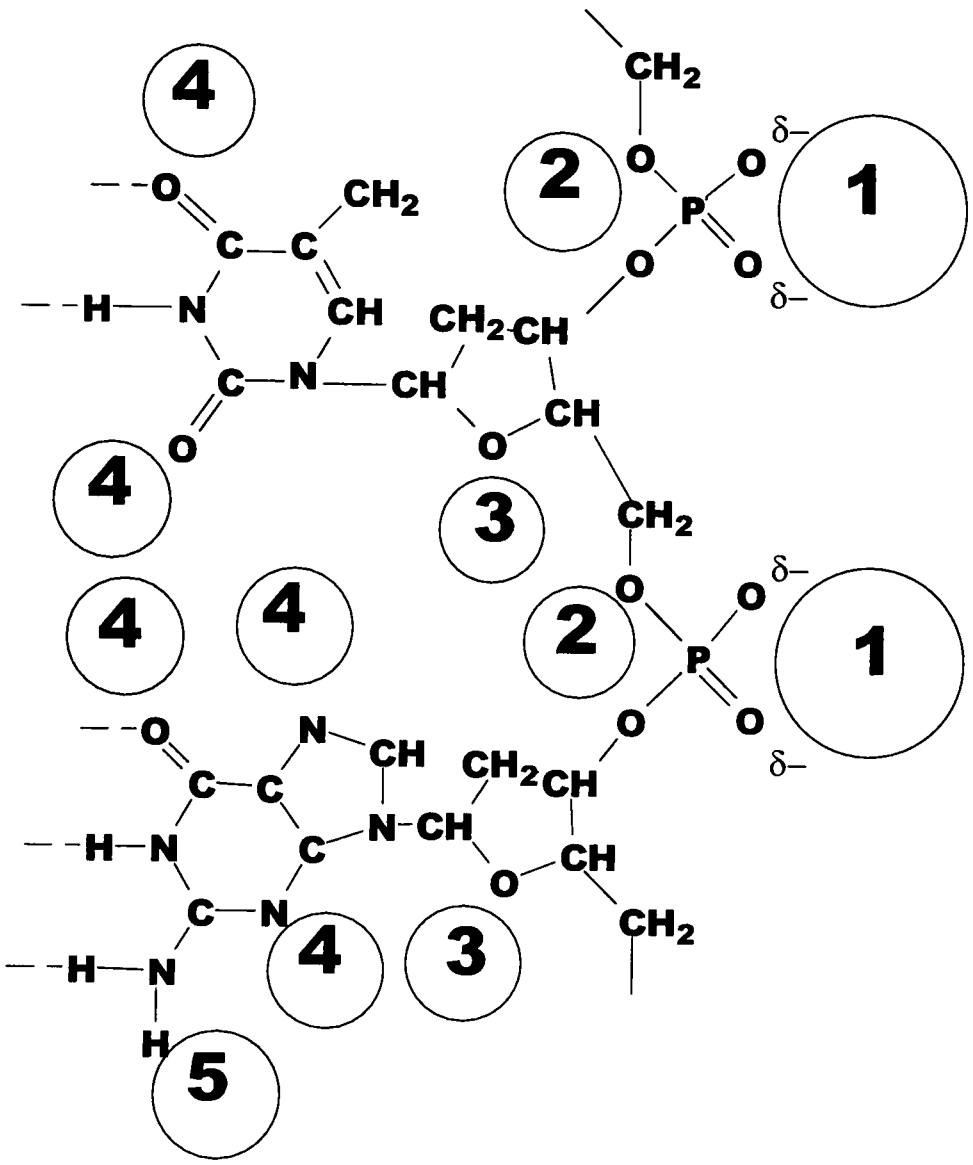

Figure 1.10.

Preferred hydration sites in B-DNA. The numbers 1 to 5 indicate strength of binding in decreasing order (Saenger 1988, adapted from Falk *et al.* 1970).

Figure 1.11.

Schematic of the interaction of radiation with DNA via the direct or indirect effect.

1) Radiation track overlays DNA

Direct damage of hydrated DNA

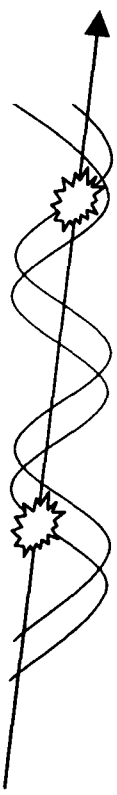

2) Radiation track overlays aqueous solution

Indirect damage

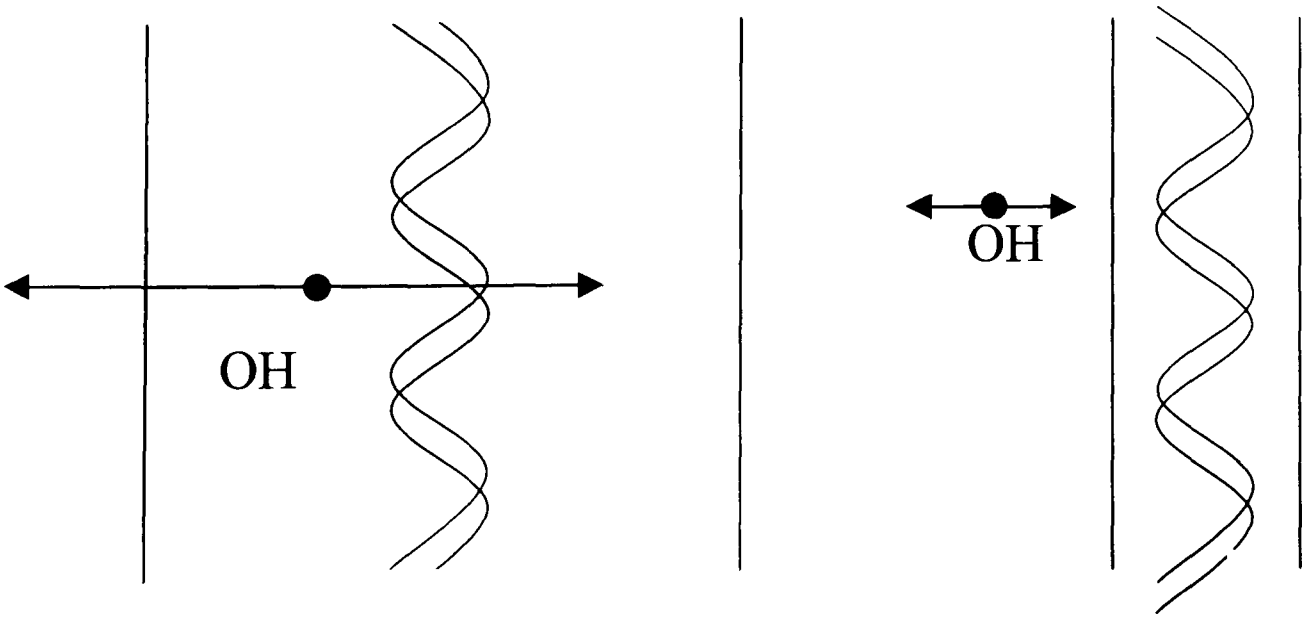

a) Low scavenger

b) Cell mimetic/High scavenger

Figure 1.12.

Mechanisms for OH radical interaction with DNA. Examples shown represent abstraction at $C_{4'}$ of the sugar moiety and addition to the nucleobases.

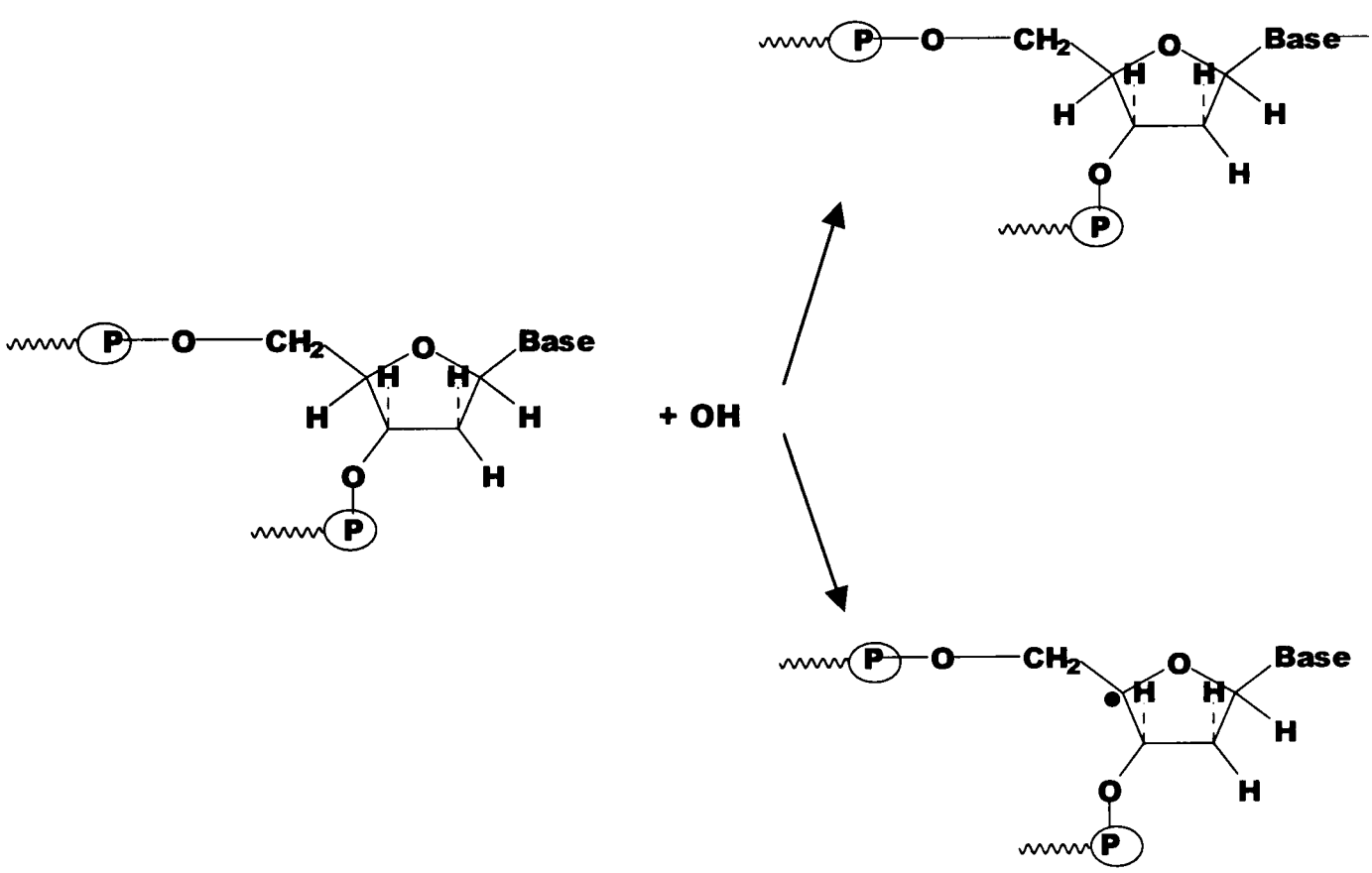

Figure 1.13.

Schematic representation of nucleotide excision repair. Note: size of excised length is not to scale (Friedberg *et al.* 1995).

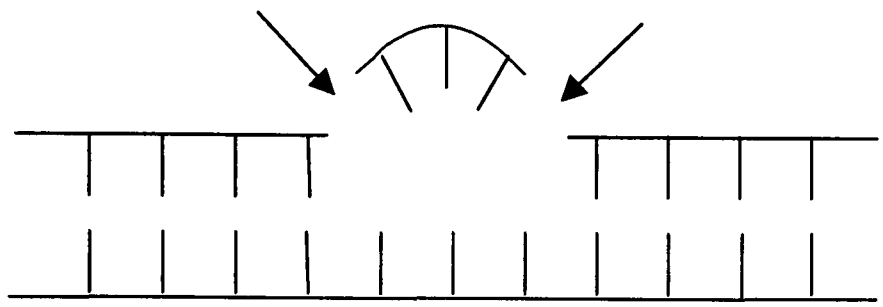

a) Excision

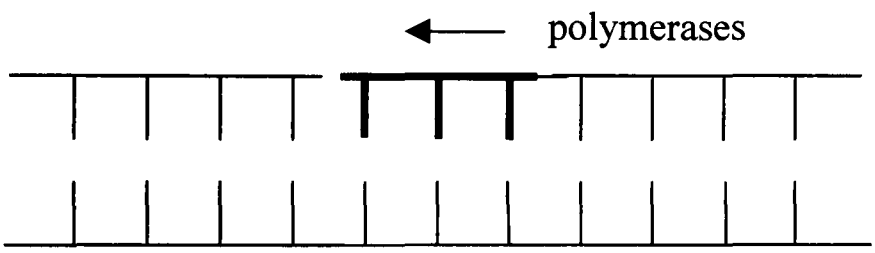

b) Repair Replication

5'

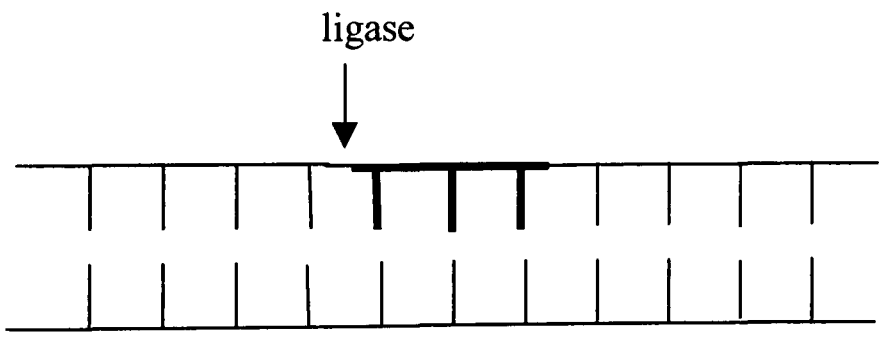

c) Rejoining

Figure 1.14.

Representation of complex damage.

a) Undamaged segment of DNA

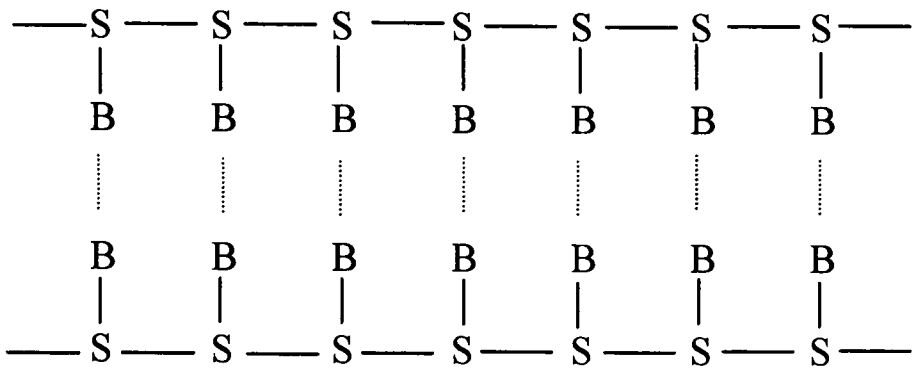

b) Simple strand break

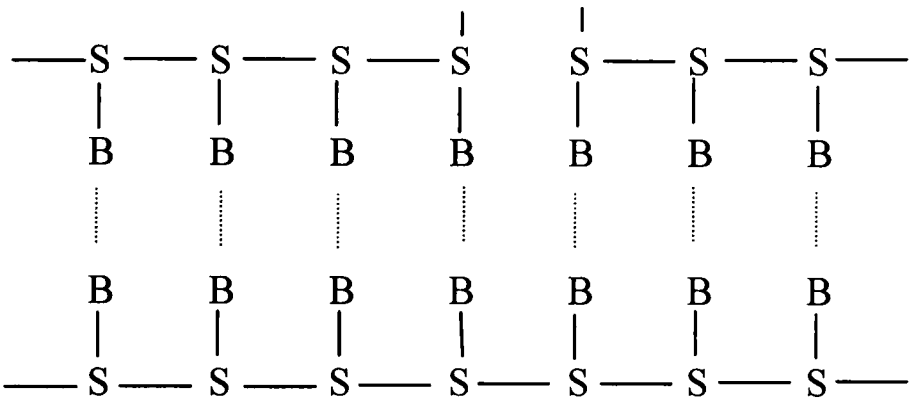

c) Complex damage site consisting of two strand breaks and a base modification in close vicinity

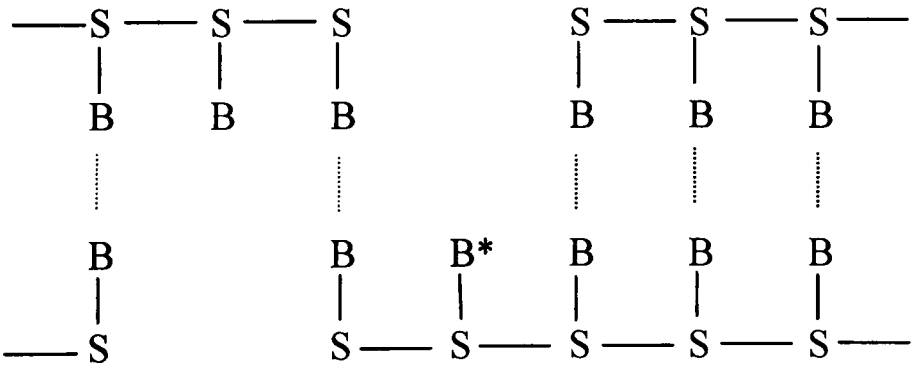

B*-Base Modification

Figure 1.15.

Low LET track illustrating representation of low energy secondary electrons.

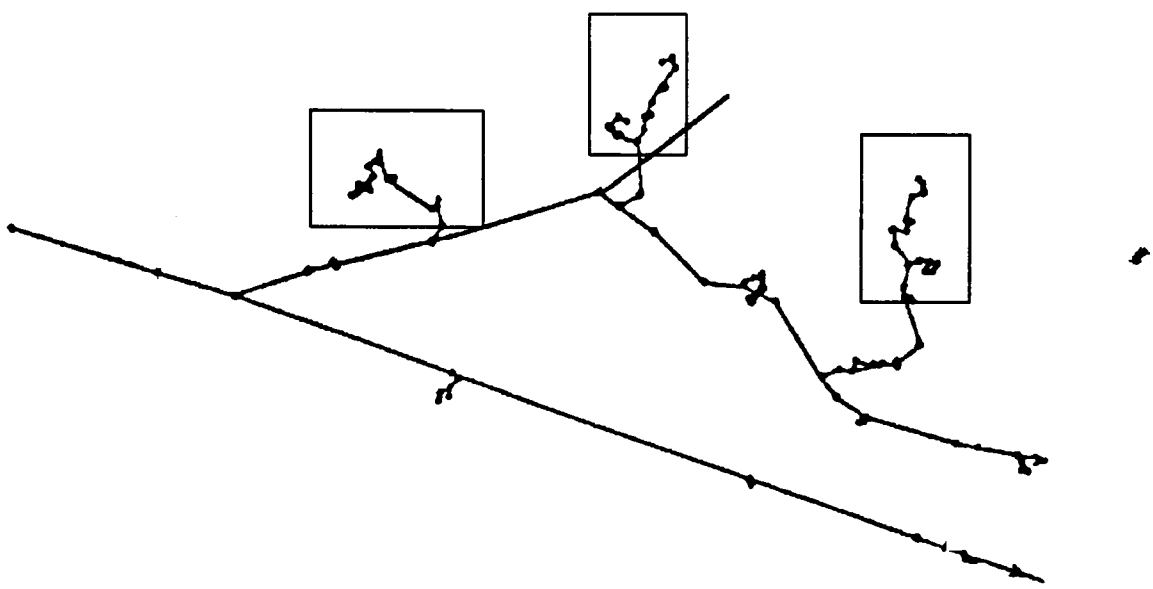

Figure 1.17.

The types of plasmid conformation depending upon degree of damage.

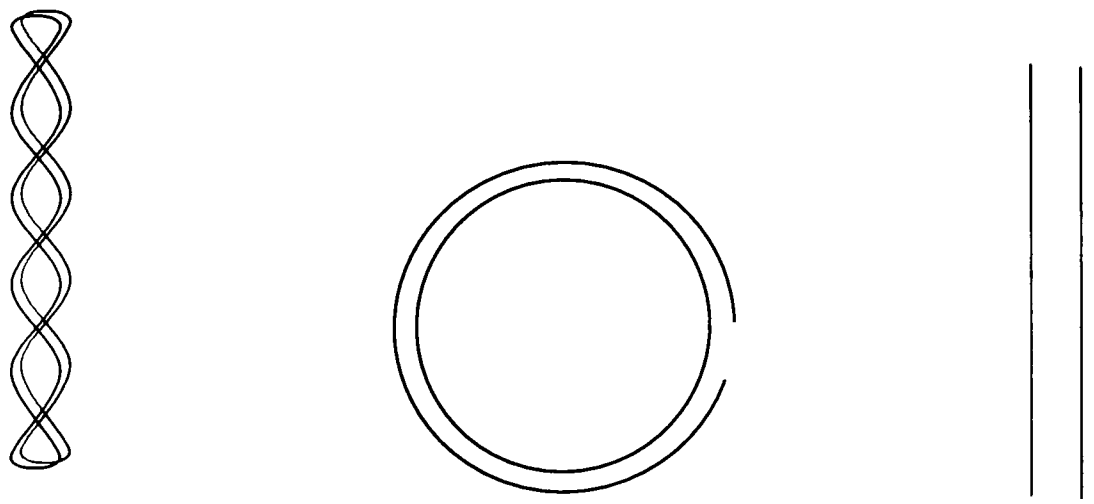

Closed Circular (≡ undamged)

Open Circular (≡ ssb)

Linear (≡dsb)

Figure 1.16.

Sample ultrasoft X-ray tracks illustrating the ionisation density on a DNA scale.

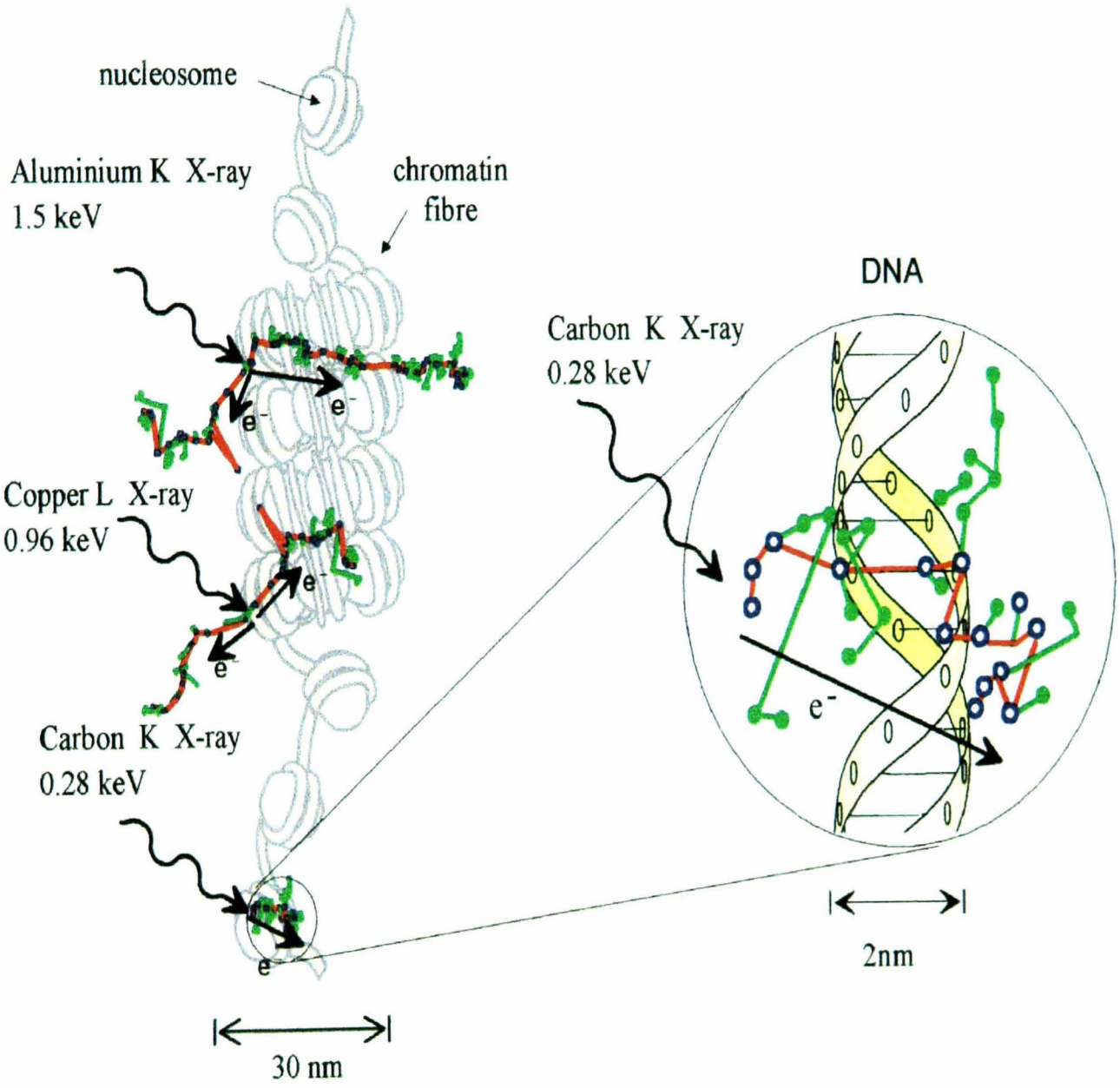

Ionisations and excitations

- primary
- secondary

Chapter 2

Materials and Methods

2.1. Plasmid Preparation

2.1.1. Culturing of E.Coli/Preparation of Solutions

A stock culture pUC18 plasmid (2686 base pairs) was obtained from an *E.Coli* HB101 (Bolivar and Backman 1979) host. All chemicals used were of the highest purity available. Yeast (autolyzed) and tryptone were both obtained from Difco laboratories.

A 5 ml ampicillin aqueous solution was made up at a concentration of 10 mg/ml, and filtered through a Millipore swinnex filter (0.22 μm). The 1 ml stock culture was split between two universals containing 5 ml of Lauria Bertani broth (10 g bacto-tryptone, 5 g bacto-yeast extract and 10 g NaCl in 1000 ml of deionized water) and 50 μl of the ampicillin solution. The two universals were sealed with paraffin paper and placed within a shaking incubator at 37^0 C, 230 rpm for 8 h.

5 g NaCl, 5 g tryptone, 2.5 g yeast and 500 ml of distilled water was added to each of two 2l flasks and the solution was adjusted to pH 7.5 by the addition of NaOH. Non-absorbent cotton wool was placed into the mouth of the flasks, the top sealed, and then the flasks autoclaved.

Three additional solutions were made up:

Solution 1: 100 ml of distilled water containing 50 mmol dm^{-3} glucose, 25 mmol dm^{-3} Tris.HCl and 10 mmol dm^{-3} EDTA adjusted to pH 8.0 was stored in the fridge following autoclaving.

Solution 2: 100 ml of distilled water containing 0.2 mol dm^{-3} NaOH and 1.0 % SDS (lauryl sulfate).

Solution 3: 100 ml of a 3.0 mol dm^{-3} potassium acetate solution containing 11.5 ml of glacial acetic acid was stored on ice prior to use.

At the end of the 8 h period, a bacterial culture was added to each of the autoclaved 2 l flasks followed by 5 ml of ampicillin solution, made up as previously descibed. The flasks were then resealed with foil and tape and placed in a shaking incubator overnight at 37^0 C and 230 rpm.

2.1.2. Harvesting and Lysis of Cells

The alkaline method for cell lysis was used as described in Sambrook *et al.* (1989) with the specifics outlined below. The contents of the two 2 l flasks were centrifuged in a JS-21 centrifuge, (Beckman) JA-10 rotor, with maximum braking at 4^0 C, for 15 min at 4000 rpm. The cell pellet was subsequently harvested by decanting off the liquid. 36 ml of solution 1 was added to the pellets that were re-suspended using a rotamixer. A lysozyme solution was prepared with the lysozyme present at a concentration of 10 mg/ml in 15 ml of 10 mmol dm^{-3} Tris.HCl (pH 8.0). The pH of the solution was adjusted to give a final pH ≥8.0, since the lysozyme becomes inactive at lower pH values. 10 ml of the lysozyme solution were then added to the pellet suspension, followed by 80 ml of solution 2. The contents of the flask were mixed and then left at room temperature for 5-10 min. 40 ml of solution 3 were subsequently added and the bottle shaken several times before placing on ice for 10 min to give a flocculent white precipitate. This was centrifuged in a JA-10 rotor, J2-21 centrifuge at 5000 rpm for 15 min at 4^0 C with zero braking. If the debris did not form a tightly packed pellet, it was necessary to centrifuge for a further 20 min. The liquid was filtered off using two pieces of cheesecloth and repeated with clean cloth after which 0.6 times the total volume of propan-2-ol was added to the filtered liquid. The solution was mixed thoroughly and stored for 10 min at room temperature before transferring to 30 ml corex tubes which were balanced prior to centrifugation at 8000 rpm for 15 min at 20^0 C with zero braking in a JS13 rotor, JS-21 centrifuge. The liquid was poured off leaving small white pellets which were washed in 70% ethanol:30% water (20^0 C). After the pellets were dried using an air line, 8 ml of TE (10 mmol dm^{-3} Tris.Cl, 1 mmol dm^{-3} EDTA, pH 8.0) was added and the tubes sealed with paraffin paper and left overnight at 4^0 C to dissolve.

2.1.3. Purification of Closed Circular DNA by Equilibrium Centrifugation in CsCl-Ethidium Bromide Gradients

The solutions from each of the tubes were pooled and for each ml of the DNA solution 1 g of CsCl was added. The solution was mixed gently and hand warmed to facilitate dissolving. 0.8 ml of a solution of ethidium bromide (10 mg/ml in water) was then added for every 10 ml of the DNA/CsCl solution which was mixed by sucking in and out of a pipette. The tube was then placed in a benchtop centrifuge and spun at

approximately 5000 rpm for 5 min at room temperature giving rise to a large amount of precipitate. The clear red solution above the precipitate was subsequently transferred to a Beckman quick seal tube and topped-up as far as possible with liquid paraffin. The tube was then sealed with a Beckman heat sealing device and a metal cap placed on top. The sample was placed in a ultracentrifuge (Beckman L-70) with a 70.1Ti rotor spun at 54k rpm for 22 h at 25^0 C with zero braking under vacuum.

At the end of the 22 h period, two bands were visible in the centre of the CsCl gradient. A relatively thin upper band is formed consisting of linear bacterial DNA and nicked circular plasmid DNA and a lower band consisting of closed circular plasmid DNA. A deep red pellet is present at the bottom of the tube consisting of ethidium bromide/RNA complexes. The lower band was extracted using a syringe inserted into the top of the tube for venting and a syringe with needle (microlance 1.1 x 40) placed into the side just beneath the lower band. The band was drawn off into the syringe and the extracted DNA mixed with a quantity of TE sufficient to give a final volume of 8 ml. This was again added to a weight in grams of CsCl equal to the volume of liquid in ml and 100 µl of ethidium bromide subsequently added. The solution was transferred to a Beckman quick seal tube and the solution centrifuged a second time as previously described.

After 22 h, the lower band was extracted from the tube as described above. The extracted fraction was then sub-divided into several Eppendorf tubes (approximately 0.5 ml in each). To remove ethidium bromide, an equal volume of water saturated butanol was added to the DNA samples in the Eppendorf tubes. The samples were then shaken and placed in a bench top centrifuge (MSE Micro Centaur) at room temperature for 3 min at 1500 rpm. After centrifugation, the aqueous, lower phase was drawn off with a plastic pipette and placed in a clean Eppendorf tube. Water saturated butanol was again added and the whole process repeated 10 times. Subsequently, the CsCl was removed from the DNA solution. The individual volumes were pooled and distilled water added to give a final volume four times the volume of the initial DNA solution. To this solution ethanol was added to double the total volume. The solution was then placed at 4^0 C overnight. The solution was transferred to Eppendorf tubes and placed in a centrifuge (Hermle Z323) at 13,000 rpm for 30 min at 4^0 C. After centrifugation, the supernatant was removed and the tubes inverted and left to dry for several hours to ensure that all of the ethanol had evaporated. The DNA was resuspended for storage in approximately 1 ml of TE (10 mmol dm^{-3} Tris.Cl, 1 mmol dm^{-3} EDTA, pH 8.0).

Samples required for current experiments were placed at 4^0 C while other samples were stored at -20^0 C.

2.2. Sample Irradiations

2.2.1. Irradiation Sources

2.2.1.1. γ-ray Irradiation

γ-ray irradiation was undertaken utilizing a sealed ^{60}Co source with peak energies at 1.173 MeV (100% abundance) and 1.332 MeV (100% abundance) and a half life of 5.26 years. Dose rates, which were determined using a Farmer type 2570 dosemeter with a type 2581 0.6cc ionisation chamber, varied between 1 Gy min^{-1} and 60 Gy min^{-1} depending upon the position of the sample relative to the source.

2.2.1.2. Hard X-ray Irradiation

Hard X-ray studies were undertaken using two different X-ray sets. A Siemens Stabilipan 1 X-ray machine was run at 250 kV (constant potential) with a compound filter of copper and aluminium, producing an X-ray spectrum with a first half-value layer of 1.2 mm of copper, giving a dose rate of 2.0 Gy min^{-1} (absorbed dose to muscle tissue). Back calculation from the half-value layer gives the mass absorption coefficient from which an average photon energy of 90 keV is calculated. A Todd Research diagnostic X-ray machine with a Machlett 50kV X-ray tube was run at 50 kV (constant potential) with an aluminium filter, producing an X-ray spectrum with a first half-value layer of 1.0mm of Al. This was run in 30 s bursts to prevent overheating, delivering 1.61 Gy (absorbed dose to muscle tissue) every 30 s. The half-value layer yields a mean photon energy of 23 keV. Dose rates were again assessed using a Farmer type 2570 dosemeter with a type 2581 0.6 cc ionisation chamber.

2.2.1.3. Ultrasoft X-ray Irradiation

An MRC cold cathode discharge tube (Goodhead and Thacker 1977, Hoshi *et al.* 1985) with the appropriate transmission target was used to produce characteristic ultrasoft X-rays (C_K, Cu_L, Al_K and Ti_K) with low bremsstrahlung contamination (<1%) as illustrated in figure 2.1. The characteristics of these X-rays are tabulated in table 2.1.

Detailed descriptions of the irradiation facility and dosimetry with the various targets are given elsewhere (Goodhead and Thacker 1977, Hill *et al.* 1997, 1998, Goodhead *et al.* 1979, 1981). The cathode potential and plasma current used for these experiments are given in table 2.2. The X-rays, produced by electron bombardment of the target, travel 5.4 cm through a flight tube continuously flushed with helium (hydrogen for C_K X-rays) at atmospheric pressure irradiating the plasmid through the Hostaphan base of the dish on which the plasmid was spread. Dosimetry was carried out using an air filled ion chamber (Neary 1970) (internal diameter 0.8 cm, volume 0.1 cm^3) with a 0.248 mg cm^{-2} aluminium window for the Cu_L, Al_K and Ti_K X-rays and a 25 μg cm^{-2} carbon window for carbon X-rays. Measurements of the ionization current were made before and after each experiment using a Keithley 616 electrometer with the ion chamber window positioned 1mm behind an empty Hostaphan based irradiation dish. Corrections were made for the variation in X-ray intensity across the sample. These experimentally determined correction factors for calculating the area weighted mean intensity over the whole sample compared to that measured at the centre are tabulated in table 2.2. The absorbed dose rate, $\dot{D}_s$, at the incident surface of the sample can be calculated from the photon fluence rate, ϕ, using

$$\dot{D}_s = \phi \left(\frac{\mu_{en}}{\rho} \right)_{\text{water}} E$$

where $(\mu_{en}/\rho)_{water}$ is the mass energy absorption coefficient of water (the value of which, at these low energies is equal to the mass attenuation coefficient $(\mu/\rho)_{water}$, given in table 2.1) for X-rays of energy, E. These ultrasoft X-rays are significantly attenuated by the sample (Henke *et al.* 1993), therefore the mean absorbed dose rate, $\dot{D}_m$, in a sample of thickness, x and density, ρ, was calculated using

$$\dot{D}_m = \dot{D}_s \frac{1 - \exp(-(\mu/\rho)_{water} \rho\ x)}{(\mu/\rho)_{water} \rho\ x}$$

The calculated mean to surface dose rate ratios and typical mean absorbed dose rates for a 7.8 μm thick sample with a density of 1 g cm^{-1} are tabulated in table 2.2 for the various ultrasoft X-ray energies.

2.2.1.4. α-particle Irradiation

Alpha particle irradiation of the solutions took place at a dose rate of approximately 24 Gy min^{-1} utilising the ^{238}Pu α-particle source with emission energies of 5.499 MeV (71.1%abundance) and 5.457 MeV (28.7% abundance) and a half life of 88 years (Goodhead *et al.* 1991). The basic set-up is illustrated in figure 2.2. The gas-tight volume between the irradiation dish and the containment chamber window is flushed with helium preventing condensation on the dish bottom which would reduce the energy and potentially the fluence of the α-particles incident on the plasmid solution. Energy measurements made using a silicon barrier detector at a position in air 3 mm above the dish base revealed an α-particle spectrum (after correction for the additional air path) with a peak energy of 3.31 MeV and a half-width at half-height of 0.25 MeV as reported by Jenner *et al.* (1993). The conversion of the energy spectrum to LET in water gives an average LET of 120 keV μm^{-1}. The absorbed dose-rate was calculated by flux measurements using CR-39 plastic track detectors (Cartwright *et al.* 1978). The measured fluence was then converted to a dose by using the mean LET of 120 keV μm^{-1} (Stevens 1989).

2.2.2. Irradiation Vessels

2.2.2.1. γ-ray

Straight 0.5 ml glass tubes or Eppendorf tubes were used when irradiating in air. Glass tubes with side arms were used when the DNA solutions were irradiated under hypoxic conditions.

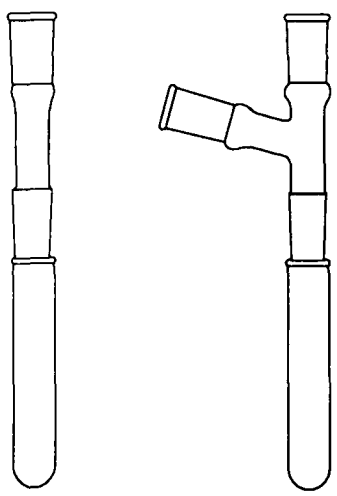

a) Straight arm glass plasmid vessel

b) Side arm glass plasmid vessel

2.2.2.2. Ultrasoft and Hard X-ray or α-particle

For all these irradiations, the plasmid solution was irradiated in glass-walled irradiation dishes (3 cm internal diameter, 3.6 cm external diameter) made with bases of 0.35 mg cm^{-2} (~2.5 μm) of Hostaphan (polyethylene terephthalate, manufactured by Hoechst). The radiation passes through the Hostaphan base before being incident on the DNA solution as illustrated in figures 2.1 and 2.2.

2.2.2.3. Independence of Strand Break Yield on Irradiation Vessel

Comparisons were undertaken with γ-ray irradiation of plasmid DNA solutions either in Eppendorf tubes, glass tubes or in Hostaphan dishes with the set-up and recovery procedures used for USX and α-particle irradiations as described in sections 2.2.2.2 and 2.3.3.2. It was found that for a given dose, there are no significant variations in the yields of strand breaks with the irradiation vessels once the necessary dose evaluations have been undertaken. Thus, any differences in the yields of DNA damage resulting from different radiation sources may be attributed to the nature of the radiation rather than variations in the radiation vessel.

2.3. Sample Preparation and Irradiation

2.3.1. DNA Stock Solutions

The DNA stock which is stored in TE (10 mmol dm^{-3} Tris.Cl, 1 mmol dm^{-3} EDTA, pH 8.0) at a concentration of 0.5 mg/ml is greater than 95 % in the undamaged, closed circular form. The concentration of DNA was determined spectrophotometrically utilising a spectrophotometer (Beckman DU 7400). The optical absorbance was determined at 260 nm for diluted DNA solutions in a 1 cm quartz cuvette. To correct for any optical absorption from either the TE or the quartz cuvette, optical absorbance of the DNA solution was measured relative to a blank cuvette containing only TE. A ratio of OD_{260}/OD_{280} was also determined to assess for protein contamination of the sample. This ratio was determined to be 1.98 within the quoted range of 1.8 to 2.0 for pure DNA samples (Sambrook, 1989).

2.3.2. Preparation of DNA Solutions

Unless otherwise stated, scavenging concentrations specific to each irradiation were obtained by the appropriate dilution of a stock, 1 mol dm^{-3} solution of Tris (pH 8.0) with distilled water. In a small number of experiments scavenging concentrations specific to each irradiation were obtained by the appropriate dilution of a stock 1 mol dm^{-3} solution of ethanol obtained by dilution of absolute ethyl alcohol with distilled water. The required volumes of the relevant diluted scavenger solution were then added to the plasmid stock to give plasmid concentrations as required. At all times the DNA/scavenger solutions were maintained at 4^0 C. For irradiations in glass tubes or Eppendorf tubes, unless otherwise stated, the plasmid stock solution of 0.5 mg/ml was diluted by a factor of 20 with a scavenging solution of specific concentration for examination. For irradiations in Hostaphan dishes, unless otherwise stated, the plasmid stock solution of 0.5 mg/ml was diluted by a factor of 10 with a scavenging solution, at a concentration specific to each experiment.

2.3.3. Irradiating Conditions

2.3.3.1. γ-ray Irradiation Conditions

20μl of the plasmid/scavenging solution was added to the glass tubes or Eppendorf tubes. In the case of irradiation in Eppendorf tubes, the lids were kept open. The DNA solutions were placed in a slide box of dimensions 10.5 cm length, 4 cm width and 4 cm height and subsequently irradiated at either 20^0 C or at 4^0 C. For irradiation at 20^0 C, samples were kept upright within the slide box by damp sawdust. For irradiations at 4^0 C, the slide box was filled with ice. To ensure secondary charged particle equilibrium the slide box containing the DNA solutions was placed on a 9 mm thickness of polmethylmethacrylate (perspex), through which it was irradiated.

Aerobic Conditions

All aerobic irradiations were carried out in Eppendorf or glass tubes without side-arms. Due to the high doses and dose rates used with the γ-ray source, there existed the possibility of oxygen depletion within the DNA solution during the irradiation. Irradiations in the dose range 500 to 2000 Gy were given either as single doses or fractionated (125 Gy/fraction) with the sample being shaken to re-equilibrate with air

between each fraction. No difference was found in the dose response between these two regimes, indicating that any oxygen depletion was not present at levels sufficient to modify the yields of DNA damage. When experimental doses greater than 2000 Gy were required these were given in fractions ≤ 500 Gy.

All post irradiation treatment takes place in the radiation vessel and in all cases the DNA solutions were kept on ice prior to any subsequent treatment.

Anaerobic Conditions

To obtain anaerobic conditions DNA samples present in glass tubes with sidearms were gassed with either N_2O (BOC) or N_2 (Air Products). The radicals present, and their relative yields, following ^{60}Co γ-ray irradiation under the various gassing conditions are summarised in table 2.3. In air, electrons are removed via an interaction with oxygen at a reaction rate constant of $1.9x10^{10}$ dm^3 mol^{-1} s^{-1} (Buxton *et al.* 1988). Under nitrous oxide, electrons are effectively converted into OH radicals; $e_{aq}^- + N_2O \rightarrow OH^- + {}^{\cdot}OH + N_2$ with a reaction rate constant of $9.1x10^9$ dm^3 mol^{-1} s^{-1} (Buxton *et al.* 1988).

A pre-bubbler, present to ensure that the gases are hydrated, was gassed for 30 min to remove all dissolved oxygen present within the water. Gassing then continued for a further 15 min prior to irradiation of the DNA solutions present, and during the irradiation. To ensure that the gassing regime employed resulted in hypoxic conditions, a solution was made up containing 1 mmol dm^{-3} methyl viologen (1,1'-dimethyl-4,4'-bipyridinium dichloride) and 0.1 mmol dm^{-3} sodium formate and gassed with N_2 as outlined above, before being irradiated with doses equivalent to those received by the plasmid solutions. The reactions that arise are outlined below.

$$ {}^{\cdot}OH + HCO_2^- \longrightarrow CO_2^{\cdot -} $$

$$ CO_2^{\cdot -} (e^-_{aq}) + MV^{2+} \longrightarrow MV^{\cdot +} $$

Colourless Blue

O_2

It was found that following the conditions outlined above, a blue solution is obtained representative of the presence of the reduced form of methyl viologen ($MV^{\cdot +}$). This confirms that gassing conditions are adequate to remove oxygen. Following irradiation, the DNA solution was subsequently transferred to an Eppendorf tube where any post irradiation treatment took place. In all cases the solutions were kept on ice prior to any subsequent treatment.

2.3.3.2. Ultra-soft and Hard X-ray and α-particle Irradiation Conditions

5 μl of the plasmid/scavenging solution was placed in Hostaphan dishes and a CR-39 plastic disc (2.84 cm diameter) positioned on top of the plasmid solution and rotated to facilitate even spreading of the solution over the entire surface area of the Hostaphan. Subsequent confocal microscopic analysis (Townsend *et al.* 1990) revealed an average thickness of the plasmid solution of 7.8 μm from six individual measurements, consistent with the calculated thickness (see section 2.3.4 for details).

Two 5 μl droplets of Tris solution, at a concentration equal to that of the irradiated solution, were placed on top of the CR-39 and a steel dish lid was placed over the sample container, both in order to minimise evaporation of the solution during the course of the experiment. All X-ray and α-particle experiments were undertaken, unless otherwise stated, at 4^0 C. To cool the solution during the course of the irradiations the dishes were placed within the irradiation rig at room temperature and cooled for 7 min prior to irradiation. Cooling was achieved by using a chiller thermo-circulator (Churchill Inst. Co. Ltd., Perivale, U.K.) which pumped a water/anti-freeze mix through a jacket surrounding the dish, ensuring that the samples were maintained at $\leq$ 4^0 C for the entire course of the irradiation.

To check whether 4^0 C was a sufficiently low temperature to ensure no strand breakage from heat labile sites, a constant dose approximately equal to that which on average will give one break per DNA molecule (D_{37}-see section 2.4.2.1), was given to the DNA solutions. These solutions contained 1 mmol dm^{-3} Tris and were maintained at temperatures ranging from 2^0 C to 10^0 C. Over this temperature range, no increase in strand break yields was observed and all values were lower than an equivalent experiment run at room temperature where heat labile sites are considered to be present. Thus, 4^0 C was considered an appropriate temperature to undertake experiments so that in the event of small fluctuations in temperature the sample is maintained at a temperature sufficiently low to ensure that strand breakage from heat labile sites is minimised.

In addition, it is necessary to ensure that the 7 min cooling period is sufficiently long for the sample and dish to reach 4^0 C prior to irradiation. Analysis using a type K, Nickel Chromium/Nickel Aluminium thermocouple together with a Kane-May 2013 temperature readout indicated that the desired temperature of 4^0 C was reached within

2-3 min of cooling. Hence 7 min was considered sufficient to ensure a sample temperature of 4^0 C.

Following irradiation, samples were subsequently recovered by removing the CR-39 and adding 25 μl of ice cold, 10 mmol dm^{-3} Tris. The CR-39 was then replaced and rotated to facilitate recovery from both the mylar and CR-39 surfaces. Typically 25 μl of the plasmid was recovered at an approximate concentration of 8 μg/ml. In all cases the DNA solutions were kept on ice prior to any subsequent treatment.

2.3.4. Confocal Analysis

The depth of the plasmid solution when irradiating with USX is of prime importance when determining the average dose that a sample receives. This is particularly true with C_K and Cu_L USX which have a very short attenuation length (see table 2.1). For accurate determinations of the dose to the DNA it is necessary to obtain accurate measurements of solution thickness. Confocal microscopic analysis of the plasmid layer was undertaken using a Biorad MRC 600 confocal inverted microscope with an Ar ion laser giving a line at 488nm. The image was viewed using a x60 oil objective lens and analysed using Biorad Comos software. Measurements were underaken on unirradiated samples, but following the same preparation and cooling procedure as for those which were to be irradiated. It is then assumed that such measurements can be applied to irradiated samples. As a result of variation in the spread of a sample over the Hostaphan base of the irradiation dishes it is necessary to undertake a number of measurements for an average thickness to be determined. To visualise the distribution of DNA on the Hostaphan, a propidium iodide stain was utilised which binds to the DNA. An average sample thickness of 7.8 μm was determined. An alternative estimate of sample thickness was made by considering uniform spread of the 5 μl DNA solution over an area defined by the CR-39 cover slip. For a diameter of 2.84 cm a predicted average thickness of 7.84 μm was determined consistent with the experimentally determined value.

Control runs were also undertaken to assess the degree of non-specific fluorescence of the propidium iodide i.e. the visibility of the stain in the absence of DNA. These measurements were undertaken after a period of 7 min cooling analogous to the experimental set-up and showed no significant non-specific fluorescence. Studies were also undertaken to reveal how this thickness varied with time to examine the effects of

evaporation which would have to be considered when long irradiation periods were used. For cooling periods up to 1 h, no significant alterations in solution thickness were determined. For times in excess of this, two subsets were apparent, a group which showed significant reduction in thickness and those in which no alterations were measured. Those in which thickness measurement changes were observed also showed evaporation of the droplets placed upon the CR-39. It was interpreted that such samples were not completely sealed, possibly as a result of small holes in the Hostaphan/dish wall join. If during experiments such evaporation was indicated then these samples were rejected. In addition, analysis was undertaken to show the plasmid DNA distribution throughout the layer. It was apparent that the plasmid DNA was distributed evenly throughout the solution with no accumulation on either the Hostaphan or CR-39 surfaces. The determination of the solution thickness of 7.8 μm can therefore be applied with confidence to be representative of the average DNA solution thickness.

2.3.5. Dialysis

If it were necessary to exchange the buffer in which the plasmid DNA was dissolved, a Pierce System 100 Microdialyzer fitted with dialysis membrane was used. Typically, 75 μl of the stock plasmid solution (see section 2.3.1) was placed into a well and the reservoir was filled with the buffer into which the plasmid is exchanged. The volume of the Microdialyzer reservoir is typically 100 ml. A magnetic stirrer present within the reservoir was placed under the well containing the plasmid and the set-up left to exchange the buffer for a minimum of 2 h. Throughout the dialysis procedure the whole apparatus was kept at 4^0 C in a cold room. Typically 60 μl of the 75 μl DNA solution placed within the well was recovered.

2.4. Post Irradiation Treatment

2.4.1. Enzyme Treatment-The Excision of Base Damage

The effects of two enzymes, formamidopyrimidine-DNA glycosylase (Fpg protein) and endonuclease III (Nth) purified from the overproducing E. coli strains JM105/pFPG230 and $\lambda N99_{cI857}$/pHIT1 respectively were examined (Generous gift from Prof. R.Wood ICRF). These enzymes excise specific base damages (table 2.4) to convert the site into a single strand break. For experiments involving the determination of base damage

yields, all DNA solutions, irrespective of gassing conditions, irradiation source and whether enzymes were to be subsequently added or not were stored on ice and subsequently ethanol precipitated. To each DNA sample solution, $1/10^{th}$ of its volume of 3 mol dm^{-3} Na acetate and three times its volume of ethanol were added. Samples were left at -20^0 C for a mimimum of 30 min and placed in a centrifuge (Hermle Z323) at 13,000 rpm for 30 min at 4^0 C. Following centrifugation, all liquid was decanted and the DNA pellets placed within an evaporator (Jouan RC 10.10.) connected to a cold trap (Jouan RCT 90) and a pump (Javac DD75) for 20 min to remove any excess ethanol. A total volume of 20 μl of activation buffer and enzyme was then added to each sample tube containing the DNA which has either been irradiated or represents an unirradiated control. Enzyme buffer consisted of 0.5 mmol dm^{-3} EDTA, 0.1 mol KCl, 40 mmol dm^{-3} Hepes, 0.5 mmol dm^{-3} dithiothreitol (DTT) and 0.2 mg/ml bovine serum albumin (BSA) at pH 8.0 (Melvin *et al.* 1998).

An Fpg stock (21 ng/μl) was stored at -20^0 C within a medium consisting of 50 % glycerol, 100 mmol dm^{-3} potassium phosphate, 0.1 mol dm^{-3} DTT, and 0.00 5% Triton X-100 at pH 6.6 (Asahara *et al.* 1989). An Nth stock at a concentration of 1.3 ng/μl was stored under similar conditions to that for Fpg. The desired quantity of enzyme to be added was determined by undertaking titrations by varying the quantities of enzymes, between 0.2μl to 5μl of the respective stocks and determining the amount of damage detected following an irradiation of approximately 50 Gy relative to irradiated samples with no enzyme present. Over this concentration range there is no variation in the yields of ssb and so addition of 1 μl of enzyme to 19 μl of the activation buffer for each DNA solution was considered to be optimal for enzyme analysis of base damage (42 ng Fpg/μg DNA, 2.6 ng Nth/μg DNA). For all DNA solutions, either irradiated or unirradiated, in the presence of enzyme, an equivalent sample was prepared under identical conditions by adding 20 μl of activation buffer but no enzyme. In both cases, the buffer or buffer/enzyme solution was squirted up and down the sides of the Eppendorf tube to ensure resuspension of the DNA. Samples were then incubated in a water bath at 37^0 C for 30 min in the case of the Nth and 1 h for the Fpg (Melvin *et al.* 1998). At the end of the incubation time, 5 μl of 0.5 mol dm^{-3} EDTA was added to stop the action of the enzyme. Samples were then placed on ice before the addition of loading buffer and analyzed by gel electrophoresis as described in section 2.4.2.

For the analysis of the additive effects of Nth and Fpg the ethanol precipitation procedure is undertaken as described above. As previously, a total volume of 20 μl of activation buffer and enzyme is then added to each sample tube. However, four sets of samples are assessed. The control set has only 20 μl of activation buffer added and the individual analysis of the effects Nth and Fpg require 19 μl of activation buffer and 1μl of the specific enzyme at concentrations as described above to be added. A final set of samples have 18 μl of activation buffer added and 1μl of Nth (1.3ng/μl) and 1μl of Fpg (21ng/μl) added. All samples are then incubated for 30 min at 37^0 C. All other post enzyme treatment and quantification is as described previously.

2.4.2. Agarose Gel Electrophoresis and Quantification

Irrespective of the radiation source, the radiation vessel and any post irradiation treatment, the determination of the amount of damage present within DNA was carried out under identical conditions by quantification of the yields of ssb and dsb. Prior to electrophoresis, a volume of loading buffer (0.1 % bromophenol blue, 30 % sucrose in TBE (89 mmol dm^{-3} Tris, 89 mmol dm^{-3} boric acid, 2 mmol dm^{-3} EDTA)) equal to half that of the recovered sample was added to the DNA solution. 20 μl of each of the DNA solutions was then placed in a well of a 1 % agarose (Sigma Type 1-A) gel in TBE at pH 7.1. Samples were subsequently run at typically 74 mV cm^{-1}, 6 mA for 17 h at 4^0 C unless otherwise stated.

Following electrophoresis the gel was stained with 30 μl of ethidium bromide (10 mg/ml) in 600 ml of TBE for approximately 1 h at 4^0 C. The gel was visualised using a UV transilluminator and the image produced using a charge coupled device (CCD) camera. Images were stored either as TIFF files on an Apple Macintosh and the relative proportions of different plasmid forms (See section 1.9 for plasmid description) determined using Collage (Fotodyne) software or as 1-D scans on a PC and analysed with Quantity One (Bio-Rad Laboratories) software. To account for the lower binding efficiency of ethidium bromide with the closed circular form, intensities within this band were multiplied by a factor of 1.4 (Milligan *et al.* 1993). Each lane of a gel was analysed individually and the relative proportions of the different forms of the plasmid present within that lane determined. Subsequently any variation in loading efficiency between lanes did not lead to errors in determination of the amounts of the different plasmid forms.

2.4.2.1. Strand Break Determination

For each radiation and scavenging concentration, a dose response for the loss of the closed circular plasmid was determined at the scavenging capacity specified. From the slope of this response, a D_{37} was calculated which, assuming Poisson statistics for strand breaks, represents the dose required to give on average one strand break per plasmid. Assuming the average mass of a base pair to be 650 Daltons and pUC18 to be 2686 bp in length, the single strand break (ssb) yield per Gray per Dalton is given by

$$\text{ssb/Gy/Da} = \frac{1}{(D_{37} \text{x} 2686 \text{x} 650)}$$

In the case of DNA double strand breaks, the proportion of linear plasmid present was determined and its dependence upon dose determined. Dependences were determined by plotting the proportion of linear plasmid DNA against dose and either a linear or quadratic line fitted to the data and an equation of the line calculated. To obtain the ssb:dsb ratio, the amount of dsbs present at a dose corresponding to the D_{37} for ssb was determined by inserting the D_{37} dose into the equation describing the dependence of the amount of linear plasmid on dose For each irradiation type and scavenging concentration, experiments were repeated at least three times.

2.4.2.2. Base Damage Determination

Dose responses for base damage, revealed as additional ssb and dsb by the action of enzyme, were determined for a fixed scavenger concentration for two sets of data, one with and one without the enzyme present, but with all other sample procedures and preparations identical. In all cases, the variation in closed circular form with dose, from which the corresponding D_{37} (section 2.4.2.1) was obtained, is determined from a minimum of 6 independent dose points. Because of the post irradiation incubation treatment (section 2.4.1) for all samples irrespective of whether they contained enzyme, heat labile sites are also included within the yields of ssb and dsb determined (section 1.6.2.3). When the dependence of the induction of enzyme sensitive sites, visualised as strand breaks, with dose is determined with enzyme present, the dose response is a measure of the number of prompt + heat labile strand breaks plus base damage sites. Thus, the ratio of the gradient of the loss of closed circular form with dose with the enzyme present:gradient with no enzyme present represents the ratio of (ssb prompt + heat labile ssb sites + base damage sites):(ssb prompt + heat labile ssb sites). In effect the ratio of gradients is equal to (base damage sites:ssb prompt + heat labile ssb sites) +

1. An approximation of base damage yields is therefore obtained assuming that heat labile sites do not contribute significantly to the total number of ssb determined i.e. the ratio of gradients is given by ssb prompt + base damage sites:ssb prompt. Therefore the presence of heat labile sites will result in an underestimation of the number of base damage sites experimentally determined. One other feature of the method results in an underestimation of base damage yields. Plasmid DNA which contains both a strand break site and a base damage site, which are sufficiently spatially separate to not give a dsb, will be undifferentiated within the detection system from DNA which contains only a single strand break. This is equivalent to the case of multiple ssbs being detected as only one single ssb which must be corrected via Poisson statistics or else minimised by using radiation doses at a level where only a small proportion of doubly hit sites are present.

A determination of the number of base damage sites/Gy/Da may readily be calculated at a specific scavenging capacity by simply multiplying a previously determined ssb/Gy/Da value (as calculated in section 2.4.2.1) by the number of base damage sites per ssb.

A measure of the complexity of damage associated with a given radiation may be determined from the ratio of dsb gradients with dose with and without enzyme present in a manner analogous to the determination of the yield of base damage sites by the ratio of ssb gradients as described above. The increase in dsb gradient may be attributed to sites of base damage being converted to single strand breaks by the enzyme in close proximity to pre-existing ssbs or another enzyme sensitive site on the complementary strand. Again this yield represents a lower estimate, as dsbs formed by the conversion of base damage sites into ssb on plasmids with pre-existing dsbs will not be recorded.

2.4.2.3. Treatment of Experimental Errors

For all experimental determinations of the yields of ssb, dsb and base damage sites all experiments are repeated a minimum of three times with the mean calculate to obtain adequate statistics. With one exception, where error bars are displayed they represent the standard deviation around this mean value. However, for the variation in OH yield with radiation energy as discussed in chapter 7 error bars are plotted as representing either the standard deviation as above or the error within the experiment, whichever is the greater. As a result of sample evaporation during the course of the experiment the mean sample dose may vary with constant incident dose. A mean sample thickness of

7.8 μm is determined, with error bars based on sample thickness varying between 9 and 5 μm and the corresponding error in the dose that such a variation will result in.

2.5. Independence of Strand Break Yields on Plasmid Concentration

From a conceptual point of view, the yield of ssb/Gy/Da should be independent of the concentration of plasmid for very dilute solutions. An increase in the plasmid concentration will result in an increased number of individual plasmids receiving damage per unit dose. However the ratio of undamaged:damaged plasmids should remain constant. This will remain true as long as the concentration of plasmid is negligible relative to the concentration of water molecules and hence radiation induced OH radicals in the solution surrounding the DNA.

To check that this assumption is valid for the range of plasmid concentrations used experimentally, a constant dose, sufficient to reduce the closed circular plasmid component to approximately 50 %, was given to a range of plasmid concentrations and the ssb yields determined. DNA stock as described in 2.3.1 was diluted with 10 mmol dm^{-3} Tris to produce several different solutions containing different concentrations of DNA as shown in table 2.5. Following irradiation, samples were diluted to the same concentration to avoid any possible concentration effects during analysis. Electrophoresis and quantification were then carried out as described in section 2.4.2.

From this analysis it was established that over the concentration range examined the yield of ssb is independent of the DNA concentration, in agreement with the observations of Milligan *et al.* (1993). Thus, for all subsequent experiments any error in precise plasmid measurements are not significant in the determination of strand break yields.

2.6. Dependence of DNA Damage Yield on Humidity

In order to examine the role of humidity in damage induction in irradiated, dried plasmid DNA it is necessary for sample preparation to induce minimal damage. A number of factors were varied and their influence on damage yields assessed. The influence of plasmid buffer was assessed by using either solutions of stock plasmid (10 mmol dm^{-3} Tris) or else plasmid DNA transferred into alternative buffers using the dialysis apparatus described in section 2.3.5. Unless otherwise stated 5 μl of the plasmid within the respective buffer was then placed onto a borosilicate glass cover

slip. In a small number of experiments, the DNA solution was placed onto graphite coated glass slides which were manufactured using a universal electron microscope shadow casting jig (Metrovac, AEI Ltd) in order to examine the importance of the surface characteristics of the borosilicate cover slips surface in generating DNA damage. For the majority of studies cover slips were not washed, however, where stated, cover slips were washed in acetone followed by distilled water and dried with an air line prior to the addition of the plasmid solution. Where specified, 1 μl of Tween 80, (Polyoxyethylene Sorbitan Monooleate) diluted by a factor of 5000 was placed onto the surface of the slides after washing, prior to the addition of the plasmid. Unless stated otherwise, after the addition of the plasmid solutions the cover slips or slides were placed onto a plastic petri dish and then either placed directly into a controlled humidity environment or else freeze dried for variable lengths of time using a micro-modulyo freeze drier (Edwards). In the latter case after the freeze drying procedure the DNA was either recovered or the petri dish containing the slide was transferred to the humidity controlled area, under equivalent conditions to those samples which were not freeze dried. The controlled humidity environment was obtained by placing 2 ml solutions of NaOH or NaCl, contained within a petri dish, ensuring separation from the DNA samples, at variable, but known concentrations, into a polyethylene box (100 mm x 100 mm x 65 mm, Merck Ltd). The concentration of the NaOH or NaCl solutions determined the humidity within the box, with the relationship between NaOH concentration and humidity summarised in table 2.6. For comparison, a saturated solution of NaCl results in a humidity of 75.28 % (Stokes 1949). For analysis with 100 % humidity, the same procedure was followed but with the addition of 2 ml of distilled water instead of NaOH or NaCl solutions. A volume of 2 ml of the NaOH or NaCl solutions was chosen as preliminary tests indicated that after 24 h a significant proportion of this solution was still present. Thus the humidity was at a value dictated by the presence of the NaOH or NaCl solutions. Once the DNA samples had been placed within the box, it was sealed and left for 24 h and maintained at room temperature. Preliminary results indicated that samples left in the humidified environment and exposed to daylight, yielded excessive amounts of damage relative to equivalent experiments run in the dark. It is proposed that this is a result of trace amounts of ethidium bromide still present within the plasmid, and so all samples placed within the humid environment were kept in the dark. Following freeze drying 3 water

molecules are anticipated to remain associated with the phosphate (Swarts *et al.* 1992). Thus the total molar mass of nucleotides will be approximately 414 g. Approximately 10 additional water molecules are bound to a nucleotide at a humidity of 70 % (Saenger 1988) resulting in an increase of mass of 180 g. It is therefore anticipated that an increase in mass of 43 % following freeze drying will signify that the DNA is in equilibrium with the environment when placed in a humidity of 70 %.

Samples were left in the humid environment for 24 h, as determinations of increases in the mass of calf thymus DNA following freeze drying indicated that >15 h was required for DNA hydration to reach equilibrium as illustrated in figure 2.3. The procedure involved freeze drying calf thymus samples for 18 h at the end of which each DNA sample was weighed and then placed in an individual 70 % humid environment where the humidity was set with NaOH as described above. At intervals, a DNA sample was removed from its humid environment, weighed and the fractional increase in mass determined. This was repeated for a number of samples with the time present within the humid environment ranging from 2 - 24 h.

For all analysis undertaken, DNA samples were recovered by adding 45 μl of 10 mmol dm^{-3} Tris. For those samples placed within the humid environment recovery took place either immediately after the 24 h period or after a variable period of time during which the DNA sample was removed from the controlled environment and left at room temperature to re-humidify. For those samples which were only exposed to freeze drying, recovery took place immediately after the freeze drying procedure.

2.7. Computer Simulations

Simulations were undertaken for Al_K USX and α-particle irradiation to determine the dependence of strand break yields on scavenging capacities and the values simulated compared with those measured experimentally following Al_K USX and α-particle irradiation. The computer simulations for these radiations are as described below.

2.7.1. Al_K USX Simulation-Single Electron

From table 2.1 it may be seen that an Al_K USX source produces photons of 1.5 keV which interact almost exclusively via the photoelectric effect producing a range of photo-electrons with variable probability with the most frequent being of 0.96 keV and an Auger-electron of 0.52 keV (Nikjoo *et al.* 1994a) (in aqueous solution > 99 % of

these interactions are with water). To simulate Al_K USX irradiation, a Monte Carlo track structure simulation code CPA100 (Terrissol and Beaudré 1990) was used to follow the history of individual 1.5 keV electrons interacting in liquid water. The code was developed to simulate the radiation chemistry of water (Terrissol *et al.* 1989). It follows the course of each primary and all secondary electrons generated until they reach thermal energies. For each inelastic collision the electrons undergo, the location, the amount of energy exchanged, the type of interaction and the time of the event is recorded. The species that are subsequently produced from each interaction are then followed and their interactions monitored as summarised in table 2.7. The likelihood of interactions, the reaction probabilities i.e. how much energy is exchanged and the types of species generated, are based on reaction cross sections which are obtained from various sources (summary in Paretzke *et al.* 1995). The order of events may be summarised as follows. Initially in the physical stage ($\leq 10^{-15}$ s) the co-ordinates and types of interaction taking place are determined. The co-ordinates and identities of these physical interactions constitute the physical track. During the pre-chemical stage at 10^{-15}-10^{-12} s the ionised and excited water molecules undergo reactions leading to the formation of water radicals and molecular products. The co-ordinates and identities of the radicals and molecular products generated constitute the chemical track.

To determine the amount and type of damage to a DNA target, the physical and chemical track generated by the passage of the single incoming electron of 1.5 keV is placed within the centre of a virtual sphere. The dimensions of the sphere are such that it contains all of the interactions associated with the electron track. A linear segment of DNA of 216 bp length is then randomly placed, using the method of μ-randomness (Kellerer 1975), within this sphere. The volume model of DNA used is as described in Nikjoo *et al.* (1994a) based on the dimensions of B-DNA (Dickerson *et al.* 1982). It consists of distinct volume regions of sugar-phosphate moiety and bases without any additional complexity of the structure being introduced. The sugar phosphate chain wraps helically around the central cylinder, which has a diameter of 1 nm, representative of the bases, and has a helical twist of 36^{0}. The total diameter of the DNA molecule is 2.3 nm with a rise for each double helical turn of 0.34 nm per base pair. The model structure also implicitly includes the first hydration shell of the DNA. It is assumed that $H_20^{\cdot+}$ resulting from interactions with the bound water layer is transferred to the DNA (La Vere *et al.* 1996). The physical track of the electron is then

assessed to ascertain whether any of the initial physical interactions lie within the volume assigned to the DNA and whether it corresponds to volumes assigned to either a sugar-phosphate moiety or a base. Any such interactions are assigned as representing direct energy deposition events within the DNA and the coordinates and the type of damage and the energy deposited are recorded.

For evaluation of indirect damage a cylindrical shell is located around the DNA segment and only those water radicals produced by the chemical track present within the cylinder are considered to be able to contribute to indirect damage of DNA. Therefore, those radicals formed outside of the cylinder are not followed and nor are those that diffuse out of the cylinder. The choice of cylindrical diameter is discussed later. Those radicals formed within the volume of the cylinder are assumed to be diffusion controlled and the path of each radical is subsequently followed and interactions recorded. The likelihood of interactions of radical species is governed by how closely they approach each other and their relative reactivities. The rate constants (k) and maximum reaction distances between species A and B (R_{AB}) are presented in table 2.7 (Nikjoo *et al.* 1997) where R_{AB} is given by $k=4\pi(D_A+D_B)R_{AB}$ (Chatterjee and Holley 1993, Terrissol and Beaudré 1990). Values for D, the coefficients of diffusion, for different radical species are presented in table 2.8 (Nikjoo *et al.* 1997). All radical species are considered to diffuse discretely with a step interval such that $L=\sqrt{(6D\delta t)}$, where L is the step size and δt is the sampling frequency which dictates the distance species are able to diffuse between sampling. The value of δt is sufficiently small so as to minimise the number of reactions which are not recorded due to radicals passing within their respective maximum reaction distance and then moving beyond that distance within the time δt. Diffusion starts at 10^{-12} s and δt is set such that L = 0.1 nm, resulting in a δt value of 6.0×10^{-13} s for OH radicals.

The diameter of the shell set around the DNA is variable and its value mimics the mean diffusion distance of OH radicals at a given scavenger concentration (section 1.6.2.1). The average diffusion distance of a radical species is given by $2.26(Dt)^{1/2}$ (Roots and Okada 1975) where D is the diffusion coefficient and t is the average lifetime of the radical species. The average lifetime of an OH radical, $(k[S])^{-1}$, within a scavenging solution is given by the inverse of the rate constant of OH radicals with the scavenger (k) multiplied by the scavenger concentration [S]. For an experimental situation with DNA present in a scavenging solution therefore, both the average lifetime and the mean

diffusion distance for OH radicals may be determined. When a simulation is undertaken therefore, parameters may be fitted to match those for an experimental scavenging scenario. A time cut-off after which radicals are no longer followed is employed within the simulation. The time cut-off value it set to be equal to the average OH radical lifetime at the particular scavenger concentration. A distance cut-off is set which dictates the diameter around the DNA cylinder within which the water radicals formed are followed. As stated, those radicals which are formed at a distance greater than this cut-off distance from the DNA target are considered unable to diffuse to and cause DNA damage and are subsequently ignored from the calculations. The distance cut-off is set to be 105 % of the average diffusion distance determined for the scavenging capacity for the particular simulation.

For simulations of the amount of damage the DNA subsequently undergoes, the direct and indirect components are treated separately. For direct interactions, if the energy deposition in the sugar-phosphate > 17.5eV (Nikjoo *et al.* 1997) a strand break is scored. For the indirect interactions, if an OH radical reaches the coordinates where the DNA chord is specified the OH radical is no longer diffused and is assumed to react either with the sugar-phosphate or the nucleobases to yield sugar or base radicals. An assumption is made that the damage is distributed 20:80 between the sugar-phosphate and the nucleobase (Scholes *et al.* 1969). It is assumed for the calculations that there is no transfer of damage from base to sugar or within the nucleobases. The probability that an OH radical which interacts with the sugar phosphate leads to a ssb is set to 65 %, based on an efficiency of 0.13 for ssb formation for OH radicals interacting with DNA (Milligan *et al.* 1993). The coordinates and number of strand breaks within the DNA model are subsequently recorded. A dsb is assumed to be formed when two or more ssbs are ≤ 10 bp apart on opposite strands.

For adequate statistics, rather than placing only a single DNA chord within the virtual sphere containing the entire chemical and physical track a number of independent random chords are placed sequentially within the sphere until the total volume of the chords is equal to the volume of the sphere. Typically this process is repeated for 1000 independent tracks and the number and types of breaks accumulated. Calculations of strand break yields are determined following the passage of each individual track. Because of this, damage to DNA such as a dsb formed from multiple track interactions is not considered within the simulation. Thus, the simulation is principally for

modelling strand breaks yields following low doses and low dose rate exposures. To calculate the ssb/Gy/Da and dsb/Gy/Da values the dose and the total mass of DNA present within the sphere must be determined. Dose deposited within the virtual sphere is given by;

$$\text{Dose (Gy)} = \frac{\text{Initial electron energy (J)}}{\rho \text{ of water (kg m}^{-3}\text{)x Volume of virtual sphere (m}^{3}\text{)}} \quad \text{(eqn. 2.1)}$$

and ssb or dsb/Gy/Da are given by;

$$\frac{\text{Number of ssb or dsb}}{\text{Dose x total number of base pairs of DNA within chords x mass of a base pair}} \quad \text{(eqn. 2.2)}$$

2.7.1.1. Al_K USX Simulation-Two Electrons

An alternative Al_K USX simulation was undertaken by simulating tracks from two electrons, one of 1 keV and one of 500 eV rather than a single 1.5 keV track as described in section 2.7.1. All details of the simulation are identical to those described in section 2.7.1 with the following additions. For each simulated scavenging capacity, with defined values for time and distance cut-offs, individual electron tracks of 1 keV and 500 eV are simulated with individual physical and chemical tracks generated. The origins of the two individual tracks are then superimposed at random orientations to form a single merged track. This track is subsequently placed within a virtual sphere which completely encompasses it and virtual DNA segments are introduced into the sphere to determine yields of DNA damage in a manner described in section 2.7.1. The process of generating two individual tracks is then repeated a large number of times to generate statistically valid data. All of the subsequent damage scoring is exactly as described in section 2.7.1.

2.7.2. α-particle Simulation

The damage induced in plasmid DNA under different scavenging capacities by irradiation with ^{238}Pu α-particles used experimentally is simulated using the Monte Carlo track structure simulation code PITS (Wilson and Nikjoo 1999). For the simulation, monoenergetic segments of 3.2 MeV α-particle tracks were used to

calculate the yields of DNA damage for comparison with the experimental data obtained with α-particles with a peak energy of 3.31 MeV (see section 2.2.1.4). The general principles for determination of DNA strand break yields, whereby DNA is placed within a virtual volume of sufficient size such that all energy deposition events and chemical species diffusion associated with the radiation track are present within it, are the same as those described above using the CPA100 code for determining DNA break yields induced by electrons, but with the following modifications. An α-particle track trajectory is effectively linear compared with that for a more scattered track associated with low LET radiation. Therefore, rather than a virtual sphere being used to encompass all of the interactions taking place associated with the radiation track, a cylinder is drawn around the segment of α-particle track, with a diameter sufficient to encompass all interactions which take place perpendicular to the main track. The use of a cylinder rather a sphere is done so as to reduce the unnecessary computing time that would arise from analysing regions large distances away from the main track within which no interactions take place.

The cylinder has a defined length into which the α-particle enters and then leaves i.e. it is not sufficiently long that the α-particle is brought to rest within it. Instead, it is of a sufficiently short length that the α-particle is assumed to have a constant LET along the axis.

The subsequent analysis of the physical and chemical tracks, the diffusion of species and the introduction of μ-random DNA chords (Kellerer 1975) with cylinders placed around the DNA of variable size was considered in the same manner as described in 2.7.1. By a means exactly analogous to that used for the electron simulation, the cylinder diameter around the DNA was varied to take into account the effect of variable scavenging capacities on the mean diffusion distance of OH radicals. In addition, a time cut-off was introduced equal to the average lifetime of the OH radical as defined by the scavenging capacity.

Unlike the electron simulation, the number of chords present within the volume around the radiation track is an input parameter whose value was adjusted to be sufficiently large to obtain statistically valid numbers of breaks but sufficiently small to optimise computing time. All parameters used to determine strand break yields are identical to those described in 2.7.1 but there are some variations in the determination of dose. For the electron simulation, the energy deposited within the virtual sphere was equal to that

of the primary electron used to simulate the action of Al_K USX since the size of the sphere was large enough to arrest all of the electrons produced. Since the α-particle is not brought to rest within the cylinder the strand break yields may not be determined in such a manner. Instead a figure is output from the simulation equal to the total energy deposited in the cylinder by the α-particle passage and it is this number instead of the initial electron energy which is input into equation 2.1 to determine strand break yields.

2.7.3. Scoring of DNA Damage

The damage present within each DNA target is scored and then classified according to the complexity. The system employed is as that described in Nikjoo *et al.* (1997) and is illustrated in figure 2.4. The simulations record the position of all breaks and thus their spatial relationships are readily determined. In a) of figure 2.4 a DNA strand with no breaks present is illustrated. In b) a simple ssb is shown which contrasts with 2 ssbs on the same DNA strand as shown in c) which for classification purposes is defined as a ssb^+. In d) and e) examples of two separate ssbs on opposite strands are shown. In d) the ssbs are > 10 bp apart and subsequently the damage is classified as 2 ssb. In e) the ssbs are ≤ 10 bp apart and this is determined to give rise to a dsb. In f) the dsb^+ classification is shown which represents one (or more) additional ssbs present near a dsb and in g) two double strand breaks are present which is classified as a dsb^{++}. Each DNA target is placed into a single category only with precedence given in the order g) to a).

In addition to the type of damage, classification is also undertaken to indicate whether damage arises from the action of the direct effect, indirectly produced OH radicals or as a combination of the two processes. Hence the proportion of damage arising wholly from the direct effect may be compared with that arising wholly from the indirect effect to illustrate the relative importance of the two processes as well as their additional combined action.

2.7.4. Treatment of Errors within Simulations

Within all simulations it is assumed that Poisson statistics apply. Subsequently the errors in the yields of ssb and dsb are given by +/- the standard deviation. If Poisson statistics apply and the total number of ssb or dsb is given by N, the standard deviation is equal to $(N)^{1/2}$.

Table 2.1.

Properties of characteristic USX in water.

X-ray	Photon energy (keV)	Dominant electron energy (keV)		Combined electron range[2] (nm)	Mass attenuation coefficient[3] (cm^2/g)	Attenuation length (μm)
		photo-	Auger-			
C_K	0.28	0.25	-	<7	5416	1.8
Cu_L	0.96[1]	0.42	0.52	~40	4640	2.2
Al_K	1.49	0.96	0.52	~70	1421	7.0
Ti_K	4.55[1]	4.02	0.52	~500	56.97	180

[1]Weighted average (Storm and Israel 1970).

[2]Combined csda (continuous slowing down approximation) range of the two electrons (single electron for C_K X-rays). Energy is generally deposited over a smaller distance due to electrons being emitted in a random direction and the tortuous path followed.

[3]Values calculated using elemental coefficients (ICRU 1970).

Table 2.2.

Parameters determined for a 7.8μm thick plasmid-suspension sample irradiated with USX in water.

X-ray	Cathode potential (kV)	Plasma current (mA)	Area weighted mean intensity over sample	Mean to surface dose rate ratios	Typical mean absorbed dose rates (Gy min^{-1})
C_K	1.5	3.0	0.85	0.233	0.5
Cu_L	2.0	8.0	0.91	0.269	0.25
Al_K	4.0	4.0	0.93	0.604	30
Ti_K	7.0	3.0	0.91	0.978	4

Table 2.3.

^{60}Co γ-irradiation G values (μmol J^{-1}) of water radicals in deoxygenated and oxygenated solutions (Scavenger concentration 10^{-4}-10^{-3} mol dm^{-3}) (Buxton 1987).

	N_2	N_2O *	O_2 **
$\cdot OH$	0.280	0.559	0.280
$\cdot H$	0.057	0.057	
e_{aq}^-	0.275		
$O_2^{\cdot -}$			0.332

* N_2O-saturated = 2.2×10^{-2} mol dm^{-3}

** O_2-saturated = 1.38×10^{-3} mol dm^{-3}

Table 2.4.

Site specificities of Fpg and Nth enzymes (Wallace 1988, Kuipers and Lafleur 1998).

Substrate Specificities	Fpg	Nth
AP Sites		
Regular	+	+
1'-oxidised	-	-
4'-oxidised	+	+
Base Modifications		
8-hydroxyguanine	+	-
Fapy-guanine	+	-
Fapy-adenine	+?	-
5,6-dihydropyrimidines	+	+
Thymine glycol	-	+

Table 2.5.

Conditions for dilution of DNA solutions for γ-ray irradiation to assess the importance of DNA concentration on strand break yields.

Sample	Concentration of DNA	Dilution Relative to Stock
5μl Stock	0.5mg/ml	1
5μl Stock + 5μl 10 mmol dm^{-3} Tris	0.25mg/ml	2
2μl Stock + 8μl 10 mmol dm^{-3} Tris	0.1mg/ml	5
1μl Stock + 9μl 10 mmol dm^{-3} Tris	0.05mg/ml	10
1μl Stock + 19μl 10 mmol dm^{-3} Tris	0.025mg/ml	20

Table 2.6.

Relative humidity obtained by solutions containing specific molarities of NaOH.

Molarity of NaOH	Humidity*
1.463	95%
3.840	85%
6.565	75%
9.792	50%

*Relative to the vapour pressure of pure water (Stokes 1949).

Table 2.7.

Reaction distances and rate constants for the reactions of radical species generated by the irradiation of water.

Reaction	Rate Constant ($dm^3\ mol^{-1}\ s^{-1}$)	Maximum Reaction Distance (nm)	Reference
$^{\cdot}OH + {}^{\cdot}OH \rightarrow H_2O_2$	$6x10^9$	0.2820	Schwarz 1969
$^{\cdot}OH + e_{aq}^- \rightarrow OH^-$	$2.5x10^{10}$	0.9054	Schwarz 1969
$^{\cdot}OH + {}^{\cdot}H \rightarrow H_2O$	$2.0x10^{10}$	0.5395	Schwarz 1969
$^{\cdot}OH + H_2 \rightarrow H + H_2O$	$4.5x10^7$	0.0015	Dorfman and Matheson 1965
$^{\cdot}OH + H_2O_2 \rightarrow HO_2 + H_2O$	$2.3x10^7$	0.0012	Burns *et al.* 1981
$^{\cdot}OH + HO_2 \rightarrow O_2 + H_2O$	$1.0x10^{10}$	0.5500	Farhataziz and Ross 1977
$e_{aq}^- + e_{aq}^- \rightarrow H_2 + OH^-$	$2.5x10^{10}$	0.1620	Schwarz 1969
$e_{aq}^- + {}^{\cdot}H \rightarrow H_2 + OH^-$	$2.5x10^{10}$	0.5740	Schwarz 1969
$e_{aq}^- + H^+ \rightarrow H$	$1.7x10^{10}$	0.3320	Schwarz 1969
$e_{aq}^- + O_2 \rightarrow O_2^{\cdot -}$	$1.9x10^{10}$	0.7600	Anbar *et al.* 1975
$e_{aq}^- + H_2O_2 \rightarrow OH + OH^-$	$1.3x10^{10}$	0.5120	Schwarz 1969
$e_{aq}^- + HO_2 \rightarrow HO_2^-$	$2.0x10^{10}$	0.8120	Burns *et al.* 1981
$e_{aq}^- + O_2^- \rightarrow HO_2^- + OH^-$	$1.3x10^{10}$	0.5200	Anbar *et al.* 1973
$^{\cdot}H + {}^{\cdot}H \rightarrow H_2$	$1.0x10^{10}$	0.1899	Schwarz 1969
$^{\cdot}H + O_2 \rightarrow HO_2$	$2.0x10^{10}$	0.5810	Dorfman and Matheson 1965
$^{\cdot}H + OH^- \rightarrow e_{aq}^- + H_2O$	$2.0x10^7$	0.0004	Anbar *et al.* 1973
$^{\cdot}H + HO_2 \rightarrow H_2O_2$	$2.0x10^{10}$	0.5860	Anbar *et al.* 1973
$^{\cdot}H + H_2O_2 \rightarrow {}^{\cdot}OH + H_2O$	$1.0x10^8$	0.0028	Anbar *et al.* 1973
$^{\cdot}H + O_2^- \rightarrow HO_2$	$2.0x10^{10}$	0.5810	Boyd *et al.* 1980

Table 2.8.

Coefficients of diffusion for various radical and molecular species (Schwarz 1969 and Burns *et al.* 1981).

Species	Coefficients of Diffusion (10^{-5} cm^2 s^{-1})
$\cdot OH$	2.8
e_{aq}^-	4.5
$\cdot H$	7.0
H_{aq}^+	9.0
H_2	5.0
H_2O_2	2.2
HO_2	2.0
O_2	2.1
OH^-	5.0

Figure 2.1.

Schematic of ultrasoft X-ray rig employed for irradiations.

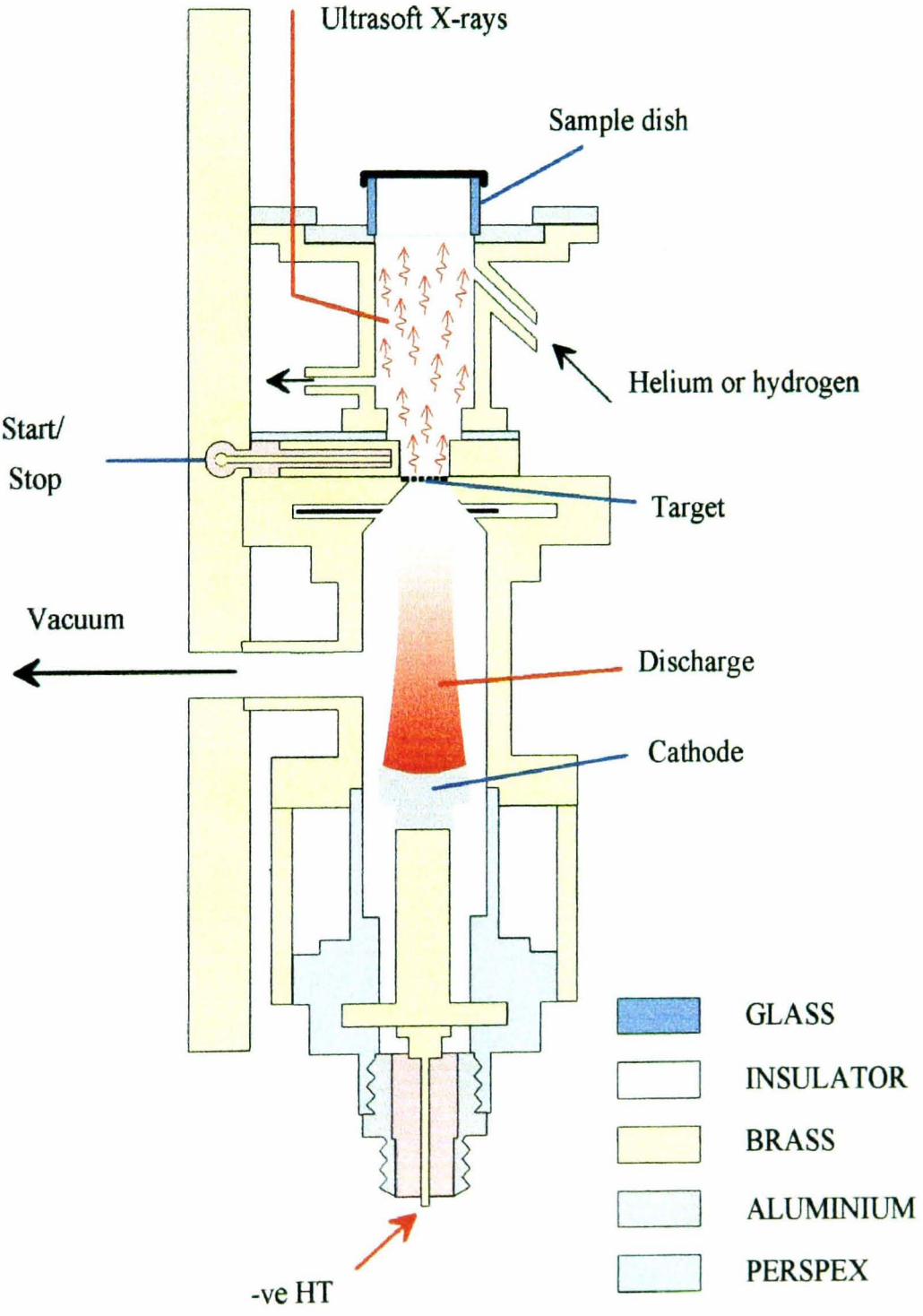

Figure 2.2.

Schematic representation of the alpha source irradiation set-up.

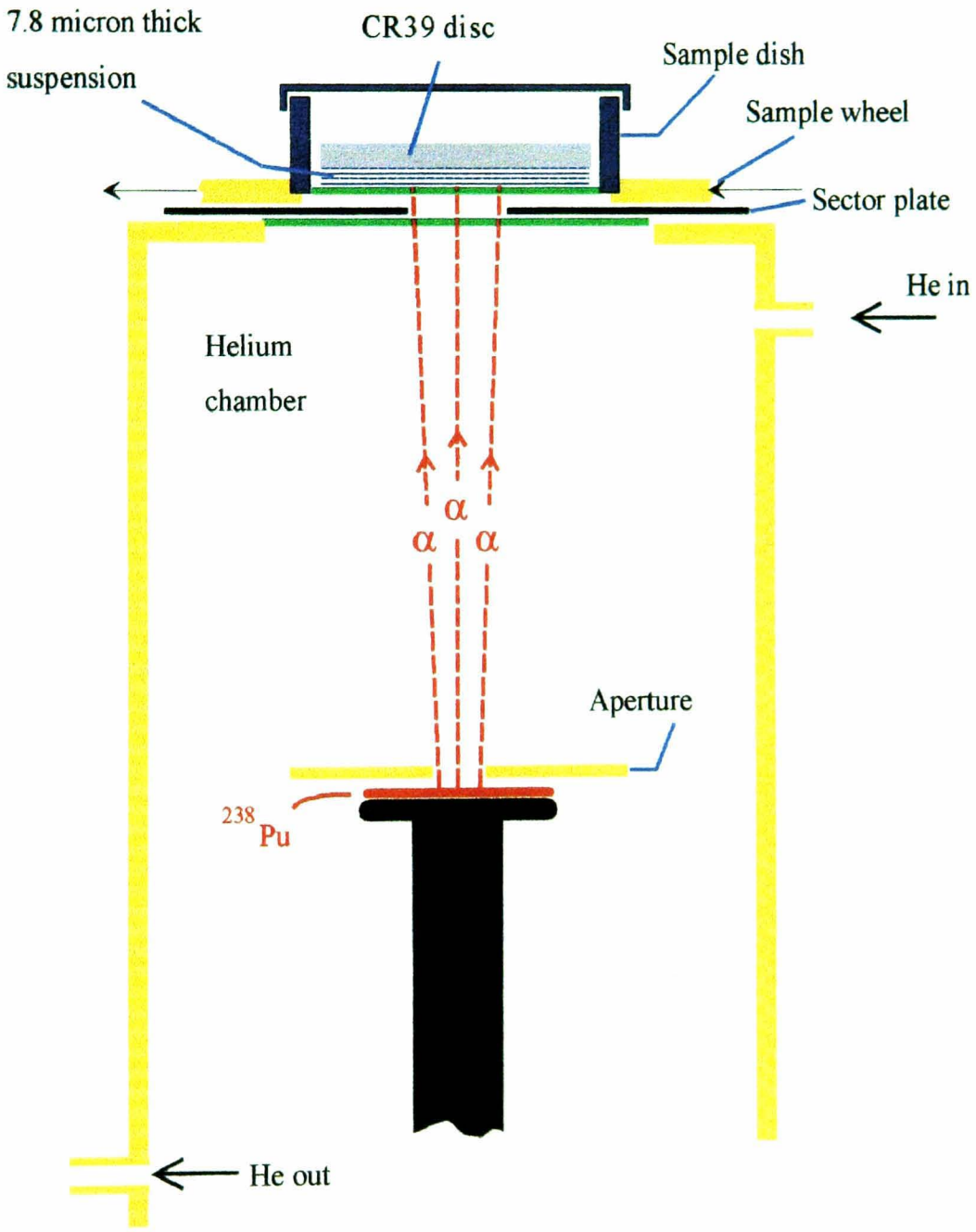

Figure 2.3.

Increases in mass of calf thymus DNA samples after freeze drying for 18 h and then placing in a 70 % humid environment set by the presence of a NaOH solution for variable periods of time.

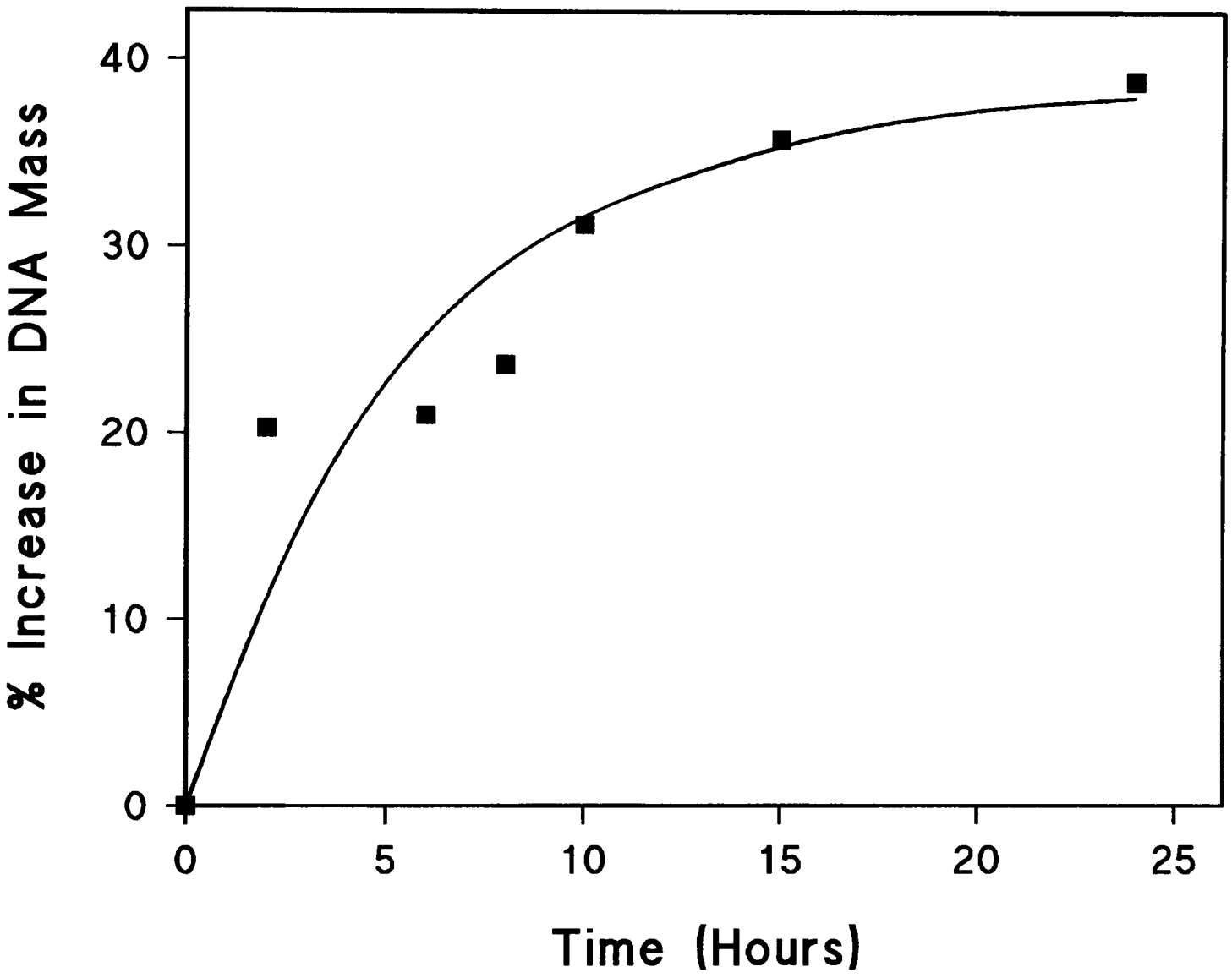

Figure 2.4.

Classification scheme of DNA breaks according to complexity as used for electron and α-particle simulations (taken from Nikjoo *et al.* 1997).

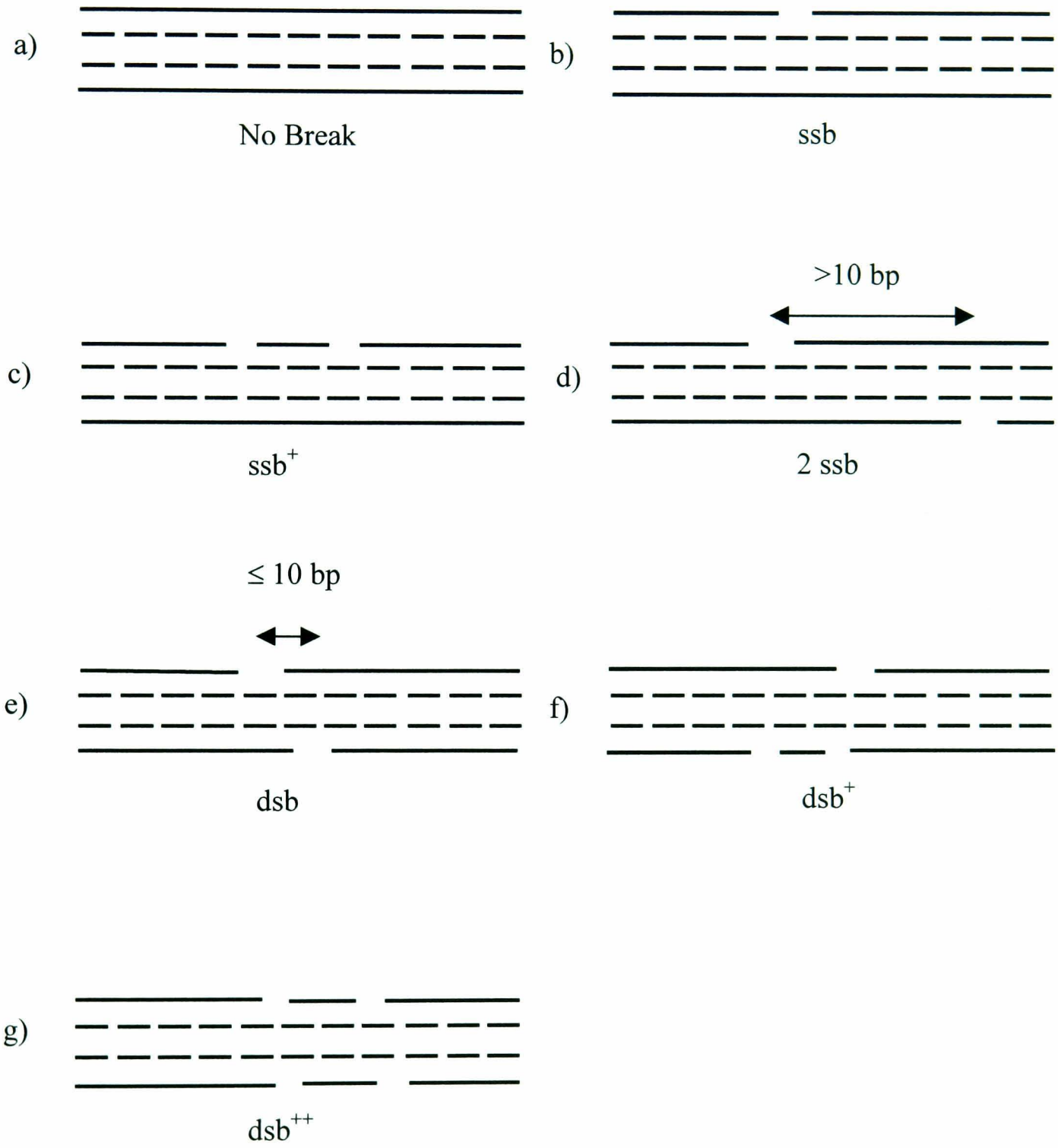

Chapter 3

Comparison of the Yield of ssb and dsb Induced in Plasmid DNA by ^{60}Co γ-ray, Al_K USX and α-particle Irradiation: Dependence on the Concentration of OH Radical Scavengers

3.1. Introduction

By quantification of radiation damage produced in plasmid DNA, investigations focus on what is considered to be the most biologically significant site for damage induced by ionising radiation in more complex biological systems. As discussed in section 1.6.2.1, ionising radiation induces damage in DNA via two possible mechanisms, direct and indirect effects. The fact that the indirect effect derives from energy deposited in the medium surrounding the DNA target, giving rise to radicals, which may subsequently diffuse to and react with the DNA, means its relative importance may be assessed. The use of OH radical scavengers, which in aqueous solution react with OH radicals to an extent dependent upon the scavenger concentration [S] and the rate constant of the reaction between the OH radicals and the scavenger (Buxton *et al.* 1988), provides an approach by which both the contribution of the indirect effect to the yield of DNA strand breaks and the relative contribution of the direct and indirect effect produced by different radiation qualities may be evaluated.

One approach to assess the contribution of the direct effect of radiation to DNA damage is to irradiate plasmid DNA in aqueous solution containing a high concentration of an OH radical scavenger, which minimises the interaction of OH radicals with DNA. As the scavenging capacity tends to ∞ the migration range of the OH radical will tend to zero and the contribution of the indirect effect will become insignificant so that all measured DNA damage may be regarded as arising from the direct effect. However, there are practical limitations to the scavenging capacities that can be used.

As discussed in section 1.5, as well as the scavenging characteristics of the medium surrounding the DNA, the ionisation density of the radiation plays a critical role in determining the amount and complexity of DNA damage in an aqueous environment (see section 1.8). At low scavenging capacities those water radicals which are formed within a radiation track and which can subsequently escape intra-track radical-radical

recombination effects are the predominant mechanism for causing damage. Radiations with high ionisation densities and a correspondingly small average distance between the sites of radical formation should produce fewer indirect DNA ssb mediated by OH radicals, due to an increase in intra-track recombination events relative to radiations with lower ionisation densities (see chapter 7 for further discussion). However, if the direct effect is considered, those radiations, which have a high ionisation density, will be more likely to give rise to damaged sites which are spatially close, forming complex damage such as dsbs, relative to isolated damage e.g. ssbs. It is therefore anticipated that with increasing ionisation density there will be a corresponding increase in the proportion of complex damage arising. Consequently, different radiations such as γ-rays, Al_K USX and α-particles have been used to irradiate plasmid DNA in aqueous solution and a range of scavenging capacities have been used to assess the role of ionisation density and diffusible water radicals in determining the yield of spatially separate ssbs and more complex damage. The formation of dsb is taken to be indicative of the capacity of the radiation to form complex damage, albeit of a simple form. Thus, the ratio of ssb:dsb may be regarded as a upper limit of the ratio of simple:complex damage associated with a particular radiation, since base damages are not included in these approaches (see chapter 5). Such information additionally provides experimental benchmarks against which computer simulations may be compared (see chapter 4).

3.2. Results

3.2.1. Dependence of the Yield of γ-ray Induced DNA Strand Breaks on Choice of Scavenger

To assess whether the yields of strand breaks induced in plasmid DNA are dependent upon the choice of scavenger, DNA was γ-ray irradiated in solution in the presence of variable concentrations of ethanol (rate constant with OH radicals 1.9×10^9 $mol^{-1}dm^3s^{-1}$) or Tris (rate constant with OH radicals 1.5×10^9 $mol^{-1}dm^3s^{-1}$) (Buxton *et al.* 1988). Irradiations were undertaken at 20^0 C under aerobic conditions and all subsequent post irradiation treatment and quantification were carried out at 20^0 C as described in section 2.4.2. By such an examination, any breaks induced by secondary Tris radicals interacting with DNA, produced by the reaction of OH radicals with Tris, would become apparent by an increased yield of ssb when irradiating DNA in Tris solutions

relative to those obtained following DNA irradiation in ethanol at equivalent scavenging capacities. There is evidence to support ethanol radicals being ineffective in inducing DNA damage (Lafleur *et al.* 1978, 1979).

A typical dependence of the amount of closed circular DNA on γ-ray irradiation dose is illustrated in figure 3.1 at a constant scavenging capacity of Tris. On the semi log plot, the loss of closed circular DNA is linear with dose. From the dose response, a D_{37} value, the dose required to reduce the amount of closed circular DNA to 37 %, was calculated from the gradient. The D_{37} value corresponds to that dose which, assuming Poisson statistics apply, results in an average of one ssb per plasmid molecule. As the scavenging capacity was varied using Tris or ethanol, D_{37} values were determined from which the yields of ssb/Gy/Da were obtained as described in section 2.4.2.1. The variation in the yield of ssb/Gy/Da with scavenging capacity is illustrated in figure 3.2 using both ethanol and Tris. Over the scavenging capacity range employed, the log of the yield of ssb/Gy/Da is approximately linear with the log of the scavenging capacity. Furthermore at 20^0 C, no significant difference between the yields of radiation-induced DNA ssb using either Tris or ethanol as the scavenger was determined, indicative of no significant contribution to the yield of ssb of secondary Tris radicals. Thus, scavenging capacity is seen as the critical variable in influencing the yield of strand breaks under these conditions rather than the choice of scavenger. For all subsequent experiments described in section 3.2.3 with DNA in aqueous solution, it was therefore decided to use Tris to set the scavenging capacities, as it is less volatile than ethanol.

3.2.2. Dependence of the Yield of Strand Breaks on Temperature

The yields of ssb induced by γ-ray irradiation of aqueous solutions of plasmid DNA at 4^0 C are presented in figure 3.3. For one set of DNA samples this temperature is maintained throughout the subsequent damage quantification procedure including during electrophoresis. For the other set of DNA samples irradiated, a temperature of 20^0 C is maintained throughout the damage analysis. Data at 4^0 C were obtained using Tris to set the scavenging capacity whereas at 20^0 C both Tris and ethanol were employed. When the yields of ssb obtained at 20^0 C were compared with those at 4^0 C, the yields of ssb are approximately linear with scavenging capacity on a log-log plot at both temperatures. However, a greater number of ssb are induced for DNA maintained at 20^0 C over the entire scavenging range employed. Quantitative examination of the

dependence of the yield of ssb on scavenging capacity at 20^0 C and 4^0 C results in the following least square fit relationships;

4^0 C response: log ssb/Gy/Da = - 0.617 (log scavenging capacity)- 4.023

20^0 C response: log ssb/Gy/Da = - 0.680 (log scavenging capacity)- 3.314

Although the gradients of the respective responses are similar they are not equal. To illustrate this point, as the scavenging capacity is varied between 10^6 s^{-1} and 10^7 s^{-1} the increased additional yield of ssb for samples at 20^0 C relative to 4^0 C decreases from 115 % to 85 %. The dependence of the excess number of ssb obtained for samples maintained at 20^0 C relative to 4^0 C on scavenging capacity based on the least square relationships above is illustrated in figure 3.4. It should be noted that the error on the gradient determined from least square analysis for the 4^0 C response is ± 0.019, whereas for the 20^0 C response it is ± 0.047. Thus, there is a significant error on the gradient accentuated by the small number of low scavenger data points for samples at 20^0 C. However, even taking into account these errors there remains a significant difference in yields of ssb between samples maintained at 20^0 C relative to 4^0 C.

The effect of temperature on the yield of ssb induced in plasmid DNA was also investigated for γ-ray, Al_K USX and α-particle irradiation at 37^0 C compared with 4^0 C but with subsequent handling and electrophoresis undertaken at 4^0 C for both sets of DNA samples (Cunniffe, unpublished data). Two representative scavenging capacities of $1.9x10^7$ s^{-1} and $1.9x10^8$ s^{-1} were investigated using ethanol to set the scavenging capacity. Following γ-ray, Al_K USX and α-particle irradiations, increases in the yields of ssb averaged for the two scavenging capacities were 23 %, 17 % and 40 % respectively, determined at 37^0 C relative to those at 4^0 C. The increase in the yields of dsb induced by these radiations was also undertaken at the same two scavenger capacities using ethanol to set the scavenging capacity. The mean increases in the yields of dsb following γ-ray, Al_K USX and α-particle irradiation of plasmid DNA in aqueous solution were 94 %, 113 % and 60 % respectively at 37^0 C relative to irradiations at 4^0 C.

3.2.3. The Effect of Radiation Quality on the Yields of DNA ssb and dsb at Different Scavenging Capacities

To assess the role of radiation quality on the induction of ssb and dsb in plasmid DNA all of the subsequent experiments were undertaken using Tris as a scavenger and all

irradiations and post-irradiation damage quantification undertaken at 4^0 C so as to minimise the contribution of heat labile sites. This is particularly important when comparing these experimentally determined yields with those obtained from simulations (see chapter 4) in which heat labile sites are not included. Solutions were prepared as described in sections 2.3 and irradiations used γ-ray, Al_K USX and α-particle radiations as described in sections 2.2.1.1 and 2.2.1.3-4. Quantification was undertaken as described in section 2.4.2.

There is a lower limit for the value of the scavenging capacity of the DNA solution that may be studied since DNA is stored in 10 mmol dm^{-3} Tris and to examine very low scavenging capacities the DNA must be dialysed. However due to the presence of impurities and adventitious scavengers, there remains a practical lower limit below which the presence of impurities dictates the scavenging capacity rather than the intentionally introduced Tris scavenger. There is also an upper limit to the scavenging capacities that may be examined for Al_K USX and α-particle irradiations since irradiation times increase with increasing scavenging capacity. The maximum dose rate obtainable for each irradiation source therefore sets the irradiation time. For longer periods of irradiation the volume of the DNA solution may change due to evaporation leading to alterations in the scavenging capacity of the solutions. Although maintaining the sample at 4^0 C helps to minimise this effect, it was necessary to impose an upper limit of 3 h for irradiation times. In addition, an upper limit of scavenging capacity was imposed upon γ-ray irradiation experiments to ensure that the majority of the interactions of the radiation track take place with water molecules rather than scavenger molecules. As such, a maximum Tris concentration of 1 mol dm^{-3} was selected.

The mean OH radical diffusion distance is dependent upon the OH radical scavenging capacity of a solution and is known to be equal to $2.26(D/k[S])^{1/2}$ where D is the diffusion coefficient, k is the rate constant of the reaction between the OH radical and the scavenger and [S] is the scavenger concentration (Roots and Okada 1975). The dependence of the mean OH radical diffusion distance on scavenging capacity is illustrated in figure 3.5. Within the cellular environment OH radicals have a mean diffusion distance of approximately 4-6 nm (Chapman and Gillespie 1981), equivalent to a scavenging capacity of $3x10^8$ s^{-1}. The dependences of the yields for ssb/Gy/Da on Tris scavenging capacity for γ-ray, Al_K USX and α-particles are shown in figure 3.6. At all scavenging capacities, the loss of closed circular DNA is log-linear with dose

allowing determinations of the respective D_{37} values and hence the values for ssb/Gy/Da. Over the scavenging capacity examined, the dependence of the yield of ssb is approximately proportional to the scavenging capacity for all three radiations, with the yields decreasing with increasing scavenging capacity. At any given scavenging capacity, the relative yield of ssb depends upon the radiation, where the yields decrease in the order γ-ray > Al_K USX > α-particle. It is apparent from the relative slopes of the three dependences that the yields of ssb tend to converge as the scavenging capacity increases. Least-square fit analysis gives the following relationships between the yields of ssb and scavenging capacity;

γ-ray: log (ssb/Gy/Da) = -0.617 (log scavenging capacity) – 4.023

α-particle: log (ssb/Gy/Da) = -0.315 (log scavenging capacity) – 7.117

Al_K USX: log (ssb/Gy/Da) = -0.408 (log scavenging capacity) – 5.882

The scavenging capacity at which the extrapolated yields of ssb from γ-ray irradiation is equal to that following α-particle irradiation may be estimated from extrapolation of the least square fit data given by;

-0.617 (log scavenging capacity) – 4.023 = -0.315 (log scavenging capacity) – 7.117

log scavenging capacity = 10.25 scavenging capacity = 1.76×10^{10} s^{-1}

Thus, in effect the extrapolation predicts that at scavenging capacities of the order of 10^{10} s^{-1} the yields of ssb for γ-ray and α-particle irradiation would be approximately equivalent.

For comparison, the yields of ssb obtained by various other groups at a range of scavenging capacities are presented in table 3.1 (Krisch *et al.* 1991, Klimczak *et al.* 1993, Milligan *et al.* 1996a). There is reasonable agreement between the present study and those of other groups although there are some differences. The reasons for any differences between the yields obtained by the various groups are discussed in section 3.3.3.

For each dose point at every scavenging capacity the yield of dsb was measured, and dose responses determined. Representative yields of dsb dependence on dose for a given scavenging capacity are presented in figure 3.7. Depending upon the shape of the dose responses either a linear quadratic or a linear relationship was fitted to the data. At all of the scavenging capacities considered for α-particle and for all but the lowest scavenging capacities examined for Al_K USX the yields of induced dsb are approximately linear with dose. For γ-ray irradiation, for scavenging capacities > 10^7 s^{-1}

the dose response for induction of dsbs is approximately linear, whereas at lower scavenging capacities the responses are approximately linear quadratic. Irrespective of the dose response dependence, the dsb/Gy/Da value was obtained by determining the yield of dsb at the dose corresponding to the D_{37} for ssb at a given scavenging capacity and multiplying the determined ssb/Gy/Da value by the proportion of linear plasmid at this D_{37} value. The variations in the yields of dsb on Tris scavenging capacity following γ-ray, Al_K USX and α-particle irradiation at 4^0 C are illustrated in figure 3.8. Irrespective of the radiation, as the scavenging capacity increases the yield of dsb decreases. At low scavenging capacities the relative order of dsb/Gy/Da is given by the yield for γ-ray > Al_K USX > α-particle. However, the relative magnitudes of the gradients for the yield of dsb against scavenging capacity is given by γ-ray > Al_K USX > α-particle. Therefore, as the scavenging capacity increases, the yield of dsb for both α-particle and Al_K USX exceed that following γ-ray irradiation. From least square fit analysis of the yield of dsb, the relationships between these yields and scavenging capacity are given by:

γ-ray: log (dsb/Gy/Da) = -0.462 (log scavenging capacity) – 6.888

α-particle: log (dsb/Gy/Da) = -0.191 (log scavenging capacity) – 9.062

Al_K USX: log (dsb/Gy/Da) = -0.322 (log scavenging capacity) – 7.835

From least square analysis, the scavenging capacity at which the yield of dsb from γ-ray irradiation is approximately equal to that from α-particle irradiation may be estimated;

-0.462 (log scavenging capacity) – 6.888 = -0.191 (log scavenging capacity) – 9.062

log scavenging capacity =8.00 scavenging capacity = 1.0×10^8 s^{-1}

The dependences of the percentage yields of dsbs relative to ssbs (dsb/ssb x100 %) calculated at the D_{37}, the dose that corresponds to a mean of 1 ssb per plasmid molecule, on scavenging capacity (section 2.4.2.1) are presented in figure 3.9. This plot represents the variation in the proportion of complex damage (as represented by dsbs) relative to isolated damage (represented by ssbs) with scavenging capacity. For all radiations, the percentage of dsb increases with increasing scavenging capacity. At any given scavenging capacity the relative values for the percentages of dsbs obtained for the three radiations is given by α-particle > Al_K USX > γ-ray. Least-square fit analysis of the data gave the following relationships between the dsb percentage and the scavenging capacity ;

γ-ray: dsb percentage @ D_{37} = 0.676 (log scavenging capacity) – 2.871

α-particle: dsb percentage @ D_{37} = 2.438 (log scavenging capacity) – 8.121

Al_K USX: dsb percentage @ D_{37} = 1.422 (log scavenging capacity) – 4.875

The ratios of ssb:dsb calculated from the least square analysis of the yields of ssb and dsb determined at different scavenging capacities are presented in table 3.2. As the scavenging capacity of the solution increases, the ratio of ssb:dsb decreases for all radiations. For the entire scavenging capacity range examined, the relative magnitudes of the ratio of ssb:dsb is given by γ-ray > Al_K USX > α-particle. Comparisons with the ratios of ssb:dsb obtained by a number of other groups are discussed in section 3.3.5 and presented in tables 3.4a and b.

For comparison with cellular values for radiation-induced DNA strand breaks (deLara *et al.* 1995 and unpublished data, Botchway *et al.* 1997), the yields of strand breaks in aqueous solution for γ-rays, α-particles and Al_K USX were determined from the least square analysis of the yields of ssb and dsb, at a scavenging capacity of 3.0×10^8 s^{-1}, and are summarised in table 3.3. This scavenging capacity represents a mean OH radical diffusion distance of 4-6 nm (see figure 3.5) approaching the value estimated for the cellular environment (Roots and Okada 1975, Ward 1991). The yields obtained with plasmid DNA are within a factor of two of those determined in V79 cells for γ-ray and Al_K USX irradiation. With α-particle irradiation the plasmid yields are a factor of 2-3 greater than those determined with cells.

3.3. Discussion

3.3.1. Generalisations

For all the strand break determinations undertaken, there are a number of generalisations that may be drawn. Firstly, the yields of both ssb and dsb depend upon the scavenging capacity of the DNA solution for all types of radiation used. As the scavenging capacity increases the yields of both ssb and dsb decrease. However, the ratio of ssb:dsb also decreases with increasing scavenging capacity leading to an increase in the yield of dsb per ssb. In addition, the yields of ssb and dsb at a given scavenging capacity are dependent upon the quality of the radiation.

3.3.2. Effect of Temperature

When the effect of temperature on the yield of radiation-induced ssb is examined, some comparative information may be obtained. From the least square fit analysis of the dependence of the yields of strand break yields on scavenging capacity, after γ-ray irradiation the yield of ssb increases by 81 % at a scavenging capacity of $1.5x10^7$ s^{-1} as the temperature for irradiation and electrophoresis is raised from 4^0 C to 20^0 C. At a scavenging capacity of $3.3x10^7$ s^{-1} over the same temperature range, the yield of ssb increases by 72 %. An average value for the increase in the yield of ssb in this range therefore is approximately 76 %. In comparison, Jones *et al.* (1994a) determined an increased yield of ssb of 52 % at a scavenging capacity of $1.5x10^7$ s^{-1} (10 mmol dm^{-3} Tris) and an increase of 102 % at a scavenging capacity of $3.3x10^7$ s^{-1} ($5x10^{-3}$ mol dm^{-3} DMSO) for a temperature of 23^0 C relative to 2^0 C. This equates to an average increase of the yield of ssb of 77 % in this scavenging capacity range, comparable with the present study. At the same scavenging capacities following treatment at 37^0 C, Jones *et al.* (1994a) revealed an average increase in the yield of ssb of ~ 90 %, relative to the yields at 2^0 C and an average increase in the yields of dsb of ~ 300 % relative to those at 2^0 C. In the present study, the yields of strand breaks increase by 23 % for ssb and 94 % for dsb induced by γ-ray irradiation at 37^0 C and electrophoresis undertaken at 4^0 C relative to both irradiation and electrophoresis at 4^0 C. There is therefore a large disparity in the increased yield of both ssb and dsb following irradiation at 37^0 C relative to 4^0 C between the present study and Jones *et al.* (1994a). This may result from the fact that samples for Jones *et al.* (1994a) were maintained at 37^0 C for 18 h prior to electrophoresis whereas in the present study samples were maintained at 37^0 C only for the course of irradiation and post irradiation treatment (approximately 1 h) before undertaking electrophoresis at 4^0 C. It has been shown however, (Jones *et al.* 1994a) that the yields of both heat labile induced ssb and dsb show a strong time dependence. The yield of heat labile ssb do not reach a plateau until DNA has been incubated at 37^0 C for 3 h whereas the yields of heat labile dsb still rise after 18 h incubation of the DNA at 37^0 C. Hence, it is anticipated that the present study will show significantly less heat induced ssb and dsb due to the reduced time at 37^0 C. However, the relevance of the procedure of maintaining the plasmid at 37^0 C for 1 h followed by electrophoresis at 4^0 C is that it effectively simulates the conditions used for the

determination of base damage as discussed in chapter 5 and assesses the yield of heat labile sites that such a procedure produces.

3.3.3. Effects of Scavenging Capacity

The dependences of the yields of ssb/Gy/Da on scavenging capacity for γ-ray, Al_K USX and α-particle irradiation (figure 3.6) is approximately linear. The reasons for this underlying linearity may be understood from assessing the competition kinetics of the reactions of OH radicals with either Tris or DNA. Since e^-_{aq} do not lead to ssb on interaction with DNA (Jones and O'Neill 1991), and the yield of ssb decreases with increasing concentrations of OH radical scavengers, Tris or ethanol, it is assumed that the OH radical is the main water radical leading to prompt ssb. If the rate constant for the reaction between OH radicals and Tris is given by k_1, the rate constant for the reaction between OH radicals and DNA given by k_2 and the yield of ssb is proportional to the concentration of OH radicals then;

$$ssb_s = ssb_o \left\{ \frac{k_2[DNA]}{k_1[Tris] + k_2[DNA]} \right\}$$

where ssb_s is the number of ssb when Tris is present and ssb_o is the number of ssb that escape the track and become homogeneously distributed when no scavenger is present. Therefore, if, as in the present study [Tris]>>[DNA] then $k_1[Tris] >> k_2[DNA]$ and the above equation approximates to;

$$\frac{ssb_s}{ssb_o} = \frac{k_2[DNA]}{k_1[Tris]}$$

$$\therefore \log (ssb_s) \propto -\log[Tris] + \text{constant}$$

Thus, a linear relationship between strand breaks and scavenging capacity is predicted with a log-log plot on the proviso that the OH radicals are principally responsible for the formation of ssb. Such an assumption will be valid at low scavenging capacity and only when the relative yields of damage due to the direct effect are neglected. That there is an approximately proportional dependence between the yields of ssb and scavenging capacity in the present study is indicative of a significant proportion of the damage arising from the indirect effect. However, the fact that the slopes illustrated in figure 3.6 are not equal to -1 is indicative of the fact that a competition kinetics approach is not completely appropriate. As the scavenging capacity increases the mean diffusion distance of OH radicals and therefore the contribution of the indirect effect is

reduced with an increasing significance of the direct effect. Further, the above competition kinetics would not apply at very high scavenging capacities since the mean diffusion distance of the OH radical is less than the molecular size of the DNA so that the reactions become non-homogeneous. At low scavenging capacities one of the above assumptions, namely that k_1[Tris]>>k_2[DNA], is no longer correct due to the reduced value of k_1[Tris.]. This has been discussed further by Milligan *et al.* (1993) and Hill (1999) and in section 1.6.2.2.

3.3.4. Effects of Radiation Quality

A comparison of the yield of DNA ssb obtained following γ-ray irradiation by various representative groups is presented in table 3.1 (Krisch *et al.* 1991, Klimczak *et al.* 1993, Milligan *et al.* 1996a). The yields presented in table 3.1 have been estimated from the respective published data. In all cases there is general consistency in the yield of strand breaks, although in the present study the yields of strand break are approximately a factor of 2 lower than the published yields. It is suggested that this disagreement reflects the fact that the published yields presented in table 3.1 were determined at room temperature. As discussed above, the yields of DNA strand breaks depend on temperature due to the conversion of heat labile sites into ssb at higher temperatures. From the yields of ssb determined at 4^0 C and 20^0 C (figure 3.3 and figure 3.4), over the scavenging capacity range 10^6 to 10^9 s^{-1}, an increase in the yields of ssb of 115 % to 39 % is estimated for DNA samples processed at 20^0 C relative to those processed at 4^0 C. The inclusion of a heat labile component to the yields of ssb in the present study at the various scavenging capacities results in good agreement with the published yields as shown by the yields corrected to include heat labile sites, presented in brackets in table 3.2.

Yields of ssb following α-particle irradiation in the present study have been estimated from least square fit data of the response of the log ssb/Gy/Da with the log scavenging capacity. Yields of $5.4x10^{-10}$ and $5.0x10^{-11}$ ssb/Gy/Da were determined at scavenging capacities of $6.6x10^6$ and $1.3x10^{10}$ s^{-1} respectively in good agreement with the study of Jones *et al.* (1993) which involved α-particle irradiation of SV40 DNA at the same scavenging capacities revealing yields of $6x10^{-10}$ and $6x10^{-11}$ ssb/Gy/Da. In the latter study electrophoresis was undertaken at room temperature so that heat labile sites contribute to the total yield of ssb. At scavenging capacities of $1.5x10^7$ and $3x10^8$ s^{-1},

the yields of ssb induced in the present study are $4.2x10^{-10}$ and $1.6x10^{-10}$ ssb/Gy/Da compared with previously determined values at these scavenging capacities of $7x10^{-10}$ and $2.5x10^{-10}$ ssb/Gy/Da (Milligan *et al.* 1996a) and $3.1x10^{-10}$ and $1.2x10^{-10}$ ssb/Gy/Da (Prise *et al.* 1999b).

This study is the first showing the variation in the yields of ssb on scavenging capacity following Al_K USX irradiation. As such, it provides information on the yields of damage induced by radiation, which has an ionisation density lying between that for γ-ray and α-particle radiation and represents a component of the ubiquitous low-energy secondary electrons in γ-ray irradiations.

As discussed, the fact that the dependence of the yield of ssb on scavenging capacity is approximately linear on the log-log plot over the majority of the scavenging capacity range investigated implies that the indirect effect contributes significantly to the pathway leading to DNA damage even at scavenging capacities as high as $1x10^9$ s^{-1} (corresponding to an average diffusion distance of the OH radical of 4-6 nm). At these higher scavenging concentrations, typical of cell mimetic conditions, however, the yields of ssb/Gy/Da for γ-ray and Al_K USX radiations are very similar whereas the yield of ssb induced by α-particles is only approximately 40 % of those of the other two radiations (figure 3.6). If the responses obtained by least square analysis of the yields of ssb for γ-ray and α-particle irradiation are extrapolated, the yields of ssb are equal for both radiations at an approximate scavenging capacity of $1.7x10^{10}$ s^{-1}. Similarly, irradiation of SV40 DNA at room temperature with ^{137}Cs γ–rays and ^4He ions (Jones *et al.* 1993) resulted in equivalent yields of ssb at a scavenging capacity of $1.3x10^{10}$ s^{-1}. Using a non-homogeneous kinetics model, Milligan *et al.* (1993) estimated the contribution of the direct effect to strand break yields induced in plasmid DNA and SV40 DNA to be approximately $2x10^{-10}$ ssb/Gy/Da. This value is consistent with the scavenging capacity at which the direct effect predominates for both γ-ray and α-particle irradiation induced ssb as determined above, assuming that heat labile sites contribute to the yields determined by Milligan *et al.* (1993).

At low scavenging capacities, the relative yields of ssb decrease with increase in ionisation density of the radiation in the order γ-ray>Al_K USX>α-particle. It is proposed that these differences are characteristic of the ionising density of the track in determining the number of water radicals which escape intra-track radical-radical events within the radiation tracks (see chapter 7 for further discussion). At low

scavenging capacities, the majority of DNA damage is produced by diffusible OH radicals that have escaped intra-track recombination events. Even at the lowest scavenging capacity used, the majority of OH radicals interact with DNA or Tris and there is little inter-track recombination at the dose rates used in these experiments. Since the mean distance between the sites of radical formation, (see section 1.5) decreases as the ionisation density of radiation increases, the number of radicals escaping the track, and therefore the yield of ssbs, decreases. At low scavenging capacities the yield of ssb is proportional to the yield of OH radicals, which escape intra-track radical-radical recombination (see chapter 7). Yields of OH radicals of 0.015 μmol J^{-1}, 0.072 μmol J^{-1} and 0.290 μmol J^{-1} were determined for α-particle, Al_K USX and γ-ray radiation respectively at a scavenging capacity of $1x10^6$ s^{-1} (see chapter 7). The yield of OH radicals for α-particle irradiation is consistent with values determined experimentally (Appleby and Schwarz 1969, Burns 1981).

3.3.5. Complex Damage Formation

An increased clustering of energy depositions associated with increased ionisation density is also expected to lead to an increased likelihood of complex damage formation relative to the formation of isolated ssb, with dsb representing a class of complex damage. Therefore with plasmid DNA, an increase in the contribution of complex lesions would be reflected as a decrease in the ratio of ssb:dsb. Additionally, the proportion of complex damage relative to ssbs would be expected to increase with increasing scavenging capacity due to the mean diffusion distance of OH radicals decreasing and therefore damage principally arising from those tracks in close proximity to the DNA. Therefore the contribution of clustered damage to the total amount of damage increases, with DNA damage arising at high scavenging capacities mainly from energy directly deposited in the DNA or in the water immediately surrounding the DNA. Hence, as the scavenger concentration increases the relative importance of the direct effect also increases. The dependence of the ratio of ssb:dsb on scavenging capacity for all of the radiations is consistent with an increased contribution of complex damage at high scavenging capacities. When the gradients of the dependences of the yields of dsb on scavenger capacity illustrated in figure 3.8 are examined, it is apparent that the gradient for alpha-particle dependence is significantly

less than that for γ-ray irradiation i.e. it shows less of a dependence on scavenging capacity, with the response for the Al_K USX lying between them.

At low scavenging capacities, where the majority of the strand breaks are due at least partly to OH radicals, the dominant mechanisms for dsb formation may be i) 2 independently induced ssbs within a few base pairs and ii) the radical transfer mechanism (Siddiqi and Bothe 1987). If the majority of the ssb induced by γ-ray radiation at a scavenging capacity of $1.5x10^5$ s^{-1} arise from a single OH radical, then given that the determined ratio of ssb:dsb is 159:1 (table 3.2) then < 1 % of these OH induced ssb are subsequently involved in the radical transfer mechanism. At these low scavenging capacities the relative yields of dsb are given by γ-ray > Al_K USX > α-particles and the dose response for the yield of dsb for γ-ray irradiation of DNA is linear quadratic (figure 3.7a) indicative of the principle mechanism for dsb generation being due to two independently produced ssb. However, as the scavenging capacity increases, there is a greater contribution of the direct effect, and only OH radicals produced near to the DNA may interact with it. At these higher scavenging capacities the dsb dose response for γ-ray irradiation of DNA is approximately linear, indicative of the mechanism for dsb generation being due to a single OH radical (Siddiqi and Bothe 1987) or multiple damage from a single track (Ward 1981, Krisch *et al.* 1991, Jones *et al.* 1993). If a single OH radical is principally responsible for the formation of dsbs then the ratios of ssb:dsb for the three radiations (figure 3.9 and table 3.2) should be similar at the different scavenging capacities. However this similarity is not seen in these studies. It is therefore concluded that a single OH radical is not principally responsible for dsb formation and subsequently the linear response for the yield of dsb with dose for α-particle over the entire scavenging capacity range examined, virtually the entire scavenging capacity range for Al_K USX and for γ-ray at high scavenging capacities (>10^7 s^{-1}) may be attributed to the action of single tracks and the formation of spatially close multiple damage sites.

In the present study following γ-ray irradiation the yields of dsb vary from $2x10^{-10}$ - $9x10^{-12}$ dsb/Gy/Da over a scavenging capacity range of $1x10^6$ to $1x10^9$ s^{-1}. In comparison over the same scavenging capacity range the yields of dsb have been found to vary between $4x10^{-10}$ - $1x10^{-11}$ dsb/Gy/Da for SV40 DNA (Krisch *et al.* 1991) and between $2x10^{-10}$ - $5x10^{-12}$ dsb/Gy/Da for plasmid DNA (Milligan *et al.* 1996a). Therefore, the yields of dsb induced by γ-ray irradiation are similar to those reported

(Krisch *et al.* 1991, Milligan *et al.* 1996a), even though the latter studies were carried out at room temperature which leads to the formation of heat labile sites which contribute to the formation of dsb.

In the present study following α-particle irradiation, the yields of dsb vary between $4.3x10^{-11}$ - $10x10^{-12}$ s^{-1} dsb/Gy/Da over a scavenging capacity range of $6.6x10^{6}$ - $1.3x10^{10}$ s^{-1}. This is in good agreement with yields of dsb determined for α-particle irradiation of SV40 DNA (Jones *et al.* 1993), which vary between $5.5x10^{-11}$ - $7x10^{-12}$ dsb/Gy/Da over the same scavenging capacity range. Again in the present study over a scavenging capacity range of $1.5x10^{7}$ - $3.0x10^{8}$ s^{-1} the yields of dsb vary between $3.7x10^{-11}$ - $2.1x10^{-11}$ dsb/Gy/Da. This also illustrates good agreement with other α-particle irradiations of plasmid DNA which have reported yields of dsb varying between $3x10^{-11}$ - $1.5x10^{-11}$ dsb/Gy/Da (Milligan *et al.* 1996a) and $3.8x10^{-11}$ - $2.3x10^{-11}$ dsb/Gy/Da (Prise *et al.* 1999a) over the same scavenging capacity range.

From least square analysis, the yields of dsb induced by γ-ray and α-particle irradiation are approximately equal at a scavenging capacity of about $1.0x10^{8}$ s^{-1}. Jones *et al.* (1993) determined that the yields of ^{4}He ion (mean LET of 102 keV μm^{-1}) induced dsb are approximately equal to the yield from γ-rays at a scavenging capacity of $3x10^{7}$ s^{-1}.

This study represents the first experimental determinations of the dependence of the yields of dsb on scavenging capacity for Al_K USX. Therefore, the yields of dsb determined are particularly important in estimating the yields of complex damage associated with Al_K USX, which has an ionisation density lying between that for ^{60}Co γ-ray and α-particle radiation. In addition they show the effectiveness of some of the low energy electrons present in γ-ray and most other irradiations. From the relationships of the yields of dsb with scavenging capacity, determined by least square fit analysis, the yields of Al_K USX dsb exceed the yields of γ-ray dsb at scavenging capacities > $6x10^{6}$ s^{-1}. Under cell mimetic scavenging capacities ($3x10^{8}$ s^{-1}) the dsb yield from Al_K USX is about 1.7 times that for γ-rays (figure 3.8).

At the D_{37} values of ssb, the dependence of the yield of dsb on scavenger capacity is illustrated in figure 3.9. Representative values for the ratio of ssb:dsb at specific scavenging capacities are presented in table 3.2. As the ionisation density of radiation increases the ratio of ssb:dsb decreases for all of the radiations. It is proposed that this increased probability of inducing a dsb per ssb with increasing scavenging capacity is consistent with complex damage becoming more significant. The increased probability

of inducing a dsb per ssb for α-particle radiation compared with γ-ray radiation for a given scavenging capacity (table 3.2) is consistent with the ionisation density of the tracks for these radiations.

The ratios of ssb:dsb determined for γ-ray and α-particle irradiation in the present study are comparable with previously published values, as summarised in tables 3.4a and 3.4b for γ-ray and α-particle irradiation respectively. Over the approximate range of scavenging capacities of $1x10^6$ s^{-1} to $1x10^{10}$ s^{-1} studied by other groups (Krisch *et al.* 1991, Jones *et al.* 1993, Klimczak *et al.* 1993, Hodgkins *et al.* 1996a and b, Milligan *et al.* 1996a) in the present study the ratio of ssb:dsb varies between 84:1 and 26:1 for γ-ray irradiation and 15:1 and 6:1 for α-particle irradiation. Thus, it may be seen from tables 3.4a and b there is overall good agreement between the present study and a variety of other studies.

The determination of the dependence of either the yield of ssb or dsb and thus the ratio of ssb:dsb on scavenging capacity for Al_K USX irradiation has not previously been investigated in detail. The determination of the yields of DNA strand breaks induced by Al_K USX irradiation is particularly important as the tracks associated with Al_K USX radiation are representative of those for low energy secondary electrons produced in all low LET irradiations, but they also have the characteristics of a densely ionising radiation as discussed above. These low energy secondary electrons are produced at the track ends of high energy photons such as ^{60}Co γ-rays and are thought to contribute approximately 30 % of the total absorbed dose (Nikjoo and Goodhead 1991). Thus the direct comparison between the yields of ssb and dsb induced by Al_K USX and ^{60}Co γ-ray irradiation highlights the relative difference between the low energy electrons induced by USX and the diverse spectrum of electron tracks induced by ^{60}Co γ-ray. At low scavenging capacities, γ-ray irradiation produces a greater yield of ssb than that induced by Al_K USX irradiation where increased intra-track radical-radical recombination occurs. However, an increased ionisation density associated with Al_K USX should give an enhanced yield of complex damage relative to ssb particularly at high scavenging capacities. At low scavenging capacities, there are a greater number of dsb following γ-ray irradiation, due to separate OH radicals leading to spatially close ssbs forming dsbs from two independent tracks (and hence with linear-quadratic dose dependence (figure 3.7a)), but as the scavenging capacity increases and the direct effect becomes more significant, the number of dsb induced by Al_K USX, predominantly from

single tracks, with linear dose dependence exceeds that induced by γ-ray. The increased complexity of damage by Al_K USX is supported by the increased probability of producing a dsb per ssb as shown in table 3.2.

In table 3.3 the yields of strand breaks obtained in plasmid DNA at cell mimetic scavenging capacities, equivalent to $3x10^{-8}$ s^{-1}, when the mean diffusion distance of the OH radical is equal to that determined within the cellular environment, are compared with those induced in irradiated V79 cells (de Lara *et al.* 1995, unpublished data, Botchway *et al.* 1997). The initial justification behind using a plasmid system is that there are fewer variables to consider than for a cellular system and that they are more controllable, and thus it is less complicated to assess the relative importance of quantities such as radiation quality and scavenging capacity. Also the parameter of scavenging capacity can be varied over a much wider range in the plasmid system. These factors are particularly important when experimental results for radiation-induced DNA damage are subsequently compared with those obtained from computer simulations, which, if computing time is to be kept to a practical length require the number of variables to be minimised and well controlled.

However, the long-term aim is to use simulations to assess more complicated biological systems. Thus, it is important to determine the extent to which the plasmid system bears similarity in its response to radiations under cell mimetic conditions, to those exhibited by cells e.g. V79. It should be noted however, that differences in strand break yields between cellular and plasmid systems may arise due to differences in yield determinations (O'Neill *et al.* 1996). For cells, in the determination of strand breaks by pulsed field gel electrophoresis or elution, a heat treatment is generally used at a temperature sufficiently high to induce heat labile sites. Additionally, with alkaline elution, ssb may arise through alkali labile sites. Cells also contain sulfhydryl (-SH) compounds which have a secondary role in chemically repairing radical sites (see review Hall 1994).

From comparison of the yields of ssb and dsb induced in plasmid DNA and mammalian cells by γ-ray irradiation (table 3.3) both the yields of ssb and dsb are similar although the plasmid yields are about a factor of two higher than those measured within cells. For α-particle irradiation, the yields of ssb and dsb are approximately a factor of 2.5 greater with plasmid DNA than cells. For α-particle and Al_K USX irradiation, computer simulated values for ssb and dsb values are also included for comparison. These

simulated values will be discussed further in chapter 4 although it should be noted that there is generally good agreement between the plasmid and simulated yields of strand breaks. With Al_K USX irradiation, both the yields of ssb and dsb for the plasmid system are approximately a factor of 1.5 greater than those in the cellular system. With all radiations, the yields of both ssb and dsb are the same order higher for the plasmid system and very similar ratios for ssb:dsb are subsequently obtained in plasmid DNA and cells. That there are an increased number of both ssb and dsb in the plasmid system relative to a cellular system is in general agreement with irradiations undertaken on naked cellular DNA and DNA complexed with histones and non-histone proteins to form chromatin structures. It is found that the chromatin structure affords protection from the formation of dsbs relative to naked DNA (Elia and Bradley 1992, Warters and Lyons 1992, Oleinick and Chiu 1994). Even though these differences may reflect the choice of scavenging capacity, the similarity in the yields of induced damage by the three radiations for the cellular and plasmid systems confirms the usefulness of the plasmid system for determining DNA damage. Furthermore, unlike the cellular system, the plasmid system allows easy, convenient and large alterations in the scavenging capacity to be made, providing an additional variable parameter for the comparison of experimentally determined yields of DNA damage with those obtained from simulations (see chapter 4).

The RBE for dsb induction in plasmid DNA at a cell mimetic scavenging capacity (mean average OH radical diffusion distance of 4-6 nm) for α-particle relative to γ-ray irradiation is determined to be 1.3. A number of cellular studies have shown the RBE for induction of dsb by α-particles is ≤ 1 (Prise *et al.* 1987, Jenner *et al.* 1992, 1993). However, small fragments produced by a multiple number of dsbs are not recorded compared with conventional PFGE detection potentially leading to an underestimation of the yield of dsb. However, as pUC18 plasmid is relatively small (2686 bp), the formation of small fragments will be less significant than for cellular DNA. Rydberg (1996) has shown an enhancement of small fragments in cells irradiated with high LET particles. Newman *et al.* (1997) have taken into account the increased number of dsb arising from the analysis of the small fragment distribution with α-particle relative to γ-ray irradiation and determined an RBE for α-particles of 1.27 in V79 cells, in good agreement with the value determined with plasmid DNA.

The RBE for Al_K USX relative to γ-ray irradiation for dsb induction in plasmid DNA at a cell mimetic scavenging capacity was determined to be 1.7. This value is slightly lower than the previously quoted values for cellular systems of 2.6 (Botchway *et al.* 1997) and 1.8 (deLara unpublished data) although again the chromatin structure within cellular DNA may afford greater protection following γ-ray irradiation than for the more densely ionising Al_K USX, effectively increasing the RBE for Al_K USX in the cellular system relative to the plasmid system.

In summary, for all three radiations the yields of ssb and dsb for plasmids follow the same trends observed for V79 cells on ionisation density of the radiations.

Table 3.1.

Yield of ssb/Gy/Da determined at room temperature for γ-ray irradiation of aqueous solution DNA by various groups -data are estimated from graphical representation. Data for the current study were obtained at 4^0 C-values that include heat labile sites are included in brackets.

Scavenging Capacity s^{-1}	ssb/Gy/Da yields Current Study pUC18 plasmid	Krisch *et al.* 1991 SV40 DNA	Milligan *et al.* 1996a pUC18 and pEC plasmid	Klimczak *et al.* 1993 pBR322 plasmid
10^6	$2x10^{-8}$ ($4x10^{-8}$)	$4x10^{-8}$	$4x10^{-8}$	$5x10^{-8}$
10^7	$5x10^{-9}$ ($8x10^{-9}$)	$9x10^{-9}$	$9x10^{-9}$	$1x10^{-8}$
10^8	$1x10^{-9}$ ($2x10^{-9}$)	$2x10^{-9}$	$2x10^{-9}$	$3x10^{-9}$
10^9	$3x10^{-10}$ ($4x10^{-10}$)	$4x10^{-10}$	$6x10^{-10}$	$6x10^{-10}$

Table 3.2.

The ratios of ssb:dsb for a range of scavenging capacities for ^{60}Co γ-rays, ^{238}Pu α-particles and Al_K USX irradiation of pUC18 DNA in aqueous solution at 4^0 C.

Tris concentration mmol dm^{-3}	Scavenging Capacity s^{-1}	Irradiation Source γ-rays	α-particles	Al_K USX
0.1	$1.5x10^5$	159:1	22:1	40:1
1.0	$1.5x10^6$	77:1	14:1	26:1
10	$1.5x10^7$	57:1	11:1	19:1
100	$1.5x10^8$	38:1	8:1	15:1

Table 3.3.

Strand break yields for pUC18 plasmid DNA at a cell mimetic equivalent scavenging capacity set by 0.2 mol dm^{-3} Tris relative to V79 cells irradiated with ^{60}Co γ-rays, ^{238}Pu α-particles and Al_K USX at 4^0 C.

Radiation Source and Biological Target	ssb/Gy/Da	dsb/Gy/Da	ssb:dsb
^{60}Co γ-rays			
pUC18 Plasmid	$5.6x10^{-10}$	$16x10^{-12}$	35:1
V79 cells	[1]$2.9x10^{-10}$	[3]$11.7x10^{-12}$	25:1
^{238}Pu α-particles			
pUC18 Plasmid	$1.6x10^{-10}$	$21x10^{-12}$	8:1
V79 cells	[1]$0.7x10^{-10}$	[3]$9.9/^{4}14.8x10^{-12}$	7:1/5:1
Simulation (see chapter 4)	$1.6x10^{-10}$	$55x10^{-12}$	3:1
Al_K USX			
pUC18 Plasmid	$4.6x10^{-10}$	$27x10^{-12}$	17:1
V79 cells	[2]$2.7x10^{-10}$	[2]$21x10^{-12}$	13:1
Simulation (see chapter 4)	$2.8x10^{-10}$	$22x10^{-12}$	13:1

[1]deLara *et al.* 1995

[2]Botchway *et al.* 1997

[3]deLara *et al.* unpublished data

[4]dsb yield multiplied by 1.27 to take into account small fragments (Newman *et al.* 1997)

Table 3.4a.

Ratios of ssb:dsb determined for a range of scavenging capacities for γ-ray irradiation of SV40* or plasmid DNA in aqueous solution.

Research Group	Scavenging capacity range s^{-1}	Ratio of ssb:dsb range
Krisch *et al.* 1991	$3x10^6$-$1.5x10^8$	150:1-40:1*
Milligan *et al.* 1996a	$6.6x10^6$-$6.6x10^9$	~100:1
Jones *et al.* 1993	$6.6x10^6$-$1.3x10^{10}$	60:1-30:1*
Hodgkins *et al.* 1996a	$1.5x10^7$-$3.0x10^8$	70:1-40:1
Klimczak *et al.* 1993	$2.0x10^8$-$6.0x10^9$	150:1-60:1

Table 3.4b.

Ratios of ssb:dsb determined for a range of scavenging capacities for α-particle irradiation of SV40* or plasmid DNA in aqueous solution.

Research Group	Scavenging capacity range s^{-1}	Ratio of ssb:dsb range	Mean LET
Milligan *et al.* 1996a	$6.6x10^6$-$6.6x10^9$	~25:1-15:1	94 keV μm^{-1}
Jones *et al.* 1993	$6.6x10^6$-$1.3x10^{10}$	~10:1*	102 keV μm^{-1}
Hodgkins *et al.* 1996b	$1.5x10^7$-$3.0x10^8$	~13:1	120 keV μm^{-1}

Figure 3.1.

Representative dose response illustrating the variation in the percentage of closed circular pUC18 DNA in aqueous solution containing 20 mmol dm^{-3} Tris and irradiated with γ-rays at 20^0 C.

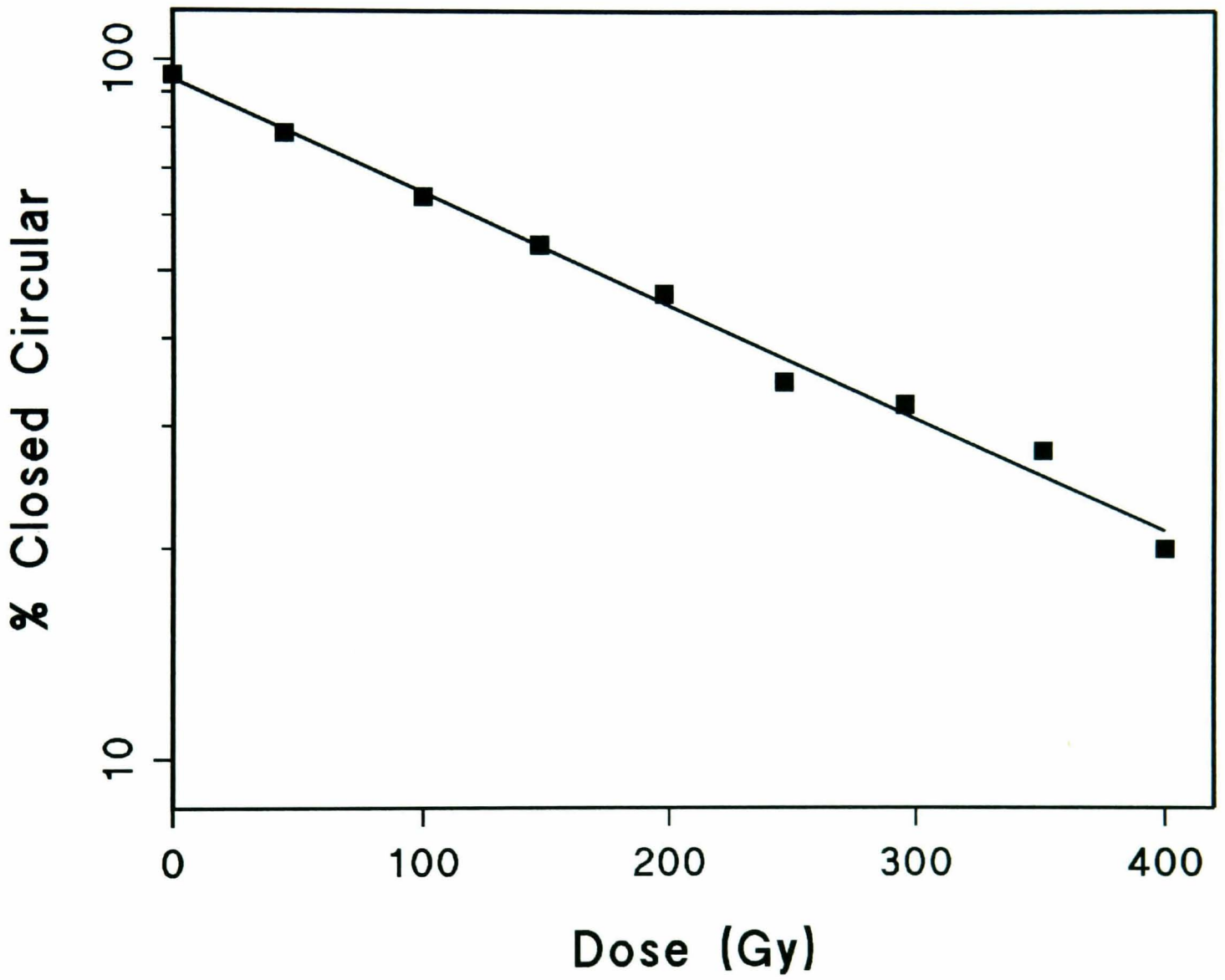

Figure 3.2.

Variation in the yield of ssb/Gy/Da on scavenging capacity, determined from the concentration of Tris or ethanol and their respective rate constants with OH radicals for γ-ray irradiation of pUC18 plasmid DNA in aqueous solution at 20^0 C.

❍ Tris

∇ Ethanol

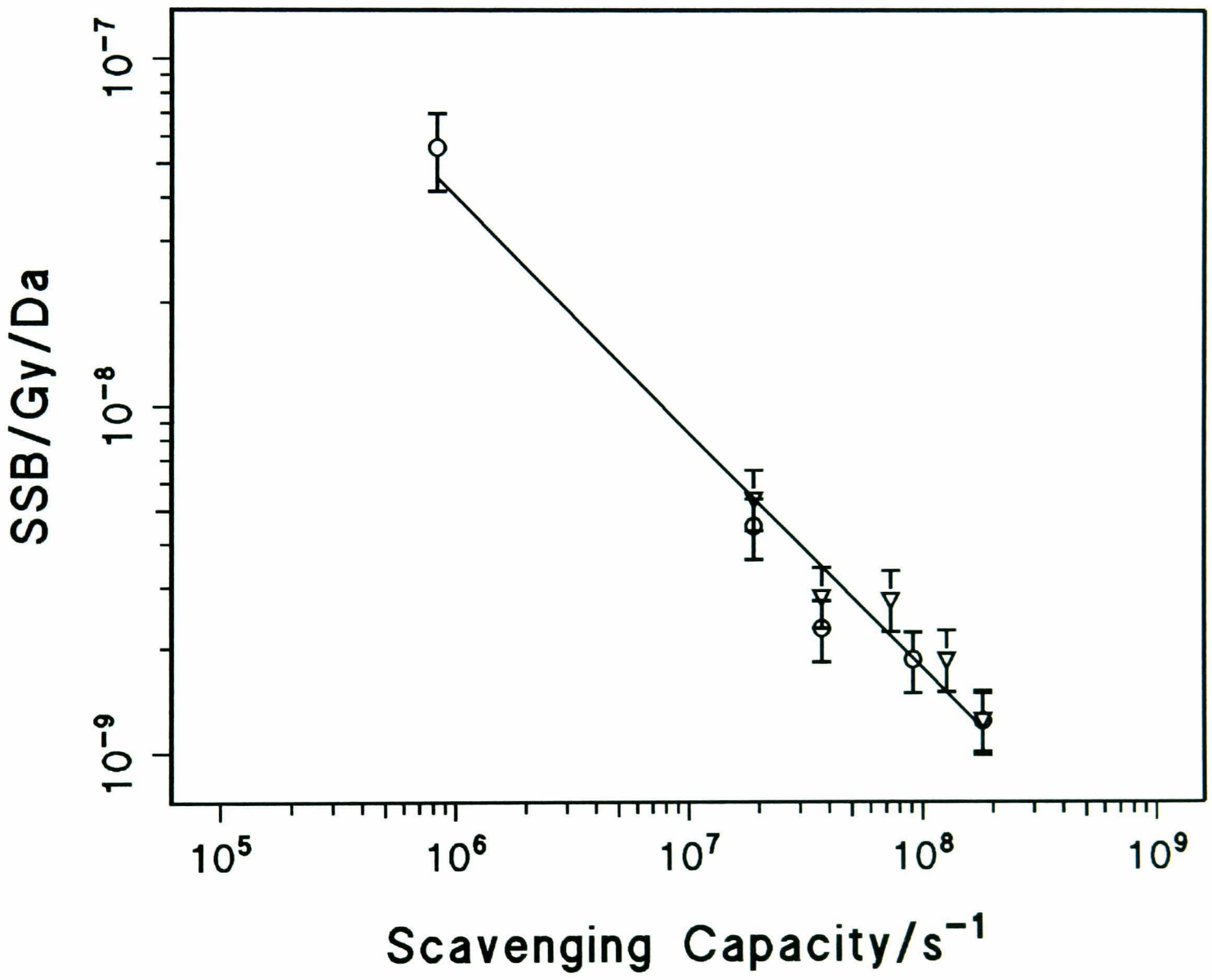

Figure 3.3.

Variation in ssb/Gy/Da on scavenging capacity resulting from changes in Tris or ethanol concentration for γ-ray irradiation of pUC18 plasmid DNA in aqueous solution at different temperatures.

❍ Tris-room temperature

∇ Ethanol-room temperature

■ Tris-4^0 C

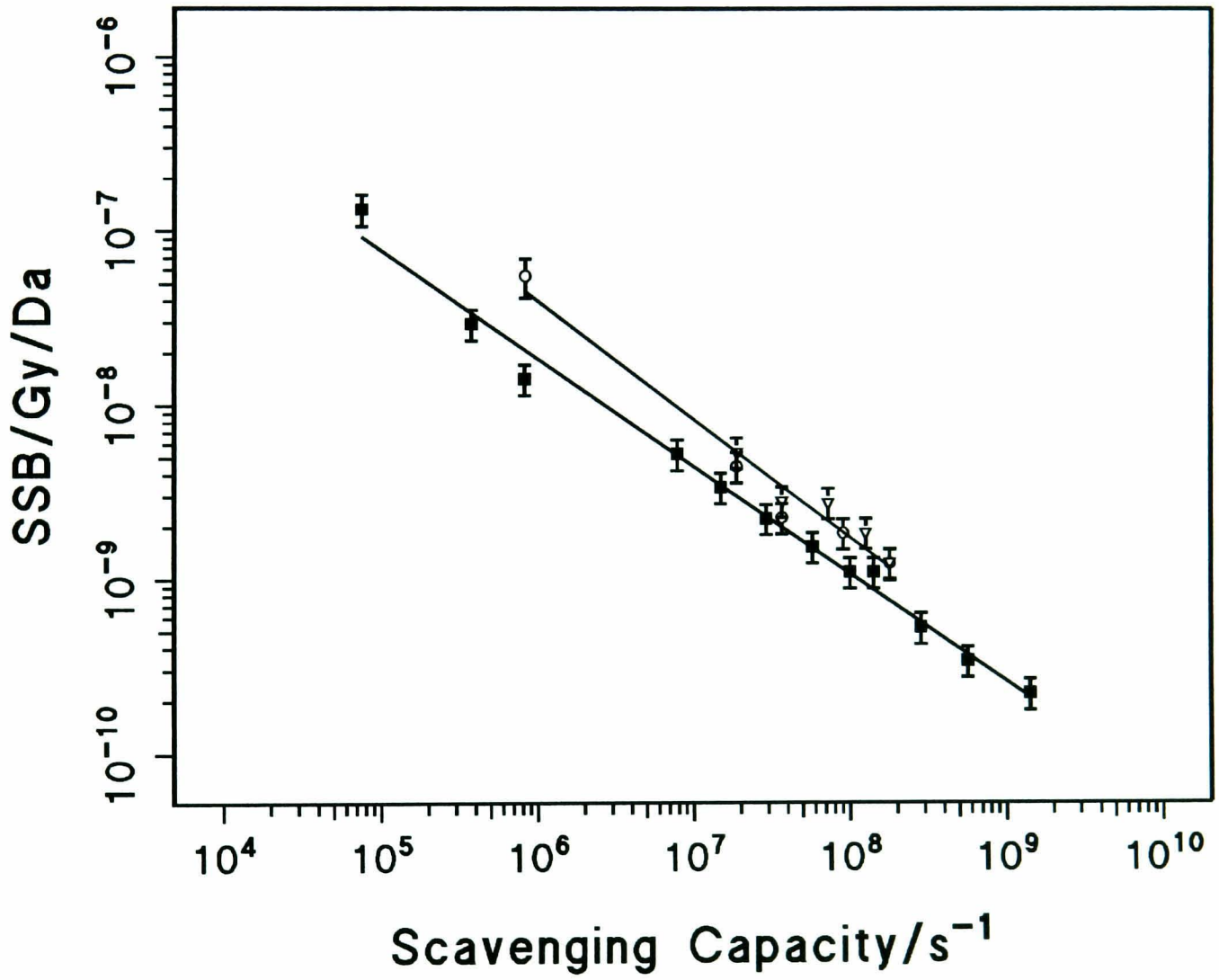

Figure 3.4.

Variation in excess number of ssb obtained with variable scavenging capacity for plasmid DNA in aqueous solution maintained at 20^0 C relative to plasmid DNA in aqueous solution at 4^0 C. Note: the graph is based on the data illustrated in figure 3.3.

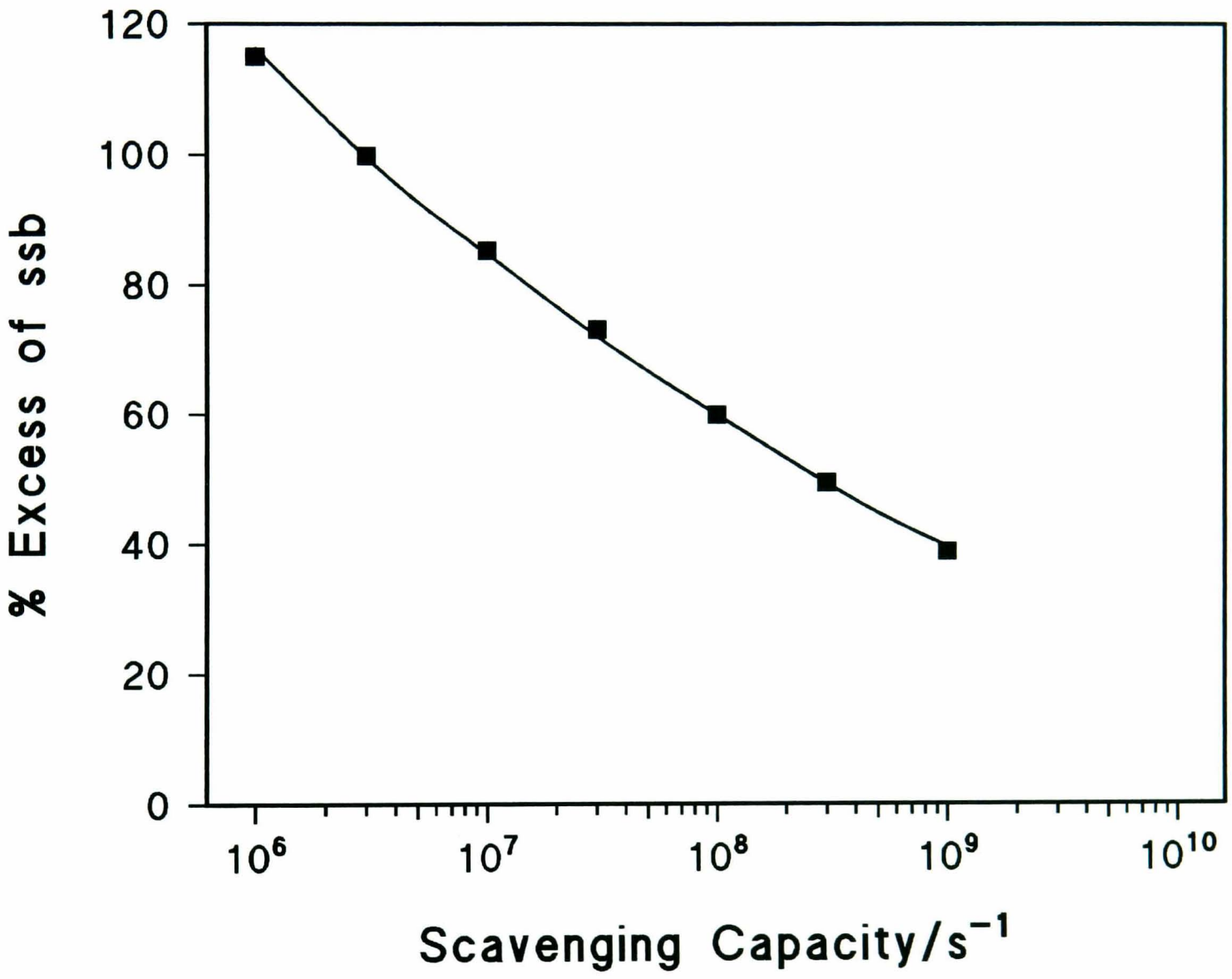

Figure 3.5.

Variation in the mean OH radical diffusion distance with OH radical scavenging capacity (Roots and Okada 1975).

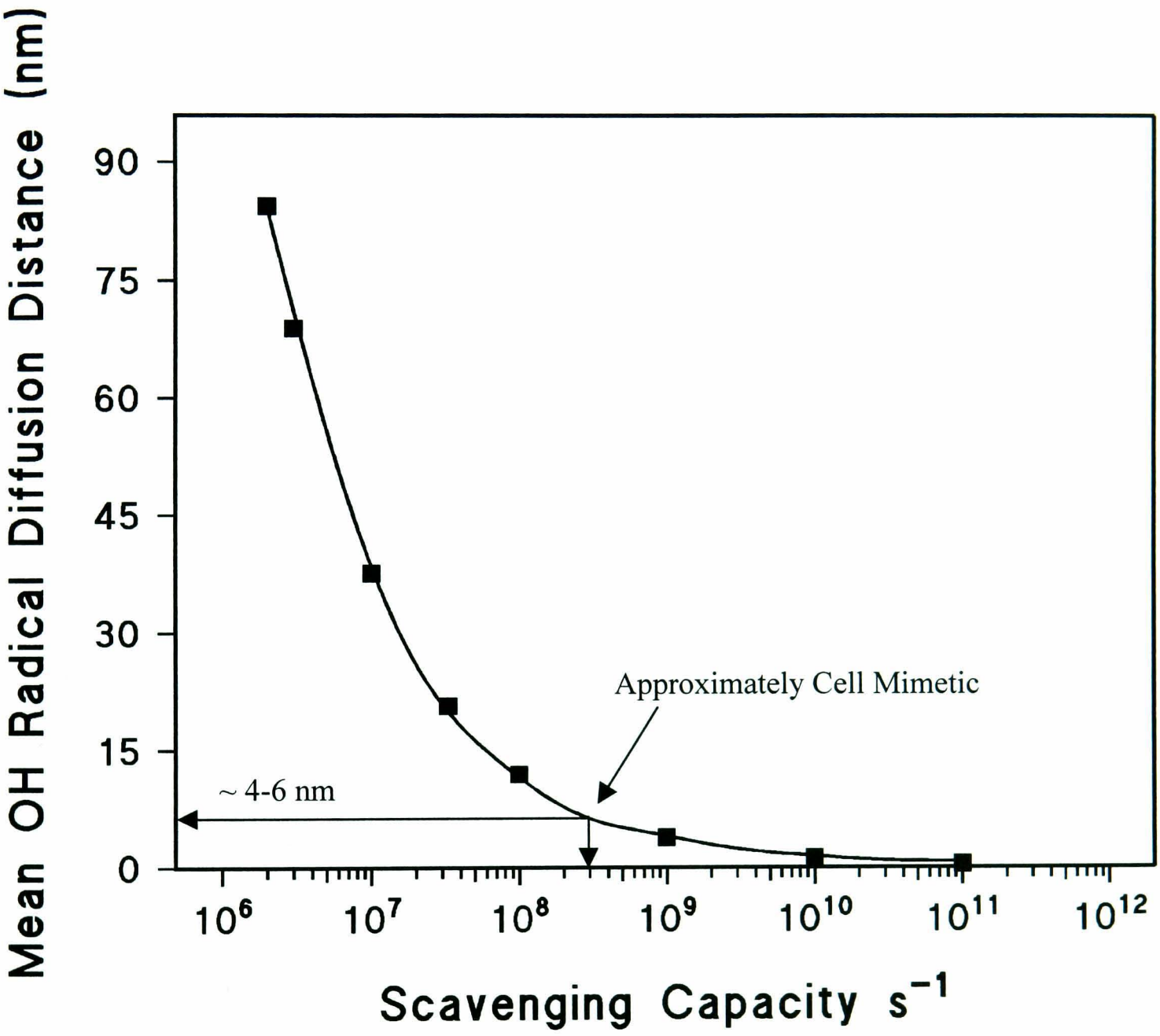

Figure 3.6.

Variation in ssb/Gy/Da on scavenging capacity resulting from changes in Tris concentration for irradiation of pUC18 DNA in aqueous solution with γ-ray, Al_K USX and α-particle at 4^0 C.

■ γ-ray

❍ Al_K USX

▲ α-particle

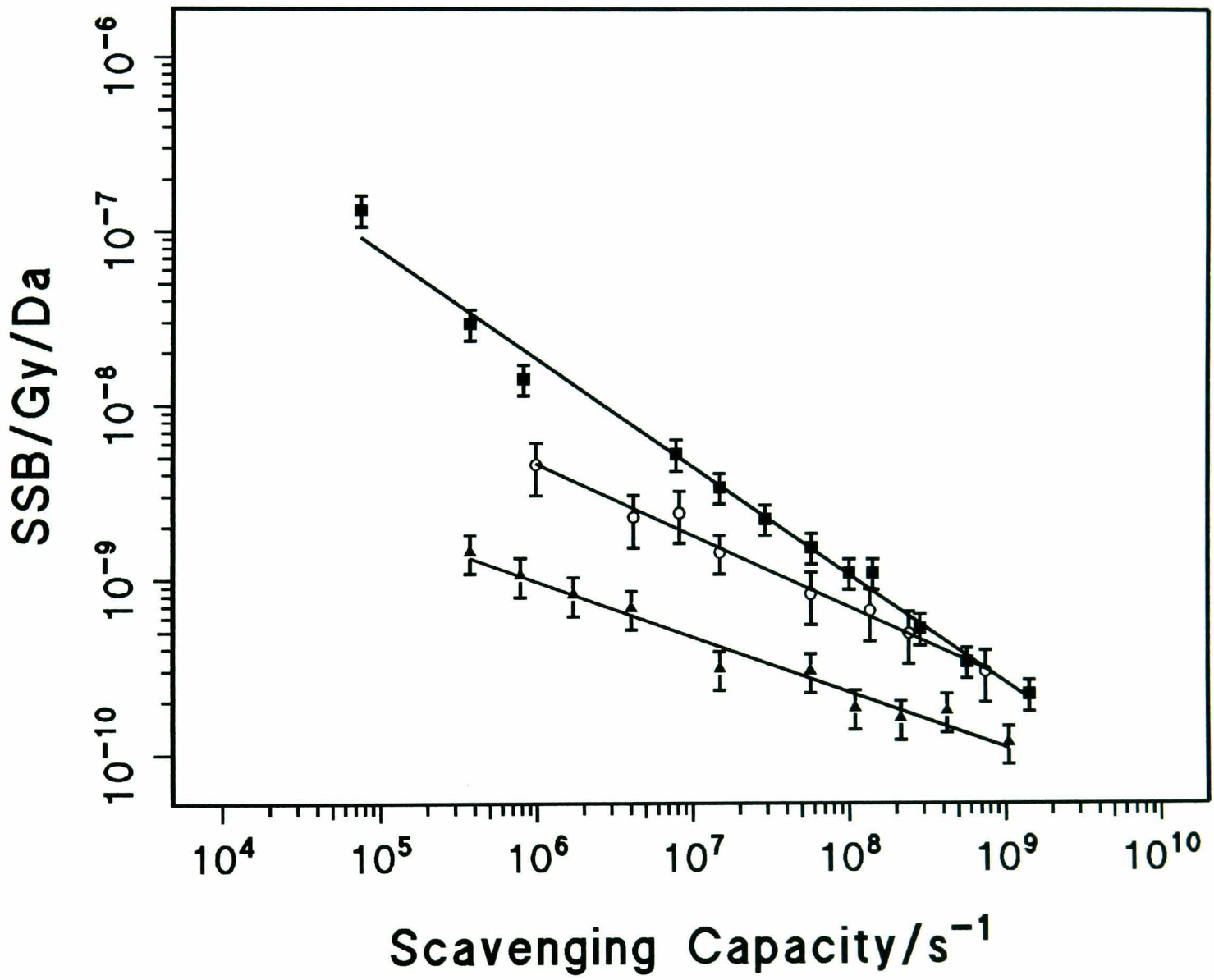

Figure 3.7.

Dependence of the percentage of linear plasmid DNA on dose for irradiation of an aqueous solution of pUC18 DNA at 4^0 C: a) ^{60}Co γ-ray irradiation DNA in 5 mmol dm^{-3} Tris solution b) α-particle irradiation in 42 mmol dm^{-3} Tris solution.

a)

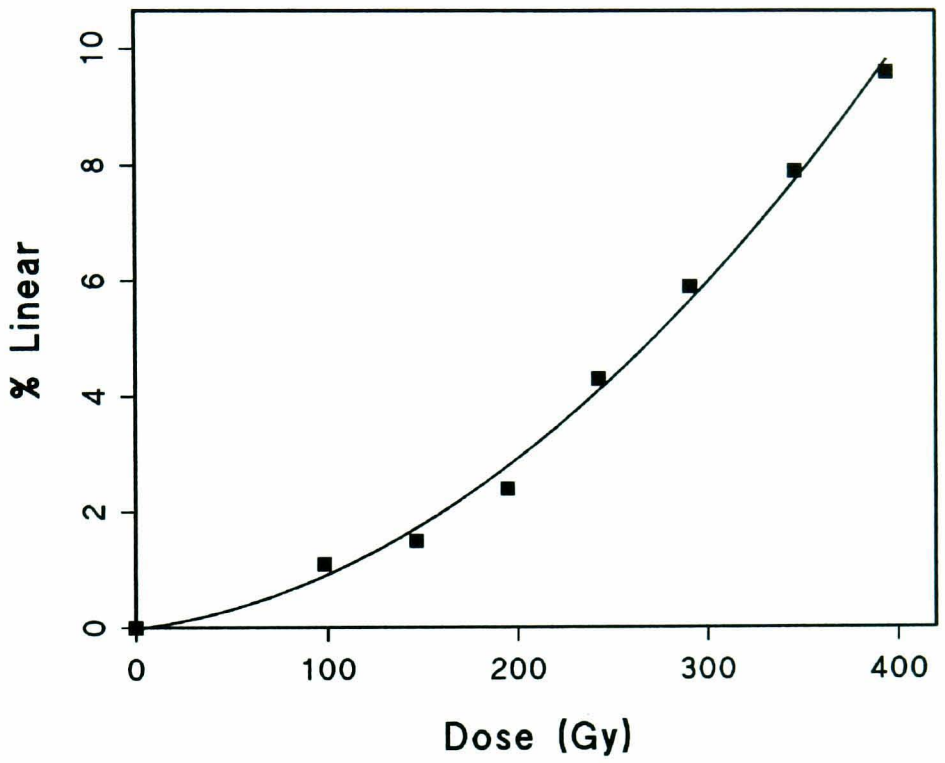

b)

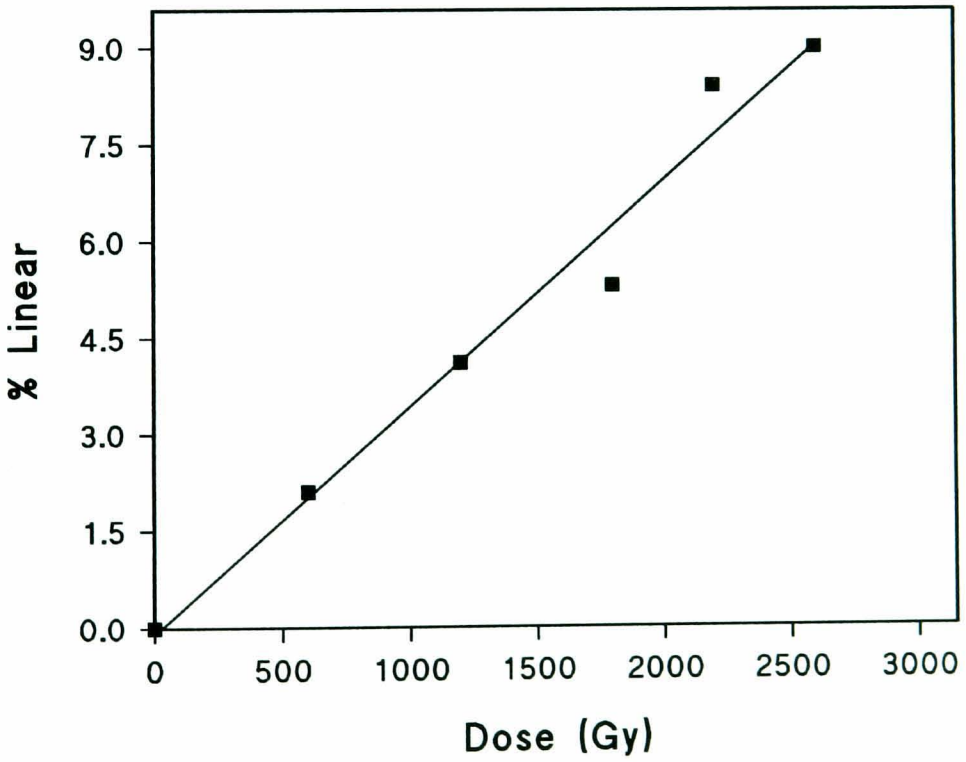

Figure 3.8.

Variation in dsb/Gy/Da on scavenging capacity resulting from changes in Tris concentration for irradiation of pUC18 DNA in aqueous solution with γ-ray, Al_K USX and α-particle at 4^0 C.

■ γ-ray

○ Al_K USX

▲ α-particle

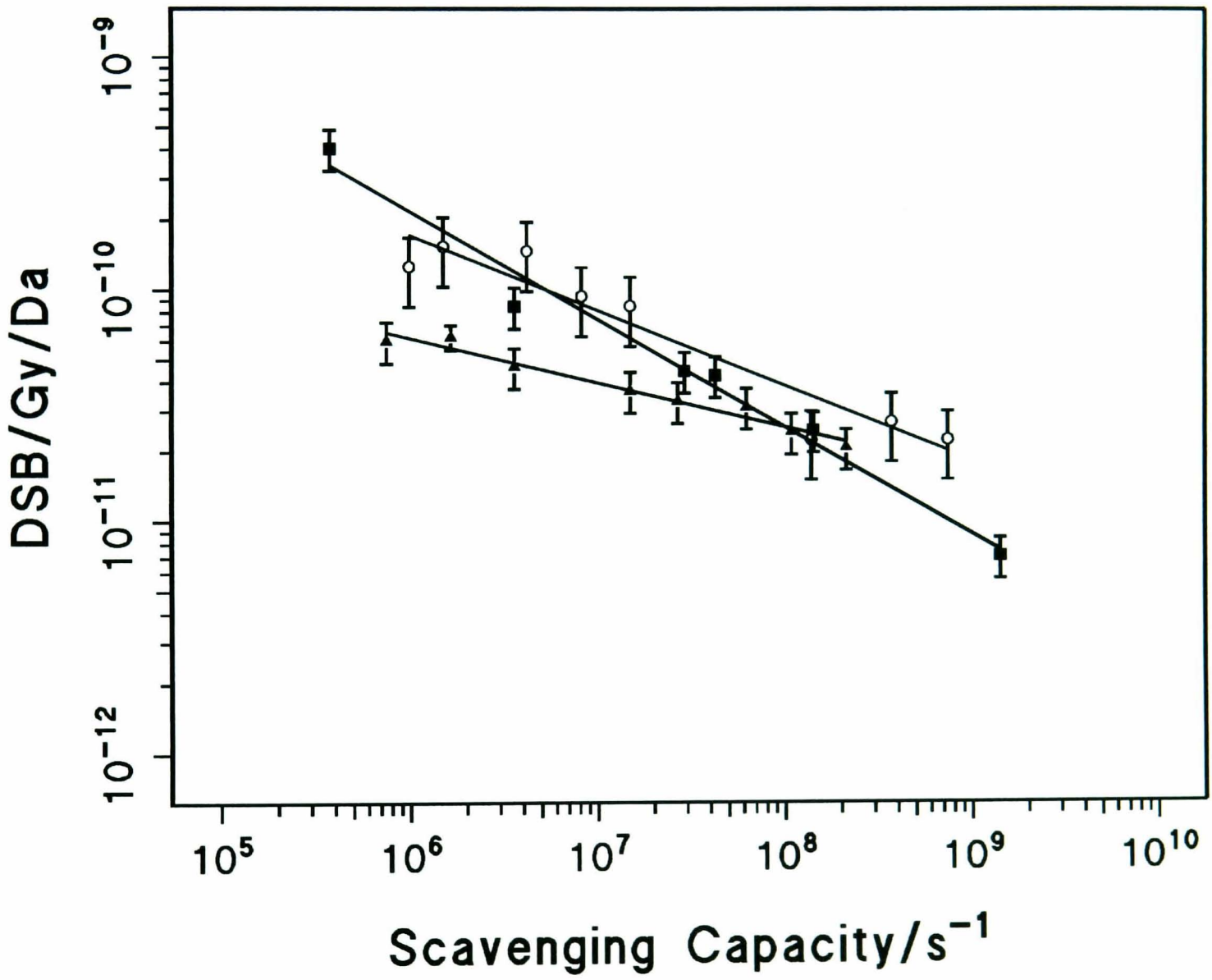

Figure 3.9.

Variation in the percentage yields of dsb at the D_{37} for ssb for specific scavenging capacities for irradiation of pUC18 DNA in aqueous solution with γ-ray, Al_K USX and α-particle at 4^0 C.

■ γ-ray

○ Al_K USX

▲ α-particle

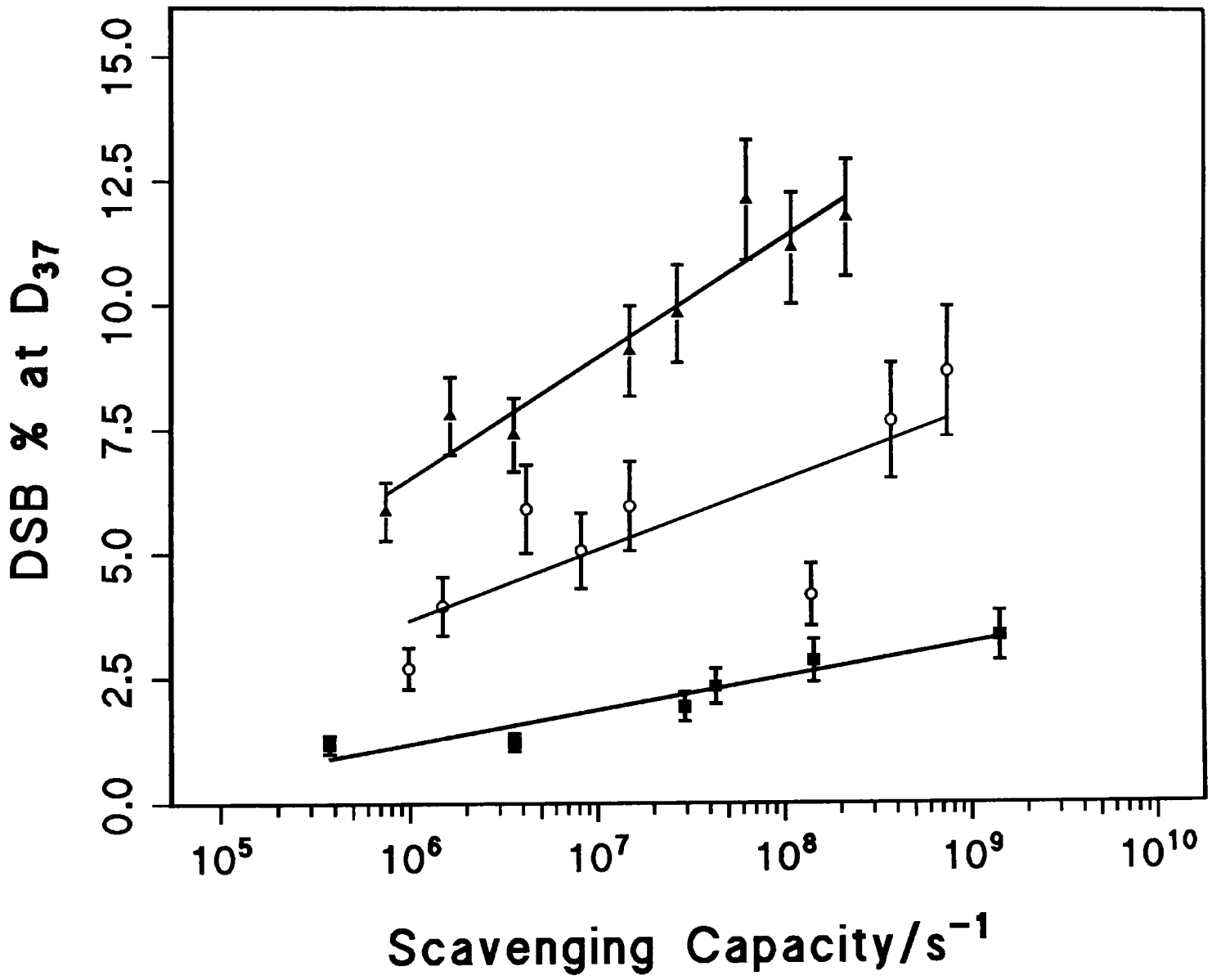

Chapter 4

The Simulation of 1.5 keV electron and α-particle Tracks and Subsequent Comparison of the Yields of DNA ssb and dsb with those Determined Experimentally

4.1. Introduction

As previously discussed in section 1.2, if simulated yields of strand breaks, determined under experimentally inaccessible conditions, are to be treated with confidence then the same simulation must produce yields of strand breaks in good agreement with those which may be experimentally determined. Of all of the yields of ssb and dsb experimentally determined within the present study, only a certain proportion are suitable for subsequent computational comparison due to certain limitations inherent within the computer analysis, principally computing time. In section 2.7, the basic principles involved in the analysis of damage induced by the passage of a radiation track are described. Analysis involves generating each physical track formed by the radiation and determining the location and magnitude of every energy deposition associated with it. Additionally, a corresponding water chemical track is produced which represents the initial condition for diffusion of all chemical species produced from the initial energy depositions associated with the physical track, and the determination of all of the reactions that these species subsequently undergo. Determinations of the yields of DNA damage are subsequently obtained by placing segments of DNA within the volume which contains the radiation tracks and examining whether energy depositions occur within the volume occupied by the DNA or whether species diffuse to and interact with the DNA as described in section 2.7.1. Hence, greater computing time is required as the size of the physical track increases and/or the diffusion distances associated with the water species increase as the scavenger concentration decreases. Increases in the physical track dimensions are associated with increases in energy of the incident photon or particle. Increases in the diffusion distances of the water species arise when the diffusion time and distance cut-off parameters within the simulation are increased, as described in section 2.7.1. These parameters are set to mimic the scavenging capacity for those experimental conditions to be simulated. At present the simulations are limited, in terms of energy, to electron

energies less than approximately 4.5 keV although scoring techniques are being developed (Bolton *et al.* 1999) to simulate higher energies. In addition codes have been developed for ion tracks so that α-particles may be simulated (Wilson and Nikjoo 1999). In terms of diffusion distances, simulations are restricted to diffusion distances of radical species and time cut-offs equivalent to experiments with scavenging capacities > $1x10^6$ s^{-1}. At present such limitations effectively make it impractical to simulate the yields of DNA ssb and dsb induced by ^{60}Co γ-ray irradiation described in chapter 3 due to energy constraints and the study described in chapter 7 where the variation in the yield of OH radicals is determined for different energy photons, due to the low scavenging capacity utilised. Thus, comparisons between simulated and experimental data previously described in chapter 3 are limited here to the simulation of the yields of strand breaks for Al_K USX and α-particle irradiations over a range of scavenging capacities > $1x10^6$ s^{-1}.

4.2. Simulations of the Yield of DNA Strand Breaks Induced by 1.5 keV electron and α-particle Irradiation of DNA

As discussed in section 2.7.1, the average diffusion distance for a radical species is given by $2.26(Dt)^{1/2}$ (Roots and Okada 1975) where D is the diffusion coefficient and t is the average lifetime of the radical species. As OH radicals are considered to be principally responsible for strand breaks (Chapman 1973, Roots and Okada 1975, von Sonntag 1987, O'Neill and Fielden 1993) the radius of the volume around the DNA within which species may diffuse and react with DNA is dictated by the OH radical scavenging capacity of the solution. The lifetime (t) of the OH radical is calculated from the inverse of the product of the scavenging capacity and the rate constant of the OH radicals and the scavenger. Therefore setting the scavenging capacity of the conditions to be simulated allows t to be determined and knowing the diffusion coefficient of the OH radical, the radius of the volume around the DNA may be calculated. Table 4.1 illustrates representative experimental scavenging capacities and calculated equivalent time cut-offs, distance cut-offs and mean OH radical diffusion distance used in the simulations. Although the average diffusion distance may readily be calculated using the equation above, this distance only represents an average value, whereas OH radicals have a range of diffusion distances around this average. Therefore, a distance cut-off based purely on the average radical diffusion distance

results in those radicals with diffusion distances greater than the average being ignored and not considered able to give rise to DNA damage. The use of the average diffusion distance may therefore lead to an underestimation in the yield of strand breaks determined. To examine this effect, the distance cut-off was varied from 0-30 nm for a fixed time cut-off value of 10^{-8} s^{-1} as illustrated in figure 4.1, where a 1 keV electron track is simulated. The average diffusion distance for an OH radical determined with a lifetime of $1x10^{-8}$ s^{-1} is equal to 11.9 nm. From figure 4.1, it is apparent that increases in the distance cut-off initially lead to a rapid increase in the yields of ssb. However, with continued increase in the distance cut-off, the yields of ssb tend towards a plateau at 30 nm. Relative to the plateau yield, the yield of ssb obtained with a distance cut-off of 11.9 nm is approximately 16 % lower. If all the ssb associated with a radiation are to be included in the simulation yield, it is important that the diffusion cut-off distance is considerably larger than the distance calculated for the average OH radical diffusion distance. However, the time required for computer simulations is proportional to the total volume within which radicals are allowed to diffuse. The time required to undertake simulations is proportional to the (diffusion cut-off distance)^3. Therefore, a compromise is necessary between including all radicals that may potentially go on to cause strand breaks and restricting computing times to within practical limits. With a time cut-off of $1x10^{-8}$ s^{-1} and a distance cut-off value of 12 nm, approximately equal to the calculated average OH radical diffusion distance, the yield of ssb is approximately 84 % of that determined for a cut-off of 30 nm. However, the increase in computing time associated with increasing the cut-off distance to 30 nm will be significant and impractical for low scavenging capacities where very long diffusion distances have to be considered. Therefore, it was decided to set a distance cut-off approximately 105 % of the average OH radical diffusion distance, as this represents a distance which results in scoring > 85 % of the ssb induced, but ensuring simulation times are maintained within practical limits. All diffusion distance cut-offs for subsequent analysis are set to 105 % of the calculated average OH radical diffusion distance for the scavenging capacities simulated. In table 4.1, the value for the cylindrical radius around the DNA is equal to 105 % of the calculated average OH radical diffusion distance at each given scavenging capacity.

4.2.1. Simulations of the Yields of DNA Strand Breaks Induced by 1.5 keV Electrons: Comparison with Experimental Data

Figures 4.2-4.6 illustrate results obtained from the simulation of the interaction of a 1.5 keV electron with DNA in aqueous solution at variable scavenging capacities; the number of tracks scored and yields of ssb and dsb are summarised in table 4.2. The simulation was undertaken by examining the interactions of a 1.5 keV electron with DNA and examining the subsequent diffusion of radicals as fully described in section 2.7.1. In figure 4.2 the yields of ssb determined from the simulation are compared with those determined experimentally for the yields of ssb following Al_K USX irradiation of plasmid DNA at 4^0 C (see chapter 3). There are restrictions to the range of scavenging capacities over which the determination of ssb and dsb may be obtained for both simulations and experimental conditions as previously described in sections 3.2.3 and 4.1. For instance, experimental yields of ssb have not been determined at scavenging capacities > 10^9 s^{-1} due to excessive radiation times and the necessity to ensure a large water:scavenger ratio so that the majority of radiation interactions effectively occur in either water or directly within the DNA and not the scavenger molecules. Simulations are limited to scavenging capacities > $2x10^6$ s^{-1} since the diffusion distances of the water radicals increase with decreasing scavenging capacities, making computing time impractical. However, comparisons between experiment and simulation can be made for the yields of ssb at scavenging capacities between $3x10^6$ and $7.5x10^8$ s^{-1} as illustrated in figure 4.2. Generally, throughout this range the dependence of the yields of ssb on scavenging capacity show a good agreement between the simulated and experimentally determined yields, with the simulated yields generally lying within the error bars of the experimentally determined yields. The simulated data clearly show that the yields of ssb have a non-linear dependence on scavenging capacity on a log-log plot. At a scavenging capacity of $3x10^8$ s^{-1}, characteristic of the cellular environment, the simulated yields of ssb are less than the experimental values by about 40 % whereas at a low scavenging capacity of $3x10^6$ s^{-1} the simulated yields of ssb are 40 % greater than those determined experimentally.

In figure 4.3 the variation in the yields of dsb with scavenger capacity determined experimentally for Al_K USX and for the 1.5 keV electron track simulation are illustrated, again revealing generally good agreement. The experimentally determined yields of dsb have a relatively large scatter associated with them due to errors inherent within USX irradiations, resulting from long irradiation times and strong dependence of

USX attenuation on sample thickness (see section 2.3.4). Within the accuracies imposed by these experimental limitations there is no significant difference between the experimental and simulated yields.

The variations in the dependences of the ratio of ssb:dsb with scavenging capacity for the simulated and experimental data are illustrated in figure 4.4. As with the yields of ssb and dsb individually there is a limited range over which both simulated and experimental data are obtainable. From the response illustrated in figure 4.4 it is apparent that as the scavenging capacity increases both the experimental and simulated ratios of ssb:dsb decreases reaching a plateau level of approximately 12:1, although this value is reached at different scavenging capacities for simulation and experiment respectively. The rate of increase in the ratio of ssb:dsb however, with decreasing scavenging capacity is greater for the simulated response especially at scavenging capacities $< 10^8$ s^{-1}. Thus, for example, at a scavenging capacity of 10^7 s^{-1} the simulated ratio of ssb:dsb is approximately 35:1 whereas the experimental ratio is approximately 17:1. However, as scavenging capacity continues to decrease the experimental ratio of ssb:dsb begins to increase rapidly so that at scavenging capacities $< 10^7$ s^{-1} the two responses effectively run parallel to each other. The ratio of ssb:dsb is very sensitive to the individual yields of damage so that if either of the values were over- or under-estimated then this would lead to a significant effect on the ratio of ssb:dsb. At a cell mimetic scavenging capacity the ratio of ssb:dsb for simulation and experiments are indistinguishable with a value of 12:1.

Figures 4.5 and 4.6 illustrate the complexity and the contribution of the direct effect respectively for formation of damage determined from simulations of 1.5 keV electrons and the dependence of these yields on scavenging capacity. In both cases only the damage arising from the yields of strand breaks is considered with no additional contribution from the simulations of base damage. In figure 4.5 the proportion of dsbs which are determined to be complex, based on the classification discussed in section 2.7.3, is shown to be strongly dependent upon the scavenging capacity at scavenging capacities $< 1x10^8$ s^{-1}. As scavenging capacity increases from $3x10^6$ to $1x10^8$ s^{-1}, the percentage of dsb classified as complex doubles from approximately 14 % to 28 %. At higher scavenging capacities the response reaches a plateau with a maximum complex proportion for dsb of approximately 31 %. That this value represents an upper limit is confirmed from simulations where all damage is considered to arise from the direct effect i.e. the yield of dsb determined within the simulations in the absence of the

chemical track. Although this results in a decreased total yield of complex dsb relative to when the chemical track is included the proportion of dsb that are classified as complex remains at approximately 30 %. To assess the contribution of directly produced strand breaks at different scavenging capacities the relative contribution of the direct effect to the yields of ssb and dsb was examined. This dependence is illustrated in figure 4.6 which represents the percentage of ssb and dsbs that are due to the direct effect only i.e. ssb (direct) / total ssb and dsb (direct) / total dsb. Within this classification a hybrid dsb that arises from two ssb, one produced via the direct effect and one from the action of OH radicals is not included within the yields of direct dsb. As the scavenging capacity increases from 10^7 s^{-1} to 10^9 s^{-1} the proportion of dsbs due to the direct effect rises from 30 % to 90 %. This illustrates the significance of the direct effect in giving rise to complex damage as determined by the yields of dsb relative to the dependence of the yield of ssb on the direct effect which rises from approximately 10 % to 65 % over the same scavenging capacity range. It should be noted that even at the lowest scavenging capacity examined of $3x10^6$ s^{-1} the direct effect still contributes approximately 20 % of the dsbs, illustrating how the contribution of directly produced dsb is significant even at relatively low scavenging capacities. At a cell mimetic scavenging capacity, approximately 30 % of the total number of dsbs are classified as complex and approximately 70 % of the dsbs arise as a result of the direct interaction. The direct contribution to the yield of ssb is approximately 45 %.

In table 4.3 comparisons are made between two different simulations of the 1.5 keV Al_K USX. A 1.5 keV Al_K USX photon will interact with water to potentially give a range of electron energies with the most common (~ 85 %) being a 0.96 keV photoelectron and a 0.52 keV Auger electron (Nikjoo *et al.* 1994a). Simulations were carried out to assess any changes in yields of DNA strand breaks obtained from simulating the Al_K USX photon with either a single electron of 1.5 keV or two lower energy electrons of 1.0 keV and 0.5 keV originating at the same point of space. The first simulation, using the single 1.5 keV electron has been used to generate the data described above. The second simulation, using the two electrons, one of 1 keV and one of 500 eV, has the individual electron tracks merged at their respective origin with random orientation to one another (see section 2.7.1.1), to form a single track which is subsequently superimposed on DNA to obtain yields of strand breakage. Comparisons of the respective yields of strand breaks obtained between the two simulations reveal an approximate 10 % decrease in the yield of ssb for the two electron simulation relative

to the simulation employing a single electron throughout the limited scavenging capacity range examined. However the yields of dsb increase by approximately 20 % for the two electron simulation relative to the single electron throughout the same scavenging capacity range. The two electron simulation therefore leads to decreases in the ratio of ssb:dsb of 20 – 25 % relative to the single electron simulations over the scavenging capacity range examined.

4.2.2. Simulations of the Yields of DNA Strand Breaks Induced by α-particles: Comparison with Experimental Data

Figures 4.7, 4.9 and 4.11 to 4.13 illustrate comparisons between the yields of strand breaks for DNA produced in aqueous solution at different scavenging capacities for simulated monoenergetic α-particle track segments of 3.2 MeV and experimental ^{238}Pu α-particle irradiation. The dependences on scavenging capacity of the yields of strand break induction in plasmid DNA at 4^0 C for α-particle irradiation are described in chapter 3. The simulated absolute yields of ssb and dsb are summarised in table 4.4. As was the case for comparisons between experimental and simulated irradiation by Al_K USX, there is a limited scavenging capacity range within which comparisons are undertaken. Again, low scavenging capacities are impractical for simulations due to the excessive computing time required and high scavenging capacities are not experimentally feasible due to the long irradiation times required and the increased probability of depositing energy in the scavenger molecules. In figure 4.7 a direct comparison is made between the yields of ssb obtained experimentally and from simulations over a scavenging capacity range of $2x10^6$ s^{-1} to $9x10^8$ s^{-1} and reveals excellent agreement. At a cell mimetic scavenging capacity of $3x10^8$ s^{-1}, there is no significant difference between the yields of ssb obtained from simulation and experiments. If a comparison is made of the yields of ssb from the simulations of the 1.5 keV electron and α-particle, illustrated in figures 4.8, it is apparent that yields of ssb are greater for the simulation of the 1.5 keV electron than for the α-particle simulation over the entire scavenging capacity range examined. In addition, it is evident that the increase in the yields of ssb with decreasing scavenging capacity, especially at lower scavenging capacities, is much greater for the 1.5 keV electron than for the α-particle simulation. Therefore the α-particle yields of ssb show significantly less dependence on scavenging capacity at scavenging capacities $<10^8$ s^{-1}.

In figure 4.9 the dependence of the yields of dsb on scavenging capacity is illustrated for the simulated and experimental data for α-particle irradiation of DNA. Direct comparison between the determinations may only be made for scavenging capacities between $1x10^7$ to $2x10^8$ s^{-1} due to the constraints of the experimental irradiation times, which are limited so as to avoid sample evaporation (see section 3.2.3). The simulated yield of dsb obtained at a scavenging capacity of $2x10^6$ s^{-1} has not been included within the plot due to the very low number of dsb (see table 4.4). However the point has been plotted along with associated error bars, which assume random Poisson scoring, to illustrate the statistical limitations. Throughout this scavenging range there is a clear difference between the simulated and experimental yields of dsb, with the simulated yields being a factor of 2-3 greater than the experimental values. At a cell mimetic scavenging capacity of $3x10^8$ s^{-1}, the experimental yields of dsb estimated from extrapolation are approximately a factor of 2.5 less than the yields of dsb obtained from the simulation.

In figure 4.10 comparisons are made between the yields of dsb obtained for the simulated 1.5 keV electron and α-particle tracks. Simulations of 1.5 keV electron tracks result in a lower yield of dsb for the α-particle simulations throughout the scavenging capacity range examined.

When the ratios of ssb:dsb determined from the simulated and experimental data are compared, there is a distinct discrepancy as shown in figure 4.11. This difference reflects the differences in the yields of dsb between experiment and simulation (see figure 4.9) since negligible differences are obtained between experimental and simulated yields of ssb (see figure 4.7). However, although the ratios of ssb:dsb are significantly different, it is apparent that the two ssb:dsb responses for experiment and simulation both show an increase in the ratio of ssb:dsb as the scavenging capacity decreases. Thus at scavenging capacities > 10^8 s^{-1} the ratios of ssb:dsb are approximately constant with values of ~ 2.5:1 and 8:1 for simulations and experiments respectively. At scavenging capacities less than this value there is a rapid increase in the ratio of ssb:dsb with values increasing to ~ 6:1 and 12:1 for simulation and experiment respectively as the scavenging capacity decreases to 10^7 s^{-1}. At a cell mimetic scavenging capacity, the ratio of ssb:dsb for the experimental data are approximately a factor of 2.5 higher than for the simulation with values of 8:1 and 2.5:1

respectively obtained. This factor is similar to that for the differences in the yields of dsb determined between experiment and from simulations.

The dependence of the yield of complex damage on scavenging capacity is shown in figure 4.12 for the α-particle simulations. It is apparent that as the scavenging capacity increases up to 10^8 s^{-1} there is an increase in the proportion of dsbs classified as complex. However, at scavenging capacities greater than this value the proportion of complex dsbs tends to a plateau at a value of approximately 65 %. This is confirmed as representing the maximum proportion of complex damage from the analysis of simulations that do not include the chemical track. The total yield of complex dsb is less than that when the chemical track is included but the proportion of dsb that are classified as complex remains the same at approximately 65 %. This value of 65 % is in contrast to the maximum yield of complex dsb for the 1.5 keV electron simulation of ~ 30 %, illustrating the increased frequency of complex damage associated with the increased ionisation density characteristic of α-particle irradiation. The dependence of the yield of ssb and dsb on scavenging capacity, due to the direct effect is shown in figure 4.13. It is apparent that as the scavenging capacity increases from 10^7 s^{-1} to 10^{10} s^{-1}, the proportion of ssb and dsb wholly attributable to the direct effect increases with increasing scavenging capacity. At scavenging capacities greater than this range, the yields tend towards a plateau especially for dsb with the yield of dsb attributable to the direct effect at the plateau being approximately 95 %. At cell mimetic values of scavenging capacity the percentage yields of ssb and dsb induced by α-particle radiation and arising from the direct effect are approximately 30 % and 70 % respectively.

4.3. Discussion

4.3.1. Limitations of Experiments and Simulations

When simulations were initially used to determine the absolute yield of strand break within DNA, only direct energy depositions were considered (Charlton *et al.* 1989, Holley *et al.* 1990). However, more recently the diffusion of radicals, namely water radicals produced in the vicinity of the DNA, have been included within such simulations so that if they interact with DNA, damage results (Nikjoo *et al.* 1994b, 1997, 1999, Moiseenko *et al.* 1998a and b). Radiation-induced DNA damage by water

radicals produced in the vicinity of DNA has been included because considerable evidence from cell studies has indicated that a significant proportion of strand breaks arise via interactions of the OH radical. However, those simulations, that have included the diffusion and interactions of radicals have generally concentrated on mean diffusion distances for radicals characteristic of those estimated for radical diffusion distances within the cellular environment. To date studies have not been undertaken to determine the dependence of the yields of DNA strand breaks on scavenging capacities distinct from the cellular environment. The extension to comparisons of the yields of strand breaks obtained experimentally and from simulations for a range of scavenging capacities allows the robustness of the simulations and the assumptions present within them to be assessed more thoroughly.

It should be noted that experimental approaches themselves have limitations. Firstly, it is assumed that the scavenger radicals are inert and do not contribute to yields of strand breaks. Secondly, an additional contribution to experimentally determined yields of strand breaks will arise from the presence of heat labile sites to an extent dependent upon the temperature of the DNA solutions. For the assessment of yields of ssb and dsb the DNA temperature is maintained at 4^0 C (see chapter 3) to minimise the presence of heat labile sites, whereas procedures such as those used for the determination of the yield of base damage sites require incubation at elevated temperatures (see chapter 5), which will induce a significant yield of heat labile sites. Thirdly, it is assumed that for the determination of the yields of strand breaks, Poisson statistics may be applied to their distribution, even for high LET radiation such as α-particles. Coupled to these points are limitations already discussed, namely the inability to determine yields of strand breaks at very high scavenging capacities ($>10^9$ s^{-1}) due to prohibitively long irradiation times and scavenging molecules constituting a significant proportion of the solution.

The simulations undertaken also have a number of general assumptions inherent within them. For the determination of the contribution of water radicals to the yields of damage and its dependence on scavenging capacity the simulations incorporate distance and time cut-offs characteristic of the scavenging capacity rather than simulating the presence of scavenger molecules and allowing them to diffuse and interact with radicals. The model of DNA used in the simulations is only an approximation without the level of complexity inherent within actual DNA. The

probabilities of strand breaks arising following the direct interaction of radiation or via the action of radicals are expressed as simple mathematical probabilities. For instance any OH radicals that interact with DNA have a 13 % probability of giving rise to a ssb and a direct deposition of energy in the sugar moiety of DNA gives rise to a ssb if the energy deposition is > 17.5 eV. No variability of these parameters or dependence on experimental variables such as scavenging capacity is incorporated in the simulations. Any significant disparities that arise between experimental and simulated yields of strand breaks may provide additional information useful for the improvement of the simulations. Of those simulations that have been undertaken, there has not been a general focus on radiations that have been used experimentally. Instead, as a result of the computing time necessary to simulate DNA damage induced by high energy electrons and photons, the majority of studies have focused on low energy electrons and photons (Goodhead and Brenner 1983, Charlton *et al.* 1989, Goodhead and Nikjoo 1989, Nikjoo and Goodhead 1991, Nikjoo *et al.* 1994a, Friedland *et al.* 1998) with some additional work undertaken on simulations with high LET radiations; α-particles and heavy ions (Charlton *et al.* 1989, Nikjoo *et al.* 1994a, 1999, Holley and Chatterjee 1996). At present high energy γ-ray induced damage has not been simulated but is being developed through the development of novel, extended scoring techniques of DNA damage (Bolton *et al.* 1999).

From the present study, a number of general characteristics are apparent. For both simulated 1.5 keV electrons and α-particle irradiation the yields of both ssb and dsb decrease with increasing scavenging capacity. As discussed for the experimental data presented in chapter 3, the mean diffusion distance of the OH radicals decreases with increasing scavenging capacity, leading to a decrease in the yield of the OH radical mediated strand breakage component. In addition, over the whole of the scavenging capacity range examined the simulated yield of ssb is greater for 1.5 keV electron simulations than for α-particle. The lower yields for α-particle simulation is due to an increased ionisation density of the tracks so that a greater degree of intra-track radical-radical recombination takes place as discussed in section 3.3.4 for experimental yields of strand breaks.

4.3.2. Yields of Strand Breaks for Electron Tracks

When experimental yields of ssb and dsb for Al_K USX are compared with simulations of 1.5 keV electrons there is a reasonable agreement in terms of absolute values and the dependence on scavenging capacity. For simulations of 1.5 keV electron at a scavenging capacity of $3x10^8$ s^{-1}, representing a mean OH radical diffusion distance of 6 nm characteristic of the cellular environment, yields of ssb and dsb of $28x10^{-11}$ ssb/Gy/Da and $2.2x10^{-11}$ dsb/Gy/Da are obtained resulting in a ratio of ssb:dsb of 13:1. Experimentally determined yields of ssb and dsb, (see chapter 3) at the same scavenging capacity following irradiation with Al_K USX, are $46x10^{-11}$ ssb/Gy/Da and $2.7x10^{-11}$ dsb/Gy/Da respectively, resulting in a ratio of ssb:dsb of 17:1. Therefore differences in the yields of ssb between experiments and simulations are greater than for dsb. At cell mimetic scavenging capacities, a high proportion of the strand breaks arise from the direct effect. However, as can be seen in figure 4.6, a greater proportion of dsb arise from the direct effect than do ssb, 70 % compared with 45 % respectively. Subsequently the yield of ssb has a greater component of OH radical mediated damage than dsb. The greater discrepancy for ssb than dsb between experiment and simulation may be indicative of an underestimation of the role of OH radicals within the simulations i.e. of the role of the indirect effect. One possible explanation for any inaccuracies in the determination of the indirect effect may lie in the way in which the experimental scavenging capacity is mimicked in the simulations by limiting the diffusion range of the OH radicals to an extent determined by the given scavenging capacity. An alternative simulation approach which may more accurately reflect the experimental system would be to introduce homogeneously distributed scavenger molecules which would be allowed to diffuse and react with radicals. One disadvantage of this approach however, is the increase in computing time required for the simulations resulting from following the diffusion and interaction of the scavenger molecules. Hence any possible benefit in the accuracy of the models must be weighed against the reduction in number of track simulations which could be undertaken per unit time and the subsequent decrease in the statistical confidence of the results.

An additional significant feature of the simulations, not determined experimentally due to limitations of using very high scavenging concentrations, is that the yields of ssb plateau at an approximate scavenging capacity of 10^9 s^{-1}.

Simulations of yields of ssb and dsb for 1.5 keV electrons have been carried out previously (Nikjoo *et al.* 1994b, 1997, 1999) at a scavenging capacity of $1x10^9$ s^{-1}.

equivalent to a mean OH radical diffusion distance of 4 nm. In the present simulation study at a scavenging capacity of $1x10^9$ s^{-1} yields of ssb and dsb have been determined to be $28x10^{-11}$ ssb/Gy/Da and $2.3x10^{-11}$ dsb/Gy/Da respectively resulting in a ratio of ssb:dsb of 12.2:1. In comparison, other studies using 1.5 keV electrons have determined the yields of ssb to be equal to $24x10^{-11}$ ssb/Gy/Da (Nikjoo *et al.* 1994b, Nikjoo *et al.* 1999) and yields of dsb have been determined to be equal to $1.6x10^{-11}$ dsb/Gy/Da (Nikjoo *et al.* 1994b) and $1.8x10^{-11}$ dsb/Gy/Da (Nikjoo *et al.* 1999) resulting in ratios of ssb:dsb of 15.0:1 and 13.3:1 respectively. Generally there is good agreement between the present simulations and previous studies. If the degree of complexity is examined, the percentage of dsb that are classified as complex is approximately 30 % at a scavenging capacity of $1x10^9$ s^{-1}, in excellent agreement with the percentage of dsb that are classified as complex of 29.4 % determined by Nikjoo *et al.* (1999).

If a comparison is made between experimental and computer simulation yields of ssb and dsb within the present study, a number of clear discrepancies are apparent between some of the simulation assumptions and the experimental reality for yields of strand breaks induced by Al_K USX. Firstly it was assumed that the radiation track associated with a 1.5 keV Al_K USX photon may be simulated by the track of a 1.5 keV electron. In actuality, the Al_K USX photon does not interact with matter to give rise to a 1.5 keV electron but interacts via the photoelectric effect, predominantly in the oxygen K-shell, to give rise to 2 electrons with a range of possible energies with the most common being a 0.96 keV photoelectron and a 0.52 keV Auger electron (Nikjoo *et al.* 1994a). Hence, two lower energy electrons are produced at a simultaneous point in space. Therefore there is a possibility that the two independent tracks may give rise to a more dense deposition of energy than that associated from only a single electron track of 1.5 keV. In addition, each of the two electrons alone have higher ionisation densities because of their lower energies. Two possible effects may arise from considering two spatially close energy tracks rather than a single track. Firstly, if the two spatially close lower energy electron tracks overlay DNA, there may be a greater probability of producing complex damage such as a dsb than that generated by a single higher energy electron track. Secondly, if the respective tracks deposit energy in water surrounding the DNA, a single electron track may result in less radical-radical recombination events than associated with two spatially close tracks due to a greater average distance between sites of radical formation.

However, in addition to a different number of tracks, the respective energy of the tracks also needs to be considered. From simulations and experiments (see chapter 7), the yield of radicals in aqueous solution which escape intra-track recombination events to become homogeneously distributed is dependent upon the energy of the radiation (Magee and Chatterjee 1978, Yamaguchi 1989, Hieda *et al.* 1994, Hill and Smith 1994, Watanabe *et al.* 1995). From the experimental examination discussed in chapter 7, at low scavenging capacities the probability of radical-radical recombination decreases with decreasing photon energy, at energies less than approximately 1.5 keV. This decrease in recombination is interpreted as resulting from the decreased total number of radicals formed with decreasing energy of the track. It is therefore predicted that the absolute yields of ssb produced via the action of radicals will increase, due to the decreased energy of the tracks leading to a decreased amount of intra-track recombination, if Al_K USX simulations are undertaken with two lower energy electrons rather than a single higher energy electron. Alternatively, there will be a decrease in the yields of ssb if there is a greater effect from an increased probability of radical-radical recombination from radicals formed from the separate tracks leading to a smaller number of radicals becoming homogeneously distributed as previously discussed. Thus, when considering ssb formation, the two potential effects may counterbalance each other, decreasing any difference in yields of ssb obtained from a two electron simulation from that obtained from a single electron track of 1.5 keV. It is anticipated that any differences in the yield of ssb will become more significant at low scavenging capacities, where the contribution of OH radicals generated by the indirect effect becomes increasingly important due to their increased average diffusion distances. If yields of dsb are considered the simulations of Al_K USX with a single 1.5 keV electron, may lead to an underestimation relative to the yield of dsb obtained from the two electron simulation. An underestimation in the yields of dsb may lead to a significant reduction in the ratio of ssb:dsb depending upon changes in the yields of ssb. Whether the yields of ssb are greater with a single or two track electron simulation will indicate which is the more prominent mechanism in the two electron simulation; either increased radical-radical interactions between tracks or reduced intra-track radical-radical recombination due to the lower numbers of radicals within each track.

The effect of simulating the yields of strand breaks induced by Al_K USX with either one or two electron tracks have been compared and is summarised in table 4.3. Comparisons of the respective yields of ssb obtained between the two simulations

indicate a 10 % lower yield for the two electron simulation relative to that for the one electron track throughout the scavenging capacity range examined. It is thus inferred that a significant contribution from radical-radical recombination of radicals produced in the two separate tracks leads to a reduction in ssb yields. This decrease counterbalances the potential increase in ssb due to an increase in the yield of OH radicals which escape intra-track radical-radical recombination, reflecting the decreased number of radicals produced in the lower energy tracks. As anticipated, the yields of dsb are about 20 % greater for the two electron simulation relative to the single electron simulation over the same scavenging capacity range. These differences in yields of ssb and dsb lead to a decrease in the relative yield of ssb to dsb of 20 – 25 % for two-electron relative to the single-electron simulations. Therefore, consideration of only a single electron track leads to the yields of damage complexity, obtained from the ratio of ssb:dsb, being underestimated. If the proportion of dsb determined to be complex (i.e. with at least one ssb in the vicinity of the dsb) are also considered for a two electron simulation, it is apparent that the simulation of a single electron track underestimates the yield of complex dsb by approximately 10 – 15 % compared with that determined for two electron simulations.

When the ratios of ssb:dsb for Al_K USX are compared between simulation and experiment as illustrated in figure 4.4, a large difference is seen with a significantly larger disparity at lower scavenging capacities where the ratio of ssb:dsb obtained from the simulations is greater. This difference may be partly explained by overestimation in the yields of ssb and underestimation of the yields of dsb from consideration of only a single 1.5 keV electron track within the simulations as discussed above. Although two electron simulations have not been undertaken at low scavenging capacities, it is anticipated that differences in the ratios of ssb:dsb between one electron and two electron simulations of Al_K USX become increasingly large at lower scavenging capacities. Simulations at high scavenging capacities reveal a significant amount of radical-radical recombination of radicals formed from the separate tracks within the two electron simulations. As the scavenging capacity decreases the mean OH radical diffusion distance increases and therefore a greater degree of radical-radical recombination of radicals from the separate tracks results. However, this may not be sufficient to explain the large difference between experimental and simulated determinations of the ratios of ssb:dsb of Al_K USX illustrated in figure 4.4 and therefore other possible explanations must be considered and will be discussed later.

However at a typical cellular scavenging capacity of $3x10^8$ s^{-1} the values for the ratio of ssb:dsb and the yields of both ssb and dsb for 1.5 keV electron simulations are within the errors associated with the experiments. Thus, for the purposes of merely determining yields of damage at such scavenging capacities it is sufficient to simulate a Al_K USX track with a single 1.5 keV electron. However by doing so, some errors may arise in determining the distribution of damage and damage complexity.

4.3.3. Yields of Strand Breaks for α-particle Tracks

The yields of ssb and dsb induced by α-particle irradiation obtained from simulations at a scavenging capacity of $3x10^8$ s^{-1}, representing a mean OH radical diffusion distance of 6 nm, are $16x10^{-11}$ ssb/Gy/Da and $5.5x10^{-11}$ dsb/Gy/Da respectively leading to a ratio of ssb:dsb of 3:1. In comparison, the experimentally determined yields of ssb and dsb described in chapter 3 induced by a 3.3 MeV α-particle are $16x10^{-11}$ ssb/Gy/Da and $2.1x10^{-11}$ dsb/Gy/Da, resulting in a ratio of ssb:dsb of 8:1. The simulated yield of ssb is not significantly different from the experimentally determined yield of ssb. In contrast there is significant difference in the yield of dsb determined from simulation and experimentally. This difference leads to significant disparities in the ratios of ssb:dsb, the possible reasons for which are discussed later. At scavenging capacities > 10^9 s^{-1}, the yields of ssb predicted from the simulations tend towards a plateau.

The comparison between experimental and simulated yields of ssb and dsb was also undertaken at varying scavenging capacities. An analysis of the complexity and mechanism for formation of damage resulting from α-particle irradiation of DNA has previously been undertaken by Nikjoo *et al.* (1999). In the present study at a scavenging capacity of $1x10^9$ s^{-1}, representing a mean OH radical diffusion distance of 4 nm, within the characteristic range of 4-6 nm for the cellular environment, simulated yields of ssb and dsb of $17x10^{-11}$ ssb/Gy/Da and $5.2x10^{-11}$ dsb/Gy/Da result in a ratio of ssb:dsb of 3.3:1 for 3.2 MeV α-particle irradiation. In an analysis with 2.0 MeV α-particles (Nikjoo *et al.* 1999), a yield of ssb of $17x10^{-11}$ ssb/Gy/Da is obtained. The yields of ssb are similar between the two simulations even though a somewhat lower yield would be expected with the higher LET 2 MeV α-particles. The yield of dsb of $4.0x10^{-11}$ dsb/Gy/Da (Nikjoo *et al.* 1999) is approximately 25 % less than from simulations of the 3.2 MeV α-particle in this study. In both cases these simulated yields are significantly higher by about a factor of 2-3 than the values determined

experimentally at a similar scavenging capacity ($3x10^8$ s^{-1}). This increase in the simulated yields of dsb results in values for the ratio of ssb:dsb which are a factor of 2-3 lower than those determined experimentally.

Within the same simulation a breakdown of damage complexity was also undertaken (Nikjoo *et al.* 1999) at a scavenging capacity of $1x10^9$ s^{-1}. At this scavenging capacity in the present study approximately 64 % of dsb are classified as complex i.e. there is an additional strand break within 10 base pairs of the dsb. This value compares well with that determined in the study of Nikjoo *et al.* (1999), in which the percentage proportion of dsb which are classified as complex is 71.3 %. This latter yield is somewhat higher than that in the present study due to the lower energy of the α-particle of 2.0 MeV used in the simulation. For instance, in the same study the simulation of a 6.0 MeV α-particle results in a lower percentage of dsb classified as complex of 53.1 %, reflecting the decrease in complexity with increasing energy of the α-particle.

One feature which may effect the relative yields of ssb and dsb in the present study is the number of individual tracks that are actually examined. Although several thousands of ssb are recorded suggesting good statistics, these ssb originate in the main from only twenty individual simulated α-particle tracks and at the lowest scavenging capacity only ten. Hence these tracks may not be truly representative and may lead to some form of skew within the results. It should be noted however, that this would not explain the large discrepancy between experimental and simulated yields of dsb observed.

In the present study, the proportion of dsb classified as complex even at scavenging capacities as low as 10^7 s^{-1} is greater than 55 %. In addition (see figure 4.13) the proportion of dsb attributable to direct effects begins to plateau at a value of approximately 55 % at scavenging capacities < 10^8 s^{-1}. The fact that the percentage of dsbs attributable to the direct effect begins to plateau at low scavenging capacities rather than continuing to decrease shows the significance of the direct effect, particularly in regard to complex damage formation, of which dsbs are an example, with densely ionising radiation such as α-particles. A direct comparison with the simulated data using a 1.5 keV electron representative of a lower density ionising track, shows that the contribution of the direct effect in inducing dsbs continues to decrease at low scavenging capacities as illustrated in figure 4.6. Comparison may also be made with the experimental determination of the contribution of the indirect effect to the total yield of strand breaks. The relative contributions of indirect DNA damage determined

for cells is approximately 60 % for ssb and dsb for low LET (Chapman *et al.* 1979, Roots *et al.* 1985, deLara *et al.* 1995) and approximately 30 % for dsb for high LET (deLara *et al.* 1995). It should be noted that the experimental indirect contribution for dsb includes hybrid dsb, in which one of the ssb is produced by the direct effect and one ssb derives from an OH radical. The yield of dsb induced by the indirect effect for Al_K USX is ~ 60 % (deLara *et al.* unpublished data). In comparison, the contribution of the indirect effect to the simulated yields of ssb and dsb for 1.5 keV electrons is approximately 55 % and 30 % respectively and for the simulated yields of ssb and dsb for the α-particle is approximately 70 % and 30 % respectively at cell mimetic conditions. As with the experimental data, the simulated indirect contribution for dsb includes hybrid dsb, in which one of the ssb is produced by the direct effect and one ssb derives from an OH radical. Hence simulated determinations for the contribution of the direct effect for ssb by 1.5 keV electrons and dsb for α-particles are in good agreement with experimental determinations. The simulated yield of dsb induced by indirect effects for 1.5 keV electrons is significantly less than that determined experimentally in cells.

One further interesting aspect of the classification of complex damage is illustrated when figures 4.5 and 4.12 are compared. Again it should be noted that the yields of complex damage do not include a contribution from base damage sites. It can be seen that with the 1.5 keV electron simulation the proportion of dsbs classified as complex reaches a plateau at approximately 30 % whereas in the α-particle case a plateau is reached at approximately 65 %. An increase in the proportion of dsb classified as complex increases with an increased ionisation density track such as that associated with α-particles. However, even when α-particle simulations under high scavenging capacities are considered, there remain a significant proportion of dsb not classified as complex. This is a confirmation of previous findings (Goodhead and Nikjoo 1989, Nikjoo *et al.* 1991) where simulations of direct effects predicted that complex damage may be generated by low LET and conversely single, isolated damage sites by high LET radiation. What changes with increases of ionisation density of the radiation is the frequency spectrum of the damage that is generated with a shift to more complex damage (Goodhead 1994). Hence it is anticipated that an increase in ionisation density leads to an increased frequency of complex damage, however less-complex damage,

such as simple dsbs and ssbs will contribute significantly to the total yield of damage associated with direct energy deposition of an α-particle track.

4.3.4. Simulation Developments

It should be stressed from the outset that simulations were originally introduced to suggest trends and dependences on variable change. Hence, primarily qualitative rather than quantitative yields of strand breaks were sought. However, simulations are also invaluable sources of quantitative information. Indeed within the present study qualitative dependences of the yields of both ssb and dsb for 1.5 keV electron and α-particle tracks with scavenging capacity obtained from the simulations have been in excellent agreement with the experimentally obtained dependences. However, it is necessary, if there is to be consistent agreement between experimental and simulated yields of damage, that certain limitations present within the simulations are addressed.

One specific aspect of the simulations that may have a significant effect on the yields of strand breaks when compared with experimental yields, especially at low scavenger concentrations, is that each radiation track in the simulations is considered separately and the damage induced therefore only arise from single track events. Thus, a DNA strand cannot be hit by a multiple number of separate tracks in the simulations. For example it is not possible to induce 2-hit dsbs due to two ssb within 10 base pairs arising from separate tracks. In the simulations dsb may only arise from depositions of energy leading to a combination of ssb from direct energy depositions and OH radicals, but where both damage mechanisms are generated by the same track. This will potentially lead to two significant differences between simulation and experiment, one concerning the yield of dsb and one the mechanism for dsb induction. Firstly, simulations will lead to an underestimation in the number of dsbs recorded with respect to experiments due to the absence of a contribution from two spatially close ssb induced by two separate tracks involving direct ssb and/or the action of OH radicals. Such an effect should be negligibly small at moderate doses under high scavenging conditions, such as cell mimetic, but it will become increasingly significant as the scavenging capacity is reduced and the average diffusion distance of OH radicals increases. This increase in the average OH diffusion distance will lead to an increase in the probability of two hit dsb arising from contributions from two separate tracks. Experimentally, the dose dependence for the induction of dsb by Al_K USX is non-linear

at low scavenging capacity (see figure 3.7) representing a significant proportion of the dsb arising from multi-track events. On increasing the scavenging capacity with Al_K USX and for all scavenging capacities with α-particles the yields of dsb are linearly dependent upon dose, from which it is inferred that the majority of dsb at high scavenging capacities arise from single track events. Other mechanisms for dsb induction e.g. radical transfer mechanisms have been discussed in chapter 3. Secondly, the proportion of dsbs resulting from the action of the direct effect illustrated in figures 4.6 and 4.13 may be overestimated at low scavenging capacity. The values quoted represent the percentage of dsbs due solely to the direct effect relative to the total number of dsbs. If the total yield of simulated dsbs are underestimated with respect to the experimental data due to the exclusion of the proportion resulting from the action of two separate OH radicals or from the combination of the direct effect and an OH radical from separate tracks, this will lead to the proportion of dsb generated purely by the direct effect being overestimated. The absence of the contribution of 2-hit dsb from separate tracks may potentially explains why the yields of dsb for the 1.5 keV electron from simulations are lower than the experimental yields presented in figure 4.3. Further support for this is shown in figure 4.3, where the simulated yields of dsb are less than the experimental yields, to an increasing extent as the scavenging capacity decreases.

A critical determinant in the relative yields of ssb and dsb and the subsequent classification of the complexity of a dsb is the base pair separation, used to define when two ssbs on separate strands give rise to a dsb. In the present study the base separation was set as ≤ 10 bp. If this value is increased, the yield of dsb increases at the expense of that of ssb. As yields of ssb are significantly greater than that of dsb over the range of scavenging capacities simulated, a larger proportional change in the yields of dsb than in the yields of ssb should result. The separation of ssb which give rise to dsb varies with the ionic strength of the DNA solution, so that the value may vary with scavenging capacity (Van Touw *et al.* 1985). However, even at the lowest scavenging capacity used this distance is expected to be close to 10. For simulations with variable scavenging capacity the separation of the base pairs could be varied. A possible explanation for the very high yields of dsb determined for the α-particle simulation relative to those determined experimentally may reflect the base pair separation to give rise to a dsb being set too high. However, the same value is used for the 1.5 keV electron simulations that give good agreement with the experimental data. In addition,

it would be difficult to account for such a large discrepancy as exists between the simulated and experimental yields of dsb purely on the basis of base pair separations alone. However, it may be informative to undertake simulations with the base pair separation varied to assess whether the electron or α-particle simulated yields of dsb are more sensitive to such variation.

A possible explanation for any disagreement between simulation and experiment may lie in the model of the DNA. At present, the model used is as described by Nikjoo *et al.* (1994a) based on the dimensions of B-DNA (Dickerson *et al.* 1982). It consists of distinct volume regions of sugar-phosphate moiety and bases without any additional complexity of the structure being introduced. The model structure also implicitly includes the first hydration shell of the DNA. It is assumed that $H_20^{\cdot+}$ resulting from interactions with the bound water layer oxidises the DNA (La Vere *et al.* 1996). Further work may assess the change in yields associated with increasing the number of hydration shells and the efficiency of transfer of charge from the water to the DNA. It may also be pertinent to consider an atomistic model of DNA in contrast to assigning volume regions to sugar phosphate and bases as currently employed. Although a volume model of DNA seems a reasonable approximation for high-energy electron irradiation an atomistic model may be more appropriate for α-particle radiation with its corresponding greater density of ionisation events. Employing such a model would not influence OH radical interactions but may change the distribution of direct events and the distances between damage sites.

The present study has focused on the role of strand breaks in determining the yields and complexity. However, there has recently been some preliminary simulations assessing the contribution of base damage sites to complex damage formation (Nikjoo *et al.* 1999). At scavenging capacities equivalent to a mean OH radical diffusion distance found within the cellular environment, with electron energy ≤ 4.5 keV the ratio of ssb:dsb is13-15:1 whereas 2 MeV α-particles lead to a ratio of ssb:dsb of 4:1. For both electron and α-particle simulations, the ratio of base damage:ssb is determined to be approximately 2:1. From chapter 5, the yields of base damage per ssb for γ-ray and α-particle radiation are estimated to be about 3:1 and 4:1 respectively under cell mimetic scavenging capacities. Such base damage yields and their dependences on scavenging capacity provide the data necessary to accurately introduce base damage into simulations. From Nikjoo *et al.* (1999) approximately 30 % of dsb following low LET

irradiation are complex (by virtue of having additional breaks in close vicinity) but with the inclusion of base damage this rises to approximately 60 %. For high LET irradiation, these values rise from approximately 70 % to 90 % following the inclusion of base damage. Thus, the inclusion of base damage will be an important consideration within simulations in determining complex damage yields. However, as for strand breaks, it is important that if base damage yields determined from simulations are to be treated with confidence then they must be in good agreement with experimental determinations. Thus it is important to undertake base damage determinations within systems which readily lend themselves to modelling and to determine mechanisms for base damage formations so that they can be correctly included within models. Both of these topics are considered within the next chapter.

Table 4.1.

Range of scavenging capacities, diffusion boundaries and diffusion cut-off times employed for 1.5 keV electron and α-particle simulations of the yields of DNA strand breaks.

Scavenging Capacity (s^{-1})	Time Cut-off (s)	Mean OH Radical Diffusion Distance[1] (nm)	Cylinder Radius Around DNA (nm)
$2x10^{6}$	$5x10^{-7}$	84.4	89.3
$3x10^{6}$	$3.3x10^{-7}$	68.9	72.9
$1x10^{7}$	$1x10^{-7}$	37.6	39.9
$3.3x10^{7}$	$3.0x10^{-8}$	20.7	21.9
$1x10^{8}$	$1x10^{-8}$	11.9	12.6
$1x10^{9}$	$1x10^{-9}$	3.8	4.0
$1x10^{10}$	$1x10^{-10}$	1.2	1.25
$1x10^{11}$	$1x10^{-11}$	0.38	0.40

[1] Roots and Okada 1975

Table 4.2.

Yields of DNA ssb and dsb and the ratio of ssb:dsb under variable scavenging capacity for 1.5 keV electron irradiation simulations.

Scavenging Capacity s^{-1}	Number of Tracks	ssb	ssb/Gy/Da	dsb	dsb/Gy/Da	ssb:dsb
$3x10^{6}$	10	4,668±68	$4.24x10^{-9}$	75±9	$6.81x10^{-11}$	62.2:1
$1x10^{7}$	50	10,979±105	$1.98x10^{-9}$	300±17	$5.41x10^{-11}$	36.6:1
$3.3x10^{7}$	250	24,482±156	$8.94x10^{-10}$	1,015±32	$3.71x10^{-11}$	24.1:1
$1x10^{8}$	500	25,413±159	$4.59x10^{-10}$	1,544±39	$2.79x10^{-11}$	16.5:1
$1x10^{9}$	500	10,532±103	$1.90x10^{-10}$	1,007±32	$1.82x10^{-11}$	10.5:1
$1x10^{10}$	500	7,973±89	$1.44x10^{-10}$	795±28	$1.43x10^{-11}$	10.0:1

Table 4.3.

Comparison between yields of ssb, dsb and the proportion of dsb classified as complex within DNA in aqueous solution from simulations employing a single 1.5 keV electron track and the summation of a 1.0 keV electron track and a 500 eV electron track originating at the same point in space for a range of scavenging capacities.

Simulation	Scavenging Capacity (s^{-1})	ssb/Gy/Da	dsb/Gy/Da	ssb:dsb	% of dsb classified as complex
1.5 keV electron	$1x10^{8}$	$4.59x10^{-10}$	$2.79x10^{-11}$	16.5:1	27.8
1.0 keV + 0.5 keV electrons	$1x10^{8}$	$4.20x10^{-10}$	$3.30x10^{-11}$	12.7:1	31.2
1.5 keV electron	$1x10^{9}$	$1.90x10^{-10}$	$1.82x10^{-11}$	10.5:1	30.8
1.0 keV + 0.5 keV electrons	$1x10^{9}$	$1.75x10^{-10}$	$2.14x10^{-11}$	8.2:1	34.6
1.5 keV electron	$1x10^{10}$	$1.44x10^{-10}$	$1.43x10^{-11}$	10.0:1	28.4
1.0 keV + 0.5 keV electrons	$1x10^{10}$	$1.33x10^{-10}$	$1.75x10^{-11}$	7.6:1	33.6

Table 4.4.

Yields of DNA ssb and dsb and the ratio of ssb:dsb under variable scavenging capacities for simulations of 3.2 MeV α-particle irradiation.

Scavenging Capacity s^{-1}	Number of Tracks	Number of Chords	ssb	ssb/Gy/da	dsb	dsb/Gy/Da	ssb:dsb
$2x10^{6}$	10	5,000	777±28	$7.77x10^{-10}$	74±9	$7.39x10^{-11}$	10.5:1
$1x10^{7}$	20	50,000	11,660±108	$4.75x10^{-10}$	1,945±44	$7.93x10^{-11}$	6.0:1
$3.3x10^{7}$	20	50,000	8,172±90	$2.95x10^{-10}$	1,992±45	$7.18x10^{-11}$	4.1:1
$1x10^{8}$	20	50,000	5,960±77	$2.05x10^{-10}$	1,835±43	$6.32x10^{-11}$	3.2:1
$1x10^{9}$	20	50,000	3,536±59	$1.12x10^{-10}$	1,502±39	$4.79x10^{-11}$	2.4:1
$1x10^{10}$	20	50,000	2,720±52	$8.67x10^{-11}$	1,098±33	$3.50x10^{-11}$	2.5:1
$1x10^{11}$	20	50,000	2,327±48	$7.42x10^{-11}$	929±30	$2.96x10^{-11}$	2.5:1

Figure 4.1.

Dependence of the yield of ssb on the variation in the cylindrical shell radius around the DNA within which the interactions of radicals are analysed. Yields of ssb are determined following the simulation of a 1 keV electron track with a time cut-off of $1x10^{-8}$ s. Note units for ssb are arbitrary.

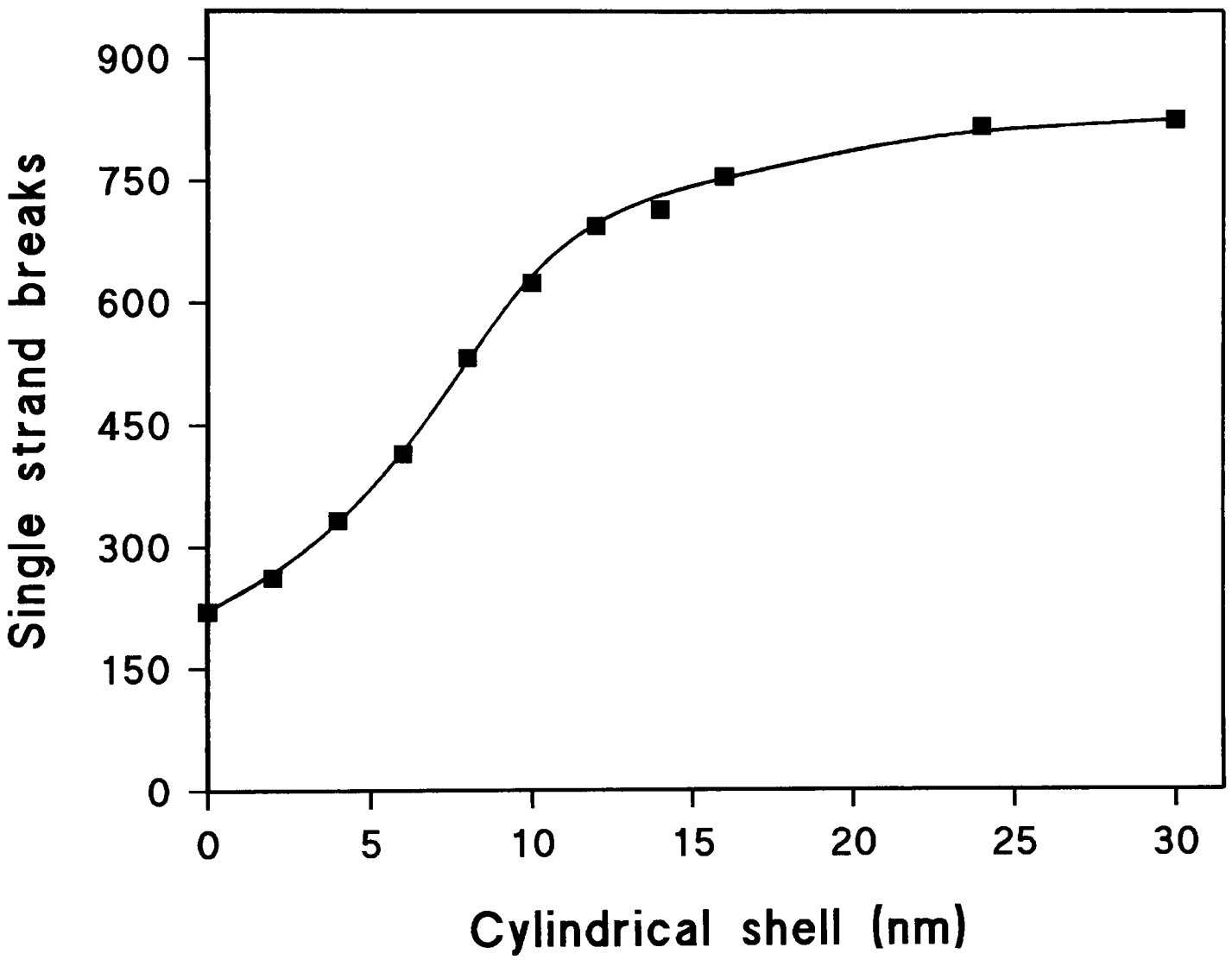

Figure 4.2.

Comparison of the dependence of the yields of ssb on scavenging capacity for experimental irradiation of pUC18 DNA with 1.5 keV Al_K USX at 4^0 C and from simulations of the yields of ssb induced by 1.5 keV electrons. Note simulation error bars are not plotted as they are less than the size of the data points.

■ Simulated 1.5 keV electron irradiation

▲ Experimental Al_K USX irradiation

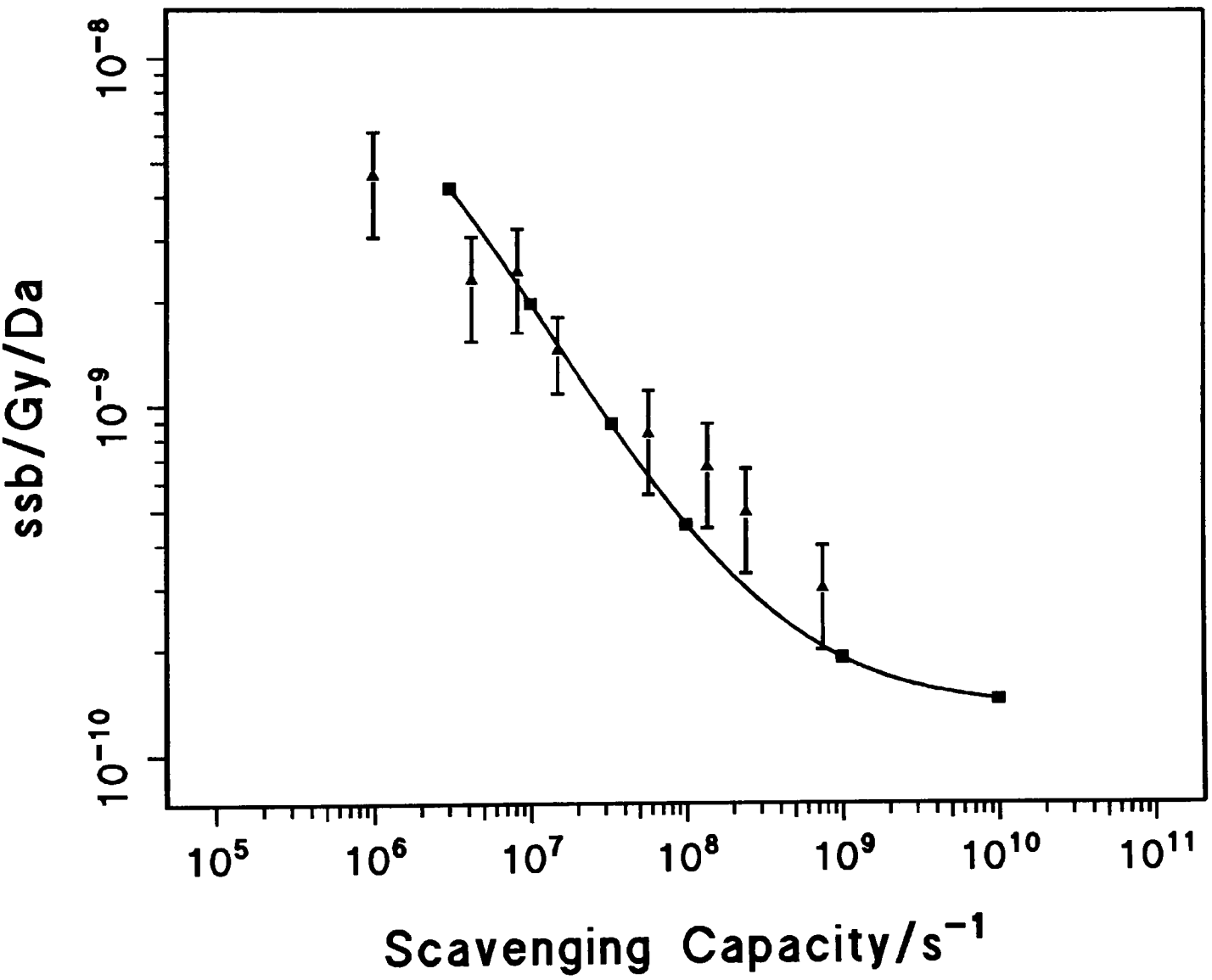

Figure 4.3.

Comparison of the dependence of the yields of dsb on scavenging capacity for experimental irradiation of pUC18 DNA with 1.5 keV Al_K USX at 4^0 C and from simulations of the yields of dsb induced by 1.5 keV electrons. Note simulation error bars are not plotted as they are less than the size of the data points.

■ Simulated 1.5 keV electron irradiation

Δ Experimental Al_K USX irradiation

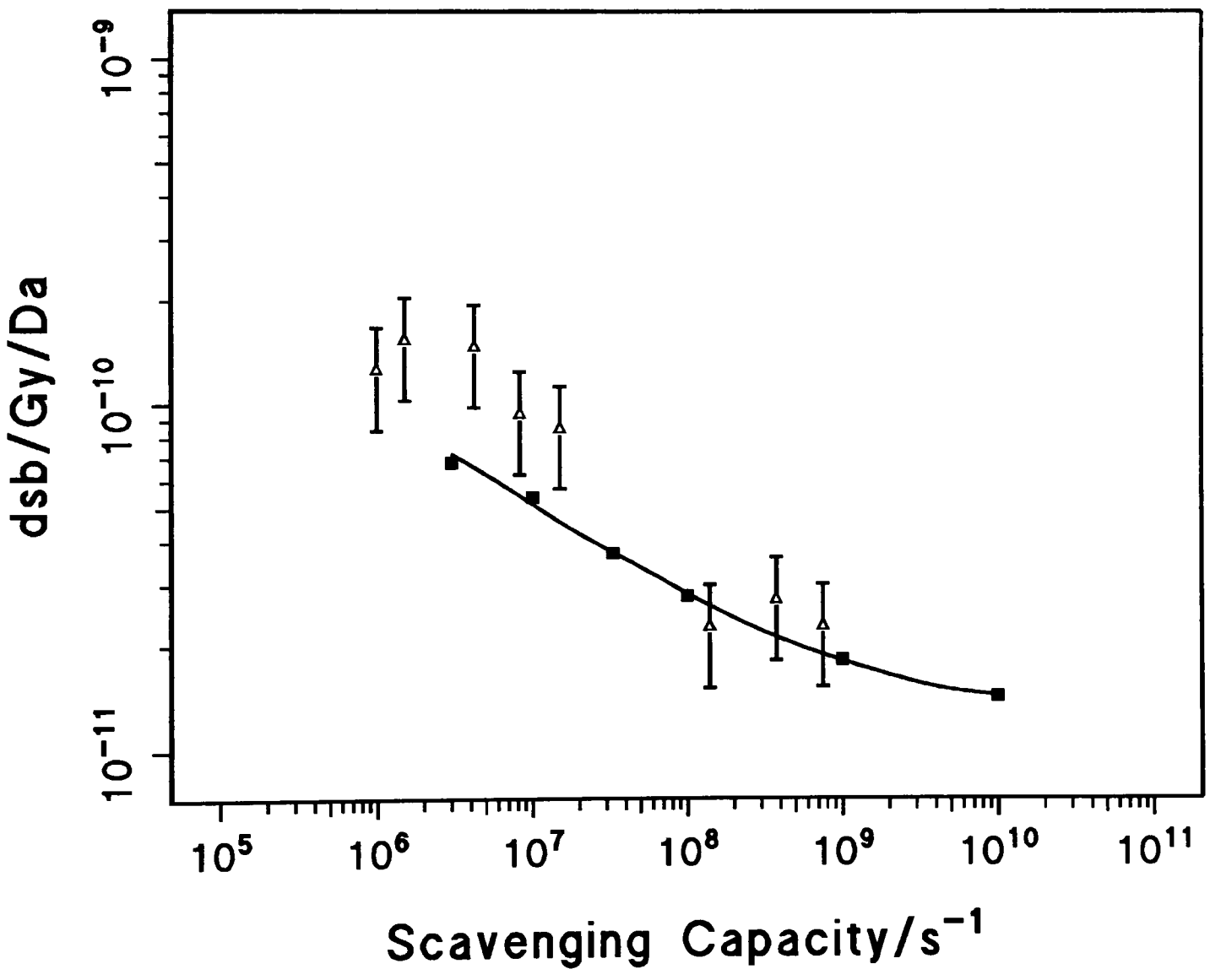

Figure 4.4.

Comparison of the ratios of ssb:dsb determined from simulations of 1.5 keV electron tracks and from experimental determination from irradiation of pUC18 DNA by 1.5 keV Al_K USX at 4^0 C. Note simulation error bars are not plotted as they are less than the size of the data points.

■ Simulated 1.5 keV electron irradiation

▲ Experimental Al_K USX irradiation

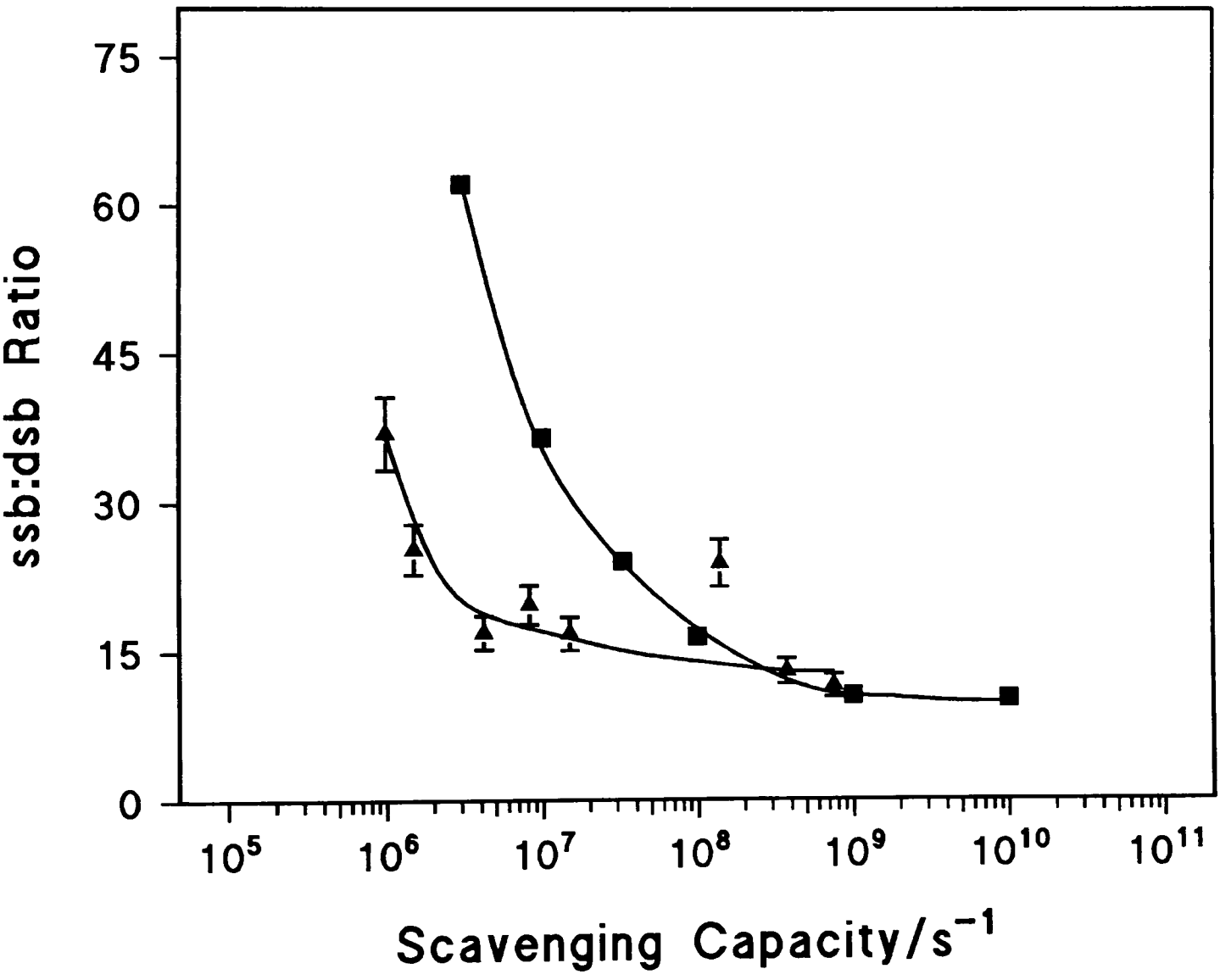

Figure 4.5.

Dependence of the proportion of dsbs, classified as complex, on scavenging capacity for the simulation of 1.5 keV electron tracks.

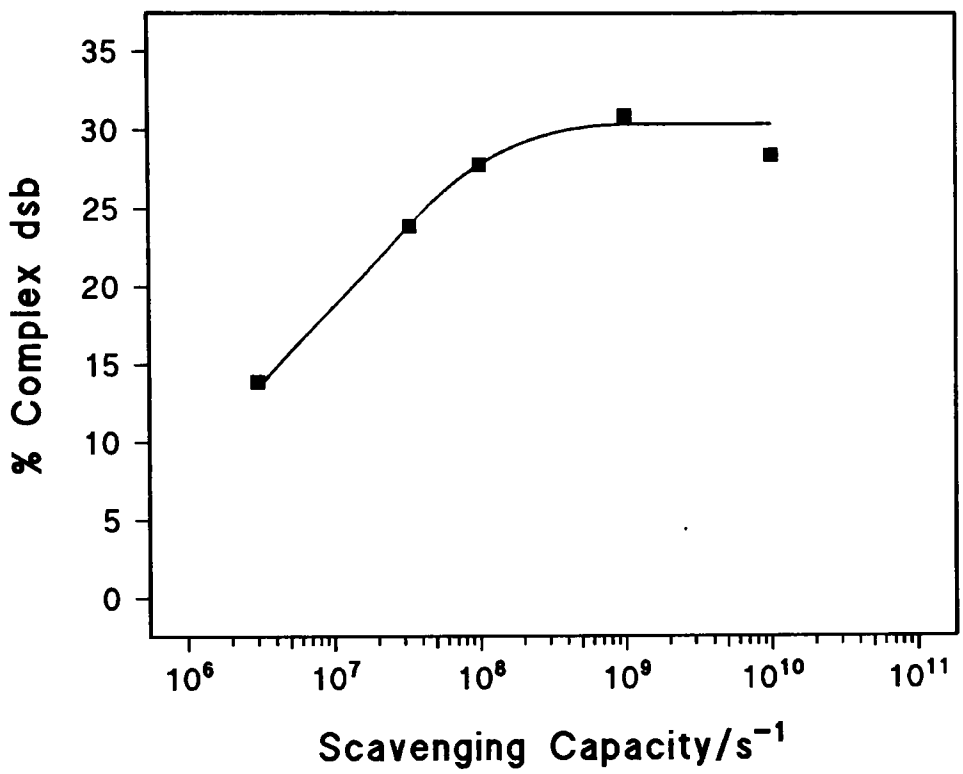

Figure 4.6.

Dependence of the yield of dsb due to the direct effect only on scavenging capacity for the simulation of 1.5 keV electron tracks.

■ Simulated yields of dsb

▲ Simulated yields of ssb

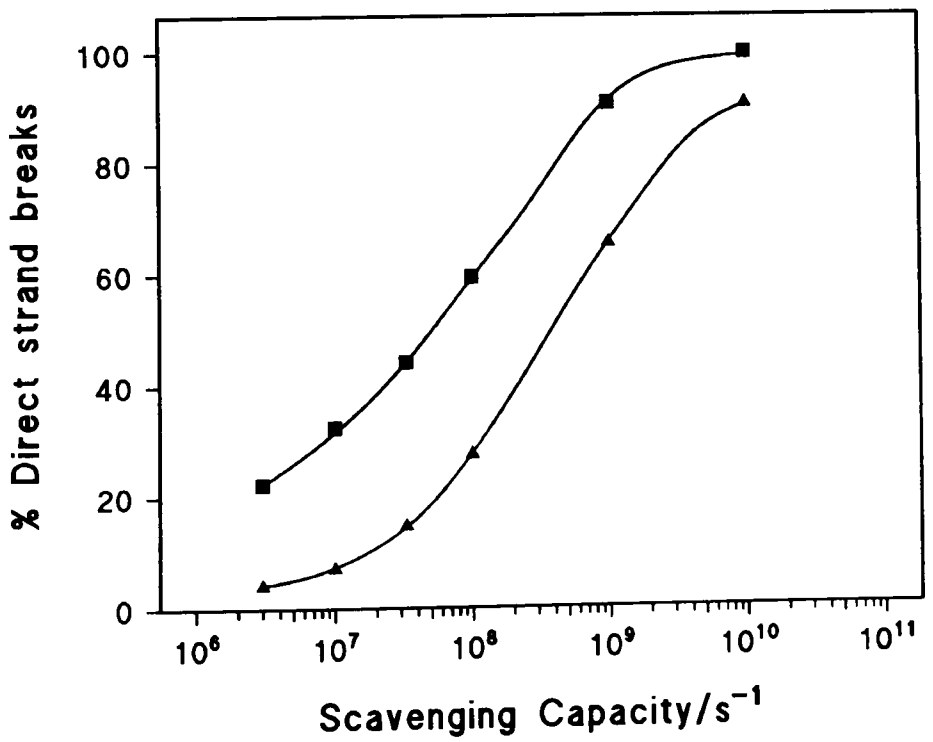

Figure 4.7.

Comparison of the dependence of yields of ssb on scavenging capacity for experimental irradiation of pUC18 DNA with ^{238}Pu α-particles at 4^0 C and from simulations of 3.2 MeV alpha particle tracks. Note simulation error bars are not plotted as they are less than the size of the data points.

■ Simulated α-particle irradiation

Δ Experimental α-particle irradiation

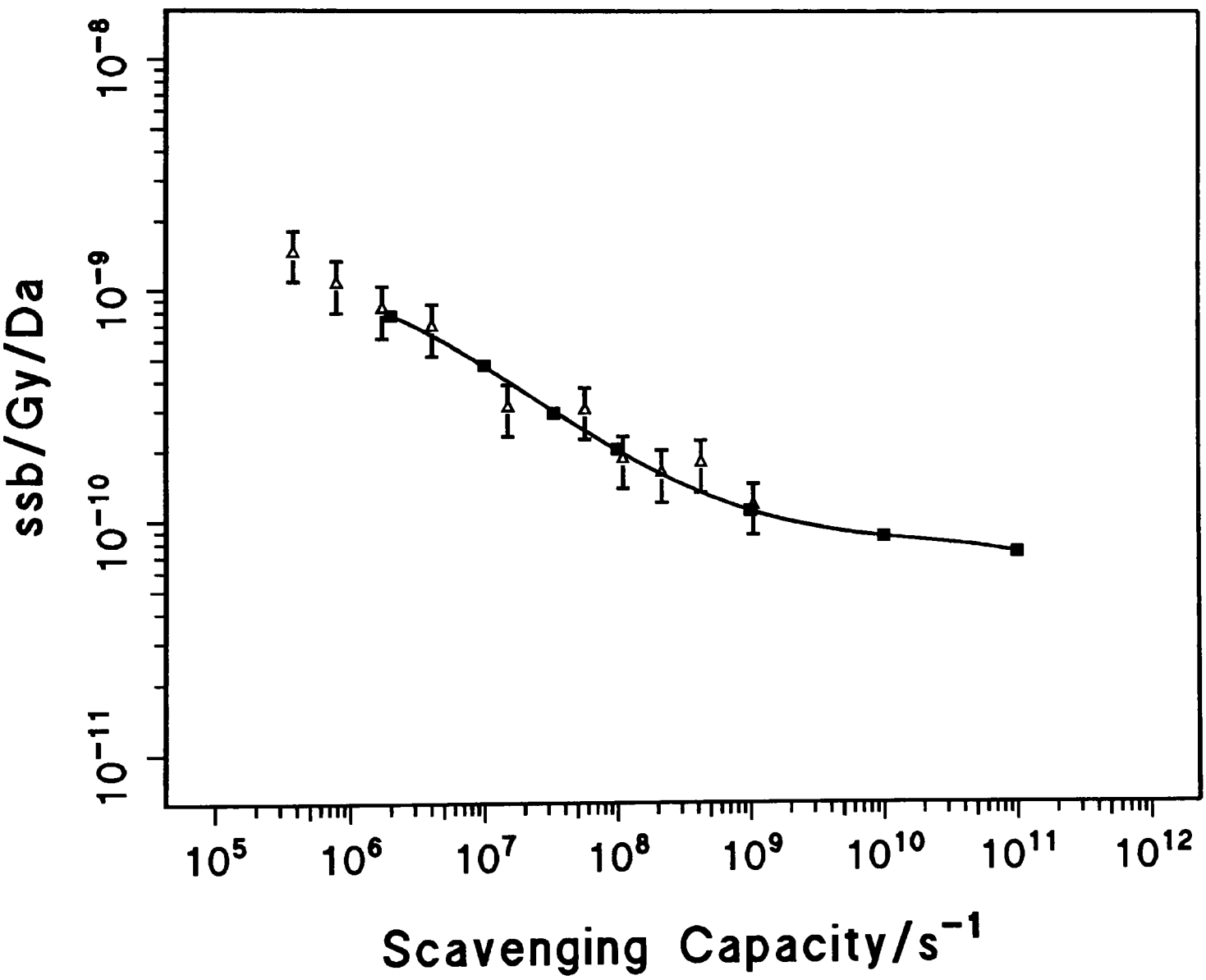

Figure 4.8.

Comparison of the dependence of yields of ssb on scavenging capacity for simulations of 1.5 keV electron and α-particle irradiation. Note simulation error bars are not plotted as they are less than the size of the data points.

■ Simulated 1.5 keV electron irradiation

▲ Simulated α-particle irradiation

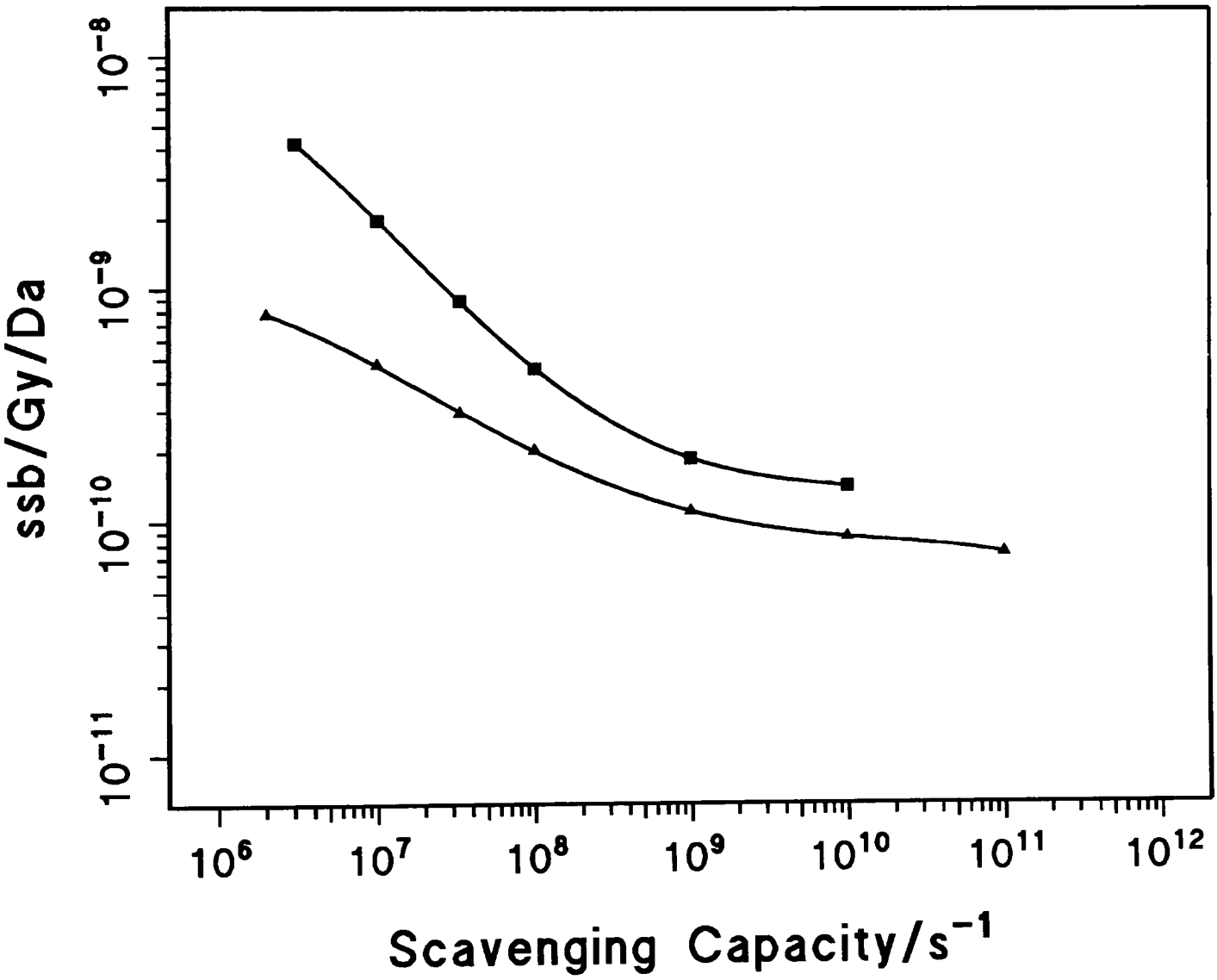

Figure 4.9.

Comparison of the dependence of the yields of dsb on scavenging capacity for irradiation of pUC18 DNA with a ^{238}Pu source at 4^0 C and from simulations of a 3.2 MeV alpha particle. Note simulation error bars are not plotted other than the point at a scavenging capacity of $2x10^6$ s^{-1} as they are less than the size of the data points.

■ Simulated α-particle irradiation

▲ Experimental α-particle irradiation

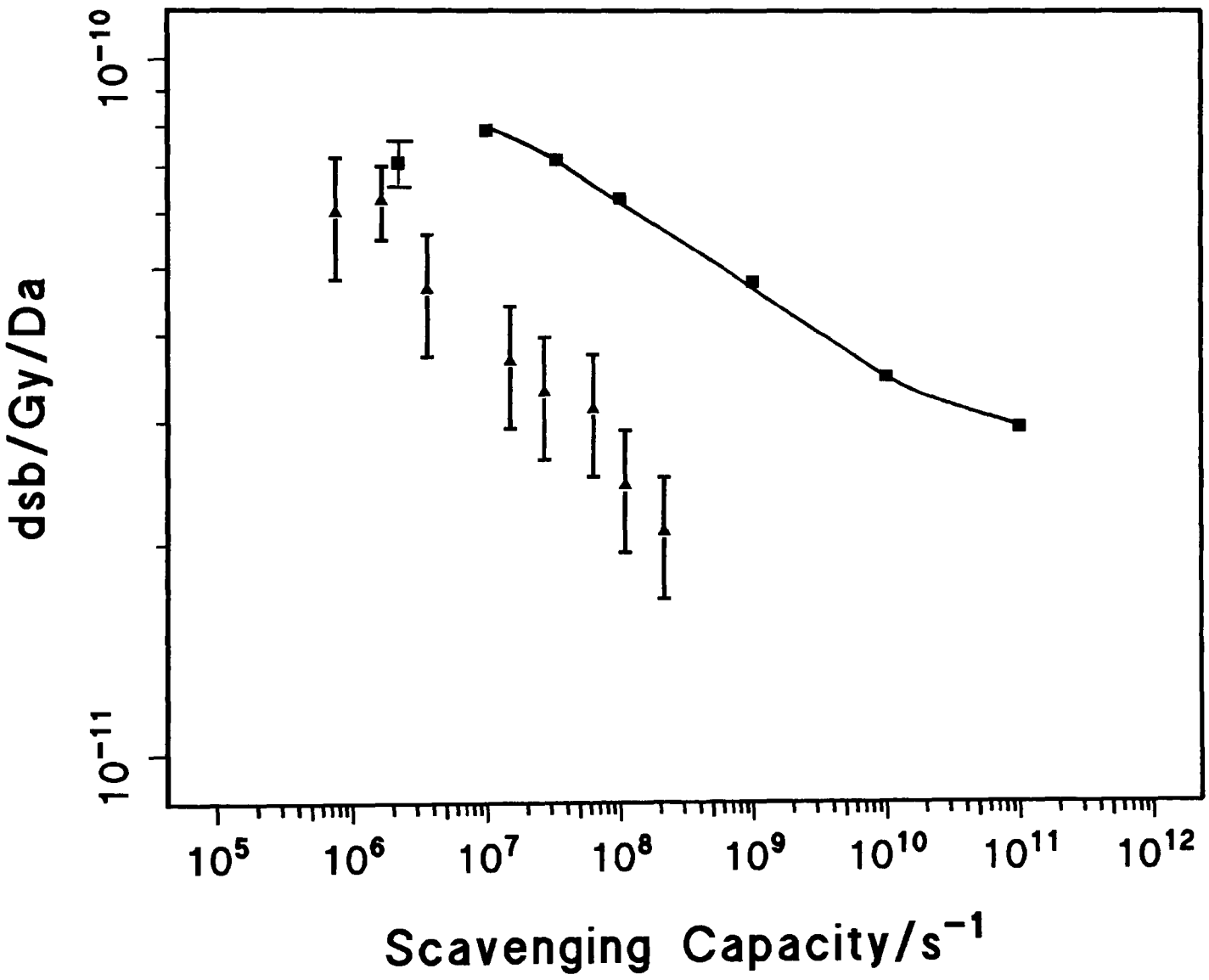

Figure 4.10.

Comparison of the dependence of the yields of dsb on scavenging capacity for simulations of 1.5 keV electron and α-particle irradiation. Note simulation error bars are not plotted as they are less than the size of the data points.

■ Simulated 1.5 keV electron irradiation

▲ Simulated α-particle irradiation

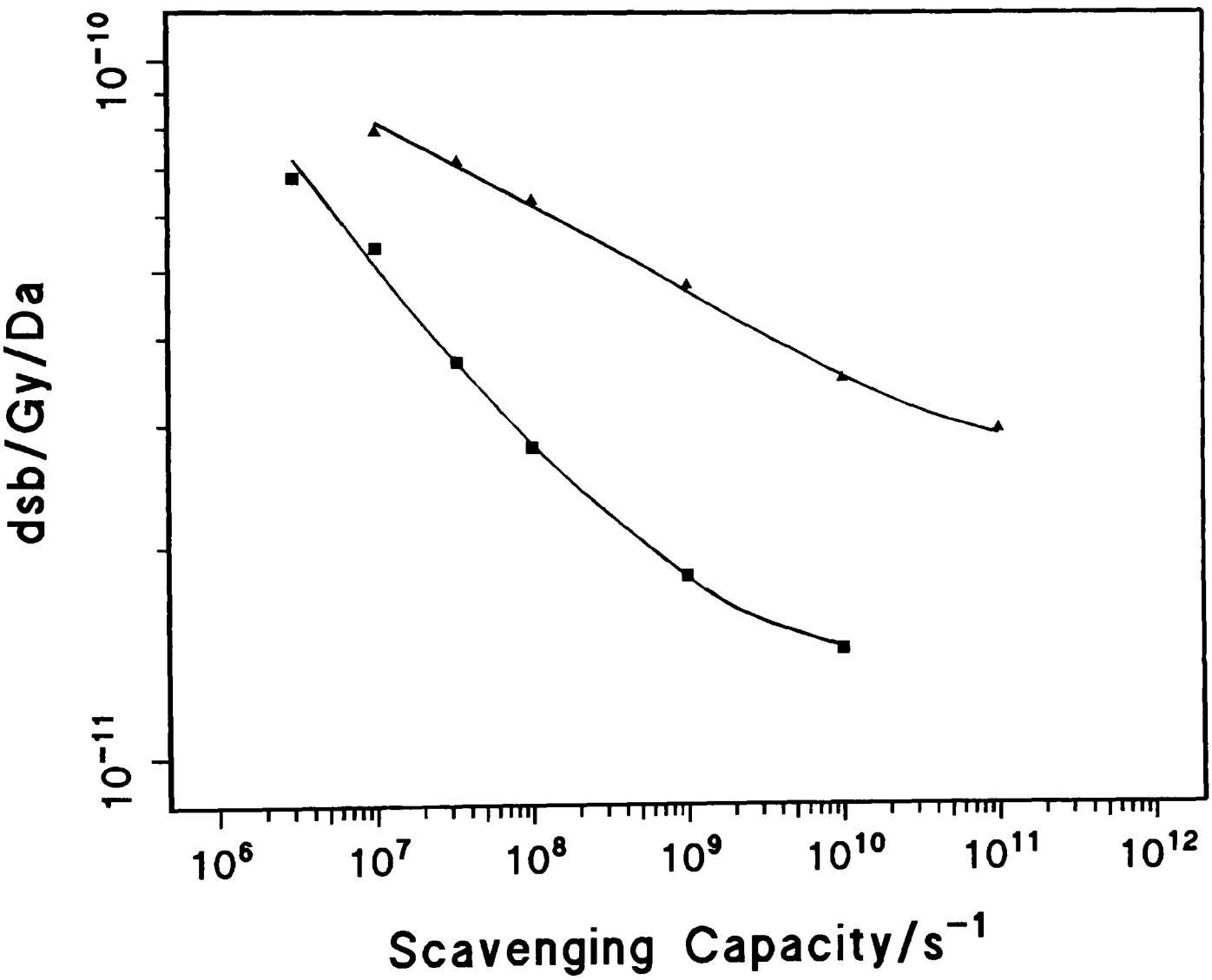

Figure 4.11.

Comparison of the ratio of ssb:dsb on scavenging capacity for experimental irradiation of pUC18 DNA with a ^{238}Pu source at 4^0 C and from simulations of a 3.2 MeV alpha particle. Note simulation error bars are not plotted as they are less than the size of the data points.

■ Simulated α-particle irradiation

▲ Experimental α-particle irradiation

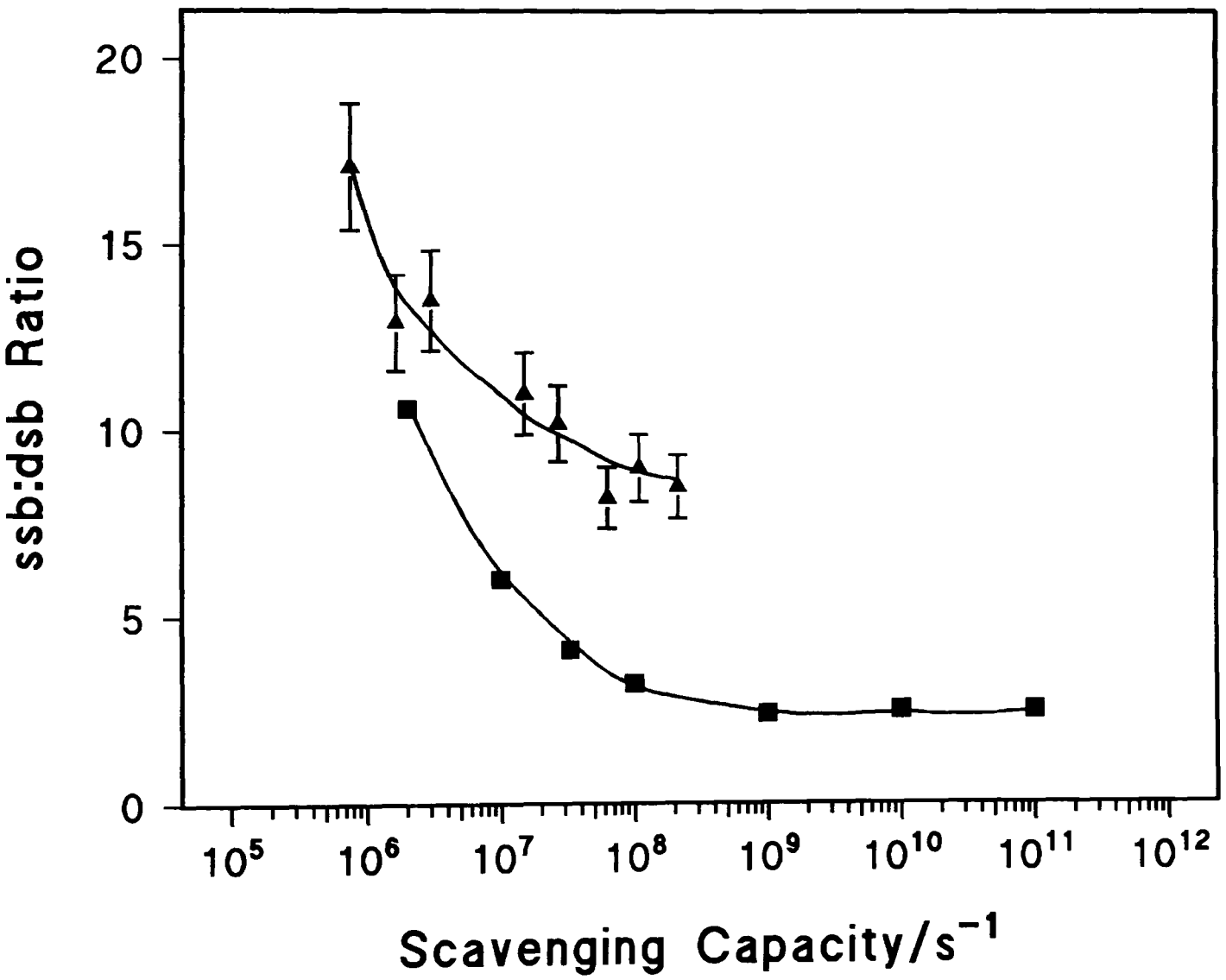

Figure 4.12.

Dependence of the proportion of dsbs classified as complex on scavenging capacity for the simulation of 3.2 MeV alpha particle tracks.

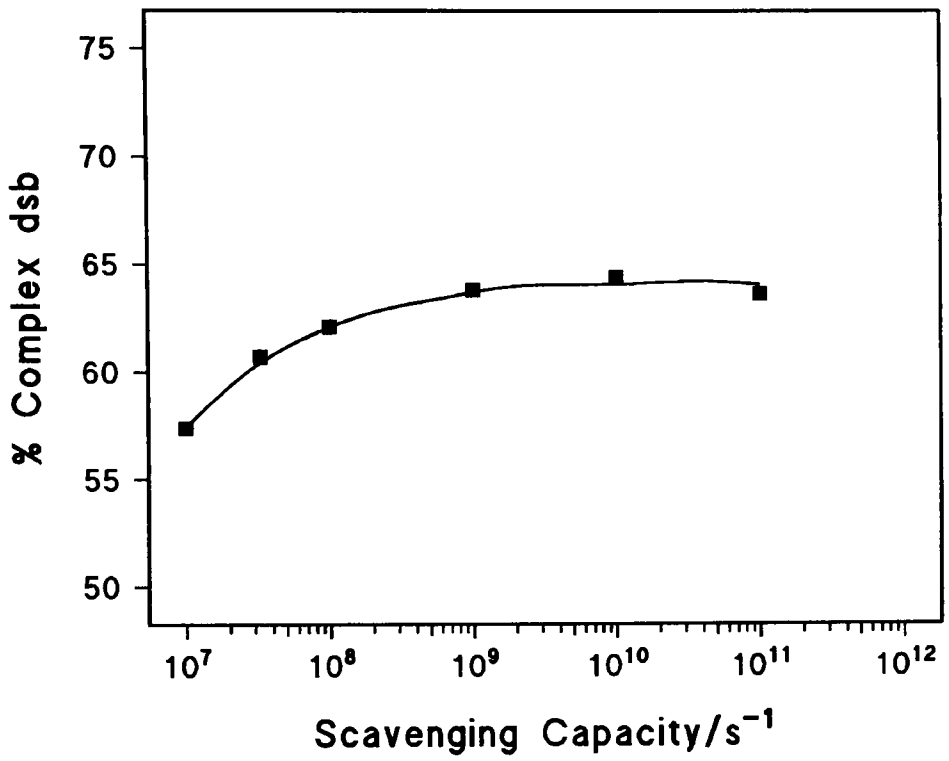

Figure 4.13.

Dependence of the proportion of ssb and dsb due to the direct effect on scavenging capacity for the simulation of 3.2 MeV alpha particle tracks.

■ Simulated yields of dsb

▲ Simulated yields of ssb

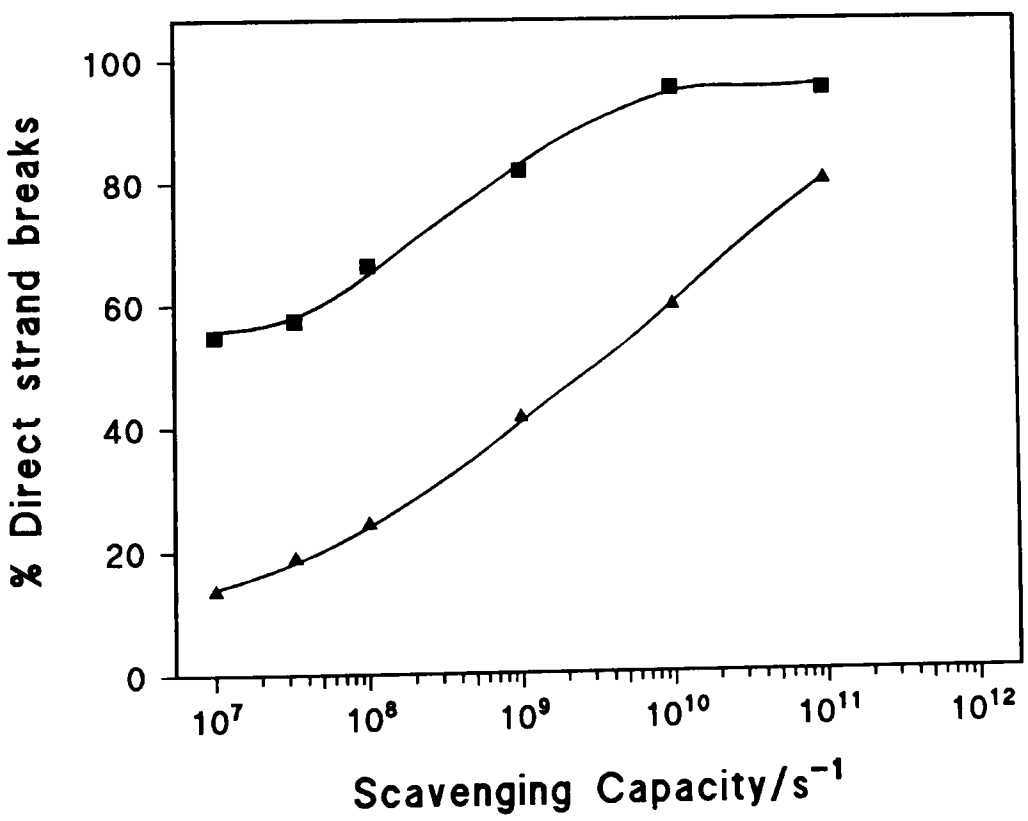

Chapter 5

Determination the Yields of Radiation-Induced Base Damage Revealed by Enzymes: Dependence of these Yields Upon Scavenging Capacity and Radiation Quality

5.1. Introduction

The determination of the yields of base damage provides information useful for both experimental and theoretical examinations. For computer simulations, experimental determinations of the yields of base damage and the ratio of strand breaks to base damage sites provide additional benchmarks for comparison and fitting. However, the majority of the determinations of the yields of base damage so far undertaken have been under low scavenging conditions rather than at scavenging capacities approaching cell mimetic conditions. From an experimental perspective, the contribution of base damages to the total damage yield may radically alter both the frequency of complex damage sites and their degree of complexity following irradiation (Nikjoo *et al.* 1999, Prise *et al.* 1999b, Sutherland *et al.* 2000). Compared with determinations considering only ssb and dsb, the inclusion of base damage sites gives a more accurate representation of the total amount of radiation-induced DNA damage and also allows assessment of the contribution of base damage sites to complex damage.

5.2. Determination of the Yields of Radiation-Induced Base Damage Sites by Enzymes

The determination of the yields of base damage may be accomplished by the use of enzymes as described in section 2.4.1. The enzymes used are Nth protein which generally excises pyrimidine base modifications and Fpg protein which generally excises purine base modifications (see table 2.4).

After irradiation, all samples underwent post-irradiation treatment consisting of precipitating the plasmid DNA and re-suspension into an activation buffer. Samples, in the presence or absence of enzyme, were incubated for a length of time specific to the enzyme used. This provides a comparison between the yields of damage obtained with and without the enzyme present and thus the number of strand breaks arising from the conversion of base damage sites into ssb via the action of the enzyme. It should be noted that as a result of the temperature of incubation necessary for enzymes to be

active, heat labile sites are included within the strand break determinations. The ratios of base damage:ssb were determined as described in section 2.4.2.2.

5.2.1. Yields of Base Damage Revealed by Nth Protein

Irradiations of plasmid DNA in aqueous solution were undertaken with γ-rays under aerobic conditions at 4^0 C using Tris as the scavenger. The irradiated DNA was precipitated and re-suspended in an activation buffer, as described in section 2.4.1. The DNA samples were then incubated in the presence or absence of Nth protein at 37^0 C for 30 min. The optimum concentration of Nth used for the determination of the yields of base damage was obtained by titration experiments as described in section 2.4.1. The dependence of the loss of closed circular DNA on γ-ray radiation dose for samples treated in the absence or presence of Nth enzyme is illustrated in figure 5.1 for a representative experiment in which the solution contained 0.1 mol dm^{-3} Tris. From figure 5.1 it can be seen that for both dependences, irrespective of whether enzyme was added, a linear response was obtained on a semi-log plot for the loss of closed circular DNA verses dose. It is thus inferred that precipitation of DNA and re-suspension into a different buffer does not result in deviation from a linear dose response for those DNA solutions that were not treated with the enzyme. When the dose responses for non-enzyme treated DNA solutions are compared with the dose responses determined for DNA solutions at equivalent scavenging capacities but maintained at 4^0 C as described in chapter 3 (i.e. from unprecipitated DNA studies), the D_{37} values for ssb are similar indicating that a relatively small number of heat-labile sites are induced by incubation at 37^0 C for 30 min. This small increase is expected as incubation of DNA solutions at 37^0 C for 30 min has previously been shown to induce only an additional 23 % ssb due to heat labile sites following γ-irradiation relative to the yields of ssb determined at 4^0 C (see section 3.2.2). The increased yield of heat sensitive labile-sites is known to be time dependent (Jones *et al.* 1994a).

From figure 5.1 it is also evident that the dose response for the loss of closed circular DNA remains linear after treatment with Nth enzyme. However, the gradient of the response for the Nth treated DNA is greater relative to that for DNA solutions that have not been treated with enzyme. This increased response in the presence of Nth is a result of radiation-generated base damage sites, which are converted to ssb by the Nth protein.

From the relative gradients of these dose dependences for the loss of closed circular DNA with and without the addition of enzyme, the numbers of base damage sites, revealed by the action of the enzyme and ssb (prompt + heat labile) were determined (see section 2.4.2.2). The variation in the ratio of base damage:ssb (revealed by the action of Nth) on the concentration of Tris scavenger following irradiation of DNA solutions with either γ-rays or α-particles is illustrated in figure 5.2. As above, irradiation was at 4^0 C and the irradiated DNA in solution was incubated in the absence or presence of Nth enzyme at 37^0 C for 30 min. As the concentration of Tris scavenger increases so too does the number of Nth sensitive base damage sites per ssb for both radiations (figure 5.2). The ratios of base damage:ssb determined at different scavenging capacities following Nth treatment are summarised in table 5.1 for γ-ray irradiation. Initially, the ratio of base damage:ssb gradually increases up to a Tris scavenging capacity of about $1.5x10^7$ s^{-1} where the value for the ratio of base damage:ssb is 0.8:1. Increasing the scavenging capacities further leads to a steeper increase in the ratio of base damage:ssb with a value of 2.8:1 at a Tris scavenging capacity of $1.4x10^9$ s^{-1}. There is an indication that the response flattens out at these high scavenging capacities. A scavenging capacity characteristic of cell mimetic conditions ($2.9x10^8$ s^{-1}) results in approximately two Nth sensitive base damage sites for every ssb produced. However it should be noted that the ratios represent lower limits as discussed in section 2.4.2.2. Firstly the actual ratio will represent the number of base damage sites:(ssb + heat labile sites). Secondly, those DNA molecules, which have a ssb and a base damage site present on the same strand, will not be discriminated from DNA molecules, which only have a ssb present. Thus this subset of damage will not contribute to the total number of base damage sites determined. This underestimation in the yield of base damage is considered in greater detail in section 5.3.3.

The variation in the ratio of base damage:ssb on scavenging concentration for irradiation with α-particles (figure 5.2) is similar to that determined for γ-ray irradiation although the ratios of base damage:ssb are greater following α-particle irradiation as shown in table 5.2. A value of 1.3:1 was obtained for the ratio of base damage:ssb after α-particle irradiation at a Tris scavenging capacity of $1.5x10^7$ s^{-1} rising to a value of 2.3:1 at a cell mimetic scavenging capacity of $2.9x10^8$ s^{-1}. At all scavenging capacities assessed, α-particle irradiation leads to approximately 0.3 more base damage sites per ssb than after γ-ray irradiation. However, the value of $(\text{base damage:ssb})_\alpha$ / (base

damage:ssb)$_\gamma$ decreases with increasing scavenging capacity from a value of 1.8 at $7.5x10^5$ s^{-1} to 1.2 at $2.9x10^8$ s^{-1} indicative of the two dependences drawing closer together at high scavenging capacities.

The increase in the ratio of base damage:ssb at high scavenging capacities may reflect oxygen depletion since irradiation of DNA samples at high scavenging concentrations requires a higher dose to produce an equivalent amount of DNA damage to that obtained at lower scavenging values. Depletion of oxygen would increase any interaction of DNA with hydrated electrons. Although the influence of oxygen depletion on the yield of strand breaks determined following high doses was previously examined in section 2.3.3.1. it was decided to extend this study given the dramatic response shown for the ratio of base damage:ssb with scavenging capacity. Because of the high doses (of the order of 1000Gy) and dose rates (approximately 52 Gy min^{-1}) any effects of radiation induced hypoxia are expected to become manifest at higher scavenging concentrations. It was therefore considered that radiation-induced hypoxia may be a possible contributory factor to the amount of base damage relative to ssb determined at high scavenger concentrations. Two sets of experiments were undertaken; One in which single dose irradiations up to a maximum of 2000 Gy were delivered and one in which equivalent doses were delivered but in maximum fractions of 250 Gy with re-equilibration of the solutions between each fraction by shaking while open to air. No differences in dose responses for the formation of Nth sensitive sites and ssb were detected between these two regimes. Therefore, to avoid any possibility of unintentional anaerobic effects at doses in excess of 500Gy, the solutions were fractionally irradiated with the largest fraction being set at 500Gy. The data in figure 5.2 were obtained by this approach.

5.2.2. Yields of Base Damage Revealed by Fpg Protein

The post-irradiation treatment of DNA solutions with Fpg enzyme is identical to the procedure utilising Nth with the exception that the incubation at 37^0 C is undertaken for 1 h rather than 30 min. The optimum concentration of Fpg that is used for base damage yield determinations is obtained by titration experiments as described in section 2.4.1. The ratios of base damage:ssb, determined at different scavenging capacities for Fpg treatment are shown in tables 5.3 and 5.4 for γ-ray and α-particle irradiation respectively and figure 5.3. As with Nth, the ratio of base damage:ssb revealed by Fpg

increases with increasing scavenging capacity. The ratio of base damage:ssb at the higher scavenging capacities is greater following α-particle irradiation than that for γ-ray irradiation. At scavenging capacities representative of those within the cellular environment, γ-ray irradiation produces approximately 1 Fpg sensitive base damage site for every ssb, whereas α-particle irradiation produces approximately 1.5 Fpg sensitive base damage site for every ssb. The ratios of base damage:ssb obtained following Nth and Fpg treatment for γ-ray irradiation are illustrated in figure 5.4. From comparison of the dependences it is apparent that the responses show similar trends, with, in both cases, the ratio of base damage:ssb increasing with increasing scavenging capacity. However, the yield of base damages detected by Nth is greater than that detected by Fpg over the entire scavenging range employed with the exception of the yields at the lowest scavenging capacities used.

5.2.3. Yields of Base Damage Revealed by Combined Treatment with Fpg and Nth

This determination of the yields of base damage was undertaken to assess whether the effect of Nth and Fpg on excision of base damage is additive or whether there is significant overlap in the spectrum of base damages recognised by the two enzymes. The procedure is identical to the separate analysis of sites sensitive to Nth and Fpg with the exception that 4 sets of DNA solutions were assessed, for base damage at specific γ-ray doses and scavenging capacities. One DNA solution contains only activation buffer, one contains activation buffer and Nth, one contains activation buffer and Fpg and one contains activation buffer to which both Nth and Fpg were added. In all cases incubation was at 37^0 C for 30 min. From comparison of the dose dependences for induction of ssb for the samples described above, addition of the enzymes simultaneously to irradiated DNA solutions resulted in yields of base damage approximately equivalent to yields obtained by the summation of the individual yields of enzyme sensitive sites. It was therefore concluded that the enzymes are effectively acting additively and only recognise a small number of the same damage sites, in accordance with previous findings (Milligan *et al.* 1999). Therefore, the ratio of base damage:ssb following irradiation at specific scavenging capacities, and subsequent treatment with either Nth or Fpg, presented in tables 5.1 - 5.4 were added, and the total yields of base damage recognised by the enzymes, per ssb, are summarised in tables 5.5 and 5.6 for γ-ray and α-particle irradiation respectively. Determination of the variation

in the yield of base damage (bd/Gy/Da) with scavenging capacity was obtained by multiplying the yield of base damage per ssb by the yield of ssb/Gy/Da at the appropriate scavenging capacity as presented in chapter 3. As previously discussed, all determinations of the ratio of base damage:ssb include a contribution from heat labile sites. Subsequently the yield of base damage sites per ssb represents a lower limit, and so too the determination of the absolute yield of base damage sites (bd/Gy/Da) shown in the final column of tables 5.5 and 5.6. Consequently it is estimated that the yields of base damage presented in tables 5.5 and 5.6 will be approximately 23 % higher after correcting for this contribution. This is discussed fully in section 5.3.3. The dependence of the yield of bd/Gy/Da on scavenging capacity following either γ-ray or α-particle irradiation is shown in figure 5.5. For both irradiations, as the scavenging capacity increases the yield of bd/Gy/Da decreases in a manner analogous to the dependence of the yield of ssb on scavenging capacity as illustrated in figure 3.6. The reason for the decrease in the yield of base damage with scavenging capacity has the same mechanistic basis as that for the decrease in the yield of ssb with scavenging capacity. Essentially OH radicals are principally responsible for the generation of base damage sites at low scavenging capacity under aerobic conditions. However, as the scavenging capacity increases, the number of OH radicals which interact with DNA at a given dose decreases resulting in lower yields of base damage. At higher scavenging capacities, the contribution of the direct effect relative to the contribution of OH radical damage becomes more prominent. Further, in a response analogous to that obtained for ssb/Gy/Da, the yields of bd/Gy/Da induced by α-particle radiation are less than those induced by γ-ray radiation over the entire scavenging capacity range examined, similar to the observations for γ-ray and α-particle radiation induced ssb/Gy/Da. As discussed in chapter 3, these differences in bd yields result from a greater number of intra-track radical-radical recombination events occurring with α-particle radiation compared with γ-ray radiation, so that fewer OH radicals escape the track and are available to interact with DNA.

5.2.4. The Complexity of Damage Involving Base Damage

If a base damage site is converted into a ssb in the vicinity of another ssb or base damage, which is also converted to a ssb, on the complementary strand then a dsb will be formed. Therefore, an increase in the yield of dsb following enzyme treatment is an

indication of base modification contributing to complex damage, which is not initially seen in the absence of the enzyme. Ratios of the yields of dsb induced by radiation but only revealed in the presence of enzyme to the yield of dsb induced in the absence of enzyme were determined over the same scavenging range employed for the determination of the ratio of base damage:ssb. The ratio of the dose response gradients for dsb_{enz}:$dsb_{no\ enz}$ is essentially constant with scavenging capacity over the range employed for both γ-ray or α-particle irradiations and treatment with either Nth or Fpg. Due to the large error associated with dsb determinations it was felt more pertinent to quote an average ratio increase over the scavenging range employed for treatment with either Nth or Fpg. Subsequently for each radiation source all ratios were summed over the entire scavenging capacity range employed irrespective of the enzyme used and an average obtained. For γ-ray and α-particle irradiation, values of 1.8 ± 0.7:1 and 1.6 ± 0.2:1 were obtained respectively for the ratios of the dose response gradients for dsb induction following treatment with or without Nth or Fpg. Hence for γ-ray and α-particle irradiation an additional 0.8 and 0.6 dsb were induced respectively following either Nth or Fpg treatment for every pre-existing dsb. By combination of these additional yields of dsb, and assuming the enzyme specificity for base damage is different as described above and that there are few damage sites with both Nth and Fpg sensitive base damages present, an additional 1.6 and 1.2 dsb are revealed by the combined action of Nth and Fpg for every dsb induced in the absence of enzyme treatment following γ-ray and α-particle irradiation respectively.

5.2.5. Mechanisms for the Dependence of the Yields of Base Damage on Scavenging Capacity

To assess the possible causes for the increase in the ratio of base damage:ssb with increasing scavenging capacity a number of factors were considered. Electrons are known to give rise to base damage on interaction with DNA (Fuciarelli *et al.* 1990). However hydrated electrons produced within the solution containing DNA rapidly react with oxygen and thus have a very low probability of interacting with DNA present at very low concentrations for γ-ray irradiation under aerobic conditions. The reaction rate constant of electrons and O_2 is 1.9×10^{10} $mmol^{-1}$ dm^3 s^{-1} (Buxton *et al.* 1988) and the concentration of O_2 in air-equilibrated water is 0.276 mmol dm^{-3}. Therefore the average lifetime of electrons in solution is 1.9×10^{-7} s. The mean diffusion distance of electrons

in solution under aerobic conditions is given by $2.26(Dt)^{1/2}$ (Roots and Okada 1975) where D is the diffusion coefficient for solvated electrons equal to $4.5x10^{-5}$ cm^2 s^{-1} (Schwarz 1969) and t is the average electron lifetime. Therefore electrons have mean diffusion distances of ~66 nm, so that electrons must be formed relatively close to DNA for interactions to occur. Additionally, the phosphate backbone of DNA, which is negatively charged, will electrostatically repel electrons in the surrounding medium, again reducing the probability of electron interactions with DNA at low ionic strength. The reaction between solvated electrons and Tris is insignificant with a rate constant of $< 10^6$ mol^{-1} dm^3 s^{-1} (Buxton *et al.* 1988). It has been shown that O_2 depletion has been eliminated as contributing to the increase in the ratio of base damage:ssb with increasing scavenging capacity (section 5.2.1). It is hypothesised here that the increase in the ratio of base damage:ssb with increasing scavenging capacity results from an increased relative yield of electrons, which can interact with DNA and induce base damage, due to variation in the ionic strength of the solution and the mean diffusion distance of the electron. These factors are influenced by the scavenging capacity, type of scavenger and the concentration of oxygen. For all of the experiments described above the scavenging capacity was set by varying the concentration of Tris. Since Tris is ionic it shields the electrostatic field around the DNA, resulting from the negatively charged phosphate backbone, to an extent dependent upon the concentration of Tris. Hence, an increase in the Tris concentration leads to an increased electrostatic shielding of the DNA to negatively charged reactants and therefore an increased probability for electrons to interact with the DNA. Additionally, as the scavenging capacity increases the relative contribution of electrons directly produced in DNA from ionisation increases relative to those produced indirectly in bulk water. Electrons produced via the direct effect i.e. ionisation of DNA, probably do not interact with oxygen and do not have to overcome electrostatic repulsion of the phosphate backbone to interact with the base moieties of DNA. Consequently, directly produced electrons have a much higher probability of interacting with DNA to cause base damage. Therefore an increase in the yields of base damage relative to ssb may be anticipated with an increase in scavenging capacity. To test the hypothesis that electrons may contribute to the formation of base damage, especially at high concentrations of Tris, and therefore contribute to the increase in the ratio of base damage:ssb with increasing scavenger concentration, two experiments were undertaken. Firstly, a non-ionic scavenger may be employed to set the scavenging capacity of the solution equivalent to that set by Tris. Due to its non-

ionic nature, any changes in the scavenger concentration will not lead to changes in the DNA electrostatic repulsion so that the probability of electrons, produced in bulk water, reacting with DNA at a given scavenging capacity may not be the same as that with Tris. Secondly, irradiations may be undertaken under anaerobic conditions in the presence of Tris. Under such conditions electrons produced in solution cannot react with oxygen and so will not be removed. Hence the potential for electrons, either directly produced or produced in the vicinity of water to cause base damage may be assessed

5.2.5.1. The Role of Electrostatic Repulsion

To examine the influence of the electrostatic repulsion associated with the phosphate backbone of the DNA, irradiations were carried out in aerated aqueous solutions comprising 1μl of DNA stock (10 mmol dm^{-3} Tris) and 19μl of 0.15 mol dm^{-3} ethanol. Such a dilution of the Tris within the DNA stock gives a final Tris concentration of 0.5 mmol dm^{-3} but the scavenging capacity of the solution is approximately equivalent to 0.2 mol dm^{-3} Tris. This results from the reaction rate constant of ethanol and OH radicals being equal to $1.9x10^9$ $mmol^{-1}$ dm^3 s^{-1}, whereas the reaction of Tris and OH radicals equals $1.5x10^9$ $mmol^{-1}$ dm^3 s^{-1} (Buxton *et al.* 1988). Therefore a 0.15 mol dm^{-3} solution of ethanol has a scavenging capacity of $2.85x10^8$ s^{-1} equivalent to a 0.19 mol dm^{-3} Tris scavenging solution. Irradiations in the presence of ethanol were undertaken in air saturated solutions with γ-ray irradiation and Nth enzyme was used to convert sensitive base damage sites into ssb. All other experimental parameters are as described above with Nth enzyme. With ethanol as a scavenger the ratio of base damage:ssb is 1.2±0.2:1. This should be compared with the ratio of base damage:ssb of 0.43:1 and 2.00:1 (table 5.1) obtained at Tris concentrations of 0.5 mmol dm^{-3} and 0.2 mol dm^{-3} respectively. Hence the ratio of base damage:ssb for irradiation of DNA in a Tris/ethanol solution lies between that obtained solely for the Tris concentration which is actually present and for a Tris concentration equivalent to the scavenging capacity of the Tris/ethanol solution. If the majority of the increase in base damage per ssb at high scavenging capacity was due to the role of electrons produced in the DNA by direct ionisation, then the ratio of base damage:ssb in the presence of either Tris or ethanol at the same scavenging capacity should be similar. As this is not the case it is inferred that the increase in the base damage per ssb at the higher scavenging capacity seen with Tris

but not ethanol is mainly due to interactions of hydrated electrons with DNA in competition with its interaction with oxygen. It is proposed that the increase in the ratio with Tris relative to that with ethanol is due to the electrostatic shielding by a high concentration of Tris. However, it is clear that electrostatic effects are not the only factor contributing to the elevated yields. Ethanol radicals are ruled out as contributing to the increased ratio of base damage:ssb as they are reported not to contribute to DNA damage (Lafleur *et al.* 1978, 1979).

5.2.5.2. Yield of Base Damage Induced Under Anaerobic Gassing Examination

Since hydrated electrons may be a precursor to base damage recognised by Nth, the determinations of the yields of base damage induced under anaerobic conditions by γ-ray irradiation of DNA in the presence of Tris at variable concentrations were undertaken. Quantification of base damage was identical to those previously undertaken with Nth. Anaerobic conditions were produced by gassing the DNA solutions at a given concentration of Tris under N_2O or N_2 for 15 min prior to irradiation and during the entire course of the irradiations as described in section 2.3.3.1. In N_2O the electrons are converted into OH radicals whereas in N_2 the yield of e^-_{aq} and OH radicals are similar.

N_2 Gassing Conditions

DNA solutions containing various concentrations of Tris were γ-ray irradiated at 4^0 C either under air or N_2. Enzyme analysis was then undertaken by the addition of Nth as described in section 2.4.1. Four sets of experiment were undertaken. Two samples were irradiated under aerobic conditions and one was treated with Nth enzyme and the other only with enzyme buffer and two samples were irradiated under N_2, again one treated with Nth enzyme and one with enzyme buffer. The yield of ssb was quantified by gel electrophoresis as described in section, 2.4.2, 2.4.2.1 and 2.4.2.2. The yields of base damage relative to that for ssb were determined both for the aerobic and anaerobic irradiation conditions and the values compared. A typical dose response for the four sample conditions is illustrated in figure 5.6. As previously shown, a linear dose log response for the loss of closed circular DNA is obtained for samples either with or without enzyme treatment and irrespective of gassing conditions. It should be noted that over all experiments performed there is no significant difference between dose

responses, in the absence of enzyme treatment, between irradiations under N_2 or aerobic conditions. However, with Nth treatment there is a significant increase in the gradient of the dose response when irradiations were undertaken under N_2 relative to irradiations under aerobic conditions. At each scavenging capacity rather than using the previously obtained ratios for base damage:ssb for irradiation in air (section 5.2.1, table 5.1) to compare with the effect of irradiation under N_2, the ratio of base damage:ssb were determined for both the aerobic and anaerobic irradiations in the same experiment to minimise any experimental inconsistencies. Irradiations carried out for DNA solutions under various scavenging capacities are summarised in table 5.7 for both aerobic and anaerobic irradiation conditions. When the ratios obtained for base damage:ssb revealed by Nth under aerobic conditions within this set of experiments are compared with those summarised in table 5.1, there is a good agreement between the two sets. Hence, the ratios obtained under anaerobic conditions do not reflect differences arising from experimental variations. From comparison of the ratios in table 5.7 it can be seen that there is a significant increase in the ratio of base damage:ssb for N_2 compared with those obtained under aerobic conditions over the range of scavenging capacities examined. The yield of base damage per ssb under N_2 increases by a factor of 2-3 compared with the equivalent yields determined under aerobic conditions over the scavenging range $7.5x10^5$-$1.4x10^8$ s^{-1}. As discussed, under aerobic conditions the lifetime of the electron is increased and it should be remembered that e^-_{aq} does not lead to ssb on interaction with DNA. As the scavenging capacity increases for irradiations under aerobic conditions the increase in the ratios of base damage:ssb is a result of the increased contribution of the direct effect and greater contribution of electrons produced in the vicinity of the DNA due to reduced electrostatic repulsion as discussed above. Since irradiating under anaerobic conditions reveals elevated ratios of base damage:ssb relative to those for aerobic conditions it is inferred that e^-_{aq} induces enzyme sensitive base damage. However, it is also possible that the base damage types under aerobic conditions may be different and affect the recognition these damages by Nth. For instance radiation may give rise to base damage sites which interact with oxygen to give sites which are no longer recognised by Nth. Therefore, in the absence of oxygen, an increased number of Nth recognised sites per ssb may be present due to the contribution of base damage arising through interactions with electrons and differences in recognition of the different types of base damage by Nth. To assess the possibility of changes in recognition of base damage produced in the presence of

oxygen by Nth, samples were irradiated under N_2O, which converts e^-_{aq} into OH radicals.

N_2O Gassing Conditions

As described in section 2.3.3.1 following irradiation under N_2O, electrons are converted into OH radicals, so that the number of OH radicals under N_2O is twice that obtained under oxygen. N_2O is an efficient scavenger of electrons with a rate constant of $9.1x10^9$ mol^{-1} dm^3 s^{-1} (Buxton *et al.* 1988) and with a concentration of $2.3x10^{-2}$ mol^{-1} dm^3 this leads to a scavenging capacity of $2.1x10^8$. For irradiation under aerobic conditions at low scavenging capacities, the number of base damage sites resulting from interactions with electrons will be minimal relative to those produced by OH radicals due to the high reactivity of electrons with oxygen and the large mean diffusion distances of the OH radicals. For irradiation under N_2O at a low scavenging capacity (e.g. 10 mmol dm^{-3} Tris) electrons do not contribute significantly to base damage except those electrons produced within a few nm of DNA. Further, since oxygen is not present, changes in recognition of damage relative to anaerobic conditions are minimised. Although with N_2O the yield of OH radicals doubles, relative to aerobic or anaerobic conditions, the ratio of base damage:ssb should remain constant compared with aerobic conditions if differences in base damage recognition by Nth are not important. Therefore, any variation in the ratio of base damage:ssb under N_2O from that obtained under aerobic conditions will be an indication of possible differences in enzyme recognition of base damage induced by OH radicals since the electron contribution to base damage should be small under both conditions.

The relative gradients for the dose response for the loss of closed circular DNA at 4^0 C for solutions containing 10 mmol dm^{-3} Tris and γ-ray irradiated under N_2O and air were compared. Irradiated samples were analysed by gel electrophoresis and staining took place as described in section 2.4.2 and quantification of strand breaks and base damage sites as described in sections 2.4.2.1 and 2.4.2.2. . To check that the samples are indeed fully anaerobic after gassing with N_2O a direct comparison was made of the yield of ssb induced under anaerobic conditions to the number induced under aerobic conditions. Assuming no air is present under N_2O conditions, the ratio of ssb induced under N_2O :aerobic conditions should be 2:1 as a result of electrons being converted to OH radicals in N_2O. The actual ratio determined is $2.1:1\pm0.6$ thus confirming that the

experimental conditions are suitable for anaerobic irradiations. That hypoxia was induced was confirmed using methyl viologen (see section 2.3.3.1).

For determination of the ratio of base damage:ssb revealed by Nth, enzyme analysis was undertaken as described in section 2.4.1 with quantification of strand breaks and base damage sites as described in sections 2.4.2.1 and 2.4.2.2. The relative dose responses for loss of closed circular DNA was compared for DNA solutions containing 10 mmol dm^{-3} Tris and γ-ray irradiated at 4^0 C under N_2O and air. As previously shown, γ-ray irradiation of DNA solutions under aerobic or anaerobic conditions gives a ratio of base damage:ssb equal to 1:1 and 2.5:1 respectively following γ-ray irradiation in the presence of 10 mmol dm^{-3} Tris and treatment with Nth as shown in table 5.7. The ratio of base damage:ssb obtained under the same conditions but saturated with N_2O is equal to (1.4±0.5):1. The ratio of base damage:ssb in N_2O is similar to that obtained under aerobic conditions and is consistent with the hypothesis that there is no significant change to the damage recognition spectrum of OH radical induced base damage in the presence of oxygen. Hence the increased yield of base damage per ssb determined under N_2 cannot be attributed predominantly to any difference in the spectrum of enzyme recognition of OH radical induced base damage and supports the hypothesis that the elevated ratio of base damage:ssb under N_2 relative to air is predominantly due to increased interaction of electrons with DNA.

5.2.5.3. Comparison with Simulation

A final piece of evidence supports the hypothesis that electron induced damage, recognised by Nth, results from the increased relative contribution of the direct effect with increasing scavenging capacity, and therefore that the number of directly produced electrons contributes to the yields of base damage. Figure 5.7a illustrates the experimental yield of base damage per ssb following Nth treatment with γ-ray irradiation as presented in figure 5.2 alongside the proportion of ssb damage arising from the direct effect as simulated for 1.5 keV electrons. Figure 5.7b illustrates the dependence on scavenging capacity of the direct effect contribution to ssb as evaluated by simulations. For this visual comparison shown in figure 5.7a the contribution from the direct effect from the simulation at the highest scavenging capacity is set to be equal to the ratio of base damage:ssb at the equivalent scavenging capacity. The values are subsequently scaled so that the zero contribution of the direct effect is set to be

equal to the point where the ratio of base damage:ssb is equal to zero. Hence, the shapes of the two responses may be directly compared. Although no definitive information may be induced from the comparison, the similarity of the two response shapes is suggestive that the direct effect may in part contribute to the enhanced ratio of base damage:ssb on increasing the scavenging capacity.

5.3. Discussion

5.3.1. Generalisations

A number of pertinent pieces of information regarding the yield of base damage have been obtained from the present study. Firstly, the yield of base damage decreases with increasing scavenging capacity for both γ-ray and α-particle irradiation due to the removal of OH radicals. However, there is an increased yield of base damage per ssb with increasing scavenging capacity following both γ-ray and α-particle irradiation.

5.3.2. Yields of Base Damage

The increase in the ratio of the yields of base damage:ssb is hypothesised to result from electrons, produced directly and indirectly, contributing to the yield of base damage sites recognised by Nth and Fpg enzymes. Predictions of the numbers of enzyme sensitive base damage sites come from a number of previous studies. Fuciarelli *et al.* (1990) have determined the yield of radiation-induced base products in DNA following γ-ray irradiation of calf thymus DNA in a phosphate buffer under aerobic conditions, by gas chromatography-mass spectrometry. The yields of cytosine glycol and thymine glycol were determined to be 19.9 and 38.1 nmol J^{-1} respectively although 5,6-dihydropyrimidine was not detected. Thus a minimum of 58 nmol J^{-1} base modifications that are substrates for Nth were determined (see table 2.4). The yields of Fapy-guanine, Fapy-adenine and 8-hydroxyguanine were determined to be 8.5, 3.6, and 59.2 nmol J^{-1} respectively leading to a minimum of 71 nmol J^{-1} of base modifications that are substrates for Fpg (see table 2.4). Thus approximately equivalent levels of Fpg and Nth sensitive sites are predicted at the equivalent of low scavenging capacities, in general agreement with the yields of base damages revealed by Nth and Fpg at 0.5 mmol dm^{-3} Tris. At a low scavenging capacity (10^6 s^{-1}) the yield of OH radicals is 0.29 μmol J^{-1} for ^{60}Co γ-ray irradiation (Buxton *et al.* 1988). In chapter 7 it is argued that the

yield of ssb at low scavenging capacities for γ-ray irradiation is proportional to the yield of OH radicals. If it is assumed that the probability of an OH radical giving a ssb is 0.13 (Milligan *et al.* 1993), then the yield of ssb is ~ 38 nmol J^{-1}. Since the yield of heat labile sites, which are converted to ssb under the conditions of the enzyme, treatment is about 10 nmol J^{-1} (see section 3.2.2) the total yield of ssb + heat labile sites is approximately 48 nmol J^{-1}. From table 5.5 the total yield of base damage at low scavenging capacities is 0.92 of the yield of prompt ssb and heat labile sites. Therefore, at low scavenging capacities, the yield of base damages recognised by Nth and Fpg is ~ 44 nmol J^{-1}, somewhat less than the yields of damage detected by analytical techniques (Fuciarelli 1990). However, although GC-MS is a very sensitive technique there is controversy over additional yields introduced through handling (Douki *et al.* 1996, Cadet *et al.* 1997) and it is only possible to identify a limited number of lesions. Thus, for example, AP sites cannot be detected. However, both enzymes are found to recognise and induce ssbs at AP sites (see table 2.4) (Baily *et al.* 1989, Kow and Wallace 1987). However, the fact that the enzymes interact additively in their base damage recognition is indicative that the number of AP sites must be small relative to base modifications.

Comparisons of the ratio of base damage:ssb obtained within the present study has been made with those determined by a number of other groups who have utilised Nth and Fpg enzymes. The majority of these studies have focused on base damage yields at low scavenging concentrations. In the current study, at a scavenging capacity of $1.5x10^7$ s^{-1}, the ratio of base damage:ssb is 0.6:1 following treatment with Fpg, consistent with several other findings. For instance, Epe *et al.* (1993) reported an approximate ratio of base damage:ssb of 1:1 following Fpg treatment at low scavenging capacities while similar ratios have been reported by a number of other groups following low-LET irradiation of DNA at low scavenging capacities (Häring *et al.* 1994, Epe *et al.* 1996, Kuipers and Lafleur 1998). In comparison, Milligan *et al.* (1996b, 1999), at an equivalent scavenging capacity, determined a ratio of base damage:ssb of 2:1 following treatment with Fpg.

At the same scavenging capacity of $1.5x10^7$ s^{-1} the present study gave a ratio of base damage:ssb of 0.8:1 with Nth, similar to that determined by a number of other groups. Epe *et al.* (1993) reported a ratio of base damage:ssb of 0.6:1 and subsequent analysis has confirmed less than 1 Nth sensitive sites per ssb, with ratios of base damage:ssb of

0.6:1 (Epe *et al.* 1996) and approximately 0.4:1 (Häring *et al.* 1994, Kuipers and Lafleur 1998) being obtained. In contrast Milligan, Ng *et al.* (1996b, 1999) reported a ratio of base damage:ssb of 1.5:1. Prise *et al.* (1999b) determined a value of 2.7:1, the latter value being ~ 2-3 fold greater than the values determined by the majority of other studies.

Even though a number of studies have been undertaken at low scavenging capacities with low LET radiation, little information is available on the ratio of base damage:ssb at high scavenging capacities or following high LET irradiation. In the present study, at scavenging capacities of $1.5x10^7$ s^{-1} and $3.0x10^8$ s^{-1} ratios of base damage:ssb of 0.8:1 and 2:1 are obtained following γ-ray irradiation and 1.3 and 2.3 following α-particle irradiation respectively following treatment with Nth. In contrast, for γ-ray and α-particle irradiations at these two scavenging capacities and subsequent Nth treatment, Prise *et al.* (1999b) determined the ratios of base damage:ssb to be 2.7:1 and 3.5:1 respectively for γ-ray irradiation and 0.8:1 and 1.5:1 for α-particle irradiation respectively. Although there is significant discrepancy between the two sets of data for both radiations, both sets of data confirm an increase in the ratio of base damage:ssb as the scavenging capacity increases.

5.3.3. Yields of Complex Damage

As discussed in section 2.4.2.2, the determinations of the ratio of base damage:ssb and the increase in dsb formation following treatment with enzyme i.e. the increase in complex damage, represent lower estimates. There are three principal reasons 1) insensitivity of the plasmid system to revealing the multiple damage, 2) reduced enzyme activity at complex damage sites and 3) heat labile sites. Firstly, a base damage site present on a plasmid which has an additional radiation-induced ssb will be undetected within the system unless the two damage sites are on separate strands and are sufficiently spatially close to form a dsb upon enzyme treatment. If the base damage site is spatially distant from the ssb, the base damage will be converted into a ssb following enzyme treatment. However, gel electrophoresis will not differentiate between a plasmid with two ssb which are not sufficiently close to form a dsb present and one containing only a single ssb, leading to only a single ssb being measured in the former case. This lack of sensitivity is minimised by using doses less than the D_{37} value for enzyme treated DNA solutions. However, this cannot reduce the lack of sensitivity

in respect of damage sites from ionisation clustering within a single track. This contribution is most relevant at high scavenging capacity. Similar arguments may be made for underestimation of enzymatically-induced dsb. Hence, radiation-induced dsb, with an additional base damage site present, will be undifferentiated from simple radiation-induced dsbs by gel electrophoresis. However, because dsb occur at lower frequencies than ssb at experimentally employed doses, it is anticipated that any underestimation will be less significant for dsb formed from multi-track effects at low scavenging capacity. However, such a proposition is only valid for DNA damage sites considered to occur independently from separate tracks. It is least likely to apply to dsb produced at high scavenging capacity.

The main basis of complex damage is that damage sites are produced spatially close as a result of ionisation clusters from a single track leading to an increased probability of base damage sites being produced near to other damage sites as the scavenging capacity increases or for high LET radiations such as α-particle irradiation. Clustered DNA damage containing base damages may reduce the efficiency of enzymes to convert a base damage into a ssb. As discussed in section 1.6.2.2 there are a number of studies examining the activity of enzymes when a base damage site occurs in close vicinity to another damage site (Chaudhry and Weinfeld 1995, Harrison *et al.* 1998, David-Cardonnier *et al.* 2000, Sutherland *et al.* 2000). These have shown that the action of the enzyme may potentially be inhibited when spatially close damage sites are produced. Specifically it appears that the enzymes' glycosylase activity is stalled when either modified bases or abasic sites are present in close vicinity to another base damage site. Thus if a base damage site is spatially close to a ssb on the opposite strand the enzyme may be inhibited and hence a dsb is not subsequently formed. In such an event the measured increase in dsbs following enzyme addition will be an underestimate. It is anticipated that the increased ionisation density of α-particle radiation will lead to more complex damage per ssb and potentially an increased number of sites in which the proximity of damage sites leads to the inhibition of the enzyme activity. Therefore, underestimation of complex damage should be greater with α-particle irradiation than γ-ray.

Analysis of the increase in dsb yields following enzyme treatment (see section 5.2.4) resulted in an additional 1.6 and 1.2 dsb, due to the conversion of base damage sites into ssb, per pre-existing dsb for γ-ray and α-particle irradiation respectively. If it is

assumed that these additional dsb arise predominantly from the existence of a ssb on the complementary strand to the excised base damage, then the total number of complex sites may be estimated. The ratios of ssb and dsb discussed in chapter 3 vary between 91:1 and 30:1 over the scavenging range of $7.5x10^5$ to $1.4x10^9$ s^{-1} following γ-ray irradiation. At the lowest scavenging capacity with γ-ray irradiation, for every 91 ssbs 1.6 base damage sites are located sufficiently spatially close to a ssb to form a dsb i.e. approximately 1 in every 50 ssb (~2 %) has a base damage site closely associated with it. At the highest scavenging capacity there are 1.6 base damage sites for every 30 ssbs i.e. approximately 1 in every 20 ssb (~5 %) has a base damage site closely associated with it. At a cell mimetic scavenging capacity approximately 1 in every 22 ssb will have an associated base damage site (~5 %). Similar arguments may be applied following α-particle irradiation. Over the scavenging capacity range ($7.5x10^5$ s^{-1} to $2.9x10^8$ s^{-1}) the ratio of ssb:dsb varies between 16:1 and 8:1. Hence at the lowest scavenging capacity there are 1.2 base damage sites for every 16 ssb i.e. approximately 1 in every 13 ssb (~8 %) has a base damage site associated with it. At the highest scavenging capacity equivalent to a cell mimetic value there are 1.2 base damage sites for every 8 ssb i.e. approximately 1 in every 7 ssb has a base damage site associated with it (~15 %). If complex damage whereby, a ssb is in close proximity to a base damage on the same strand has a similar yield to complex damage determined where the damages are on different strands, then the yields of complex damage are at least twice as great as the value estimated above. Hence, if the values determined for cell mimetic conditions of 5 % and 15 % are considered then at least 10 % and 30 % of ssb have an associated base damage for γ-ray and α-particle radiation respectively. If the yield of prompt dsbs (see chapter 3) under cell mimetic conditions are included, the yields of complex damage increase to ~13 % and 42 % for γ-ray and α-particle radiation respectively. As stated above, these are only lower limits of ssb which have an associated base damage or ssb for the three principal reasons given above, namely that the plasmid system underestimates the yield of complex damage, there may be reduced enzyme activity at the complex damage sites and heat labile sites also contribute.

Consideration of heat labile sites is based upon the increase in the yield of dsb of 94 % determined for γ-ray irradiated DNA solutions incubated at 37^0 C for 30 min as described in section 3.2.2. Therefore, the increase in dsb relative to prompt dsb (at 4^0 C)

following enzyme treatment (at 37^0 C) may actually be a factor of 2 higher than the values presented above. As the ratios of dsb (enzyme present):dsb (no enzyme) were determined at 37^0 C the amount of complex damage will be considerably higher than the figures quoted above if heat labile sites are considered. It was shown that at cell mimetic scavenging capacities after γ-ray irradiation 1 in every 22 ssb and after α-particle 1 in every 7 ssb (see above), would have a spatially close base damage site on the opposite strand. If the heat labile correction is undertaken these reduce to 1 in 11 ssb for γ-ray and 1 in 3.5 ssb for α-particle irradiation. In terms of absolute complex yields, the figures of ~ 13 % and 42 % quoted above for the yields of complex damage following γ-ray and α-particle irradiation respectively will increase to 23 % and 72 % if heat labile sites are included. This compares well with Cunniffe and O'Neill (1999) who determined the contribution of complex DNA ssb in plasmids following γ-ray and α-particle irradiation to be 43 % and 56 % respectively. As further comparison Nikjoo *et al.* (1999) have undertaken simulations of DNA damage including base damage. After 4.5 keV electron and 2.0 MeV α-particle irradiation (of higher LET than was used in the experiments), complex DNA ssb comprise 46 % and 93 % respectively of the total yield of ssb.

As discussed in sections 1.6.2.3 and 2.4.2.2 radiation-induced heat labile sites may be converted into ssb when DNA solutions are treated with heat post-irradiation. Heat labile sites will be present for both sets of samples, independent of the treatment with enzyme. For those samples to which no enzyme was added, the total number of ssbs determined is equal to the number of prompt ssbs plus the number of heat labile sites. For those samples to which enzyme is added, the total number of ssbs corresponds to the number of prompt ssbs + the number of heat labile sites + the number of base damage sites converted to ssbs by the enzyme. Therefore the ratio of gradients for the two dose responses in the absence or presence of enzyme is given by;

$$\frac{\text{enzyme sensitive base damage sites} + (\text{ssb})_{\text{prompt}} + (\text{ssb})_{\text{heat labile}}}{(\text{ssb})_{\text{prompt}} + (\text{ssb})_{\text{heat labile}}}$$

Therefore the ratios quoted as base damage:ssb in fact represents base damage:$((\text{ssb})_{\text{prompt}} + (\text{ssb})_{\text{heat labile}})$. Considering γ-ray irradiation of plasmid DNA in 10 mmol dm^{-3} Tris and treated with Nth, a ratio for the base damage:ssb of 0.84:1 was determined. However, in section 3.2.2 it was shown that the yield of ssb increases by approximately 23 % due to heat labile sites for γ-ray irradiated plasmid DNA incubated

at 37^0 C for 30 min in enzyme buffer. Therefore the ratio of base damage:prompt ssb is approximately 23 % larger, resulting in a ratio of base damage to prompt ssb of 1:1 at 10 mmol dm^{-3} Tris. Ratios for base damage:ssb determined by the addition of Nth over all of the scavenging capacities considered are approximately 23 % lower than the ratio of base damage: prompt ssb if heat labile sites are considered. However, the ratios presented in tables 5.1-5.7 represent the ratio of base damage:ssb (prompt + heat labile) since simple corrections cannot easily be undertaken for all base damage determinations. As discussed in section 1.6.2.3, the yield of heat labile sites is dependent upon the length of time that the samples are exposed to elevated temperatures, with a maximum yield of heat labile ssb occurring at times in excess of 5 h (Jones *et al.*1994a). Hence the length of time for incubation, has a critical role in the yield of heat labile ssbs determined and consequently on the ratio of base damage:ssb. However, there is variability in the incubation time at 37^0 C for the studies using the two enzymes. Nth incubation is undertaken for 30 min, whereas for Fpg it is 1 h. This difference may lead to the ratios for base damage:ssb determined with Fpg being reduced relative to those determined with Nth due to an increased quantity of heat labile sites resulting from longer incubation times. Thus the yields of base damage presented in tables 5.5 and 5.6 should be at least 23 % higher.

5.3.4. Dependence of Base Damage Yields on Scavenging Capacity

From the increased value for the ratio of base damage:ssb with increasing scavenging capacity presented in tables 5.5 and 5.6, it is suggested that electron-induced base damage sites occur more frequently per ssb at higher scavenging capacities especially when using ionic scavengers. Firstly the direct effect becomes relatively more prominent at higher scavenging capacities and therefore a greater proportion of the damage is from electrons produced within the DNA as a result of direct ionisation. Secondly, an additional mechanism for the increased contribution of electrons to the yields of base damage is the electrostatic shielding of the phosphate backbone of DNA as the concentration of Tris increases. The competition for electrons by oxygen and DNA leads to proportionally more electrons reacting with DNA due to electrostatic shielding so that the reactivity of electrons with DNA increases relative to its reactivity with oxygen. Additionally, there are fewer interactions between electrons and OH radicals as the concentration of OH radical scavenger increases due to reduction in the average diffusion distance of OH radicals with increasing scavenging capacities. Tris

reacts preferentially with OH radicals but is unreactive with electrons. Hence the probability of interactions between OH radicals and electrons decreases with increasing Tris concentration. Thus a greater proportion of electrons may be available to react subsequently with DNA. The relative importance of the direct effect and electrostatic shielding in the yields of base damage may be estimated by examining the relative ratios of base damage:ssb determined with ethanol and Tris under equivalent scavenging capacities. As presented in section 5.2.5.1, at an approximate cell mimetic scavenging capacity of $2.9x10^8$ s^{-1} the ratio of base damage:ssb is 1.2:1 with Nth when the scavenging capacity is set by ethanol and 2.0:1 when set by Tris. It is proposed that of the 2 base damage sites per ssb with Tris that 0.8 are due to hydrated electrons that result from electrostatic shielding leading to the difference in the ratios of base damage:ssb between these two scavengers. At low scavenging capacities of Tris, where the direct effect may be considered to be negligible and the majority of damage sites arise from the action of OH radicals, the yields of Nth sensitive base damage sites vary between 0.4-0.8 per ssb. With 0.15 mol dm^{-3} ethanol, 1.2 base damages were recorded per ssb. Therefore, it is estimated that of these 1.2 base damages per ssb that 0.4-0.8 arise from OH radicals, assuming the yield of base damages per ssb per OH radical is independent of the scavenger concentration, and 0.4-0.8 from direct effects. These values lead to an approximate ratio of direct to indirect base damage of 50:50 under cell mimetic conditions. If figure 5.7b is examined, from the simulation of the relative contribution of the direct effect approximately 0.19 mol dm^{-3} Tris i.e. a scavenging capacity of $2.9x10^8$ s^{-1}, the direct effect contributes approximately 45 % of the total yield of ssb, consistent with the above calculations. At a similar scavenging capacity of $1.4x10^8$ s^{-1}, for DNA irradiated under anaerobic conditions in Tris, a ratio of Nth sensitive base damage sites:ssb of 3.2:1 is obtained as shown in table 5.7. As alterations in base recognition do not contribute significantly (see section 5.2.5.2) as a potential explanation for this rise, as previously discussed, it is suggested as due to electrons produced in the solution surrounding the DNA. Therefore, approximately 1.2 additional base damage sites arise from electron interactions with DNA under anaerobic conditions compared with aerobic conditions.

Significant evidence has been presented that the increase in the ratio of base damage:ssb with increasing scavenging capacity is due to the interaction of electrons with DNA to cause base damage under both aerobic and anaerobic conditions. One particularly important area where the role of electrons in causing base damage should

be considered will be within computer simulations of DNA damage. Although presently simulations follow the diffusion of a range of species that are generated following the passage of a radiation track, damage resulting from diffusible radicals is generally considered to be exclusively as a result of the interaction of OH radicals with DNA, both in the induction of strand breaks and base damage sites. If electrons are considered to contribute to the yields of base damage to an extent dependent upon the scavenging capacity, this will become particularly important for simulations of cell mimetic conditions, which are considered to have approximate scavenging capacities of $2.9x10^{-8}$ s^{-1}. In the present study this scavenging capacity results in a ratio of base damage:ssb of 3:1 following γ-ray irradiations compared with only 1:1 to 1.4:1 at low scavenging capacities (see table 5.5). At these low scavenging capacities under aerobic conditions the majority of damage will arise from OH radical interactions. Hence ignoring the contribution of electrons within simulations will have a negligible effect on the simulated yield of base damage at low scavenger capacity. However as the scavenging capacity increases the error of ignoring electron contributions to the formation of base damage is anticipated to become increasingly significant.

In conclusion, it is shown with DNA that the yields of base damage sites per ssb increase with increasing scavenging capacity and that a proportion of base damage sites are produced by interactions with electrons. The scavenging capacity dependence arises from two separate contributions. Firstly, the proportion of damage due to the direct effect increases with increasing scavenging capacity leading to a greater proportion of electrons generated by direct ionisations. Secondly, with the use of an ionic scavenger, such as Tris, increasing the scavenging capacity leads to shielding of the electrostatic repulsion of the phosphate backbone increasing the probability of interactions between DNA and electrons produced by the interaction of radiation with water.

The main experimental finding is that the inclusion of base damage leads to a significant increase in radiation-induced complexity of DNA damage. At cell mimetic scavenging capacities, the yields of complex damage determined from the yields of prompt dsb are only approximately 5 % and 15 % of the yield of ssb following γ-ray and α-particle irradiation respectively. However, if base damage sites are included as revealed by the plasmid assay, the yield of complex lesions rises to 23 % and 72 % respectively relative to the yields of ssb. These represent lower limit estimates of complex lesions due to the nature of the plasmid assay, as discussed above. Therefore,

the influence of base damage on the repairability of DNA lesions produced within cells may be significant. Further, the experimental results indicate that the determination of yields of complex damage by simulations will be significantly underestimated if base damages are not included unless other pathways are artificially increased to compensate.

Table 5.1.

Variation in the ratio of base damage:ssb for ^{60}Co γ-ray irradiation of pUC18 DNA in aerated aqueous solution on scavenging capacity as revealed by treatment with Nth.

Tris Concentration mmol dm^{-3}	Scavenging Capacity $/s^{-1}$	Base Damage:ssb
0.5	$7.5x10^5$	0.43 ± 0.09:1
10.0	$1.5x10^7$	0.84 ± 0.15:1
95.5	$1.4x10^8$	1.52 ± 0.22:1
190.5	$2.9x10^8$	2.00 ± 0.11:1
950.5	$1.4x10^9$	2.76 ± 0.74:1

Table 5.2.

Variation in the ratio of base damage:ssb for ^{238}Pu α-particle irradiation of pUC18 DNA in aerated aqueous solution on scavenging capacity as revealed by treatment with Nth.

Tris Concentration mmol dm^{-3}	Scavenging Capacity $/s^{-1}$	Base Damage:ssb
0.5	$7.5x10^5$	0.77 ±0.21:1
10	$1.5x10^7$	1.33 ±0.16:1
48	$7.2x10^7$	1.72 ± 0.37:1
95.5	$1.4x10^8$	1.72 ± 0.16:1
190.5	$2.9x10^8$	2.32 ±0.34:1

Table 5.3.

Variation in the ratio of base damage:ssb for ^{60}Co γ-ray irradiation of pUC18 DNA in aerated aqueous solution on scavenging capacity as revealed by treatment with Fpg.

Tris Concentration mmol dm^{-3}	Scavenging Capacity /s^{-1}	Base Damage:ssb
0.5	$7.5x10^5$	0.49±0.19:1
10.0	$1.5x10^7$	0.56±0.09:1
190.5	$2.9x10^8$	0.95±0.22:1
950.5	$1.4x10^9$	2.09±0.54:1

Table 5.4.

Variation in the ratio of base damage:ssb for ^{238}Pu α-particle irradiation of pUC18 DNA in aerated aqueous solution on scavenging capacity as revealed by treatment with Fpg.

Tris Concentration mmol dm^{-3}	Scavenging Capacity /s^{-1}	Base Damage:ssb
0.5	$7.5x10^5$	0.31±0.18:1
10.0	$1.5x10^7$	0.80±0.21:1
190.5	$2.9x10^8$	1.53±0.43:1

Table 5.5.

Variation in the ratio of base damage:ssb for ^{60}Co γ-ray irradiation of pUC18 DNA in aerated aqueous solution on scavenging capacity as revealed by the summation of ratios obtained following independent treatments of Nth (table 5.1) and Fpg (table 5.3).

Tris Concentration mmol dm^{-3}	Scavenging Capacity $/s^{-1}$	Base Damage:ssb	bd/Gy/Da
0.5	$7.5x10^{5}$	0.92:1	$2.07x10^{-8}$
10.0	$1.5x10^{7}$	1.40:1	$4.96x10^{-9}$
190.5	$2.9x10^{8}$	2.95:1	$1.68x10^{-9}$
950.5	$1.4x10^{9}$	4.85:1	$1.05x10^{-9}$

Table 5.6.

Variation in the ratio of base damage:ssb for ^{238}Pu α-particle irradiation of pUC18 DNA in aerated aqueous solution with scavenging capacity as revealed by the summation of ratios obtained following independent treatments of Nth (table 5.2) and Fpg (table 5.4).

Tris Concentration mmol dm^{-3}	Scavenging Capacity $/s^{-1}$	Base Damage:ssb	bd/Gy/Da
0.5	$7.5x10^{5}$	1.1:1	$1.2x10^{-9}$
10.0	$1.5x10^{7}$	2.1:1	$8.8x10^{-10}$
190.5	$2.9x10^{8}$	3.9:1	$6.4x10^{-10}$

Table 5.7.

Variation in the ratio of base damage:ssb for ^{60}Co γ-irradiation of pUC18 DNA in aqueous solution at various scavenging capacities under aerobic or anaerobic conditions. The samples were treated with Nth following irradiation.

Tris Concentration mmol dm^{-3}	Scavenging Capacity $/s^{-1}$	Base Damage:ssb	
		Air	N_2
0.5	$7.5x10^5$	0.5±0.2:1	1.5±0.3:1
10.0	$1.5x10^7$	1.0±0.3:1	2.5±0.6:1
95.5	$1.4x10^8$	1.7±0.4:1	3.2±0.6:1

Figure 5.1.

Variation in the dose response for loss of closed circular pUC18 DNA in aqueous solution containing 0.1 mol dm^{-3} Tris irradiated with ^{60}Co γ-ray under aerobic conditions and subsequently treated with or without Nth protein at 37^0 C for 30 min in enzyme buffer.

▲ DNA and buffer only ■ DNA treated with Nth

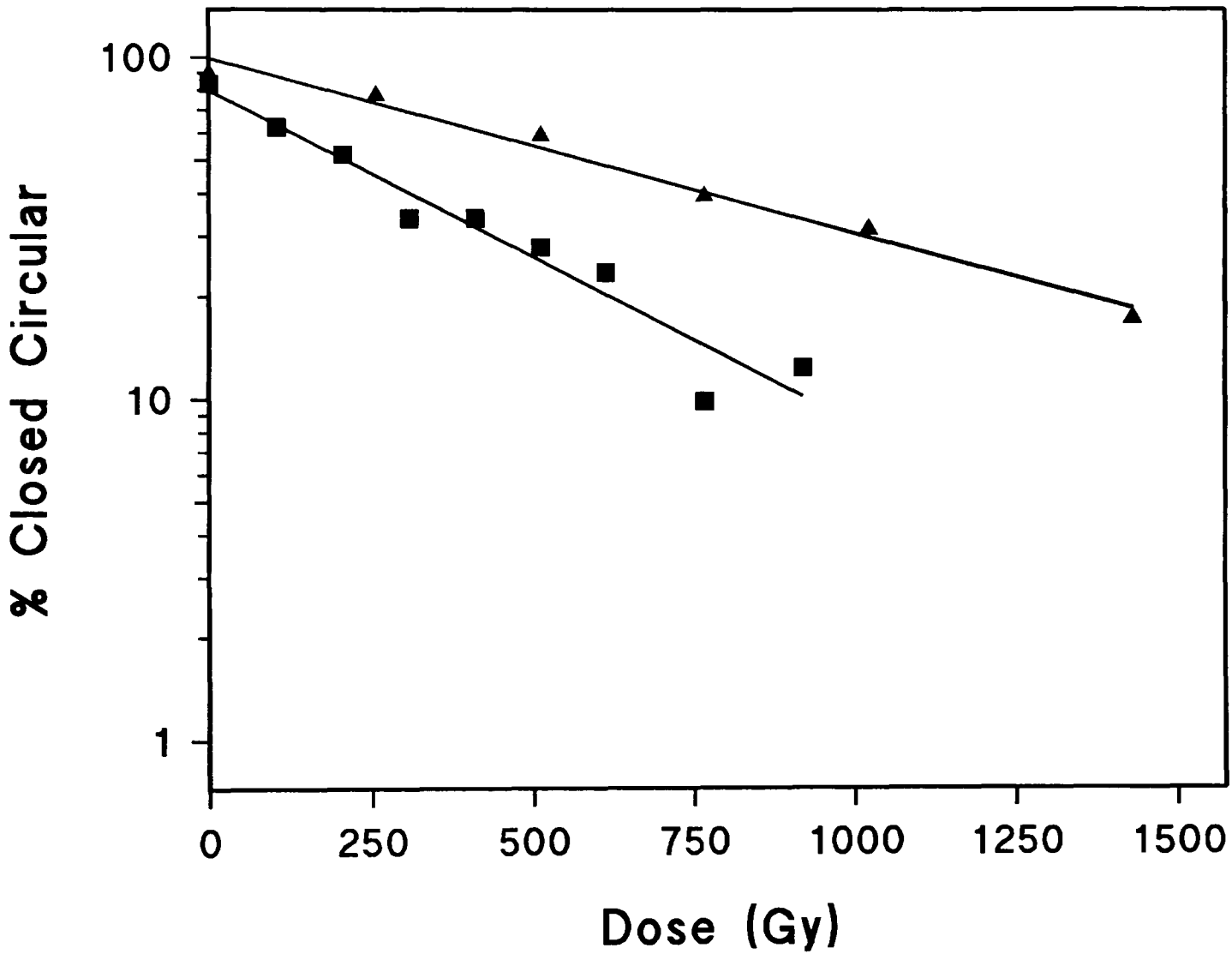

Figure 5.2.

Variation in the ratio of base damage:ssb on scavenging capacity in pUC18 DNA as revealed by Nth following ^{60}Co γ-ray (▲) and ^{238}Pu α-particle (○) irradiation under aerobic conditions.

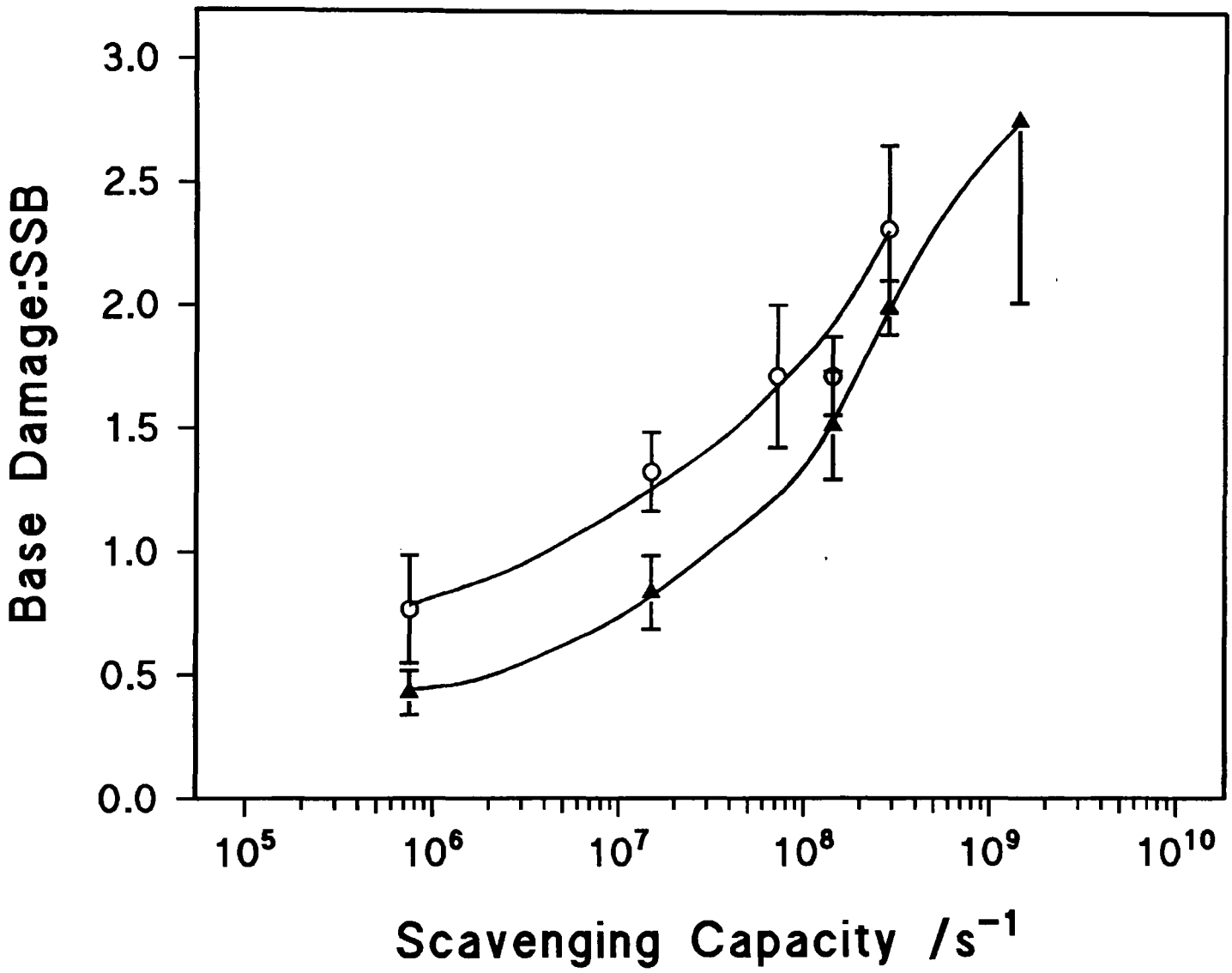

Figure 5.3.

Variation in the ratio of base damage:ssb with scavenging capacity in pUC18 DNA as revealed by Fpg following ^{60}Co γ-ray (▲) and ^{238}Pu α-particle (❍) irradiation under aerobic conditions.

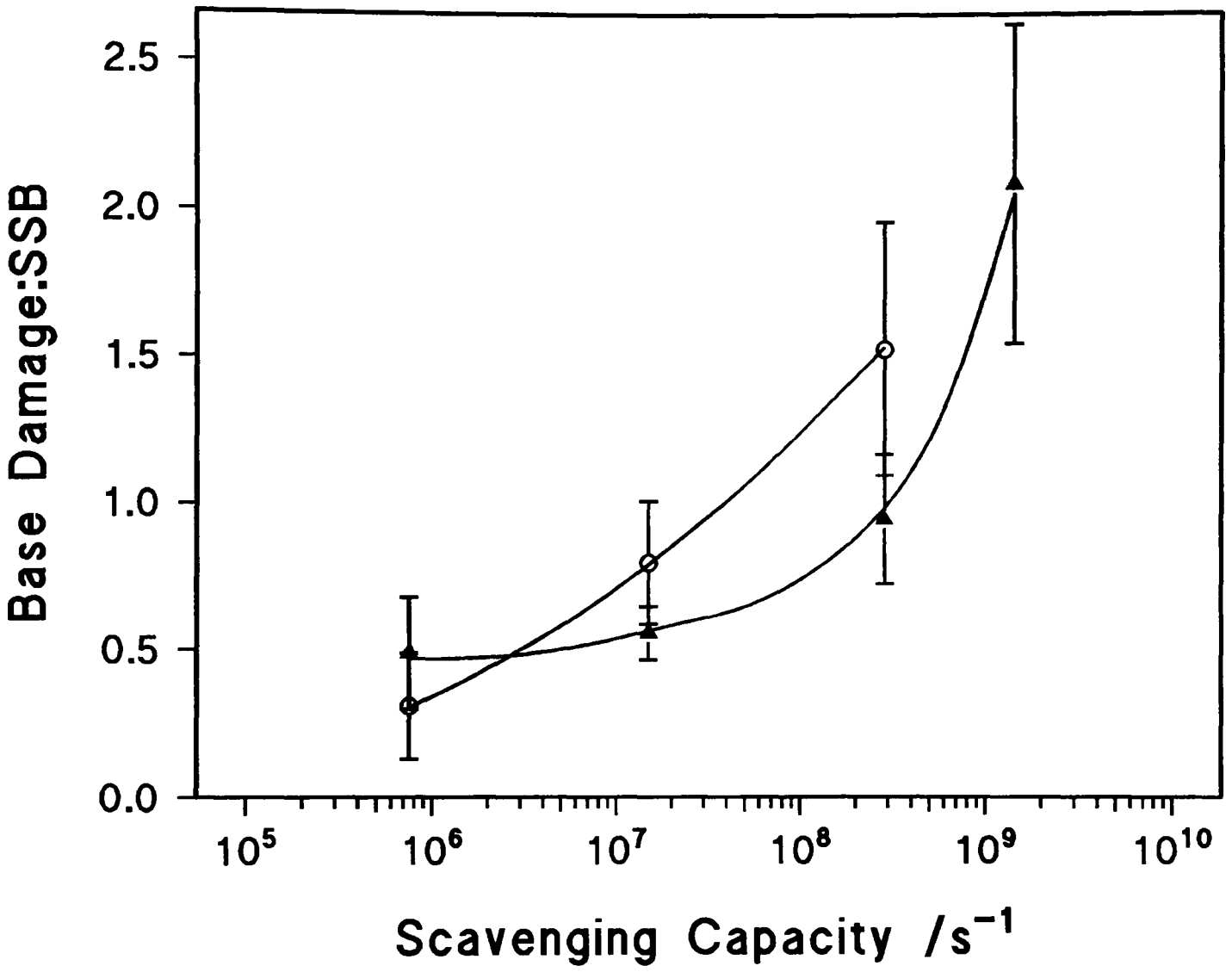

Figure 5.4.

Variation in the relative yield of base damage with scavenging capacity determined following treatment with Nth (○) and Fpg (▲) of pUC18 DNA in aerated aqueous solution irradiated with ^{60}Co γ-rays.

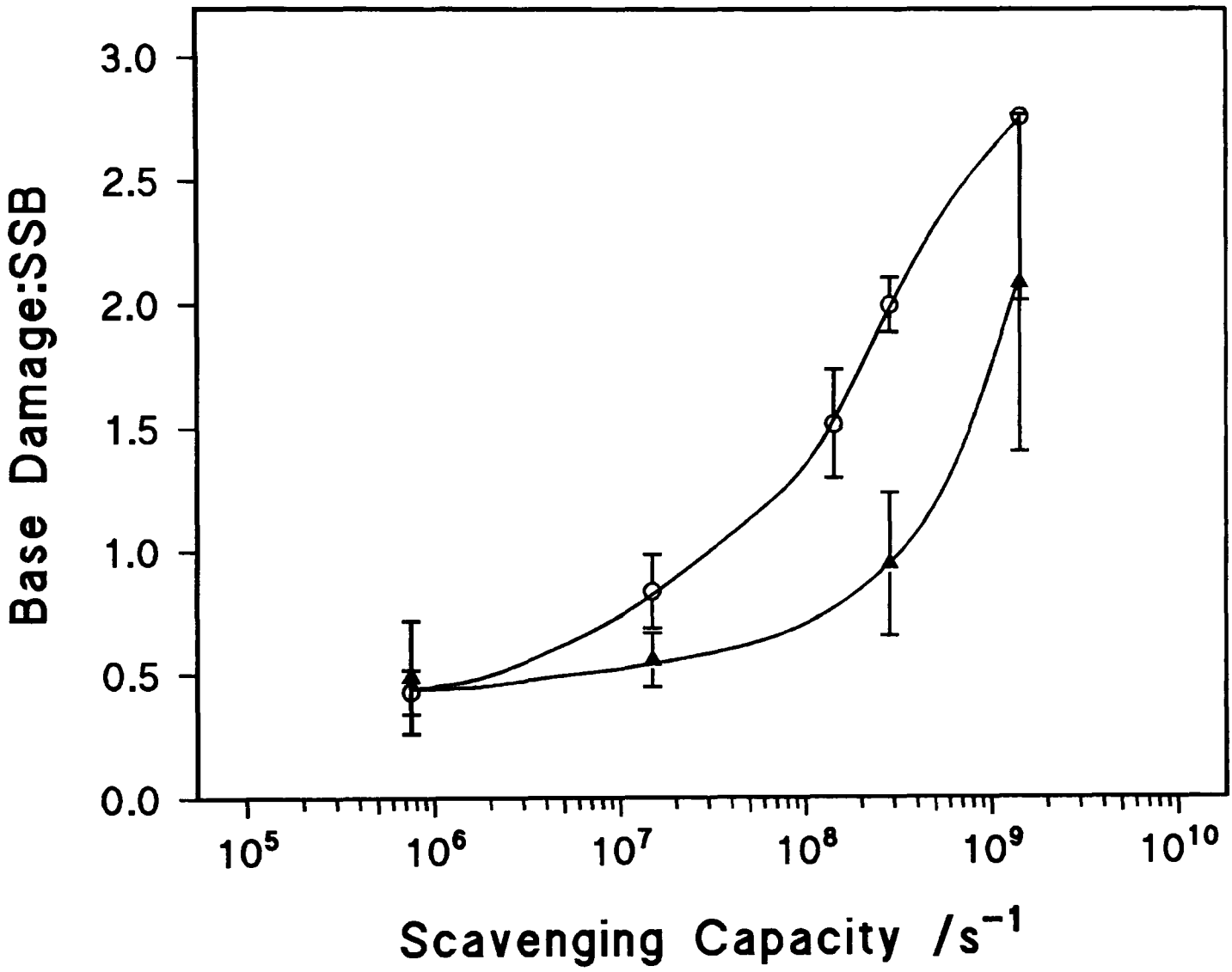

Figure 5.5.

Variation in the yields of base damage on scavenging capacity determined for pUC18 DNA irradiated in aerobic aqueous solution with ^{60}Co γ-ray (▲) and ^{238}Pu α-particle sources (○) and subsequently treated with Nth and Fpg. Note: yields are obtained by the summation of individual yields obtained following independent treatments of Nth and Fpg.

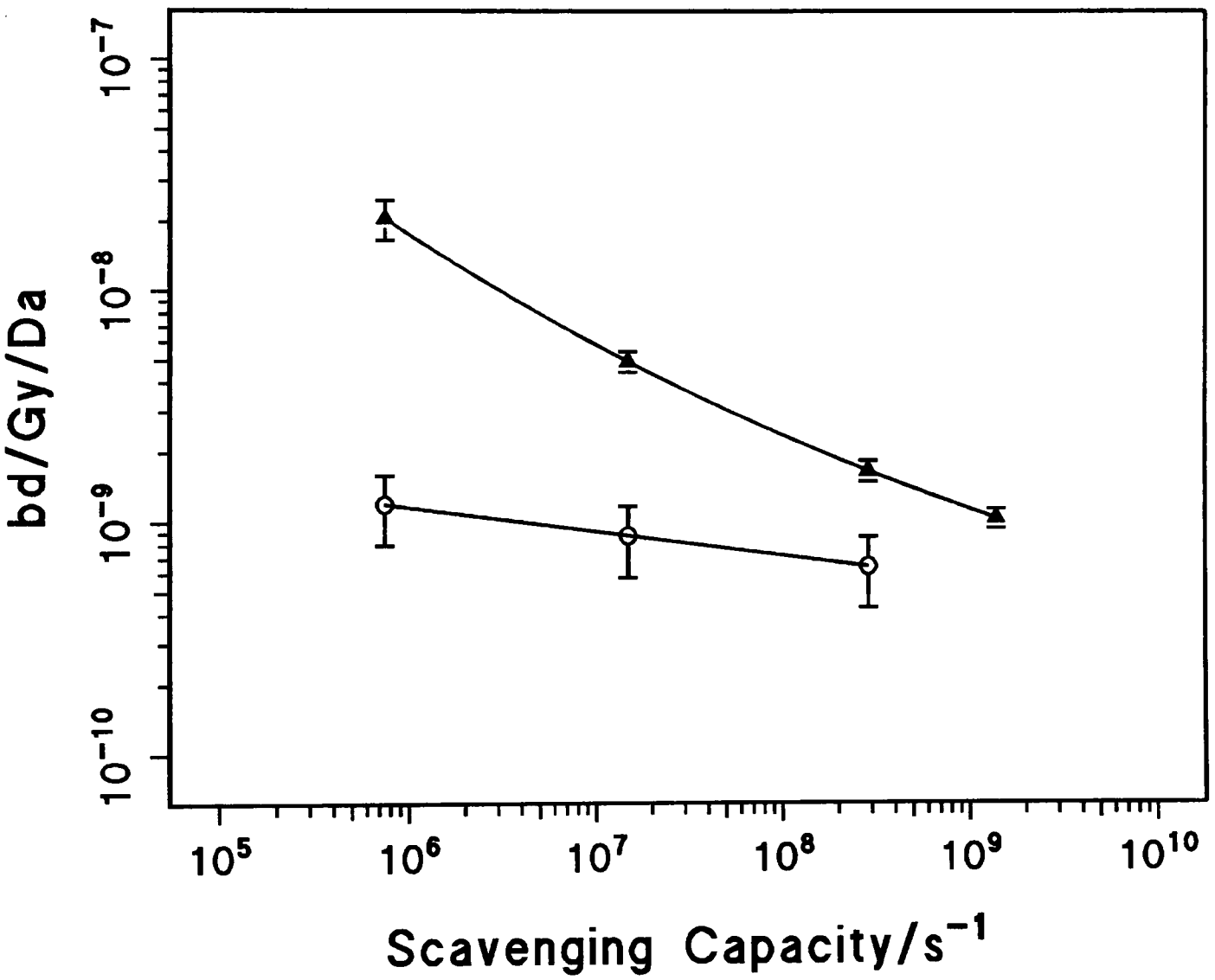

Figure 5.6.

The dose responses for loss of closed circular pUC18 DNA in aqueous solution containing 0.1 mol dm^{-3} Tris irradiated with ^{60}Co γ-ray either under air or N_2. The samples were treated post-irradiation with either enzyme buffer only or enzyme buffer containing Nth.

▼ N_2: DNA treated with buffer only ◆ Air: DNA treated with buffer only ■ Air: DNA treated with Nth ▲ N_2: DNA treated with Nth

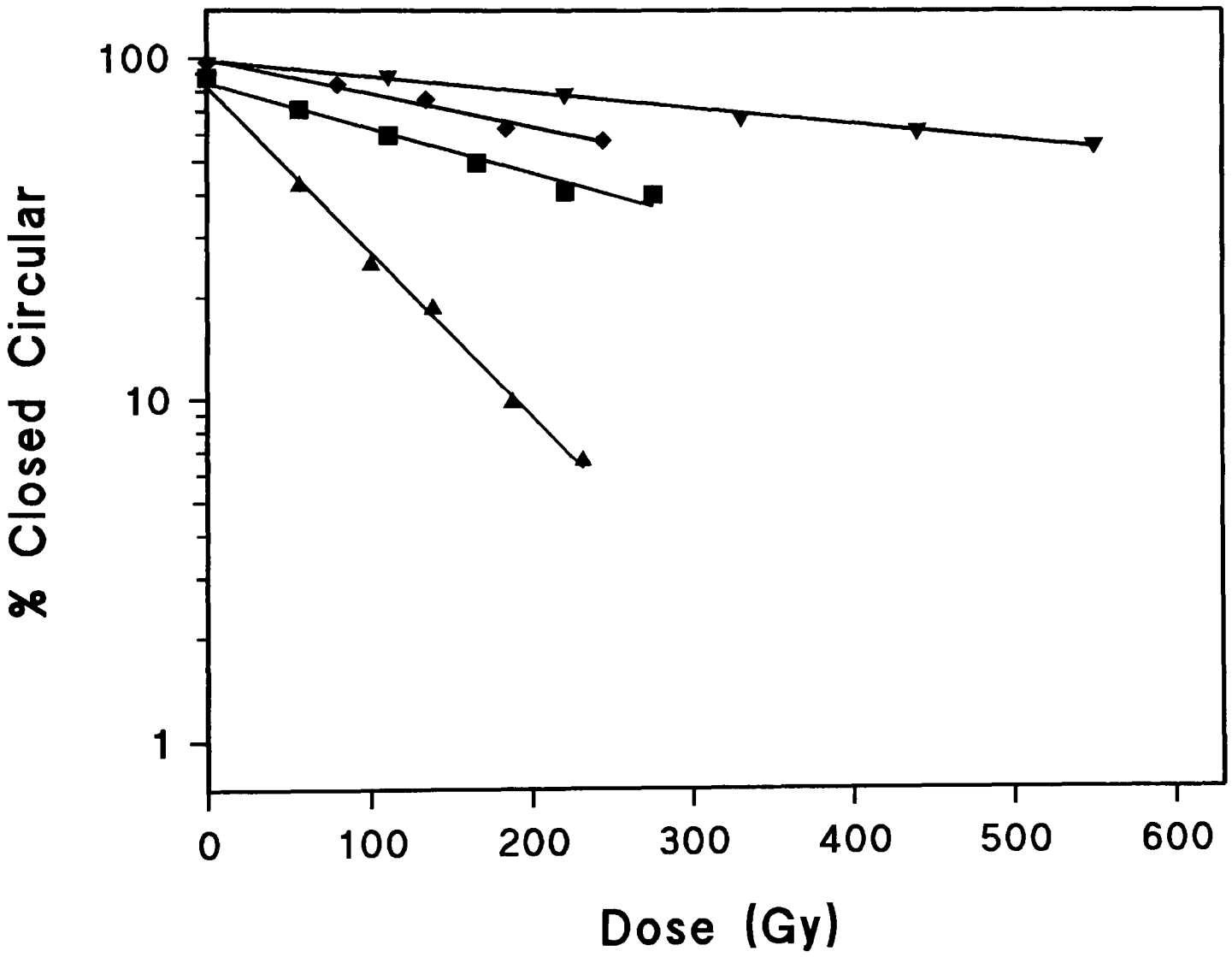

Figure 5.7.

a) Comparison of the shape of response between the ratio of base damage:ssb for ^{60}Co γ-ray irradiated pUC18 DNA in aerated aqueous solution treated with Nth (○) and the contribution of the direct effect calculated from simulations of 1.5 keV electrons (▲) (shown in 5.7b) under variable scavenger concentrations. The two responses are normalised so that the maximum value for the direct effect is set to be equal to the maximum ratio of base damage:ssb and the value of zero for the percentage contribution of the direct effect is set to be equal to the value of zero for the ratio of base damage:ssb.

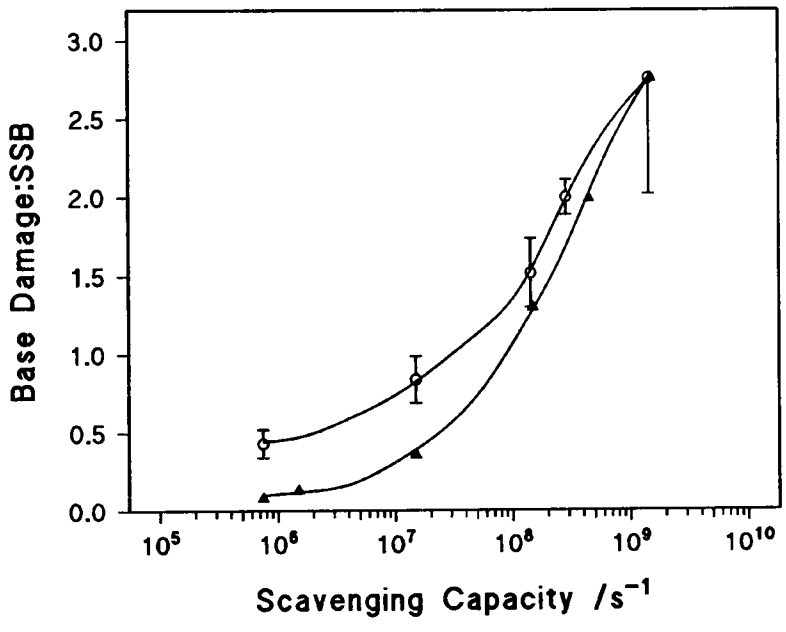

b) The contribution of the direct effect calculated from simulations of 1.5 keV electrons under variable scavenger capacities.

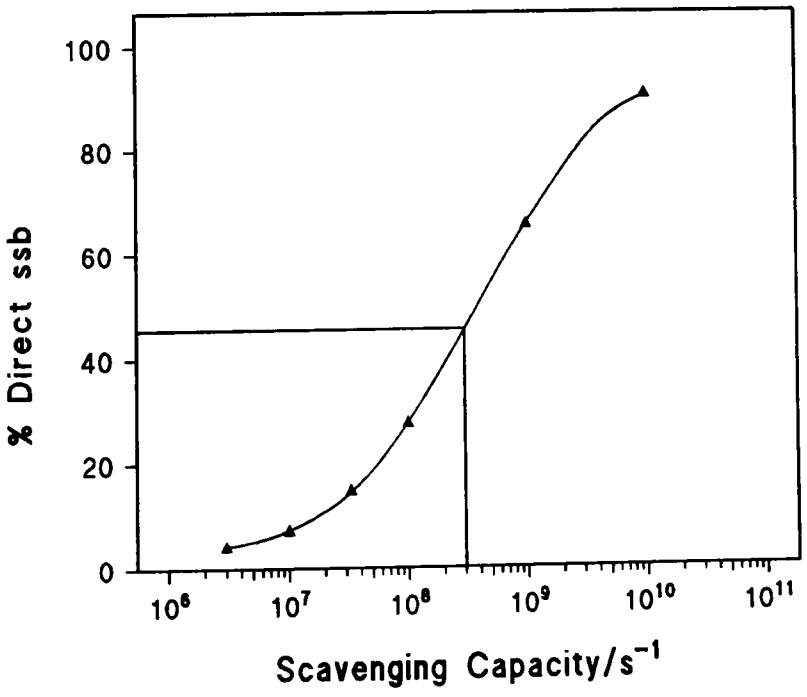

Chapter 6

Experimental Procedures for Obtaining DNA Samples at Variable Humidities

6.1. Introduction

It is very difficult to study the direct effects of radiation in DNA in an aqueous environment since the contribution of diffusible water radicals to DNA damage is significant (see chapter 3). However, the contribution of the direct effect may be assessed by examining the dependence of strand break yields on the humidity around the DNA so that the effects of diffusible radicals are minimised. Section 1.6.1 described how the number of water molecules bound to DNA alters with varying humidity, dictating the effective target size of DNA. The contribution of the direct effect to DNA damage is therefore intrinsically linked to air humidity with alterations subsequently influencing the total contribution of the direct effect and reflecting the dependence of the direct effect on the amount of bound water in the DNA (Ito *et al.* 1993).

6.2. Results

A series of experiments were undertaken to establish suitable conditions for irradiation of closed circular plasmid DNA at different humidities to simulate the action of the direct effect. For measurements of ssb and specifically dsb yields to be determined accurately, it is necessary for the handling procedure, undertaken in order to obtain samples at specified humidities, to result in a minimal amount of damage prior to irradiation. Subsequently, damage levels were assessed under various conditions in order to optimise the procedure (see section 2.6 for details). Initially, the recovery of DNA stock solutions (10 mmol dm^{-3} Tris, 1mmol dm^{-3} EDTA. See section 2.3.1) placed within variable humidity conditions was investigated. DNA solutions were placed onto glass cover slips and placed in a controlled environment for 24 h, sufficiently long to allow the DNA to reach equilibrium (figure 2.3), at room temperature with four different concentrations of NaOH, to set relative humidities of 95 %, 85 %, 70 % and 50 %, before removal from the environment and immediate recovery. The cover slips containing the DNA solutions were placed within a separate area than the NaOH solutions within the controlled environment. Thus, it was ensured that DNA and NaOH did not come into direct contact. The percentages of DNA present

in the closed circular form, determined by analysis and quantification carried out as described in section 2.4.2, are presented in column 1 of table 6.1. As can be seen, there is excessive damage indicated by the loss of closed circular plasmid DNA under all humidities. It is also evident that there is a strong decrease in the amount of closed circular DNA recovered as the relative humidity is decreased. To assess whether this degradation was associated with NaOH rather than merely the relative humidity, an additional sample was equilibrated for the same period of time in an environment containing a saturated solution of NaCl which gives a relative humidity of 75 %. This condition resulted in 26.7 % of the plasmid population remaining in the closed circular form. Therefore the amount of DNA damage is comparable when the humidity was set to 70 % -75 % by the presence of either a saturated solution of NaCl or a suitable NaOH solution. It was subsequently decided to control the humidity by the use of NaOH solutions. The effect on DNA damage levels of removing the sample from the controlled humidity environment after 24 h and leaving it to re-hydrate for 4 h at room temperature and humidity prior to recovery is shown in column 2, table 6.1. No significant effect was observed on the amount of undamaged plasmid DNA recovered by the introduction of this re-hydration period and thus it was not subsequently used.

The effect of dialysing the plasmid from the 10 mmol dm^{-3} Tris, 1mmol dm^{-3} EDTA solution into a number of other buffers on DNA damage levels is summarised in the remaining columns (3-7) of table 6.1. Only dialysing into a solution containing a very high concentration of NaCl (1 mol dm^{-3}) has a significant effect on minimising damage of the plasmid DNA. Employing 1mmol dm^{-3} EDTA (columns 4 and 5, table 6.1) illustrates the repeatability of the experimental procedure. Identical experiments carried out on different days result in significant variations in the amount of closed circular DNA recovered.

The effects of freeze drying the stock DNA solutions for 24 h (10 mmol dm^{-3} Tris, 1mmol dm^{-3} EDTA) on glass slides prior to introduction into the humid environment are shown in table 6.2 for two separate experiments carried out on different days. As previously described, the humidity was established using NaOH solutions and the samples were maintained in the humid environment for 24 h at room temperature prior to recovery and quantification. Comparisons of the results obtained and shown in table 6.2 with those illustrated in column 1 of table 6.1 under equivalent humidities indicate that the initial freeze drying step significantly decreases the amount of damaged plasmid recovered. Variations in the yields of closed circular DNA following

immediate recovery after variable freeze drying periods are presented in column 1 of table 6.3. It is apparent that there is no significant variation in the amount of DNA damage with freeze drying times.

Placing plasmid DNA on glass cover slips results in levels of DNA degradation which are too great to undertake subsequent experiments to determine the yields of DNA damage induced by radiation. Therefore, surface characteristics of the glass slides were examined. The glass cover slip was either treated with different solutions or coated with graphite (see section 2.6). In columns 1-7 of table 6.3, stock DNA (10 mmol dm^{-3} Tris, 1mmol dm^{-3} EDTA) was placed on glass cover slips before freeze drying. Columns 2-5 of table 6.3 illustrate that cleaning the glass cover slip with acetone and/or placing a layer of Tween on the glass surface slightly decreases the amount of DNA damage arising following freeze drying, although the experimental variation is significant as seen when columns 3 and 4 of table 6.3 are compared. When samples which were placed on cleaned surfaces are introduced into the NaOH-controlled humidity environment for 24 h, high yields of DNA damage were obtained. As an alternative to glass cover slips, glass slides were coated with graphite (see section 2.6). The results are shown in columns 8 and 9 of table 6.3. When the plasmid is recovered immediately following freeze drying for 3 h, the plasmid DNA is virtually undamaged relative to untreated DNA. This low level of damage would be acceptable for subsequent irradiation studies, although the humidity was not controlled. However, if a similar sample was then placed within a 70% humidity environment for 24 h, a large amount of damage again arises following recovery of the DNA as shown in column 9 of table 6.3. Therefore, due to the high levels of open circular DNA induced following introduction into the humid environment, irrespective of the variation of a variety of conditions, radiation experiments were not undertaken with DNA samples utilising the techniques described above.

6.3. Discussion

In order to investigate the influence of humidity upon radiation-induced DNA damage it is a pre-requisite that DNA damage induced by the experimental procedure for a specified hydration level (see section 1.6.1) is insignificant. In addition, if damage occurs as part of the procedure it is desirable that it is induced at a consistent level allowing correction of the results. Such DNA damage induction through handling will not significantly effect determination of the yields of radiation induced ssb as the yield

of radiation induced ssb may simply be determined by subtracting the yield of ssb induced in unirradiated controls from the total number of ssbs following irradiation. However non-radiation induced ssb will prevent accurate determination of the yield of radiation-induced dsb due to the possibility of the presence of radiation-induced ssbs being spatially close to handling induced ssbs and giving rise to dsbs. For this reason the experiments undertaken on the role of hydration level on yields of damage have focused on obtaining DNA samples with low and repeatable levels of damage induced as a result of the handling procedures. A number of factors contribute to damage induced in unirradiated DNA within a controlled humidity environment. Starting with a solution of DNA equilibrated within a given humidity (column 1 table 6.1) it is apparent that significant amounts of damage are present, so that any radiation induced dsb breaks would be difficult to quantify. Such a procedure, of placing DNA onto a glass surface and then placing within a controlled humid environment to allow to equilibrate, for obtaining DNA at specified levels of hydration for subsequent radiation experimentation is clearly unsuitable. It is postulated that the DNA damage may result from shearing of the plasmid during the dehydration/rehydration procedures, potentially exacerbated by electrostatic repulsion between the phosphate groups of the DNA. When the level of hydration of the DNA is reduced, the shielding of this repulsion is also reduced leading to the DNA becoming less stable. To try and overcome this, two areas of investigation were undertaken. Firstly, the DNA was not recovered immediately after the sample was removed from the humidity controlled environment. Instead it was left to rehydrate, potentially stabilising the structure, making it less prone to damage when recovered. Secondly the plasmid was dialysed into several other buffers with varying concentrations of salt. It is thought that the presence of salts within the buffer may stabilise the DNA structure by shielding the electrostatic repulsion associated with the phosphate groups, again potentially reducing the amount of recovery induced damage. Leaving the DNA prior to rehydration does not lead to a significant reduction in the amount of DNA damage (column 2, table 6.1). With different buffers it can be seen that, with one exception, there is little variation in the level of damage. Only dialysis of the DNA into solutions containing a high concentration of NaCl (1 mol dm^{-3}) has a significant effect in reducing the quantity of damage. However the level of damage is still unacceptable for subsequent radiation experiments. Further, such a high salt concentration may lead to alterations in the conformation of the DNA, which could lead to changes in radiation sensitivity

(Balasubramanian *et al.* 1998, Milano and Bernhard 1999). Generally all of the various changes in salt concentration and rehydration times shown in table 6.1 lead to significant levels of DNA damage and as such are therefore unacceptable for radiation sensitivity studies at various humidities.

In an attempt to overcome the problem of high levels of damage, an alternative approach of freeze drying the samples before equilibrating in a controlled humidity environment was examined. It may be seen in table 6.2 that freeze drying significantly increases the amount of undamaged plasmid compared with the various conditions reported in table 6.1. However, damage levels are still unacceptably high for radiation experiments. The decrease in damage levels following freeze drying is thought to be due to a decreased binding between the DNA and the glass surface subsequently leading to less shearing when recovery is attempted. Cleaning the surface with detergent to minimise surface adhesion had little effect on the amount of damage induced. The least amount of damage was obtained with a graphite surface where 97 % of the plasmid is recovered immediately following freeze drying, indicative of insignificant damage induction in the DNA. These levels of damage would be acceptable for subsequent radiation experiments. However, if a sample is then equilibrated at a humidity of 70 %, a large amount of damage is induced following recovery (column 9 table 6.3).

That 97 % recovery is achieved for a graphite surface indicates that damage was not predominantly produced by the freeze drying procedure or subsequent recovery of the DNA. Therefore it is suggested that the DNA damage is induced during the time in the controlled humidity procedure. It is concluded that either the use of NaOH to control humidity or the extended time (24 h) required for the plasmid to equilibrate fully at room temperature, is responsible. Since a saturated NaCl solution used to control the humidity produces equivalent amounts of damage to that when NaOH is used, it is inferred that the hydrating solution does not contribute significantly to the amount of DNA damage. The time of 24 h was chosen since measurements of calf thymus DNA indicated that at least 15 h was required for the DNA to reach an equilibrium level of hydration (see figure 2.3 and section 2.6). That a period of at least 24 h is required for DNA to reach equilibrium under different levels of hydration is supported by studies on radiation-induced base damage as a function of hydration (Swarts *et al.* 1992) where long equilibration periods were required prior to irradiation.

A number of other groups have examined dry DNA and the damage induced following irradiation. Folkard *et al.* (1999), have undertaken irradiations of dry DNA in which DNA in solution is placed onto a glass cover slip and then cooled to approximately – 12^0 C and freeze-dried for about 40 min at 10^{-5} mbar. Samples were subsequently stored under dry nitrogen before being irradiated and then recovered with TE buffer. Michael *et al.* (1994) and Folkard *et al.* (1993) placed DNA in an EDTA solution onto a polycarbonate filter or gold disk, which was then placed in a vacuum in the irradiation chamber for subsequent exposure to radiation. Control samples (Michael *et al.* 1994) which were not exposed to radiation showed 10-20 % lower levels of closed circular DNA than the stock (> 90 % in the closed circular form) after re-exposure to atmospheric pressure and recovered with TE. Such levels of damage associated with handling are consistent with the current findings using freeze drying and add further support to the equilibration of DNA samples at a given humidity being a crucial step in inducing DNA damage. It is essential to minimise even further non-radiation induced DNA damage before radiation experiments may subsequently be undertaken.

Table 6.1.

Variations in percentage of pUC18 DNA recovered in the closed circular form following recovery of samples placed in humid environments for 24 h at 20^0 C with varying buffers, recovery techniques and hydration. Variations in DNA hydration are achieved by altering the relative humidity of the environment through changes in the concentration of NaOH solutions present.

Relative Humidity	10 mmol dm^{-3} Tris, 1 mmol dm^{-3} EDTA. Recover Immediately (1)	10 mmol dm^{-3} Tris, 1 mmol dm^{-3} EDTA. Rehydrate for 4 h prior to recovery (2)	1 mmol dm^{-3} Tris, 1 mmol dm^{-3} EDTA. Recover Immediately (3)	1 mmol dm^{-3} EDTA. Recover Immediately (4)	1 mmol dm^{-3} EDTA. Recover Immediately (5)	1 mmol dm^{-3} Phosphate Buffer. Recover Immediately (6)	1 mol dm^{-3} NaCl, 10 mmol dm^{-3} Tris, 1 mmol dm^{-3} EDTA. Recover Immediately (7)
95%	57.6	55.8	46.9	37.5	49.1	61.1	82.9
85%	48.6	51.7	25.4	33.2	49	49.1	78.4
70%	33.4	36.7	15.7	16.1	31.5	36.4	74.2
50%	11.0	10.7	0.0	0.0	7.1	10.5	49.6

Table 6.2.

Variation in percentage of closed circular DNA recovered following freeze drying for 24 h and placed in variably humid environment for 24 h at 20^0 C.

Humidity	10 mmol dm^{-3} Tris, 1 mmol dm^{-3} EDTA, DNA Solution. Recover Immediately. Day 1	10 mmol dm^{-3} Tris, 1 mmol dm^{-3} EDTA, DNA Solution. Recover Immediately. Day 2
100%	81.7	90.1
95%	74.4	88.5
85%	72.2	86.8
70%	59.1	76.2

Table 6.3. Variations in percentage of pUC18 DNA present in 10 mmol dm^{-3} Tris, 1mmol dm^{-3} EDTA buffer recovered in the closed circular form following changes in humidity, sample surface and freeze drying time.

Length of time for freeze drying	(No Humidity control)	Slide cleaning (No humidity control)		Slide cleaning (No humidity control)		70 % humidity for 24 h		Freeze dried on graphite	
		No Cleaning	Acetone	Acetone	Acetone +Tween	Acetone	Acetone + Tween	No Humidity control	70% humidity for 24 h
	(1)	(2)	(3)	(4)	(5)	(6)	(7)	(8)	(9)
7 min	74%								
45 min	76%								
1.5 h	75%								
2 h				94% (mean)	94% (mean)				
3 h	66%	77% (mean)	79% (mean)			~75% (mean)	~75% (mean)	97%	70%
6 h	72%								

Chapter 7

The Dependence of OH Radical Yield in Aqueous Solution on the Energy of Incoming Photon Irradiation

7.1. Introduction

The variation in DNA strand break yields with radiation quality described in chapter 3 emphasises the importance of the ionisation density of the radiation track and the extent to which intra-track radical-radical recombination and the amount of DNA damage that arises depends upon the radiation quality. The study was extended by determining experimentally how the variation in ultra-soft X-ray (USX) photon energy influences the density of radicals that are generated in water and potentially go on to initiate DNA damage, and in particular clustered DNA damage. In effect, the yield of OH radicals which escape intra-track radical-radical interactions in water to become homogeneously distributed, has been utilised as an indicator of the ionisation density of the low energy secondary electron tracks produced following USX photon absorption in water (see section 1.5). A number of studies have been undertaken to model the radiation chemistry of water, following the time dependent yields of primary radicals (Magee and Chatterjee 1978, Yamaguchi 1989, Pimblott 1992, LaVerne and Pimblott 1993a and b, Hill and Smith 1994, Pimblott and Green 1995, Pimblott and LaVerne 1997, 1998, Moiseenko *et al.* 1998a). The majority of these models have focused on γ-rays, hard X-rays and high-energy electrons. From theoretical investigations of the dependence of radical yields on the photon energy of the radiation, it has been postulated that the yield of OH radicals, generated from radiation tracks in water and which escape intra-track recombination events to become homogeneously distributed, is dependent upon the energy of the radiation (Magee and Chatterjee 1978, Yamaguchi 1989, Hieda *et al.* 1994, Hill and Smith 1994, Watanabe *et al.* 1995, Fulford *et al.* 1999).

From simulations and pulse radiolysis studies, the majority of intra-track radical-radical interactions, in water, occur at times $<10^{-6}$ s after which the remaining radicals may be regarded as homogeneously distributed (Jonah *et al.* 1973, 1976, Pimblott and LaVerne 1997, 1998). The relationship between the scavenging capacity of a solution and the average lifetime of OH radicals is discussed in section 1.5. If the scavenging capacity is

sufficiently low then the average OH radical lifetime will be $>10^6$ s and the radicals may be considered to be homogeneously distributed.

The aim here was to determine experimentally the dependence of the yield of OH radicals that escape intra-track recombination events in water on the photon energy of the incident radiation. From a modelling standpoint, this information provides experimental benchmarks against which track simulations may be compared and hence leads to subsequent refinement of these models. From a biological point of view, the importance of ionisation density associated with specific radiation energies can be assessed by the relative yields of damage.

7.2. Principles of the Method

The objective of determining OH radical yields in water at times when they have become homogeneously distributed ($>10^{-6}$ s, see figure 1.6) is achieved by effectively using plasmid DNA within an aqueous solution containing a given concentration of a OH radical scavenger. Tris was used as the OH radical scavenger and is present as a probe to sample the number of OH radicals present at 10^{-6}s. The concentration of the OH radical scavenger (Tris) used sets the lifetime of the OH radicals by knowing the reaction rate constant for the reaction of OH radicals with Tris (Buxton *et al.* 1988). Thus a scavenging concentration is selected so that the lifetime of OH radicals is 10^{-6} s, sufficiently high to ensure that the majority of homogeneously distributed radicals interact with either the scavenger or DNA in a fixed proportion and the OH radicals are not removed as a consequence of radical-radical interactions involving homogeneously distributed radicals, including the OH radical (Jonah and Miller 1977, Pimblott and Green 1995, Pimblott and LaVerne 1997, 1998). Plasmid DNA reacts competitively with Tris for OH radicals (Milligan *et al.* 1996a) to give rise to readily detectable single strand breaks (ssb) the yield of which is subsequently determined. Therefore only those OH radicals formed within a radiation track and which subsequently escape intra-track radical-radical recombinations induce DNA ssb and are effectively measured. Consequently the yield of ssb within the DNA probe is proportional to the yield of OH radical species escaping radical-radical intra-track recombination events, a reflection of the ionisation density of the track. Two assumptions are inherent if such an interpretation of ssb data is to be inferred. Firstly, that the probability of OH radicals interacting with DNA in competition with a fixed scavenger concentration is

independent of the photon energy. Secondly, it is assumed that the primary yield of radicals produced per unit dose is independent of photon energy.

An aqueous solution containing plasmid DNA and Tris at a concentration of 0.66 mmol dm^{-3} (pH 7.0) is obtained by dilution of DNA stock in a scavenging solution as described in sections 2.3.1 and 2.3.2 with the exception that the DNA solution containing 0.66 mmol dm^{-3} Tris was obtained by diluting 3.3 μl of the DNA stock which contains 10 mmol dm^{-3} Tris with 46.7 μl of triple distilled water resulting in a final DNA concentration of 33 ng/μl, equivalent to a base pair concentration of 51μmol dm^{-3}. The same procedure for obtaining DNA solutions for irradiation was used irrespective of the irradiation vessel.

Sample treatment, radiation sources and dosimetry are described in section 2.2. Radiation sources used were the ^{60}Co γ-ray source, the Siemens Stabilipan and Todd Research X-ray sets and the USX sources producing characteristics X-rays for C_K, Cu_L, Al_K and Ti_K. ^{60}Co γ-ray irradiations of the aerated DNA solutions were carried out at 4^0 C in non-arm glass tubes whereas for all other irradiations, the solutions were placed in Hostaphan based dishes. Post irradiation treatment was as described in (2.4.2) with samples being maintained at 4^0 C throughout to minimise the contribution of heat labile sites.

7.3. Results

The dependence of the loss of closed circular plasmid on radiation dose is shown in figure 7.1 for irradiation of the plasmid DNA solution containing 0.66 mmol dm^{-3} Tris with ^{60}Co γ radiation, 50 kV (constant potential) diagnostic X-rays and Al_K USX. At this concentration of Tris equivalent to a scavenging capacity of 10^6 s^{-1}, the majority of OH radicals present are homogeneously distributed. As with strand break analysis (Chapter 3, figure 3.1), the amount of undamaged plasmid decreases exponentially with dose for each radiation. The yields of ssb induced, calculated from the slope of the dose responses, are dependent upon the energy of the radiation. For example, the yield of ssb is greater for ^{60}Co γ-rays than Al_K USX based upon these slopes. The yields of ssb/Gy/Da calculated from the dose dependences for radiations of different photo-energies are shown in table 7.1 together with the respective photon energies. The dependence of the yields of ssb/Gy/Da on photon energy is shown in figure 7.2a. The dependence of the yield of homogeneously distributed OH radicals on photon energy is

illustrated in figure 7.2b. The yields of ssb/Gy/Da have been converted into yields of homogeneous OH radicals by normalising the yield of ssbs for a given radiation relative to the yield for ^{60}Co γ-ray and taking G (OH) = 0.29 μmol J^{-1} for ^{60}Co γ radiation at 10^{-6} s (Buxton *et al.* 1988). The yield of OH radicals increases with increasing photon energy for values of E > 1keV. Below 1keV the yield of OH radicals increases with decreasing photon energy. For comparison, from the least square fit analysis of the yields of ssb for ^{60}Co γ-ray and α-particle irradiation described in chapter 3, the yield of OH radicals calculated for α-particles at 10^{-6} s^{-1} is 0.015 μmol J^{-1}.

Since the attenuation of X-rays through the sample becomes increasingly large at lower energies (see tables 2.1 and 2.2) it was important to assess whether the changes in G (OH) determined with varying photon energy reflect attenuation. An accurate determination of the sample thickness was obtained by confocal microscopy prior to irradiation as described in section 2.3.4. From this analysis, it was also apparent that the DNA is distributed evenly throughout the solution and that there is no accumulation on the Hostaphan base of the irradiation dishes, the CR-39 or the dish-wall surfaces. However, consideration must also be given to maintaining a constant sample thickness throughout the course of the experiment. Any evaporation during the course of the irradiation leads to variation in attenuation of the dose and subsequently a discrepancy between actual and assumed doses. The confocal analysis revealed that over extended periods of time (> 1 h) evaporation becomes significant in a certain proportion of the samples. The use of a cooled samples and dishes, droplets placed on top of the CR-39 disc and lids placed on top of the dishes minimises evaporation. However those samples where evaporation remains significant are characterised by the reduction in size of the droplets placed on top of the CR-39 discs and can subsequently be rejected from analysis. The minimisation of evaporation rate is essential with the Cu_L and C_K USX as long irradiation times were required due to their low dose rates of 0.25 and 0.5 Gy min^{-1} respectively. Due to the low number of ssb/Gy/Da with Cu_L USX, long irradiation times were also required to give measurable breakage yields. Since the mass attenuation coefficients for Cu_L and C_K USX are similar in water (See table 2.1), the difference in ssb/Gy/Da yields illustrated in table 7.1 between these two energies is indicative of a difference in OH radical yield rather than a response resulting merely from variations in attenuation factors. This supports the conclusion that any problems

associated with sample thickness and the subsequent attenuation of USX sources has been controlled, although they remain the largest source of error.

Further examination of figure 7.2b illustrates that the dependence of OH radical yield on photon energy passes through a minimum at ~1-2 keV. The experimental data have subsequently been compared with that obtained from simulations. Figure 7.3 illustrates comparisons between these experimentally determined yields of OH radicals and those obtained from various theoretical simulations. In all cases there is partial agreement between the simulated and experimentally determined dependences although there are some variations in responses (see discussion).

7.4. Discussion

From simulations, it is apparent that low linear energy transfer (LET) radiation i.e. γ-rays, X-rays and high-energy electrons produce low energy, secondary electrons, which contribute approximately 30% of the absorbed dose (Nikjoo and Goodhead 1991) as a result of the subsequent interactions of the primary incident electrons or, in the case of photon irradiation, of the Compton and photoelectric electrons (section 1.3.1). These low energy electrons may be represented by characteristic ultra-soft X-rays (USX) which interact almost exclusively via the photoelectric effect producing isolated tracks of single or paired electrons with small well defined energies (in water > 99% of these X-ray interactions are with oxygen). Carbon K X-rays produce a single photo-electron since they can ionise only the outer shell of oxygen, while for other X-ray energies an Auger-electron usually accompanies the photo-electron after oxygen K-shell ionisation, as indicated in table 2.1. The majority of studies employing USX have highlighted these low energy secondary electrons to be the predominant contributor to biologically complex DNA damage (Goodhead and Thacker 1977, Kobayashi *et al.* 1987, Goodhead and Nikjoo 1989, 1990, Botchway *et al.* 1997, Nikjoo *et al.* 1997). An increase in ionisation density is generally considered to give rise to an increased proportion and complexity of DNA damage which is less susceptible to cellular repair processes than damage produced by more sparsely distributed ionisations (Blöcher 1988, Prise *et al.* 1989, 1994, Jenner *et al.* 1993, Hodgkins *et al.* 1996a and b, Botchway *et al.* 1997).

The main finding of the present study is that the experimentally determined yields of ssb are dependent upon the photon energy of the radiations used. As the photon energy

is reduced there is a decrease in the number of ssb/Gy/Da to a minimum value at 1-2 keV below which further decreases in photon energy result in an increased number of ssb/Gy/Da. The scavenging capacity of 0.66 mmol dm^{-3} Tris corresponds to a reaction time of 1μs, sufficiently long for OH radicals to become homogeneously distributed (Jonah *et al.* 1973, 1976, Pimblott and LaVerne 1997, 1998). The plasmid is also at a low concentration and thus both Tris and DNA are at concentrations insufficient to influence intra-track, radical-radical interactions but sufficiently high to interact with the majority of homogeneous OH radicals in competition with their loss by inter-track radical-radical interactions at the dose rates used. Since the plasmid is at a low concentration, it should be noted that an absolute measure of the number of radicals present is not obtained but the number of radicals is sampled for comparison between different radiation energies. From simulations with electrons of energy > 1keV, the initial yield of ionisation and excitations is independent of the electron energy (Pimblott and LaVerne 1997, 1998). Therefore, observed differences in the yields of ssb on photon energy do not arise from differences in initial OH radical yields but reflect differences in the number of OH radicals that become homogeneously distributed. Thus the number of ssb induced in plasmid DNA is proportional to the number of OH radicals escaping intra-track events and becoming homogeneously distributed. Differences in the homogeneously distributed yield of OH radicals are dependent upon the photon energy of the radiation and are therefore a reflection of the relative spatial distributions of the species that are formed within the radiation track.

When these results are compared with those obtained experimentally from Fricke dosimetric methods (≥ 2 keV) (Freyer *et al.* 1989, Watanabe *et al.* 1995, Yamaguchi 1997) and from theoretical calculations (Magee and Chatterjee 1978, Yamaguchi 1989, Hill and Smith 1994) there is partial agreement. However, with Fricke dosimetry, the yield of Fe^{3+} it determined from the interaction of Fe^{2+} with H atoms and OH radicals and the molecular product, H_2O_2. Therefore, the yield of OH radicals is not directly determined using the Fricke system. The reaction with H_2O_2 potentially compensates for any reduction in the yield of OH radicals as a result of intra-track recombination events. In figure 7.3 the experimental dependence of OH radical yields on photon energy (table 7.1) is compared with various theoretical simulations for electrons or photons of different energy. The calculation of Magee and Chatterjee (1978) (figure 7.3a) for monoenergetic electrons and Yamaguchi (1989) (figure 7.3c) for

monoenergetic photons both used a prescribed diffusion model. In these simulations, tracks are broken up into a finite number of track entities in which diffusion controlled reaction kinetics is described using a set of simultaneous differential equations which represent the concentration and diffusion constant for each species and the rates of reaction between each of the species. These simulations were then essentially fitted to the limited high-energy electron and photon experimental data. The Monte Carlo electron simulations of Hill and Smith (1994) (figure 7.3b) and Terrissol and Beaudré (1990) and personal communication from H.Nikjoo (figure 7.3d) followed the evolution of events, from the initial interactions, production of chemically reactive species and their subsequent diffusion controlled reactions. The Monte Carlo method allows the stochastic nature of the radiation tracks to be followed.

In the case of the Magee and Chatterjee model (1978) the general shape of the response is similar to that obtained experimentally but the actual response is shifted towards lower energies, with the minimum OH radical yield occurring at 0.5 keV compared with the experimental value at ~1.5 keV. In comparison, the Hill and Smith model (1994) gives a minimum at approximately 1 keV with the depth similar to that determined experimentally. In addition, the subsequent rise in OH radical yields at the lower energies is less steep than that found experimentally. The model of Terrissol and Beaudré (1990) predicts a similar value of energy for the minimum OH yield to the experiment value, although, with the exception at lower energies, there is a greater OH yield throughout the energy range examined than determined experimentally. In the Yamaguchi (1989) model a minimum occurs at a similar value to the Magee and Chatterjee (1978) model at around 0.5 keV. Over the entire energy range, the simulated OH radical yield (Yamaguchi 1989) shows less of a dependence upon energy than the dependences determined either experimentally or by the other three models (Magee and Chatterjee 1978, Terrissol and Beaudré 1990, Hill and Smith 1994) examined. Some differences in the yields of OH radicals between photons and electrons of a given energy are to be expected since the photon interaction results in two electrons (photo and Auger) of lower energies produced from the same atom. In the case of two electrons in addition to their higher individual ionisation densities there may be some overlap of the respective tracks. This will give rise to a greater number of radical-radical interactions between radicals formed within the individual tracks and between the two respective electron tracks and consequently an expected decrease in the homogeneously distributed yield of OH radicals at 10^{-6} sec (see section 4.2.1)

The decrease in the number of OH radicals escaping intra-track radical-radical interactions in the energy range of the photons from 1.25 MeV to 1.5 keV is a good indication of an increase in ionisation density of the track with decreasing energy. In biological systems when the track overlays the DNA such increases in ionisation density with decreasing energy of incident radiation would be expected to lead to a corresponding increase in complexity of DNA damage, resulting from local clustering of ionisations on the scale of DNA and its immediate surroundings (Nikjoo *et al.* 1997). Indeed, this increase in track ionisation density leading to more complex DNA damage is supported by experimental findings of an increase in the number of DNA dsb for V79 cells irradiated with USX of different energy (Botchway *et al.* 1997, de Lara *et al.* unpublished data) which represent the simplest measurable form of complex damage within cells, with decreasing photon energy of the radiation. When the data of de Lara *et al.* (unpublished) are extended to lower energies such as C_K USX the yield of dsb are slightly greater than that induced by Cu_L USX indicating a continued increase in ionisation density of the radiation. The upturn in the OH radical yields at these lower energies may be explained in terms of the total number of radicals that are formed within the radiation track. In section 1.5 (figure 1.6) it was discussed how the probability of intra-track radical-radical recombination events depends upon not only the ionisation density of the track but also the total number of radicals that are generated. Approximately 4-5 ionisations are produced per 100 eV so that C_K produces 12-13 ionisations and Cu_L produces a total of 40-50 ionisations. The solid angle around any one radical within which diffusion results in a possible interaction with another radical becomes progressively smaller as the total number of radicals generated decreases. As photon energy decreases a point is reached where the increased probability of intra-track radical-radical events due to the decrease in distance between sites of radical formation is offset by the decreased angle through which diffusion results in a possible interaction. From the experimental data this turning point is at approximately 1-2 keV. At lower energies the decrease in the total number of radicals formed becomes the dominant factor in determining the probability of radical-radical events. Subsequently at energies such as that associated with C_K USX, the OH radical yield increases relative to that for photons of higher energies such as Al_K USX.

Table 7.1.

Variation in the yield of single strand breaks produced in pUC18 DNA at 4^0 C with incident photon energy in an aqueous solution containing 0.66 mmol dm^{-3} Tris.

	Energy	Single Strand Break Yield/ Gy/Da	Yield of OH Radicals[1] μmol J^{-1}
Gamma ^{60}Co	1.25 MeV average	$18.80x10^{-9}$	0.290
Titanium X-ray K-shell emission	4.55 keV	$5.81x10^{-9}$	0.090
Aluminium X-ray K-shell emission	1.49 keV	$4.66x10^{-9}$	0.072
Copper X-ray L-shell emission	0.96 keV	$5.3x10^{-9}$	0.082
Carbon X-ray K-shell emission	0.28 keV	$16.66x10^{-9}$	0.257
Siemens Stabilipan 1 X-ray set	250 kV (constant potential) 90 keV average	$15.31x10^{-9}$	0.236
TODD Research machine Machlett X-ray set	50 kV (constant potential) 23keV average	$13.03x10^{-9}$	0.201

$$\frac{^1G(OH)_{radiation}}{G(OH)_{Co\text{-}60\ \gamma\text{-}rays}} = \frac{(ssb/Gy/Da)_{radiation}}{(ssb/Gy/Da)_{Co\text{-}60\ \gamma\text{-}rays}}$$

Figure 7.1.

The dose dependence for the loss of closed circular plasmid determined for photons of varying incident energy. Irradiations were undertaken in an aqueous solution containing pUC18 (33ng/μl) and 0.66 mmol dm^{-3} Tris at 4^0 C.

▼ Al_K USX ■ Diagnostic 50 kV (constant potential) X-ray ▲ ^{60}Co γ-ray

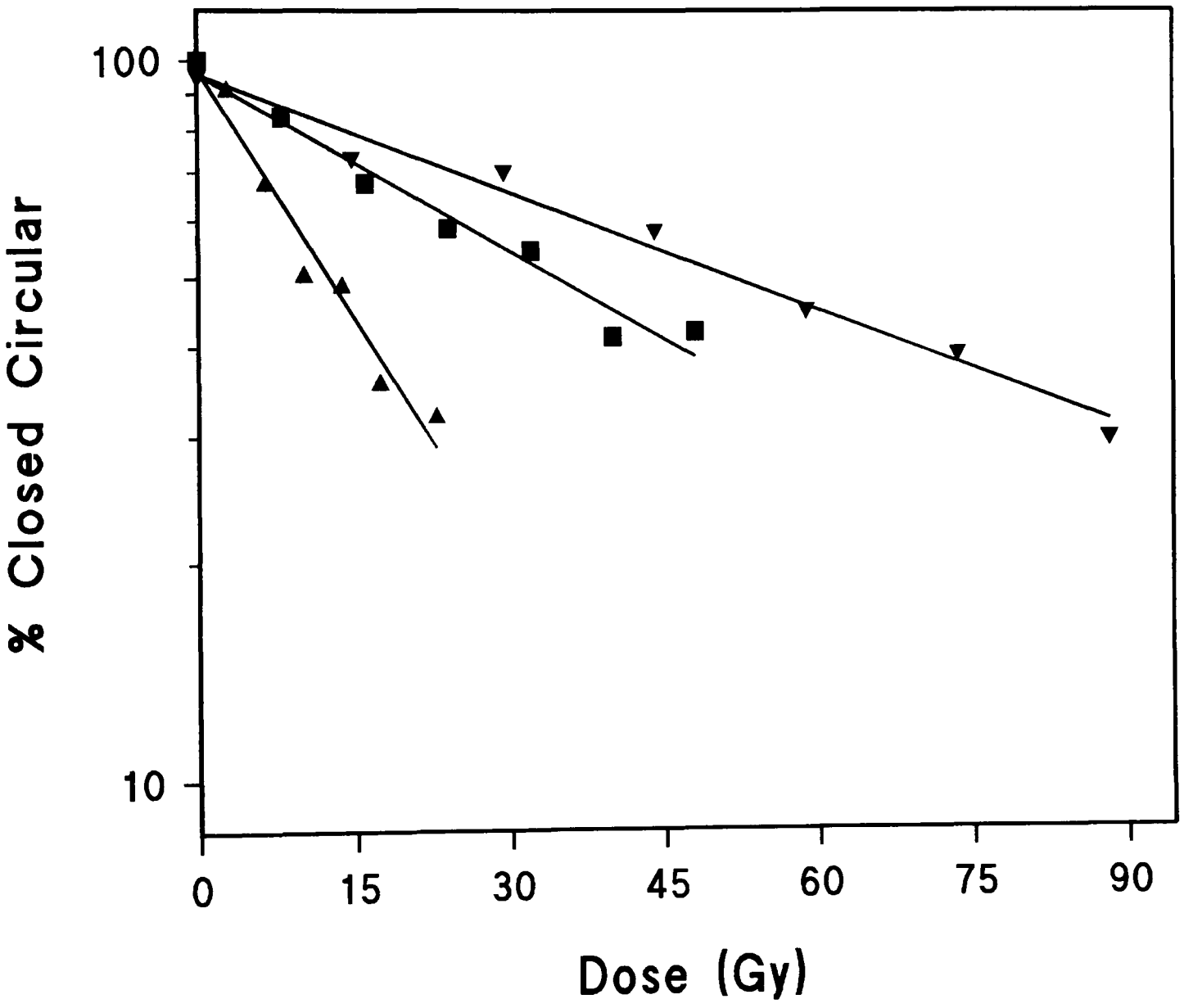

Figure 7.2.

Experimental dependence on incident photon energy determined in pUC18 DNA of a) yield of single strand breaks b) yield of OH radicals (see text for determination). Irradiations were undertaken in an aqueous solution containing DNA (33ng/μl) and 0.66 mmol dm^{-3} Tris at 4^0 C.

● C_K USX ○ Cu_L USX ▼ Al_K USX ■ Ti_K USX

❐ TODD Research X-ray set ◆ Siemens X-ray set ▲ ^{60}Co γ-ray

a)

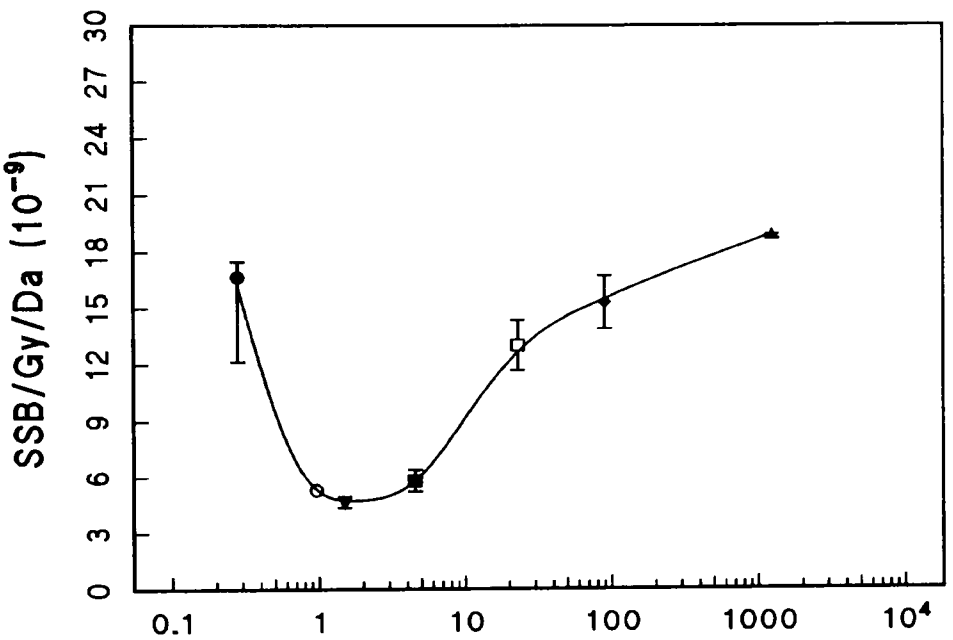

b)

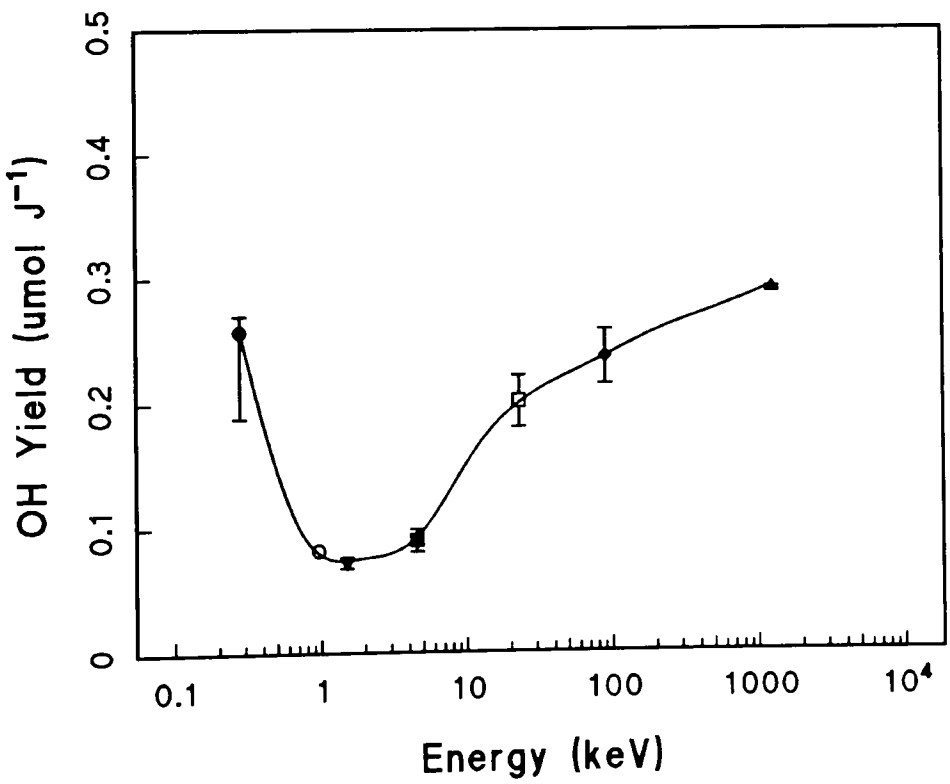

Figure 7.3.

Comparison between the dependence on photon energy of the experimentally determined yields of OH radicals (See table 7.1) and the simulated yields of OH radicals determined by (a) Magee and Chatterjee 1978, (b) Hill and Smith 1994, (c) Yamaguchi 1989, (d) Terrissol and Beaudré (1990) and personal communication from H.Nikjoo. a), b) and d) simulate the passage of mono-energetic electrons whereas c) simulates mono-energetic photons.

● C_K USX ○ Cu_L USX ▼ Al_K USX ■ Ti_K USX

❒ TODD Research X-ray set ◆ Siemens X-ray set ▲ ^{60}Co γ-ray

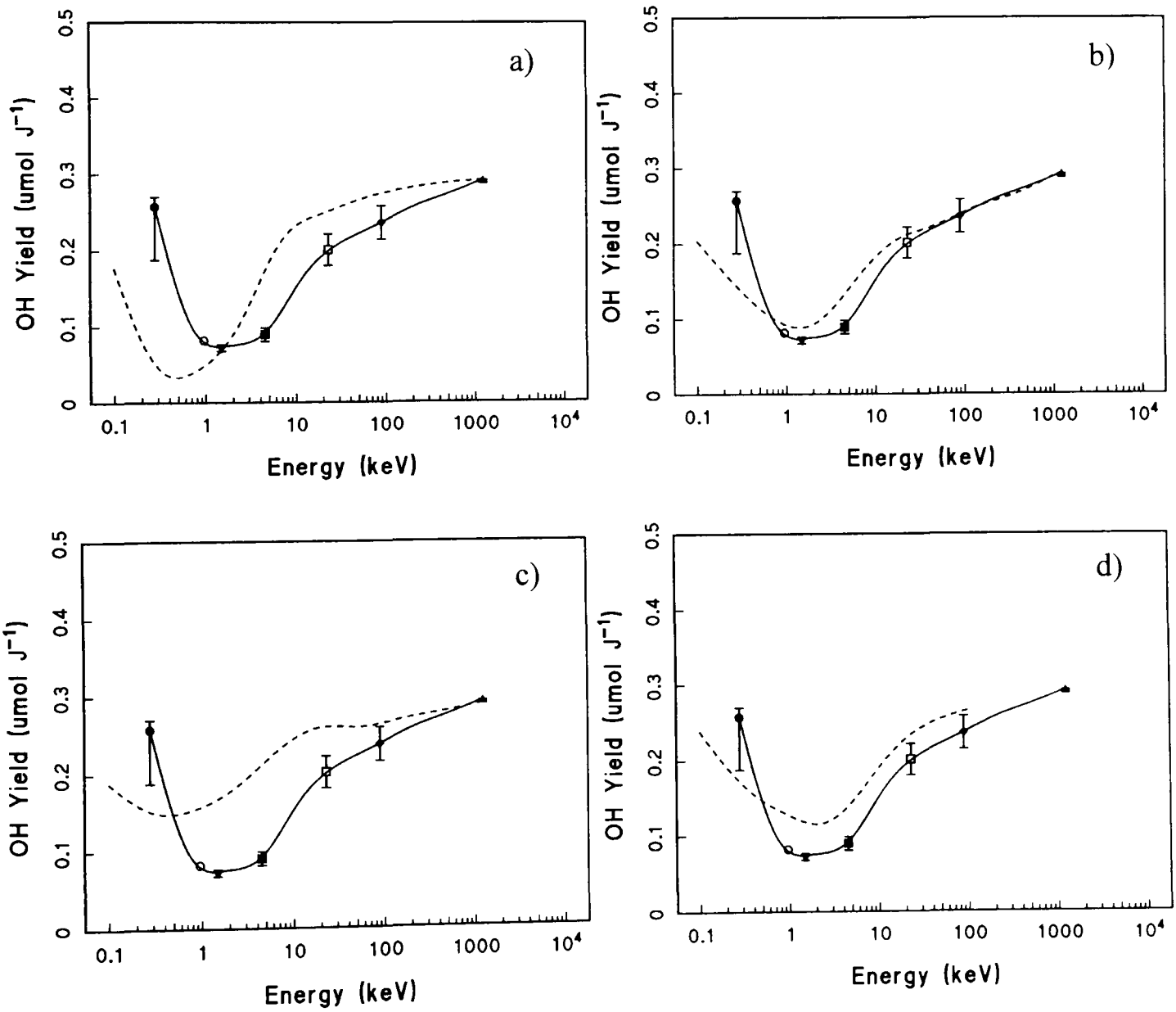

Chapter 8

Conclusions

8.1. Discussion

The importance of ionising radiation in giving rise to complex DNA damage has been hypothesised in a large number of studies, within both computer simulations (Goodhead *et al.* 1980, 1981, 1985, Ward 1985, Goodhead 1989, 1992, Goodhead and Nikjoo 1989, 1990, Charlton *et al.* 1989, Brenner and Ward 1992, Michalik 1992, Nikjoo *et al.* 1997, 1998, 1999,) and experimentally. Experimental studies have provided indirect evidence for the biological significance of clustered DNA damage as indicated by the relative repairability of strand breaks (Jenner *et al* 1993, Prise *et al.* 1994, Cunniffe and O'Neill 1999) and from studies to assess enzyme activity within clustered damage sites (Chaudhry and Weinfeld 1995, Harrison *et al.* 1998, David-Cordonnier *et al.* 2000). The present study has contributed information pertaining to both of these fields. The role of the energy and ionisation density of radiation has been assessed experimentally by determining the spectrum of DNA damage associated with changes in the relative amount of indirect and direct damage through modifying the scavenging capacity and thus the DNA environment. The use of a plasmid system for the determination of experimental yields of damage has proved an excellent tool, as such a system allows variables to be altered precisely and independently in order to assess their relative importance. In addition, because of the underlying simplicity of the system, consisting as it does of naked DNA within an aqueous solution, it provides an excellent system for comparisons with yields of damage from computer simulations which have now been undertaken. Simulations do not consider the effects of such factors as repair or radiation attenuation, which might be present within a multi-compartmental cellular system.

From an experimental point of view, damage determinations have focused on yields of both simple isolated DNA damage and of more complex forms of DNA damage. The former has been achieved by determining the yields of isolated ssb and base damage. The latter by determining the yields of dsb, which represent the simplest form of complex damage, and of base damage sites which are sufficiently spatially close to either one another or to a ssb to form a dsb when the base damages are converted into

ssb via the action of base excision enzymes. From the perspective of assessing the role of both the energy and ionisation density of radiation in determining the type and quantity of radiation damage, the determination of the yields of both simple and complex damage provides pertinent information.

8.1.1. Scavenging Capacity and the Mean OH Radical Diffusion Distance

When plasmid DNA is irradiated in aqueous solution, the yield of radiation-induced isolated ssbs and base damage sites and more complex dsb are dependent upon the scavenging capacity of the solution. As the scavenging capacity increases, there is a corresponding decrease in the role of the indirect effect resulting from the reduction in the mean diffusion distance of OH radicals leading to a decrease in the yields of ssb, base damage and dsb. Subsequently, a greater proportion of damage arises from either the direct effect or OH radicals produced from a radiation track lying very closely to the DNA. This shift in damage mechanisms results in an increased proportion of damage sites lying in close vicinity to one another leading to an increase in complex damage relative to more isolated damages. Such an alteration in damage type is reflected in the decrease in the ratio of ssb:dsb, effectively representing the ratio of isolated damage:complex damage, as the scavenging capacity increases i.e. the proportion of complex damage increases with increasing scavenging capacity.

8.1.2. Ionisation Density

Two aspects of the current study illustrate the importance of ionisation density of the radiation track in determining the types and yields of damage and the dependence of the yield of OH radicals on radiation energy. One involved irradiating plasmid DNA with different radiations and determining the yield of strand breaks under variable scavenging capacities, in order to establish the yield of damage attributable to the indirect effect. The other has been undertaken with plasmid DNA irradiated with photons of various energies at a constant low scavenging capacity, effectively resulting in all damage being attributed to the indirect effect.

From the determination of the yield of ssb at low scavenging capacities it is established that the yield of OH radicals which escape intra-track radical-radical reactions decreases with decreasing photon energy, reflecting an increased ionisation density of the resulting low-energy secondary electron track generated. However, for photon energies < 1.5 keV, the yield of ssb increases due to a decreased proportion of OH

radicals involved in intra-track radical-radical recombination since a smaller number of radicals are actually produced. It is anticipated that with such low energy radiations, although there is an increase in ionisation density, a point will eventually be reached where both the frequency and degree of complexity of complex damage yields also decreases due to very few ionisations occurring per track.

The role of ionisation density over a range of scavenging capacities irradiations was examined with γ-ray, Al_K USX and α-particles. The yields of isolated ssbs generated within the plasmid DNA is dependent upon the reciprocal of the ionising density, decreasing significantly with increasing ionisation density. An increase in ionisation density effectively results in the average distance between ionisations within the radiation track decreasing, so that fewer OH radicals escape from the radiation track. At low scavenging capacities the relatively small amount of radical-radical recombination associated with low LET radiation leads to a large yield of ssb compared with that for higher LET radiation. However, this type of damage is of an isolated nature and has been shown to be rapidly repaired within the cellular environment (see review Friedberg *et al.* 1995). Of potentially more biologically significance is the increased yields of complex damage with increasing ionisation density estimated from the determination of the yields of dsb, taken to be representative of complex damage.

From experimentally determined values of the ratio of ssb:dsb, the relative prevalence of simple and complex damage is strongly dependent upon ionisation density. In addition the ratio of ssb:dsb shows less of a dependence on scavenging capacity with increased ionisation density, as an increased prevalence of spatially close damage sites associated with high density ionisation tracks leads to a shift from isolated ssb to the potentially biologically more significant complex damage.

8.1.3. Simulations

Although the plasmid experimental system is invaluable for generating strand break yields for comparison with computer simulations, it is difficult to divide complex damage into sub-categories determined by the degree of complexity for experimental data. This is particularly important, as with the majority of experimental studies the only types of complex damage determined are dsb. However, a range of investigations has indicated that dsbs themselves do not appear to represent a specifically significant form of biological damage (Prise *et al.* 1987, Goodhead and Nikjoo 1989, Nikjoo *et al.*

1991, Fox and Prise 1992, Jenner *et al.* 1992). However, what may be more significant are dsb that have additional spatially close damage sites. Simulations provide an excellent method for examining both the types of complex damage arising and also the source of their generation (direct or by OH radical), as the exact location of each event associated with a radiation track is known and its position relative to DNA obtained. In addition, simulated yields of damage allow a direct comparison to be made with the yields of damage obtained experimentally to assess the validity and robustness of the simulations.

With simulations of α-particle and 1.5 keV electron tracks the proportion of damage attributable to the direct effect and also the proportion of dsb that are classified as complex increases with increasing scavenging capacity. As scavenging capacity increases for both track simulations the importance of the direct effect increases in line with the decreased diffusion distance of OH radicals, in a manner analogous to the experimental dependences. As the proportion of damage attributable to the direct effect increases the proportion of dsbs classified as complex increases reflecting a shift in damage mechanisms from single isolated events, characteristic of spatially distant OH radicals, to clustering of damage sites, associated with the direct effect and from OH radicals produced close to the DNA. The contribution to damage from the direct effect and the proportion of dsb classified as complex is significantly less with 1.5 keV electrons than α-particles. Under cell mimetic conditions the proportion of dsb classified as complex is approximately 30 and 65 % for the Al_K USX and α-particle simulations respectively.

A 1.5 keV Al_K USX typically interacts with matter to give rise to two electrons, with the most common combination being one of 0.96 keV and one of 0.52 keV leading to conjecture as to whether it is applicable to simulate a Al_K USX track with a single 1.5 keV electron or whether it would be more appropriate to do so with two lower energy electrons which are generated with the same initial position in space. Comparisons of the two simulation techniques reveal an approximate 10 % decrease in the yields of ssb and a 20 % increase in the yields of dsb when two track simulations are compared with single track simulations. In addition the proportion of dsb classified as complex increased by approximately 15 % following two track simulations.

Comparisons of results obtained experimentally and from simulations reveal good agreement over a range of scavenging capacities for yields of ssb and dsb for Al_K USX

irradiation and for the yields of ssb for α-particle irradiation. Such an agreement increases the confidence in the assumptions inherent within the simulations (e.g. percentage likelihood of an OH radical giving rise to a ssb and maximum distance between ssb on opposite strands which result in a dsb) and that the yields of complex damage obtained from the simulations are a reasonable representation of what is taking place within experimental systems. However, there is some disparity between the yields of dsb obtained experimentally for α-particle irradiation and from simulation and possible reasons have been discussed.

8.1.4. Base Damage

Although computer simulations can at present provide information on the spectrum of the yields of strand breaks they generally, as in the current study, do not include the contribution of base damage when determining the yields of total and complex damage. One of the principal reasons for the absence of base damage from simulations is due to the minimal amount of experimental data available on the yields of base damage at different scavenging capacities. The yields of base damage, determined within the current study using enzymes which convert base damage into ssb are dependent upon conditions i.e. scavenging capacity and the type of radiation. It is the extent of this variability and its dependence on various parameters that must be determined experimentally if base damage sites are to be introduced into simulations.

At low scavenging capacities, the majority of base damage sites are produced by isolated OH radicals as for ssb. However as the scavenging capacity approaches values more characteristic of the cellular environment, base damage sites are, to an increasing extent, generated by the direct effect and OH radicals produced in close vicinity to the DNA resulting in a greater likelihood of base damage sites being spatially close to other lesions. In addition at these higher scavenging capacities a greater proportion of base damage sites are generated by the reaction of electrons with DNA.

The contribution of electrons to the yields of base damage sites has a strong scavenging capacity dependence due to two independent mechanisms. Firstly, an increased proportion of the total damage arises from the direct effect as scavenging capacity increases, so that a greater proportion of electrons are produced directly within, and react with, the DNA. Secondly, if the scavenging capacity is set with an ionic scavenger, then electrons produced indirectly close to the DNA have an increased

ability to interact with the DNA, since the electrostatic repulsion of the phosphate backbone is reduced by the presence of the ionic scavenger. At scavenging capacities representative of those found within the cellular environment the ratio of base damage:ssb is approximately 3:1 and 4:1 compared with only 1:1 and 1:1 at low scavenging capacities for γ-ray and α-particle irradiation respectively.

The number of ssb that have an additional base damage site in close vicinity have been determined. The yield of DNA ssb damage sites which are complex following enzyme treatment, i.e. have an additional damage site in close vicinity is 23 % and 72 % following γ-ray and α-particle irradiation respectively. The yield of complex damage therefore which is not apparent as dsb is significant. In addition non-dsb complex damage may also be biologically significant. Indeed, evidence is becoming available that such damage may compromise repair.

8.2. Future Work

Determinations of the yields of ssb and dsb have revealed the importance of including the contribution of heat labile sites. This is particularly important when the yields of dsb are to be determined due to the relatively low yield of dsb compared with those for ssb and thus the greater sensitivity to changes in yields induced by small numbers of additional heat labile sites. An area which subsequently requires further investigation is a more accurate determination of the yield of heat labile sites. It would be of particularly usefulness when base damage sites and their role in complexity are to be considered. Because base damage sites are determined via the use of enzymes which require incubation at temperatures of 37^0 C, heat labile sites are readily induced. However incubation takes place for a variable period of time and hence for an accurate determination of the contribution of heat labile sites an accurate time course for their induction is required.

The accurate determination of base damage sites is a very important area if the total yields of complex damage are to be determined both experimentally and within simulations. However, if base damages are to be simulated, alterations may have to be made to current simulations to accommodate the variability in the mechanisms of base damage formation. Due to experimental evidence supporting the potential importance of electron reactions with DNA in the formation of base damage it will be necessary to include the diffusion and interactions of electrons within simulations in a manner

analogous to that undertaken for OH radicals. However, for OH interactions, variations in the yields of damage due to differences in scavenging capacity can readily be simulated by adjusting the mean OH radical diffusion distance accordingly. This is not so readily undertaken with the electron contribution to base damage, as although the mean electron diffusion distance will have a scavenging capacity dependence there will be an additional factor to consider. The potential for electrons produced in solution to interact with the DNA is dependent upon the probability of overcoming the electrostatic repulsion associated with the phosphate backbone of the DNA. Therefore the importance of the electron contribution to base damage will be variable depending upon the ionic strength of the scavenger. If accurate simulations are to be undertaken they must incorporate a variable probability of electron-DNA reactions for electrons produced in solution that is dependent upon the scavenging capacity. Therefore if simulations of yields of base damage are to be obtained for the cellular environment a determination of the ionic strength of the solution surrounding the cellular DNA is required to determine to what extent the repulsive phosphate electrostatic field is overcome. It is apparent however that if true values for the complexity of DNA damage are to be obtained then it is a requisite that base damage is included. This is apparent from the very large change in complex damage obtained experimentally once the contribution of base damage is included. Hence for accurate determinations of the yields of complex damage within simulations it is a requirement that the yields of base damage are included and all mechanisms for their generation are fully integrated. For the accurate incorporation of base damage into simulations however further experimental benchmarks are required. In particular the determination of base damage yields in cells using the same enzymatic approaches as have been employed within the plasmid system are necessary.

The characteristics of the DNA model structure employed within the simulations will also influence the yields and spectrum of damage obtained. Currently volumes are assigned to sugar phosphate and bases. However, an atomistic model of DNA may also be considered. Although a volume model of DNA may be adequate for high-energy electron irradiation an atomistic model may be more appropriate for α-particle radiation with its corresponding greater density of ionisation events. Employing such a model would not influence OH radical interactions but may change the distribution of direct events and the distances between damage sites. In addition present DNA models

typically include a number of water molecules to represent the first hydration shell of the DNA with the assumption that $H_20^{\cdot+}$ resulting from interactions with the bound water layer is transferred to the DNA (La Vere *et al.* 1996). To assess the validity of including only the first hydration shell and assuming complete radical transfer from this shell, experimental benchmarks are required. Thus, further work to assess the variation in the direct effect with different DNA hydration levels, potentially by varying the relative humidity as previously discussed, is required.

References

- G.E.Adams and R.L.Wilson, Pulse radiolysis of the oxidation of organic radicals in aqueous solution. Trans. Faraday Soc. **65**, 1981-1987 (1969a).
- G.E.Adams and R.L.Wilson, Pulse radiolysis studies on the oxidation of organic radicals in aqueous solution. Trans. Faraday Soc. **65**, 2981-2987 (1969b).
- B.N.Ames, M.K.Shigenaga and T.M.Hagen, Oxidants, antioxidants and the degenerative diseases of aging. Proc. Natl. Acad. Sci. USA **90**, 7915-7922 (1993).
- M.Anbar, M.Bambenek and A.B.Ross, Selected specific rates of reactions of transients from water in aqueous solution. 1. Hydrated electron. Nat. Stand. Ref. Data Systems, Nat. Bur. Stand. Vol. 43 (NSRDS-NBS-43) (1973).
- M.Anbar, Farhataziz and A.B.Ross, Selected specific rates of reactions of transients from water in aqueous solution. II.Hydrogen atom. Nat. Stand. Ref. Data Systems, Nat. Bur. Stand. Vol. 51 (NSRDS-NBS-51) (1975).
- A.Appleby and H.A.Schwarz, Radical and molecular yields in water irradiated by γ-rays and heavy ions. J. Phys. Chem. **73**, 1937-1941 (1969).
- H.Asahara, P.W.Wistort, J.F.Bank, R.H.Bakerian and R.P.Cunningham, Purification and characterization of *Escherichia coli* endonuclease III from the cloned Nth gene. Biochem. **28**, 4444-4449 (1989).
- I.S.Ayene, C.J.Koch and R.E.Krisch, Role of scavenger-derived radicals in the induction of double-strand and single-strand breaks in irradiated DNA. Radiat. Res. **142**, 133-143 (1995).
- V.Baily, W.G.Verly, T.R.O'Connor and J.Laval, Mechanism of DNA strand nicking by apurinic/apyrimidinic sites by *Escherichia coli* [formamidopyrimidine]-DNA glycosylase. Biochem. J. **262**, 581-589 (1989).
- B.Balasubramanian, W.K.Pogozelski and T.D.Tullius, DNA strand breaking by the hydroxyl radical is governed by the accessible surface of the hydrogen atoms of the DNA backbone. Proc. Natl. Acad. Sci. USA **95**, 9738-9743 (1998).
- R.V.Bensasson, E.J.Land and T.G.Truscott, *Excited states and free radicals in biology and medicine*. Oxford University Press. New York (1993).
- D.Blöcher, DNA double-strand break repair determines the RBE of α-particles. Int. J. Radiat. Biol. **54**, 761-771 (1988).

- S.Boiteux, E.Gajewski, J.Laval and M.Dizdaroglu, Substrate specificity of the *Escherichia coli* Fpg protein (Formamidopyrimidine-DNA glycosylase): excision of purine lesions in DNA produced by ionizing radiation or photosensitization. Biochem. **31**, 106-110 (1992).
- F.Bolivar and K.Backman, Plasmids of *Escherichia coli* as cloning vectors. Meth. Enz. **68**, 245-267 (1979).
- C.E.Bolton, H.Nikjoo and D.T.Goodhead, Computational modelling of medium- to high-energy electron-induced DNA damage. Eleventh ICRR, 284 (1999).
- S.W.Botchway, D.L. Stevens, M.A.Hill, T.J.Jenner and P.O'Neill, Induction and rejoining of DNA double-strand breaks in chinese hamster V79-4 cells irradiated with characteristic aluminium K and copper L ultrasoft X-Rays. Radiat. Res. **148**, 317-324 (1997).
- A.W.Boyd, M.B.Carver and R.S.Dixon, Computed and experimental product concentrations in the radiolysis of water. Radiat. Phys. Chem. **15**, 177-185 (1980).
- A.P.Breen and J.A.Murphy, Reactions of oxyl radicals with DNA. Free Rad. Biol. Med. **18**, 1033-1077 (1995).
- L.H.Breimer, Enzymatic excision from gamma-irradiated polydeoxyribo-nucleotides of adenine residues whose imidazole rings have been ruptured. Nucleic Acids Res. **12**, 6359-6367 (1984).
- L.H.Breimer and T.Lindahl, DNA glycosylaseactivities for thymine residues damaged by ring saturation, fragmentation or ring contraction are functions of Endonuclease-III in *Escherichia-Coli*. J.Biol.Chem. **259**, 5543-5548 (1984).
- D.J.Brenner and J.F.Ward, Constraints on energy deposition and target size of multiply-damaged sites associated with DNA double strand breaks. Int. J. Radiat. Biol. **61**, 737-748 (1992).
- W.G.Burns, Effect of radiation type in water radiolysis. J. Chem. Soc. Faraday Trans. 1 **77**, 2803-2813 (1981).
- W.G.Burns, R.May and K.F.Baverstock, Oxygen as a product of water radiolysis in high LET tracks. I. The origin of the hydroperoxyl radical in water radiolysis. Radiat. Res. **86**, 1-19 (1981).
- C.J.Burrows and J.G.Muller, Oxidative nucleobase modifications leading to strand scission. Chem. Rev. **98**, 1109-1151 (1998).

- G.V.Buxton, Radiation chemistry in the liquid state: (1) water and homogeneous aqueous solutions. *Radiation Chemistry-Principles and applications*. edited by Farhataziz and M.A.J.Rodgers VCH Publishers Inc, New York (1987).
- G.V.Buxton, C.L.Greenstock, W.P.Helman and A.B.Ross, Critical review of rate constants for reactions of hydrated electrons, hydrogen atoms and hydroxyl radicals ($^{\cdot}OH/^{\cdot}O^{-}$) in aqueous solution. J. Phys. Chem. Reference Data **17**, 513-886 (1988).
- E.Cadenas, Biochemistry of oxygen-toxicity. Annu. Rev. Biochem. **58**, 79-110 (1989).
- J.Cadet, T.Douki and J-L.Ravant, Artifacts associated with the measurement of oxidized DNA bases. Environ. Health Persp. **105**, 1034-1039 (1997).
- B.G.Cartwright, E.K.Shirk and P.B.Prise, A nuclear-track-recording polymer of unique sensitivity and resolution. Nucl. Inst. Meth. **153**, 457-460 (1978).
- J.D.Chapman, A.P.Reuvers, J.P.Borsa and C.L.Greenstock, Chemical radioprotection and radiosensitization of mammalian cells growing in vitro. Radiat. Res. **56**, 291-306 (1973).
- J.D.Chapman, S.D.Doern, A.P.Reuvers, C.J.Gillespie, A.Chatterjee, E.A.Blakely, K.C.Smith and C.A.Tobias, Radioprotection by DMSO of mammalian cells exposed to X-rays and to heavy charged-particle beams. Rad. Environ. Biophys. **16**, 29-41 (1979).
- J.D.Chapman and C.J.Gillespie, radiation-induced events and their time scale in mammalian cells. Adv. Radiat. Res. **9**, 143-198 (1981).
- D.E.Charlton, H.Nikjoo and J.L.Humm, Calculation of initial yields of single- and double-strand breaks in cell nuclei from electrons, protons and alpha particles. Int. J. Radiat. Biol. **56**, 1-19 (1989).
- A.Chatterjee and W.R.Holley, Computer simulation of initial events in the biochemical mechanisms of DNA damage. Adv. Radiat. Biol. **17**, 181-226 (1993).
- M.A.Chaudhry and M.Weinfeld, The action of *Escherichia coli* endonuclease III on multiply damaged sites in DNA. J. Mol. Biol. **249**, 914-922 (1995).
- R.Cox, J.Thacker, D.T.Goodhead and R.J.Munson, Mutation and inactivation of mammalian cells by various ionizing radiations. Nature **267**, 425-427 (1977).
- S.Cunniffe and P.O'Neill, The complexity of radiation-induced DNA damage as revealed by exposure to cell extracts. Radiat. Res. **152**, 421-427 (1999).

- R.Datta, A.Cole and S.Robinson, Use of track-end alpha particles from ^{241}Am to study radiosensitive sites in CHO cells. Radiat. Res. **65**, 139-151 (1976).
- M-H.David-Cordonnier, J.Laval and P.O'Neill, Clustered DNA damage: influence on damage excision by XRS5 nuclear extracts and *Escherichia coli* Fpg and Endonuclease III. J. Biol. Chem. **275**, 11865-11873 (2000).
- D.J.Deeble and C.von Sonntag, The UV absorption spectra of the C(5) and C(6) OH adduct radicals of uracil and thymine derivatives. A pulse radiolysis study. Z. Naturforsch. **40c**, 925-928 (1985).
- C.M.deLara, T.J.Jenner, K.M.S.Townsend, S.J.Marsden and P.O'Neill, The effect of dimethyl sulfoxide on the induction of DNA double-strand breaks in V79-4 mammalian cells by alpha particles. Radiat. Res. **144**, 43-49 (1995).
- B.Demple and S.Linn, DNA N-glycosylases and UV repair. Nature **287**, 203-208 (1980).
- R.E.Dickerson, H.E.Drew, B.N.Conner, R.N.Wing, A.V.Fratini and M.L.Kopka, Anatomy of A-, B- and Z-DNA. Science **216**, 475-485 (1982).
- M.Dizdaroglu, J.Laval and S.Boiteux, Substrate specificity of the *Escherichia coli* endonuclease III. Excision of thymine and cytosine derived lesions in DNA produced by radiation generated free radicals. Biochem. **32**, 12105-12111 (1993).
- L.M.Dorfman and M.S.Matheson, Pulse radiolysis. Prog. React. Kin. **3**, 237-301 (1965).
- T.Douki, T.Delatour, F.Bianchini and J.Cadet, Observation and prevention of an artifactual formation of oxidised DNA bases and nucleosides in the GC-EIMS method. Carcinogenesis **17**, 347-353 (1996).
- T.Douki and J.Cadet, Modification of DNA bases by photosensitized one-electron oxidation. Int. J. Radiat. Biol. **75**, 571-581 (1999).
- I.G.Draganić, M.T.Nenadović and Z.D.Draganić, Radiolysis of HCOOH + O_2 at pH 1.3-13 and the yields of primary products in γ radiolysis of water. J. Phys. Chem. **73**, 2564-2570 (1969).
- M.C.Elia and M.O.Bradley, Influence of chromatin structure on the induction of DNA double strand breaks by ionizing radiation. Can. Res. **52**, 1580-1586 (1992).
- M.Elkind, Repair processes in radiation biology. Radiat. Res. **100**, 425-449 (1984).

- B.Epe, M.Pflaum, M.Häring, J.Hegler and H.Rüdiger, Use of repair endonucleases to characterize DNA damage induced by reactive oxygen species in cellular and cell free systems. Toxicol. Lett. **67**, 57-72 (1993).
- B.Epe, D.Ballmaier, I.Roussyn, K.Briviba and H.Sies, DNA damage by peroxynitrite characterized with DNA repair enzymes. Nucleic Acids Res. **24**. 4105-4110 (1996).
- M.Falk, A.G.Poole and C.G.Goymour, Infrared study of the state of water in the hydration shell of DNA. Can.J.Chem. **48**, 1536-1542 (1970).
- Farhataziz and A.B.Ross, Selected specific rates of reactions of transients from water in aqueous solution. III.Hydroxyl radical and perhydroxyl radical and their radical ions. Nat. Stand. Ref. Data Systems, Nat. Bur. Stand. Vol. 59 (NSRDS-NBS-59) (1977).
- *Radiation Chemistry Principles and Applications*. edited by Farhataziz and M.A.J.Rodgers. VCH Publications Inc, (1987).
- M.B.Flick, R.L.Warters, L.S.Yasui and R.E.Krisch, Measurement of radiation-induced DNA damage using gel electrophoresis or neutral filter elution shows an increased frequency of DNA strand breaks after exposure to pH 9.6. Radiat. Res. **119**, 452-465 (1989).
- M.Folkard, K.M.Prise, B.Vojnovic, S.Davies, M.J.Roper and B.D.Michael, Measurement of DNA damage by electrons with energies between 25 and 4000 eV. Int. J. Radiat. Biol. **64**, 651-658 (1993).
- M.Folkard, K.M.Prise, B.Vojnovic, H.C.Newman, M.J.Roper, K.J.Hollis and B.D.Michael, Conventional and microbeam studies using low-energy charged particles relevant to risk assessment and the mechanisms of radiation action. Radiat. Prot. Dosim. **61**, 215-218 (1995).
- M.Folkard, K.M.Prise, B.Brocklehurst and B.D.Michael, DNA damage induction in dry and hydrated DNA by synchrotron radiation, J. Phys. B: At. Mol. Opt. Phys. **32**. 2753-2761 (1999).
- J.C.Fox and K.M.Prise, DNA lesions, linear energy transfer and radiosensitive mutants. *Radiation Science: Of Molecules, Mice and Men*. edited by H.Denekamp and D.G.Hirst, Brit. J. Radiol. Suppl. **24**. pp. 1-89 (1992).
- D. Frankenberg, M.Frankenberg-Schwager, D.Blöcher and R.Harbich, Evidence for DNA double-strand breaks as the critical lesions in yeast cells irradiated with

sparsley or densely ionising radiation under oxic or anoxic conditions. Radiat. Res. **88**, 524-532 (1981).

- D. Frankenberg, M.Frankenberg-Schwager and R.Harbich, The contribution of OH* in densely ionising electron track ends of particle tracks to the induction of DNA double strand breaks. Radiat. Prot. Dosim. **31**, 249-252 (1990).
- M.Frankenberg-Schwager, Induction, repair and biological relevance of radiation-induced DNA lesions in eukaryotic cells. Radiat. Environ. Biophys. **29**, 273-292 (1990).
- D.Freifelder and B.Trumbo, Matching of single-strand breaks to form double-strand breaks in DNA. Biopoly. **7**, 681-693 (1969).
- J.P.Freyer, M.E.Schiliiaci and M.R.Raju, Measurement of the G-value for 1.5 keV X-rays. Int. J. Radiat. Biol. **56**, 885-892 (1989).
- E.C.Friedberg, G.Walker and W. Siede, *DNA Repair and Mutagenesis*. American Society of Microbiology, Washington DC (1985).
- W.Friedland, P.Jacob, H.G.Paretzke and T.Stork, Monte Carlo simulation of production of short DNA fragments by low-linear energy transfer radiation using higher-order DNA models. Radiat. Res. **150**, 170-182 (1998).
- A.F.Fuciarelli, B.J.Wegher, W.F.Blakely and M.Dizdaroglu, Yields of radiation-induced base products in DNA: effects of DNA conformation and gassing conditions. Int. J. Radiat. Biol. **58**, 397-415 (1990).
- J.Fulford, P.Bonner, D.T.Goodhead, M.A.Hill and P.O'Neill, Experimental determination of the dependence of OH radical yield on photon energy: a comparison with theoretical simulations. J. Phys. Chem. A **103**, 11345-11349 (1999).
- D.T.Goodhead and J.Thacker, Inactivation and mutation of cultured mammalian cells by aluminium characteristic ultra-soft X-rays. 1. Properties of aluminium X-rays and preliminary experiments with Chinese hamster cells. Int. J. Radiat. Biol. **31**, 541-559 (1977).
- D.T.Goodhead, J.Thacker and R.Cox, Effectiveness of 0.3 keV carbon ultrasoft X-rays for the inactivation and mutation of cultured mammalian cells. Int. J. Radiat. Biol. **36**, 101-114 (1979).

- D.T.Goodhead, R.J. Munson, J.Thacker and R.Cox, Mutation and inactivation of cultured mammalian cells exposed to beams of accelerated heavy ions IV. Biological interpretation. Int. J. Radiat. Biol. **37**, 135-167 (1980).
- D.T.Goodhead, J.Thacker and R.Cox, Is selective absorption of ultrasoft x-rays biologically important in mammalian cells? Phys. Med. Biol. **26**, 1115-1127 (1981).
- D.T.Goodhead and D.J.Brenner, Estimation of a single property of low LET radiations which correlates with biological effectiveness. Phys. Med. Biol. **28**, 485-492 (1983).
- D.T.Goodhead, D.E.Charlton, W.E.Wilson and H.G.Paretzke, Current biophysical approaches to the undertstanding of biological effects of radiation in terms of local energy deposition. *Proceedings of the Fifth Symposium on Neutron Dosimetry.* edited by H.Schraubem M.Burger and J.Booz. Commission of the European Communities, Luxembourg pp 57-68 (1985).
- D.T.Goodhead, Relationship of microdosimetric techniques to applications in biological systems. *The Dosimetry of Ionising Radiations, Vol II.* edited by K.R. Kase, B.E. Bjarngaard and F.H. Attix. Academic Press, Orlando pp 1-89 (1987).
- D.T.Goodhead, The initial physical damage produced by ionizing radiation, Int. J. Radiat. Biol. **56**, 623-634 (1989).
- D.T.Goodhead and H.Nikjoo, Track structure analysis of ultrasoft X-rays compared to high- and low-LET radiations. Int. J. Radiat. Biol. **55**, 513-529 (1989).
- D.T.Goodhead and H.Nikjoo, Current status of ultrasoft x-rays and track structure analysis as tools for testing and developing biophysical models of radiation action. Radiat. Prot. Dosim. **31**, 343-350 (1990).
- D.T.Goodhead, D.A.Bance, A.Stretch and R.E.Wilkinson, A versatile plutonium-238 irradiator for radiobiological studies with α-particles. Int. J. Radiat. Biol. **59**, 195-210 (1991).
- D.T.Goodhead, Radiation tracks in biological materials: initial damage in cells, DNA and associated structures. *Genes, Cancer and Radiation Protection.* edited by M.L.Mendelsohn. National Council on Radiation Protection and Measurements, Bethesda pp 25-37 (1992).
- D.T.Goodhead, J.Thacker and R.Cox, Effects of radiations of different qualities on cells: molecular mechanisms of damage and repair. Int. J. Radiat. Biol. **63**, 543-556 (1993).

- D.T.Goodhead, Initial events in the cellular effects of ionising radiation: clustered damage in DNA. Int. J. Radiat. Biol. **65**, 7-17 (1994).
- L.I.Grossweiner, Electron motions in aqueous systems-a survey. Photochem. and Photobiol. **28**, 97-108 (1978).
- E.H.Grubbé, Priority in the therapeutic use of X-Rays. Radiology **21**, 156-162 (1933).
- E.J.Hall, *Radiobiology for the radiologist*, 4th edition. J.B.Lippincott Co., Philadelphia (1994).
- R.Hanai, M.Yazu and K.Hieda, On the experimental distinction between ssbs and dsbs in circular DNA. Int. J. Radiat. Biol. **73**, 475-479 (1998).
- M.Häring, H.Rüdiger, B.Demple, S.Boiteux and B.Epe, Recognition of oxidized abasic sites by repair endonucleases. Nucleic Acids Res. **22**, 2010-2015 (1994).
- L.Harrison, Z. Hatahet, A.A.Purmal and S.S.Wallace, Multiply damaged sites in DNA: interactions with *Escherichia coli* endonucleases III and VIII. Nucleic Acids Res. **26**, 932-941 (1998).
- J.Heilmann, H.Rink, G.Taucher-Scholz and G.Kraft, DNA strand break induction and rejoining and cellular recovery in mammalian cells after heavy-ion irradiation. Radiat. Res. **135**, 46-55 (1993).
- J.Heilmann, G.Taucher-Scholz and G.Kraft, Induction of DNA double-strand breaks in CHO-K1 cells by carbon ions, Int. J. Radiat. Biol. **68**, 153-162 (1995).
- B.L.Henke, E.M.Gullikson and J.C.Davis, X-ray interactions: photoabsorption, scattering, transmission and reflection at E = 50-30,000 eV, Z = 1-92. Atomic Data and Nuclear Data Tables **54**, 181-342 (1993).
- E.S.Henle, R.Roots, W.R.Holley and A.Chatterjee, DNA strand breakage is correlated with unaltered base release after gamma irradiation. Radiat. Res. **143**, 144-150 (1995).
- K.Hieda, Y.Hayakawa, A.Ito, K.Kobayashi and T.Ito, Wavelength dependence of the formation of single-strand breaks and base changes in DNA by the ultraviolet radiation above 150 nm. Photochem. Photobiol. **44**, 379-383 (1986).
- K.Hieda, DNA-damage induced by vacuum and soft-X-ray photons from synchrotron-radiation. Int. J. Radiat. Biol. **66**, 561-567 (1994).

- K.Hieda, K.Suzuki, T.Hirona, M.Suzuki and Y.Furusawa, Single- and double-strand breaks in pBR322 DNA by vacuum-UV from 8.3 to 20.7 eV. J. Radiat. Res. **35**, 104-111 (1994).
- K.Hieda, T.Hirona, A. Azami, M.Suzuki, Y.Furusawa, H.Maezawa, N. Usamis, A. Yokoya and K.Kobayashi, Single- and double-strand breaks in pBR322 plasmid DNA by monochromatic X-rays on and off the K-absorption peak of phosphorus. Int. J. Radiat. Biol. **70**, 437-445 (1996).
- M.A.Hill and F.A.Smith, Calculation of initial and primary yields in the radiolysis of water. Radiat. Phys. Chem. **43**, 265-280 (1994).
- M.A.Hill, D.L.Stevens, D.A.Bance and D.T.Goodhead, A versatile mammalian cell irradiation rig for low dose rate ultrasoft X-ray studies. *Microdosimetry: an interdisciplinary approach.* edited by D.T.Goodhead, P.O'Neill and H.G.Menzel. The Royal Society of Chemistry, Cambridge, U.K. pp 203-206 (1997).
- M.A.Hill, M.D.Vecchia, K.M.S.Townsend and D.T.Goodhead, Production and dosimetry of copper L ultrasoft x-rays for biological and biochemical investigations. Phys. Med. Biol. **43**, 351-363 (1998).
- M.A.Hill, Radiation damage to DNA: The importance of track structure. Radiat. Measure. **31**, 15-23 (1999).
- P.S.Hodgkins, M.P.Fairman and P.O'Neill, Rejoining of gamma-radiation-induced single-strand breaks in plasmid DNA by human cell extracts: dependence on the concentration of the hydroxyl radical scavenger, Tris. Radiat. Res. **145**, 24-30 (1996a).
- P.S.Hodgkins, P.O'Neill, D.L.Stevens and M.P.Fairman, The severity of alpha-particle-induced DNA damage is revealed by exposure to cell-free extracts. Radiat. Res. **146**, 660-667 (1996b).
- W.R.Holley, A.Chatterjee, and J.L.Magee, Production of DNA strand breaks by direct effects of heavy charged particles. Radiat. Res. **121**, 161-168 (1990).
- W.R.Holley and A.Chatterjee, Clusters of DNA damage induced by ionizing radiation: Formation of short DNA fragments. I. Theoretical modelling. Radiat. Res. **145**, 188-199 (1996).
- M.Hoshi, D.T.Goodhead, D.J.Brenner, D.A.Bance, J.J.Chmielewski, M.A.Paciotti and J.N.Bradbury, Dosimetry comparison and characterisation of an Al K ultrasoft

x-ray beam from an MRC cold-cathode source. Phys. Med. Biol. **30**, 1029-1041 (1985).

- F.Hutchinson, Chemical changes induced in DNA by ionizing radiation, Prog. Nucleic. Acid Res. Mol. Biol. **32**, 115-154 (1985).
- F.Hutchinson, Formation of two double-strand breaks in the same DNA molecule by a single high-energy photon or ionizing particle. Int. J. Radiat. Biol. **70**, 505-512 (1996).
- ICRU, Linear Energy Transfer. *ICRU Report 16*. ICRU, Washington DC (1970).
- M.Isildar, M.N.Schuchmann, D.Schulte-Frohlinde and C.von Sonntag, Oxygen uptake in the radiolysis of aqueous solutions of nucleic acids and their constituents. Int. J. Radiat. Biol. **41**, 525-533 (1982).
- T.Ito, S.C.Baker, C.D.Stickley, J.G.Peak and M.J.Peak, Dependence of the yield of strand breaks induced by γ-rays in DNA on the physical conditions of exposure: water content and temperature. Int. J. Radiat. Biol. **63**, 289-296 (1993).
- T.J.Jenner, M.Belli, D.T.Goodhead, F.Ianzini, G.Simone and M.A.Tabocchini, Direct comparison of biological effectiveness of protons and alpha-particles of the same LET. Int. J. Radiat. Biol. **61**, 631-637 (1992).
- T.J.Jenner, C.M.deLara, P.O'Neill and D.L.Stevens, Induction and rejoining of DNA double-strand breaks in V79-4 mammalian cells following γ- and α-irradiation. Int. J. Radiat. Biol. **64**, 265-273 (1993).
- C.D.Jonah, E.J.Hart and M.S.Matheson, Yields and decay of the hydrated electron at times greater than 200 picoseconds. J. Phys. Chem. **77**, 1838-1843 (1973).
- C.D.Jonah, M.S.Matheson, J.R.Millar and E.J.Hart, Yield and decay of the hydrated electron from 100 ps to 3 ns. J. Phys. Chem. **80**, 1267-1270 (1976).
- C.D.Jonah and J.R.Miller, Yield and decay of the OH radical from 200 ps to 3 ns. J. Phys. Chem. **81**, 1974-1977 (1977).
- G.D.D.Jones and P.O'Neill, Kinetics of radiation induced strand break formation in single stranded pyrimidine polynucleotides in the presence and absence of oxygen: a time resolved light scattering study. Int. J. Radiat. Biol. **59**, 1127-1145 (1991).
- G.D.D.Jones, J.R.Milligan, J.F.Ward, P.M.Calabro-Jones and J.A.Aguilera, Yield of strand breaks as a function of scavenger concentration and LET for SV40 irradiated with ^{4}He ions. Radiat. Res. **136** 190-196 (1993).

- G.D.D.Jones, T.V.Boswell and J.F.Ward, Effects of postirradiation temperature on the yields of radiation-induced single and double-strand breakage in SV40 DNA. Radiat. Res. **138,** 291-296 (1994a).
- G.D.D.Jones, T.V.Boswell, J.Lee, J.R.Milligan, J.F.Ward and M.Weinfeld, A comparison of DNA damages produced under conditions of direct and indirect action of radiation. Int. J. Radiat. Biol. **66**, 441-445 (1994b).
- H.L.Katcher and S.S.Wallace, Characterization of the *Escherichia-coli* X-ray endonuclease, endonuclease-III. Biochem. **22**, 4071-4081 (1983).
- A.M.Kellerer, Fundamentals of microdosimetry. Dosim. Ion. Radiat. **1**, 77-162 (1975).
- U.Klimczak, D.C.Ludwig, F.Mark, P.Rettberg and D.Schulte-Frohlinde, Irradiation of plasmid and phage DNA in water-alcohol mixtures: strand breaks and lethal damage as a function of scavenger concentration. Int. J. Radiat. Biol. **64**, 497-510 (1993).
- K.Kobayashi, K.Heida, H.Maezawa, M.Ando and T.Ito, Monochromatic X-ray irradiation system (0.08-0.4 nm) for radiation biology studies using synchrotron radiation at the photon factory. J. Radiat. Res. **28**, 243-253 (1987).
- Y.W.Kow and S.S.Wallace, Mechanism of action of *Escherichia coli* endonuclease III. Biochem. **26**, 8200-8206 (1987).
- K.K.Krane, *Introductory nuclear physics*. John Wiley & Sons, New York (1988).
- R.E.Krisch, M.B.Flick and C.N.Trumbore, Radiation chemical mechanisms of single- and double-strand break formation in irradiated SV40 DNA. Radiat. Res. **126**, 251-259 (1991).
- G.K.Kuipers and M.V.M.Lafleur, Characterization of DNA damage induced by gamma-radiation-derived water radicals, using DNA repair enzymes. Int. J. Radiat. Biol. **74**, 511-519 (1998).
- A.Kupperman, Diffusion model of the radiation chemistry of aqueous solutions. *Radiation Research*. edited by G.Silini. North-Holland Publishing Co. Amsterdam pp 212-234 (1967).
- M.V.M.Lafleur, J.Woldhuis and H.Loman, Alkali-labile sites and post-irradiation effects in single-stranded DNA induced by H radicals. Int. J. Radiat. Biol. **33**, 273-281 (1978).

- M.V.M.Lafleur, M van Heuval, J.Woldhuis and H.Loman, Alkali-labile sites and post-irradiation effects in gamma-irradiated biologically active double-stranded DNA in aqueous solution. Int. J. Radiat. Biol. **36**, 241-247 (1979).
- T.La Vere, D.Becker and M.D.Sevilla, Yields of OH in gamma-irradiated DNA as a function of DNA hydration: hole transfer in competition with OH formation. Radiat. Res. **145**, 673-680 (1996).
- J.A.LaVerne and S.M.Pimblott, Yields of hydroxyl radical and hydrated electron scavenging reactions in aqueous solutions of biological interest. Radiat. Res. **135**, 16-23 (1993a).
- J.A.LaVerne and S.M.Pimblott, Diffusion-kinetic modelling of the cooperative effect of scavengers on the scavenged yield of the hydroxyl radical. J. Chem. Faraday Trans. **89**, 3527-3532 (1993b).
- M.Löbrich, P.K.Cooper and B.Rydberg, Non-random distribution of DNA double-strand breaks induced by particle irradiation. Int. J. Radiat. Biol. **70**, 493-503 (1996).
- M.Löbrich, Induction and repair of DNA double-strand breaks in human fibroblasts after particle irradiation. Adv. Space Res. **22**, 551-560 (1998).
- C.Lücke-Huhle, Biological relevance of alkali-labile sites in double-stranded DNA after γ-irradiation. Int. J. Radiat. Biol. **27**, 1-6 (1975).
- J.L.Magee and A.Chatterjee, Theory of the chemical effects of high-energy electrons. J. Phys. Chem. **82**, 2219-2226 (1978).
- J.L.Magee and A.Chatterjee, A spur unfolding model for the radiolysis of water. Radiat. Phys. Chem. **15**, 125-132 (1980).
- T.Melvin, S.M.T.Cunniffe, P.O'Neill, A.W.Parker and T.Roldan-Arjona, Guanine is the target for direct ionisation damage in DNA as detected using excision enzymes. Nucleic Acids Res. **26**, 4935-4942 (1998).
- B.D.Michael, K.M.Prise, M.Folkard, B.Vojnovic, B.Brocklehurst, I.H.Munro and A.Hopkirk, Action spectra for single- and double-strand break induction in plasmid DNA: studies using synchrotron radiation. Int. J. Radiat. Biol. **66**, 569-572 (1994).
- V. Michalik, Model of DNA damage induced by radiation of different quality. Int. J. Radiat. Biol. **62**, 9-20 (1992).
- M.T.Milano and W.A.Bernhard, The effect of packing and conformation on free radical yields in films of variably hydrated DNA. Radiat. Res. **151**, 39-49 (1999).

- J.R.Milligan, J.A.Aguilera and J.F.Ward, Variation of single-strand yield with scavenger concentration for plasmid DNA irradiated in aqueous solution. Radiat. Res. **133**, 151-157 (1993).
- J.R.Milligan and J.F.Ward, Yield of single-strand breaks due to attack on DNA by scavenger-derived radicals. Radiat. Res. **137**, 295-299 (1994).
- J.R.Milligan, J.Y-Y.Ng, C.C.L.Wu, J.A.Aguilera, C.F.Fahey and J.F.Ward, DNA repair by thiols in air shows two radicals make a double-strand break. Radiat. Res. **143**, 273-280 (1995).
- J.R.Milligan, J.A.Aguilera, C.C.L.Wu, J.Y-Y.Ng and J.F.Ward, The difference that linear energy transfer makes to precursors of DNA strand breaks. Radiat. Res. **145**, 442-448 (1996a).
- J.R.Milligan, J.Y-Y.Ng, C.C.L.Wu, J.A.Aguilera, J.F.Ward, Y.W.Kow, S.S.Wallace and R.P.Cunningham, Methyperoxyl radicals as intermediates in the damage to DNA irradiated in aqueous dimethyl sulfoxide with gamma rays. Radiat. Res. **146**, 436-443 (1996b).
- J.R.Milligan, C.C.L.Wu, J.Y-Y.Ng, J.A.Aguilera and J.F.Ward, Characterization of the reaction rate coefficient of DNA with the hydroxyl radical. Radiat. Res. **146**, 510-513 (1996c).
- J.R.Milligan, J.A.Aguilera, C.C.Wu, R.A.Paglinawan, T-T.D.Nguyen, D.Wu and J.F.Ward, Effect of hydroxyl radical scavenging capacity on clustering of DNA damage. Radiat. Res. **148**, 325-329 (1997).
- J.R.Milligan, J.A.Aguilera, T-T.D.Nguyen, J.F.Ward, Y.W.Kow, B.He and R.P.Cunningham, Yield of DNA strand breaks after base oxidation of plasmid DNA. Radiat. Res. **151**, 334-342 (1999).
- V.V.Moiseenko, R.N.Hamm, A.J.Walker and W.V.Prestwich, Modelling DNA damage induced by different energy photons and tritium beta-particles. Int. J. Radiat. Biol. **74**, 533-550 (1998a).
- V.V.Moiseenko, R.N.Hamm, A.J.Walker and W.V.Prestwich, The cellular environment in computer simulations of radiation-induced damage to DNA. Radiat. Environ. Biophys. **37**, 167-172 (1998b).
- A.Mozumder and J.L.Magee, Model of tracks of ionizing radiations for radical reaction mechanisms. Radiat.Res. **28**, 203-214 (1966).

- National Council on Radiation Protection and Measurements (NCRP). Evaluation of occupational and environmental exposures to radon and radon daughters in the united states. *NCRP Report 78*. National Council on Radiation Protection and Measurements, Washington, D.C (1984).
- National Research Council, Committee on the Biological Effects of Ionizing Radiation. *Health Risks of Radon and Other Internally Deposited Alpha Emitters (BIER IV)*. National Academy Press, Washingdon DC (1988).
- National Research Council, Committee on the Biological Effects of Ionizing Radiation. *Health Effects of Exposure to Radon (BIER VI)*. National Academy Press, Washingdon DC (1998).
- G.J.Neary, Irradiation of simple biological specimens by charged particles. *The uses of cyclotrons in chemistry, metallurgy and biology*. edited by C.B. Amphlett. Butterworth, London pp 194-203 (1970).
- H.C.Newman, K.M.Prise, M.Folkard and B.D.Michael, DNA double-strand break distribution in X-ray and α-particle irradiated V79 cells: evidence for non-random breakage. Int. J. Radiat. Biol. **71**, 347-363 (1997).
- H.Nikjoo and D.T.Goodhead, Track structure analysis illustrating the prominent role of low-energy electrons in radiobiological effects of low-LET radiations. Phys. Med. Biol. **36**, 229-238 (1991).
- H. Nikjoo, D.T. Goodhead, D.E. Charlton and H.G. Paretzke, Energy deposition in small cylinder targets by monoenergetic electrons. Int. J. Radiat. Biol. **60**, 739-756 (1991).
- H.Nikjoo, D.E.Charlton and D.T.Goodhead, Monte Carlo track structure studies of energy deposition and calculation of initial DSB and RBE. Adv. Space Res. **14**, 161-180 (1994a).
- H.Nikjoo, P.O'Neill, M.Terrissol and D.T.Goodhead, Modelling of radiation-induced DNA damage: the early physical and chemical event. Int. J. Radiat. Biol. **66**, 453-457 (1994b).
- H.Nikjoo, M.Terrissol, R.N.Hamm, J.E.Turner, S.Uehara, H.G.Paretzke and D.T.Goodhead, Comparison of energy deposition in small cylindrical volumes by electrons generated by Monte Carlo track structure codes for gaseous and liquid water. Radiat. Prot. Dosim. **52**, 165-169 (1994c).

- H.Nikjoo, P.O'Neill, D.T.Goodhead and M.Terrissol, Computational modelling of low-energy electron-induced DNA damage by early physical and chemical events. Int. J. Radiat. Biol. **71**, 467-483 (1997).
- H.Nikjoo, S.Uehara, W.E.Wilson, M.Hoshi and D.T.Goodhead, Track structure in radiation biology: theory and applications. Int. J. Radiat. Biol. **73**, 355-364 (1998).
- H.Nikjoo, P.O'Neill, M.Terrissol and D.T.Goodhead, Quantitative modelling of DNA damage using Monte Carlo track structure method. Radiat. Environ. Biophys. **38**, 31-38 (1999).
- J.Nygren and G.Ahnström, DNA double and single-strand breaks induced by accelerated He^{2+} and N^{6+} ions in human cells: relative biological effectiveness is dependent on the relative contribution of the direct and indirect effects. Int. J. Radiat. Biol. **70**, 421-427 (1996).
- T.R.O'Connor and J.Laval, Physical association of the 2, 6-diamino-4-hydroxy-5N-formamidopyrimidine-DNA glycosylase of *Escherichia-coli* and an activity nicking DNA at apurinic apyrimidinic sites. Proc. Natl. Acad. Sci. USA **86**, 5222-5226 (1989).
- N.L.Oleinick and S.M.Chiu, Nuclear and chromatin structures and their influence on the radiosensitivity of DNA. Radiat. Prot. Dosim. **52**, 353-358 (1994).
- P.O'Neill and E.M.Fielden, Primary free radical processes in DNA. Adv. Radiat. Biol. **17**, 53-119 (1993).
- P.O'Neill, S.M.T.Cunniffe, D.L.Stevens, S.W.Botchway and H.Nikjoo, Strand break induction in DNA by aluminium K ultrasoft x-rays: Comparison of experimental data and track structure analysis. *Microdosimetry: an interdisciplinary approach*. edited by D.T.Goodhead, P.O'Neill and H.G.Menzel. The Royal Society of Chemistry, Cambridge, U.K. pp 81-84 (1997).
- A.Ozols, K.M.Prise and B.D.Michael, A comparison of the radiosensitivity of relaxed and supercoiled plasmid DNA. Int. J. Radiat. Biol. **75**, 83-90 (1999).
- H.G.Paretzke, Radiation track structure theory. *Kinetics of Nonhomogeneous Processes*. edited by G.R. Freeman. Wiley, New York pp 89-170 (1987).
- H.G.Paretzke, D.T.Goodhead, I.G.Kaplan and M.Terrissol, *Atomic and molecular data for radiotherapy and radiation research*. IAEA-TECDOC-799, Vienna (1995).

- J.G.Peak, T.Ito, F.T.Robb and M.J.Peak, DNA damage produced by exposure of supercoiled plasmid DNA to high- and low-LET ionizing radiation: effects of hydroxyl radicals quenchers. Int. J. Radiat. Biol. **67**, 1-6 (1995).
- S.M.Pimblott, Investigation of various factors influencing the effect of scavengers on the radiation chemistry following the high-energy radiolysis of water. J. Phys. Chem. **96**, 4485-4491 (1992).
- S.M.Pimblott and N.J.B.Green, *Recent advances in the kinetics of radiolytic processes. Vol. 3.* edited by R.G.Compton and G.Hancock. Elsevier, Amsterdam, pp 117-174 (1995).
- S.M.Pimblott and J.A.LaVerne, Stochastic simulation of the electron radiolysis of water and aqueous solutions. J. Phys. Chem. A **101**, 5828-5838 (1997).
- S.M.Pimblott and J.A.LaVerne, Effect of electron energy on the radiation chemistry of liquid water. Radiat. Res. **150**, 159-169 (1998).
- W.K.Pogozelski and T.D.Tullius, Oxidative strand scission of nucleic acids: routes initiated by hydrogen abstraction from the sugar moiety. Chem. Rev. **98**, 1089-1107 (1998).
- W.K.Pogozelski, M.A.Xapos and W.F.Blakely, Quantitative assessment of the contribution of clustered damage to DNA double-strand breaks induced by ^{60}Co gamma rays and fission neutrons, Radiat. Res. **151**, 442-448 (1999).
- K.M.Prise, S.Davies and B.D.Michael, The relationship between radiation-induced DNA double strand breaks and cell kill in hamster V79 fibroblasts irradiated with 250 kVp X-rays, 2.3 MeV neutrons or ^{238}Pu α-particles. Int. J. Radiat. Biol. **52**, 893-902 (1987).
- K.M.Prise, M.Folkard, S.Davies and B.D.Michael, Measurement of DNA damage and cell killing in chinese hamster V79 cells irradiated with aluminium characteristic ultrasoft X rays. Radiat. Res. **117**, 489-499 (1989).
- K.M.Prise, S.Davies and B.D.Michael, Evidence for induction of DNA double-strand breaks at paired radical sites. Radiat. Res. **134**, 102-106 (1993).
- K.M.Prise, M.Folkard, H.C.Newman and B.D.Michael, Effect of radiation quality on lesion complexity in cellular DNA. Int. J. Radiat. Biol. **66**, 537-542 (1994).
- K.M.Prise, G Ahnström, M.Belli, J.Carlsson, D.Frankenberg, J.Keiffer, M.Löbrich, B.D.Michael, J.Nygren, G.Simone and B.Sternlöw, A review of dsb induction data for varying quality radiation. Int. J. Radiat. Biol. **74**, 173-184 (1998).

- K.M.Prise, N.E.Gillies and B.D.Michael, Further evidence for double-strand breaks originating from a paired radical precursor from studies of oxygen fixation processes. Radiat. Res. **151**, 635-641 (1999a).
- K.M.Prise, C.H.L.Pullar and B.D.Michael, A study of endonuclease III-sensitive sites in irradiated DNA: detection of alpha-particle-induced oxidative damage. Carcinogenesis **20**, 905-909 (1999b).
- R.Roots and S.Okada, Estimation of life times and diffusion distances of radicals involved in X-ray-induced strand breaks or killing of mammalian cells. Radiat. Res. **64**, 306-320 (1975).
- R.Roots, A.Chatterjee, P.Chang, L.Lommel and E.A.Blakely, Characterization of the hydroxyl radical-induced damage after sparsely and densely ionizing irradiation. Int. J. Radiat. Biol. **47**, 157-166 (1985).
- R.Roots, W.Holley, A.Chatterjee, M.Irizarry and G.Kraft, The formation of strand breaks in DNA after high-LET irradiation: a comparison of data from in vitro and cellular systems. Int. J. Radiat. Biol. **58**, 55-69 (1990).
- A.B.Ross, Selected specific rates of reactions of transients from water in aqueous solution. 1. Hydrated electron, supplemental data. Nat. Stand. Ref. Data Systems, Nat. Bur. Stand. Vol. 43 Suppl. (NSRDS-NBS-43 Suppl.) (1975).
- B.Rydberg, Clusters of DNA damage induced by ionizing radiation: formation of short DNA fragments. II. Experimental detection. Radiat. Res. **145**, 200-209 (1996).
- W.Saenger, *Principles of nucleic acid structure*. Springer-Verlag, New York (1988).
- J.Sambrook, E.F.Fritsch and T.Maniatis, *Molecular Cloning, A Laboratory Manual. 2nd Edition*, Cold Spring Harbor Laboratory Press, New York. (1989).
- A.Sancar and G.B.Sancar, DNA-repair enzymes. Annu. Rev. Biochem. **57**, 29-67 (1988).
- G.Scholes, R.L.Willson and M.Ebert, Pulse radiolysis of aqueous solutions of deoxyrobonucleotides and of DNA: reaction with hydroxy-radicals. Chem. Comm.17-18 (1969).
- R.H.Schuler and B.Behar, Proc. *5th Tihany Symp. on Radiation Chemistry*, edited by J.Dobo, P.Hedvig and R.Schiller, Akademai Kaido, Budapest pp 183 (1983).

- H.A.Schwarz, Applications of the spur diffusion model to the radiation chemistry of aqueous solutions. J. Phys. Chem. **73**, 1928-1937 (1969).
- M.A.Siddiqi and E.Bothe, Single- and double-strand break formation in DNA irradiated in aqueous solution: dependence on dose and scavenger concentration. Radiat. Res. **112**, 449-463 (1987).
- H.Sies, *Oxidative stress: oxidants and antioxidants*. edited by H.Sies. New York Academic, New York (1991).
- M.Spotheim-Maurizot, M Charlier and R.Sabattier, DNA radiolysis by fast neutrons. Int. J. Radiat. Biol. **57**, 301-313 (1990).
- A.A.Stankus, M.A.Xapus, C.J.Kolanko, H.M.Gerstenberg and W.F.Blakely, Energy deposition events produced by fission neutrons in aqueous solutions of plasmid DNA. Int. J. Radiat. Biol. **68**, 1-9 (1995).
- J.Stanton, G.Taucher-Scholz, M.Schneider, J.Heilmann and G.Kraft, Protection of DNA from high LET radiation by two OH radical scavengers, tris (hydroxymethyl) amino-methane and 2-mercaptoethanol. Radiat. Environ. Biophys. **32**, 21-32 (1993).
- S.Steenken, Purines-bases, nucleosides and nucleotides-aqueous-solution redox chemistry and transformation reactions of their radical cations and e^- and OH adducts. Chem. Rev. **89**, 503-520 (1989).
- D.L.Stevens, H.Nikjoo and D.T.Goodhead, Stopping powers and ranges of protons, deuterons and alpha-particles in selected materials. Part 2. Deuterons, energy=10 keV to 20 MeV. MRC Radiobiology Unit Monograph 89/1, Chilton, UK (1989).
- R.H.Stokes, Standard solutions for humidity control at 25^0 C. Ind. Eng. Chem. **41**, 2013 (1949).
- E.Storm and H.I.Israel, Photon cross sections from 1 keV to 100 MeV for elements Z=1 to Z=100. Nucl. Data Tables, **A7**, 565-688 (1970).
- B.M.Sutherland, P.V.Bennet, O.Sidorkina and J.Laval, Clustered DNA damages induced in isolated DNA and in human cells by low doses of ionising radiation. Proc. Natl. Acad. Sci. USA **97**, 103-108 (2000).
- S.G.Swarts, M.D.Sevilla, D.Becker, C.J.Tokar and K.T.Wheeler, Radiation-induced DNA damage as a function of hydration. Radiat. Res. **129**, 333-344 (1992).
- G. Taucher-Scholz, J.A.Stanton, M.Schneider and G.Kraft, Induction of DNA breaks in SV40 by heavy ions. Adv. Space Res. **12**, 73-80 (1992).

- G. Taucher-Scholz and G.Kraft, Influence of radiation quality on the yield of DNA strand breaks in SV40 DNA irradiated in solution. Radiat. Res. **151**, 595-604 (1999).
- J.Tchou, H.Kasai, S.Shibutani, M.H.Chung, J.Laval, A.P.Grollman and S.Nishimura, 8-oxoguanine (8-hydroxyguanine) DNA glycosylase and its substrate-specificity. Proc. Natl. Acad. Sci. USA **88**, 4690-4694 (1991).
- M.Terrissol, M.C.Bordage, V.Caudrelier and P.Segur, Cross sections for 0.025 eV-1 keV electrons and 10 eV-1 keV photons. *Atomic and Molecular Data for Radiotherapy*. IAEA-TECDOC-506, Vienna pp 219-233 (1989).
- M.Terrissol and A.Beaudré, Simulation of space and time evolution of radiolytic species induced by electrons in water. Radiat. Prot. Dosim. **31**, 171-175 (1990).
- J.Thacker, A.Stretch and D.T.Goodhead, The mutagenecity of α-particles from plutonium-238. Radiat. Res. **92**, 343-352 (1982).
- J.Thacker, Radiation-induced mutations in mammalian cells at low doses and low dose rates. *Advances in Radiation Biology, Vol 16.* edited by O.F.Nygaard, W.K.Sinclair and J.T.Lett. Academic, San Diego pp. 77-124 (1992).
- H.Tomita, M.Kai, T. Kusama and A.Ito, Strand break formation in plasmid DNA irradiated in aqueous solution: effect of medium temperature and hydroxyl radical scavenger concentration. J. Radiat. Res. **36**, 46-55 (1995).
- H.Tomita, M.Kai, T. Kusama and A.Ito, Monte Carlo simulation of physiochemical processes of liquid water radiolysis. Radiat. Environ. Biophys. **36**, 105-116 (1997).
- H.Tomita, M.Kai, T. Kusama and A.Ito, Monte Carlo simulation of DNA strand-break induction in supercoiled plasmid pBR322 DNA from indirect effects. Radiat. Environ. Biophys. **36**, 235-241 (1998).
- K.M.S.Townsend, A.Stretch, D.L.Stevens and D.T.Goodhead, Thickness measurements on V79-4 cells. A comparison between laser scanning confocal microscopy and electron microscopy. Int. J. Radiat. Biol. **58**, 499-503 (1990).
- M.-J.B Tunis and J.E.Hearst, On the hydration of DNA.II. Base composition dependence of the net hydration of DNA. Biopolymers **6**, 1345-1353 (1968).
- J.E.Turner, R.N.Hamm, H.A.Wright, R.H.Ritchie, J.L.Magee, A.Chatterjee and W.E.Bolch, Studies to link the basic radiation physics and chemistry of liquid water. Radiat. Phys. Chem. **32**, 503-510 (1988).

- L.Udovičić, F.Mark, E.Bothe and D.Schulte-Frohlinde, Non-Homogeneous kinetics of single stranded calf-thymus DNA and low-molecular weight scavengers for OH radicals: a comparison of experimental data and theoretical models. Int. J. Radiat. Biol. **59**, 677-697 (1991).
- Y. Umrania, H.Nikjoo and J.M.Goodfellow, A knowledge-based model of DNA hydration. Int. J. Radiat. Biol. **67**, 145-152 (1995).
- G.P. van der Schans, Gamma-ray induced double-strand breaks in DNA resulting from randomly-inflicted single-strand breaks: temporal local denaturation, a new radiation phenomenom? Int. J. Radiat. Biol. **33**, 105-120 (1978).
- J.H. van Touw, J.B.Verberne, J.Retèl and H.Loman, Radiation-induced strand breaks in φX174 replicative form DNA: an improved experimental and theoretical approach. Int. J. Radiat. Biol. **48**, 567-578 (1985).
- *Computational Approaches in Molecular Radiation Biology. Monte Carlo Methods*. edited by M.N.Varma and A.Chatterjee. Plenum Press, New York (1994).
- C. von Sonntag, U.Hagen, A.Schon-Bopp and D.Schulte-Frohlinde. Radiation-induced strand breaks in DNA: chemical and enzymatic analysis of end groups and mechanistic approaches. Adv. Radiat. Biol. **9**, 109-142 (1981).
- C. von Sonntag, *The Chemical Basis of Radiation Biology*. Taylor and Francis, Basingstoke, UK. pp 117-166 (1987).
- H.M.Vriesendorp and D.W. van Bekkum, *Susceptibility to total body irradiation. Response to Total Body Irradiation in Different Species*. edited by J.J.Broerse and T.MacVittie. Martinus Nijhoff, Amsterdam (1984).
- S.S.Wallace, AP endonuclease and DNA glycosylases that recognize oxidative DNA damage. Environ. Mutagen. **12**, 431-477 (1988).
- S.S.Wallace, DNA damages processed by base excision repair: biological consequences. Int. J. Radiat. Biol. **66**, 579-589 (1994).
- J.F.Ward and I.Kuo, Strand breaks, base release and postirradiation changes in DNA γ-irradiated in dilute O_2-saturated aqueous solution. Radiat. Res. **66**, 485-498 (1976).
- J.F.Ward, Some biochemical consequences of the spatial distribution of ionizing radiation-produced free radicals. Radiat. Res. **86**, 185-195 (1981).
- J.F.Ward, E.I.Joner and W.F.Blakely, Effects of inhibitors of DNA strand break repair on HeLa cell radiosensitivity. Cancer Res. **44**, 59-63 (1984).

- J.F.Ward, Biochemistry of DNA lesions, Radiat. Res. **104**, S103-S111 (1985).
- J.F.Ward, DNA damage produced by ionizing radiation in mammalian cells: identities, mechanisms for formation and reparability. Prog. Nucleic Acid. Res. Mol. Biol. **35**, 95-125 (1988).
- J.F.Ward, Mechanisms of radiation action on DNA in model systems-their relevance to cellular DNA. *Early effects of radiation on DNA*. edited by E.M.Fielden and P.O'Neill. NATO ASI series H vol. 54, Springer-Verlag, New York pp 1-16 (1991).
- J.F.Ward, The complexity of DNA damage: relevance to biological consequences. Int. J. Radiat. Biol. **66**, 427-432 (1994).
- R.L.Warters and B.W.Lyons, Variation in radiation-induced formation of DNA double-strand breaks as a function of chromatin structure. Radiat. Res. **130**, 309-318 (1992).
- R.Watanabe, N.Usami and K.Kobayashi, Oxidataion yield of the ferrous ion in a Fricke solution irradiated with monochromatic synchrotron soft X-rays in the 1.8-10 keV region. Int. J. Radiat. Biol. **68**, 113-120 (1995).
- R.L.Willson, The reaction of oxygen with radiation-induced free radicals in DNA and related compounds. Int. J. Radiat. Biol. **17**, 349-358 (1970).
- W.E.Wilson and H.Nikjoo, A Monte Carlo code for positive ion track simulation. Radiat. Environ. Biophys. **38**, 97-104 (1999).
- B.Wolf and S.Hanlon, Structural transitions of deoxyribonucleic acid in aqueous electrolyte solutions.II. The role of hydration. Biochem. **14**, 1661-1670 (1975).
- M.A.Xapos and W.K.Pogozelski, Modelling the yield of double-strand breaks due to formation of multiply damaged sites in irradiated plasmid DNA. Radiat. Res. **146**, 668-672 (1996).
- H.Yamaguchi, A spur diffusion model applied to estimate yields of species in water irradiated by monoenergetic photons of 50 eV-2 MeV. Radiat. Phys. Chem. **34**, 801-807 (1989).
- H.Yamaguchi, Calculation of G-value of Fricke dosimeter irradiated by photons of 100 eV-10 MeV. *Microdosimetry: an interdisciplinary approach*. edited by D.T.Goodhead, P.O'Neill and H.G.Menzel. The Royal Society of Chemistry, Cambridge, U.K. pp 97-100 (1997).